



Swansea University  
Prifysgol Abertawe



## Swansea University E-Theses

---

# The photodegradation resistance of polymer coatings for pre-finished steels.

Cashmore, Samantha

### How to cite:

---

Cashmore, Samantha (2010) *The photodegradation resistance of polymer coatings for pre-finished steels..* thesis, Swansea University.

<http://cronfa.swan.ac.uk/Record/cronfa42963>

### Use policy:

---

This item is brought to you by Swansea University. Any person downloading material is agreeing to abide by the terms of the repository licence: copies of full text items may be used or reproduced in any format or medium, without prior permission for personal research or study, educational or non-commercial purposes only. The copyright for any work remains with the original author unless otherwise specified. The full-text must not be sold in any format or medium without the formal permission of the copyright holder. Permission for multiple reproductions should be obtained from the original author.

Authors are personally responsible for adhering to copyright and publisher restrictions when uploading content to the repository.

Please link to the metadata record in the Swansea University repository, Cronfa (link given in the citation reference above.)

<http://www.swansea.ac.uk/library/researchsupport/ris-support/>

# The Photodegradation Resistance of Polymer Coatings for Pre-finished Steels

**Samantha Cashmore**

2010

A Thesis Submitted to Swansea University for the Degree of  
Engineering Doctorate (EngD)

ProQuest Number: 10821353

All rights reserved

INFORMATION TO ALL USERS

The quality of this reproduction is dependent upon the quality of the copy submitted.

In the unlikely event that the author did not send a complete manuscript and there are missing pages, these will be noted. Also, if material had to be removed, a note will indicate the deletion.



ProQuest 10821353

Published by ProQuest LLC (2018). Copyright of the Dissertation is held by the Author.

All rights reserved.

This work is protected against unauthorized copying under Title 17, United States Code  
Microform Edition © ProQuest LLC.

ProQuest LLC.  
789 East Eisenhower Parkway  
P.O. Box 1346  
Ann Arbor, MI 48106 – 1346





## DECLARATION

This work has not previously been accepted in substance for any degree and is not being concurrently submitted in candidature for any degree.

Signed .. ..... (candidate)

Date ..... 1/1/2021 .....

## STATEMENT 1

This thesis is the result of my own investigations, except where otherwise stated. Where correction services have been used, the extent and nature of the correction is clearly marked in a footnote(s).

Other sources are acknowledged by footnotes giving explicit references. A bibliography is appended.

Signed .. ..... (candidate)

Date ..... 1/8/2021 .....

## STATEMENT 2

I hereby give consent for my thesis, if accepted, to be available for photocopying and for inter-library loan, and for the title and summary to be made available to outside organisations.

Signed ..... (candidate)

Date ..... 1/8/2021 .....

## Summary of Thesis

The focus of this EngD Thesis was the investigation into improving the resistance to weathering, of coatings for pre-finished steel applications, namely poly (vinyl chloride) (PVC).

The addition of stabilisers and their influence on photodegradation was assessed and measured by gloss and colour change after artificial weathering, as well as measuring the carbon dioxide (CO<sub>2</sub>) evolution using the flat panel reactor. The resistance to photodegradation titanium dioxide (TiO<sub>2</sub>) pigmented PVC coatings has been shown to be improved significantly by the addition of Hydrotalcite (HT) in atmospheres of all humidities. This stabilisation reflects the ability of HT to remove hydrochloric acid within the film, reducing dehydrochlorination and therefore coating degradation.

Similarly, improved resistance to photodegradation and the signs of coating failure was achieved by the use of barrier coatings. Both stabilised PVC clear coats and nano-metric physical vapour deposition (PVD) sputtered coatings were successful at reducing the level of degradation of the TiO<sub>2</sub> pigmented PVC base coating. Although showing little difference in some areas of degradation measured, the ultra-violet absorber (UVA) and hindered amine light stabiliser (HALS) stabilised clear PVC top coats proved to be successful at reducing the level of localised degradation and associated colour change that was evident.

Recognising the environmental impact of the use of solvents in PVC coating systems, polyethylene (PE) was identified as alternative polymer coating for external applications. Techniques used to measure the photodegradation of PVC, such as CO<sub>2</sub> evolution, have also proved to be a suitable testing technique for polyethylene coatings, even when stabilised. Oxidation induction experiments were also carried out on the stabilised and pigmented PE and combined with the CO<sub>2</sub> evolution data, provided an insight into the degradation mechanisms of this polymer.

## **Acknowledgements**

Firstly, I would like to thank my sponsors, EPSRC and Corus Colors. A special thanks should go to Paul Jones and Jon Elvins, my industrial supervisors, who have continually shown interest in my studies and encouraged me throughout the four years.

A huge thanks must go to my supervisors in Swansea University, Cris Arnold, Sue Alston and especially Dave Worsley and Andrew Robinson. All have shared their interest, expertise and offered a tremendous amount of support through the years.

After the years of studying in the Materials Engineering Department, I have made some wonderful friends. We have shared some special times and to Dai, Bruce and Lee, I am very thankful that I was able to come to work and thoroughly enjoy every day.

Last but by no means least, without the love and support of my friends, colleagues at Tata, family and especially Michael, I would not be writing this. For accompanying me on numerous visits to Port Talbot to change experiments at unsociable hours, patience and support at times of self-doubting, I am eternally grateful to him.

*To Grandma*

|          |  |           |
|----------|--|-----------|
| <b>1</b> | <b>Introduction.....</b>                                   | <b>17</b> |
| 1.1      | Pre-Finished Steel .....                                   | 2         |
| 1.2      | Constituents of Paint .....                                | 3         |
| 1.2.2    | Coil Coating Process .....                                 | 8         |
| 1.2.3    | Polymer Coated Steels .....                                | 10        |
| 1.3      | Mechanisms of Polymer Photodegradation .....               | 10        |
| 1.3.1    | Photochemistry .....                                       | 10        |
| 1.3.2    | General Mechanism of Polymer Degradation.....              | 15        |
| 1.3.3    | Polyethylene and Poly (vinyl chloride) .....               | 23        |
| 1.4      | Titanium Dioxide .....                                     | 25        |
| 1.4.1    | Structure of TiO <sub>2</sub> .....                        | 26        |
| 1.4.2    | Manufacture of TiO <sub>2</sub> [28] .....                 | 27        |
| 1.4.3    | Photoactivity of TiO <sub>2</sub> .....                    | 31        |
| 1.5      | The Effect of Photodegradation on Coating Durability ..... | 35        |
| 1.5.1    | Gloss Loss and Chalking.....                               | 35        |
| 1.5.2    | Colour Change .....  | 36        |
| 1.5.3    | Delamination .....   | 36        |
| 1.5.4    | Crazing and Cracking.....                                  | 36        |
| 1.5.5    | Weight Loss and Film Thickness Change.....                 | 36        |
| 1.6      | Stabilisation against Photodegradation .....               | 37        |
| 1.6.1    | Additives .....  | 37        |
| 1.6.2    | Barrier Layers.....  | 44        |
| 1.7      | Weathering and Accelerated Exposure .....                  | 45        |
| 1.7.1    | Natural Exposure.....                                      | 46        |
| 1.7.2    | Artificial Exposure .....                                  | 47        |
| 1.8      | Degradation Measurement Techniques.....                    | 49        |
| 1.8.1    | Physical Testing Techniques.....                           | 49        |
| 1.8.2    | Chemical Test Methods to Quantify Degradation .....        | 50        |
| 1.8.3    | Oxidation Induction Characteristics.....                   | 56        |
| 1.9      | Introduction to Investigation.....                         | 57        |
| 1.9.1    | Motivation .....   | 57        |
| 1.9.2    | Structure of Thesis .....                                  | 57        |
| 1.10     | References .....   | 60        |
| <b>2</b> | <b>Experimental Procedures.....</b>                        | <b>65</b> |
| 2.1      | Coating Formulations.....                                  | 65        |
| 2.1.1    | PVC Paint Formulations .....                               | 65        |
| 2.1.2    | Polyethylene.....  | 67        |
| 2.2      | Sample Preparation .....                                   | 68        |
| 2.2.1    | PVC.....   | 68        |
| 2.2.2    | Polyethylene Coatings.....                                 | 71        |
| 2.2.3    | Plasma Vapour Deposition Coating of PVC Samples .....      | 74        |
| 2.3      | Accelerated Weathering.....                                | 76        |
| 2.3.1    | Fourier Transform Infrared Spectrophotometer.....          | 76        |

|       |   |    |
|-------|---|----|
| 2.3.2 | Carbon Dioxide Reactor.....                         | 76 |
| 2.3.3 | Automatic Data Collection Programme (Evolgas) ..... | 79 |
| 2.3.4 | Atmospheric Condition Experimentation .....         | 82 |
| 2.4   | DSC.....  | 83 |
| 2.5   | Commercial Accelerated Weathering .....             | 84 |
| 2.5.1 | QUVA .....  | 84 |
| 2.5.2 | Gloss Measurement.....                              | 85 |
| 2.5.3 | Colour Measurement.....                             | 86 |
| 2.5.4 | UV Vis Spectrophotometer .....                      | 86 |
| 2.5.5 | Weight Loss Apparatus .....                         | 88 |
| 2.6   | References .....                                    | 89 |

### **3 The Effects of Humidity on TiO<sub>2</sub> Photocatalysed Photodegradation ..... 90**

|       |  |     |
|-------|--|-----|
| 3.1   | Introduction.....  | 91  |
| 3.1.1 | Aims and Objectives .....  | 91  |
| 3.2   | Experimental Procedure .....   | 92  |
| 3.2.1 | Model PVC Coatings .....   | 92  |
| 3.2.2 | Polyethylene Samples .....   | 92  |
| 3.2.3 | Photodegradation Irradiation Apparatus and Data Collection .....                           | 93  |
| 3.2.4 | Control of Relative Humidity above 32%.....  | 94  |
| 3.2.5 | In-situ Assessment of Effect of Varying Humidity below 32% RH..                            | 96  |
| 3.2.6 | Gloss Retention during QUVA Weathering of Near Commercial HT Containing PVC Plastisol..... | 97  |
| 3.3   | Results and Discussion.....  | 98  |
| 3.3.1 | Effect of TiO <sub>2</sub> addition on PVC Photodegradation in Ambient Conditions .....    | 98  |
| 3.3.2 | The Effect of Humidity on UPVC Photodegradation .....                                      | 100 |
| 3.3.3 | The Effect of Hydrotalcite Addition on UPVC Photodegradation ..                            | 102 |
| 3.3.4 | The Influence of Varying Levels of HT Addition .....                                       | 104 |
| 3.3.5 | Influence of Humidity on the HT Stabilised System .....                                    | 106 |
| 3.3.6 | The Effect of HT Addition on Gloss Performance of Weathered PVC Samples                    | 107 |
| 3.4   | The Effect of Humidity on Polyethylene Photodegradation.....                               | 108 |
| 3.5   | Conclusions .....  | 114 |
| 3.6   | References .....   | 116 |

### **4 The Effect of Clear Top Coats on Improving the Weathering Resistance of PVC Systems..... 118**

|       |                              |     |
|-------|------------------------------|-----|
| 4.1   | Introduction.....            | 119 |
| 4.1.1 | Aims and Objectives .....    | 119 |
| 4.2   | Experimental Techniques..... | 120 |
| 4.2.1 | Sample Preparation .....     | 120 |
| 4.2.2 | Accelerated Weathering.....  | 122 |
| 4.2.3 | Gloss and Colour Change..... | 123 |

|       |  |     |
|-------|--|-----|
| 4.2.4 | Colour Change Measurements .....   | 123 |
| 4.2.5 | Weight loss.....   | 124 |
| 4.2.6 | Imaging .....  | 124 |
| 4.3   | Results and Discussion.....  | 125 |
| 4.3.1 | Commercial Systems.....  | 125 |
| 4.3.2 | Fully Formulated Clear Coat Systems .....  | 132 |
| 4.3.3 | Photodegradation of TiO <sub>2</sub> Pigmented HPS 200 with Clear Coat<br>Lacquers 147 |     |
| 4.4   | Conclusions.....   | 149 |
| 4.5   | References .....   | 151 |

## **5 Nano-scale Coatings for the Improved Weathering Resistance of PVC ..... 152**

|       |  |     |
|-------|--|-----|
| 5.1   | Introduction.....  | 153 |
| 5.1.1 | Aims and Objective.....                                  | 153 |
| 5.2   | Experimental .....                                       | 154 |
| 5.2.1 | Barrier Coatings for Improved PVC Photodegradation ..... | 154 |
| 5.2.2 | Wedge Coated Fully Formulated Model PVC Coating .....    | 155 |
| 5.2.3 | Accelerated Weathering .....                             | 157 |
| 5.3   | Results and Discussion.....                              | 158 |
| 5.3.1 | CO <sub>2</sub> Evolution .....                          | 158 |
| 5.3.2 | Aluminum and Titanium Wedge Coated PVC.....              | 171 |
| 5.4   | Conclusions.....   | 175 |
| 5.5   | References .....   | 177 |

## **6 Polyethylene Photodegradation & Development of Accelerated Testing Techniques..... 178**

|       |   |     |
|-------|---|-----|
| 6.1   | Introduction.....   | 179 |
| 6.1.1 | Aims and Objectives .....   | 179 |
| 6.2   | Experimental .....  | 180 |
| 6.2.1 | Pigments and Stabilisers .....                                      | 180 |
| 6.2.2 | Sample Preparation .....  | 181 |
| 6.2.3 | Accelerated Weathering .....  | 181 |
| 6.2.4 | CO <sub>2</sub> Reactor .....                                       | 181 |
| 6.2.5 | Differential Scanning Calorimetry (DSC) .....                       | 182 |
| 6.2.6 | Development of Technique for In-situ Oxidation Induction Profiles   | 183 |
| 6.3   | Results and Discussion.....   | 185 |
| 6.3.1 | In-situ CO <sub>2</sub> Evolution Profiles of PE .....              | 185 |
| 6.3.2 | In-situ CO <sub>2</sub> Evolution of Artificially Weathered PE..... | 192 |
| 6.3.3 | Measurement of Oxidation Induction Temperatures (OIT).....          | 199 |
| 6.3.4 | Development of In-situ UV Irradiated PE Oxidation Profiles.....     | 208 |
| 6.4   | Conclusions.....  | 215 |
| 6.5   | References .....  | 218 |

**7 Conclusions and Future Work.....219**  
7.1 Conclusions..... 220  
7.2 Future Work ..... 222  
**8 Appendices .....223**



# Nomenclature

AH - Phenolic Anti Oxidant  
Al - Aluminium  
AO -Anti Oxidant  
ATR - Attenuated Total Reflectance  
ca - Circa  
CaF<sub>2</sub> - Calcium Fluoride  
CO<sub>2</sub> - Carbon Dioxide  
CTC - Charge Transfer Complexes  
Cu - Copper  
DSC - Differential Scanning Calorimetry  
FTIR - Fourier Transform Infrared Spectrophotometer  
HALS - Hindered Amine Light Stabilisers  
HBP -Hydroxy-benzophenone  
HCl - Hydrogen Chloride  
HT - Hydrotalcite  
IC - Internal Conversion (Catalyst)  
IR - Infrared  
ISC - Inter-system Crossing  
ITO - Indium Tin Oxide  
MEK - Methyl Ethyl Ketone  
MIR - Mid Infrared  
NIR - Near Infrared  
OIT - Oxidation Induction Temperature  
PE - Polyethylene  
PET - Polyethylene terephthalate  
PHR - Per Hundred Resin  
PP - Polypropylene  
PU - Polyurethane  
PVC - Poly Vinyl Chloride  
PVD - Plasma Vapour Deposition  
PVDF - Polyvinylidene Fluoride  
RH - Relative Humidity  
SED - Solvent Emissions Directive  
SEM - Scanning Electron Microscope  
THF - Tetrahydrofuran  
Ti - Titanium  
TiO<sub>2</sub> - Titanium Dioxide  
UPVC - Unplasticised Poly Vinyl Chloride  
UVA - Ultra Violet Absorber  
UVAs - Ultraviolet Absorbers  
VOC - Volatile Organic Compound

# Table of Figures

## Chapter 1

|   |    |
|---|----|
| Figure 1-1 Coating Layers of an Organically Coated Steel Product.....   | 2  |
| Figure 1-2 Coil Coating Line .....  | 9  |
| Figure 1-3 Energy Levels of Excited States.....   | 12 |
| Figure 1-4 Deactivation Pathways Jablonski Diagram [10].....  | 12 |
| Figure 1-5 Radiative Deactivation of Excited States .....   | 15 |
| Figure 1-6 Formation of Chromophores in Type A and B Polymers .....   | 16 |
| Figure 1-7 Chromophoric Groups in Type A and B polymers[19].....  | 17 |
| Figure 1-8 Absorption Spectra of Some Common Polymers (coating thickness shown in brackets) [21] .....            | 18 |
| Figure 1-9 Bolland-Gee Auto-oxidation Mechanism [22].....   | 18 |
| Figure 1-10 Overview of the Free Radical Degradation Mechanism [11].....  | 19 |
| Figure 1-11 Chromophores and Photochemical Reactions[19] .....  | 20 |
| Figure 1-12 Cage recombination effect.....  | 20 |
| Figure 1-13 Crosslinking Reaction in the Polymer.....   | 22 |
| Figure 1-14 Disproportionation Reaction to Produce Ketone and Alcohol functions                                   | 22 |
| Figure 1-15 Flow diagram of Photo-Oxidation Reactions in Polymers [24] .....                                      | 23 |
| Figure 1-16 PE Structure.....   | 24 |
| Figure 1-17 PVC Structure .....   | 24 |
| Figure 1-18 Crystal Structures of Anatase and Rutile [21].....  | 27 |
| Figure 1-19 The Sulphate and Chloride Process.....  | 29 |
| Figure 1-20 Typical Fluid Energy Mill.....  | 31 |
| Figure 1-21 Valence and Conduction Bands, a) Partially -filled band, b) Large band gap, c) Smaller band gap ..... | 32 |
| Figure 1-22 Chalking and its Effects .....  | 35 |
| Figure 1-23 Influences and Effects of Photodegradation.....   | 37 |
| Figure 1-24 Keto/enol Tautomerism Energy Dissipation Mechanism in Hydroxyl-benzophenone.....                      | 39 |
| Figure 1-25 Benzotriazole Stabilisation Mechanism in Hydroxy-phenyl-benzotriazole .....                           | 39 |
| Figure 1-26 Cyclic Mechanism of HALS Stabilisation [20] .....   | 43 |
| Figure 1-27 Spectrum of Different Light Sources .....   | 48 |
| Figure 1-28 Flat Panel Irradiation Apparatus.....   | 54 |
| Figure 1-29 CO <sub>2</sub> Evolution Rate for Different Photoactive Grades of TiO <sub>2</sub> [19]...           | 55 |
| Figure 1-30 Typical Oxidation Induction Characteristics.....  | 56 |

## Chapter 2

|  |    |
|--|----|
| Figure 2-1 - 'Draw Down' Coating Technique .....                               | 68 |
| Figure 2-2 Coating of Primed Steel .....                                       | 69 |
| Figure 2-3 - Torque Rheometer .....  | 71 |
| Figure 2-4 - Compression Moulder.....  | 73 |
| Figure 2-5 - 'Sandwich Like' Arrangement of Steel Plates, PET and Polymer..... | 73 |
| Figure 2-6 PVD Coating Chamber.....  | 74 |
| Figure 2-7 Deposition Target.....  | 75 |
| Figure 2-8 Schematic of Instrument Set Up.....                                 | 76 |

|  |    |
|--|----|
| Figure 2-9 Schematic of Experimental Apparatus .....   | 77 |
| Figure 2-10 The Instantaneous Response of the System to Injections of 100microL<br>CO <sub>2</sub> ..... | 78 |
| Figure 2-11 Cumulative Effect of the Injections.....   | 79 |
| Figure 2-12 The Evolgas Scan Control User Interface .....  | 80 |
| Figure 2-13 The Evolgas Timer Control User Interface .....   | 80 |
| Figure 2-14 - Interface for Adjusting Area Parameters .....  | 81 |
| Figure 2-15 Screen Showing Test Progress and Log File.....   | 82 |
| Figure 2-16 Schematic of Apparatus Used to Introduce and Measure the Effect of RH<br>.....               | 83 |
| Figure 2-17 - Jade DSC.....  | 83 |
| Figure 2-18 - Aluminium Sample Pans.....   | 84 |
| Figure 2-19 QUVA Weatherometer.....  | 85 |
| Figure 2-20 Integration Sphere of UV Vis Spectrophotometer .....   | 87 |

### Chapter 3

|  |     |
|--|-----|
| Figure 3-1 FTIR CO <sub>2</sub> Transmission Spectrum as a function of irradiation time for a<br>model PVC/TiO <sub>2</sub> film. ....                                   | 94  |
| Figure 3-2 Apparatus for In-Situ Control of Relative Humidity above 32%.....   | 95  |
| Figure 3-3 Apparatus for In-situ assessment of Effect of Varying Humidity below<br>32% RH.....   | 97  |
| Figure 3-4 Typical CO <sub>2</sub> evolution kinetics from a 30PHR TiO <sub>2</sub> PVC film irradiated<br>under typical lab conditions of ca 40% relative humidity..... | 98  |
| Figure 3-5 The Mechanism of TiO <sub>2</sub> Catalysed PVC Photodegradation .....  | 99  |
| Figure 3-6 Typical CO <sub>2</sub> Evolution Profiles for UPVC in Varying Relative Humidities<br>.....   | 100 |
| Figure 3-7 CO <sub>2</sub> Evolution Rates for UPVC at Varying Relative Humidities<br>Controlled Using Saturated Salt Solutions.....                                     | 100 |
| Figure 3-8 CO <sub>2</sub> Evolution Rates for UPVC at Relative Humidities Less Than 43%<br>.....  | 101 |
| Figure 3-9 Typical CO <sub>2</sub> evolution Kinetic Effects of a 5% (PHR) HT Addition on of<br>a 30PHR TiO <sub>2</sub> /PVC film.....                                  | 103 |
| Figure 3-10 Schematic of Ion Exchange Mechanism [50].....  | 103 |
| Figure 3-11 Typical CO <sub>2</sub> Evolution Profiles for HT Pigmented UPVC.....  | 104 |
| Figure 3-12 CO <sub>2</sub> Evolution Rates for HT Pigmented UPVC at 32%RH.....  | 105 |
| Figure 3-13 The Effect Of Varying RH on 4%HT UPVC CO <sub>2</sub> Evolution Rates ....   | 106 |
| Figure 3-14 The Change in Gloss Level After QUVA Weathering.....   | 107 |
| Figure 3-15 Typical CO <sub>2</sub> Evolution Profiles for PE at Varying RH.....   | 109 |
| Figure 3-16 CO <sub>2</sub> Evolution Rates for TiO <sub>2</sub> Pigmented PE at Varying RH .....  | 109 |
| Figure 3-17 Comparison of the CO <sub>2</sub> Evolution Rates for TiO <sub>2</sub> Pigmented PE and<br>PVC at Varying RH .....   | 110 |

### Chapter 4

|   |     |
|---|-----|
| Figure 4-1 Change in Gloss Retention of Near Commercial Lacquered HPS200 ....                     | 125 |
| Figure 4-2 Change in Colour of Near Commercial Lacquered HPS200 after 2100hrs<br>Weathering ..... | 126 |
| Figure 4-3 Change in Total Reflectance between 350nm and 780nm after 2100hrs<br>Weathering .....  | 127 |

|  |     |
|--|-----|
| Figure 4-4 Average Gloss Retention Values for 2 PU Lacquered Samples .....   | 128 |
| Figure 4-5 The Change in Reflectance at the Respective Wavelength.....   | 129 |
| Figure 4-6 Reflectance Spectra between 350nm and 780nm for a Non-Lacquered<br>HPS200 Before and After Weathering.....                    | 129 |
| Figure 4-7 Reflectance Spectra between 350nm and 780nm for a 20 Micron Clear<br>HPS200 Lacquered Sample Before and After Weathering..... | 130 |
| Figure 4-8 Reflectance Spectra between 350nm and 780nm for a 40 Micron Clear<br>HPS200 Lacquered Sample Before and After Weathering..... | 130 |
| Figure 4-9 Reflectance Spectra between 350nm and 780nm for a High Performance<br>Lacquered Sample Before and After Weathering .....      | 131 |
| Figure 4-10 Reflectance Spectra between 350nm and 780nm for a PU Lacquered<br>Sample Before and After Weathering .....                   | 131 |
| Figure 4-11 The Gloss Retention after 2100hrs Weathering of HBP Stabilised<br>Lacquer.....   | 133 |
| Figure 4-12 The Gloss Retention after 2100hrs Weathering of Chimisorb 81<br>Stabilised Lacquer.....                                      | 134 |
| Figure 4-13 The Gloss Retention after 2100hrs Weathering of Tinuvin 571 Stabilised<br>Lacquer.....                                       | 134 |
| Figure 4-14 The Gloss Retention after 2100hrs Weathering of Tinuvin 765 Stabilised<br>Lacquer.....                                       | 135 |
| Figure 4-15 The Gloss Retention after 2100hrs Weathering of Tinuvin Mix Stabilised<br>Lacquer.....                                       | 135 |
| Figure 4-16 CO <sub>2</sub> Evolution Rates for HBP .....  | 136 |
| Figure 4-17 CO <sub>2</sub> Evolution Rates for Chimisorb 81 .....   | 137 |
| Figure 4-18 CO <sub>2</sub> Evolution Rates for Tinuvin 571 .....  | 137 |
| Figure 4-19 CO <sub>2</sub> Evolution Rates for Tinuvin 765 .....  | 138 |
| Figure 4-20 CO <sub>2</sub> Evolution Rates for Tinuvin Mix .....  | 138 |
| Figure 4-21 Average CO <sub>2</sub> Evolution Rate for Various Loading Levels of Additives<br>.....                                      | 140 |
| Figure 4-22 Change in Reflectance Spectrum after 1200hrs .....   | 141 |
| Figure 4-23 Sample Matrix After 2100hrs QUV Weathering .....   | 142 |
| Figure 4-24 Lacquer- NoAdditive, 2% HBP & 5% Tinuvin 571 Images after<br>Weathering .....  | 143 |
| Figure 4-25 Mass Loss of Free Film Clear Top Coats after UVA Exposure.....   | 144 |
| Figure 4-26 Gloss Retention of Free Films after 1400hrs QUVA Exposure.....   | 145 |
| Figure 4-27 UV Vis Reflectance of Free Films at 385nm .....  | 146 |
| Figure 4-28 Ranking of Durability Characteristics of a HBP Stabilised Clear Coat   | 148 |
| Figure 4-29 Ranking of Durability Characteristics of Chimisorb 81 Stabilised Clear<br>Coat .....   | 148 |
| Figure 4-30 Photoactivity Ranking of All Clear Coats.....  | 149 |

## Chapter 5

|   |     |
|---|-----|
| Figure 5-1 Model PVC Coated Sample for PVD Coating .....  | 154 |
| Figure 5-2 Deposition Coating Chamber .....   | 155 |
| Figure 5-3 Schematic of Technique Used to Produce the Aluminium Wedge Coated<br>PVC Sample..... | 156 |
| Figure 5-4 Typical CO <sub>2</sub> Evolution Profile for ITO Coated PVC Samples .....           | 158 |
| Figure 5-5 CO <sub>2</sub> Evolution Profiles for ITO Coated PVC .....                          | 159 |
| Figure 5-6 CO <sub>2</sub> Evolution Profiles for Aluminium Coated PVC.....                     | 160 |

|   |     |
|---|-----|
| Figure 5-7 CO <sub>2</sub> Evolution Profiles for Copper Coated PVC .....                           | 161 |
| Figure 5-8 CO <sub>2</sub> Evolution Profiles for Alumina Coated PVC .....                          | 162 |
| Figure 5-9 CO <sub>2</sub> Evolution Profiles for Zirconia Coated PVC.....                          | 163 |
| Figure 5-10 CO <sub>2</sub> Evolution Profiles for Titanium Coated PVC .....                        | 164 |
| Figure 5-11 CO <sub>2</sub> Evolution Profile for Model PVC in the Absence of a Barrier Layer ..... | 165 |
| Figure 5-12 CO <sub>2</sub> Evolution Volumes at 1000 Minutes.....                                  | 167 |
| Figure 5-13 Formation on Microcracks in Deposited Coating .....                                     | 169 |
| Figure 5-14 CO <sub>2</sub> Evolution Volumes at 1000 Minutes .....                                 | 170 |
| Figure 5-15 Aluminium Wedge Coated PVC .....  | 171 |
| Figure 5-16 Titanium Wedge Coated PVC.....  | 171 |
| Figure 5-17 Aluminium Wedge Coated PVC Before and After 1000h hours QUVA Weathering .....           | 172 |
| Figure 5-18 Titanium Wedge Coated PVC Before and After 1000h hours QUVA Weathering .....            | 172 |
| Figure 5-19 Scanned Images of Aluminum Wedge Coated PVC Sample During QUVA Weathering.....          | 173 |
| Figure 5-20 Scanned Images of Titanium Wedge Coated PVC Sample During QUVA Weathering.....          | 174 |
| Figure 5-21 CO <sub>2</sub> Evolution Rates for Various Coatings.....                               | 176 |

## Chapter 6

|   |     |
|---|-----|
| Figure 6-1 UV Vis. Spectrum of Various Options for Furnace Lid.....                                     | 184 |
| Figure 6-2 CO <sub>2</sub> Evolution Curve for Virgin and Stabilised PE .....                           | 185 |
| Figure 6-3 CO <sub>2</sub> Evolution Curve for TiO <sub>2</sub> Pigmented PE .....                      | 186 |
| Figure 6-4 CO <sub>2</sub> Evolution Rates for Virgin and Stabilised PE .....                           | 186 |
| Figure 6-5 CO <sub>2</sub> Evolution Rates for TiO <sub>2</sub> Pigmented PE .....                      | 187 |
| Figure 6-6 Formation of CO <sub>2</sub> during oxidation of PE.....                                     | 190 |
| Figure 6-7 CO <sub>2</sub> Profiles for Virgin and Stabilised PE after Varying QUV Exposure .....       | 192 |
| Figure 6-8 CO <sub>2</sub> Profiles for TiO <sub>2</sub> Pigmented PE after Varying QUV Exposure ....   | 193 |
| Figure 6-9 CO <sub>2</sub> Evolution Rates for Virgin and Stabilised PE after Varying QUV Exposure..... | 193 |
| Figure 6-10 CO <sub>2</sub> Profiles TiO <sub>2</sub> Pigmented PE after Varying QUV Exposure.....      | 194 |
| Figure 6-11 The Influence of QUV Exposure on Degradation Rate .....                                     | 195 |
| Figure 6-12 The Influence of QUV Exposure on Degradation Rate .....                                     | 196 |
| Figure 6-13 CO <sub>2</sub> Evolved at 250 Minutes of Testing In Flat Panel Reactor.....                | 197 |
| Figure 6-14 Typical PE DSC Oxidation Profile .....  | 200 |
| Figure 6-15 Oxidation Induction Profiles for Virgin PE after QUV Exposure .....                         | 200 |
| Figure 6-16 Peak Oxidation Induction Temperatures for Virgin PE .....                                   | 201 |
| Figure 6-17 Oxidation Induction Profiles for Tinuvin and Virgin PE.....                                 | 202 |
| Figure 6-18 Oxidation Induction Profiles for Irganox and Virgin PE .....                                | 202 |
| Figure 6-19 Oxidation Induction Profiles for 50% TiO <sub>2</sub> and Virgin PE .....                   | 203 |
| Figure 6-20 Oxidation Induction Times after QUV Exposure .....  | 203 |
| Figure 6-21 Influence of QUV Exposure on Oxidation Induction Temperature.....                           | 204 |
| Figure 6-22 Influence of QUV Exposure on Oxidation Induction Temperature Using a Short DSC Ramp.....    | 206 |
| Figure 6-23 Influence of Surface Removal on OIT .....   | 207 |
| Figure 6-24 The In-situ UV-OIT Test Equipment .....   | 209 |

|   |     |
|---|-----|
| Figure 6-25 OIT Profiles for Exposed Virgin PE .....  | 210 |
| Figure 6-26 OIT for PE with Varying UV Exposure.....  | 210 |
| Figure 6-27 OIT Profiles for Tinuvin Stabilised PE .....                                      | 211 |
| Figure 6-28 OIT Profiles for Irganox Stabilised Virgin PE.....                                | 212 |
| Figure 6-29 OIT Profiles for 50% TiO <sub>2</sub> Pigmented Virgin PE.....                    | 212 |
| Figure 6-30 Influence of UV Irradiation on OIT during In-Situ Irradiation.....                | 213 |
| Figure 6-31 The Decrease in OIT as a Result of In-Situ UV Irradiation, after<br>Exposure..... | 214 |

# Index of Tables

## Chapter 1

|  |    |
|--|----|
| Table 1-1 Paint Components [1] .....                             | 4  |
| Table 1-2 Selected Polymer Resin Types and Their Properties..... | 5  |
| Table 1-3 Annual VOC Emissions [2].....                          | 6  |
| Table 1-4 Required Cleavage Energies for Bonds[11] .....         | 13 |
| Table 1-5 Typical Types of Particle Coagulation .....            | 30 |
| Table 1-6 Common Characteristic Group Frequencies.....           | 51 |

## Chapter 2

|  |    |
|--|----|
| Table 2-1 Formulations of Clear Top Coats .....      | 67 |
| Table 2-2 Clear Coat Lacquers Systems Compared ..... | 70 |

## Chapter 3

|   |    |
|---|----|
| Table 3-1 Sample Matrix .....   | 92 |
| Table 3-2 Salt Solutions and Respective Achievable Relative Humidity..... | 96 |

## Chapter 4

|   |     |
|---|-----|
| Table 4-1 Sample Matrix for Commercial Lacquer Comparison ..... | 120 |
| Table 4-2 Stabilisers Tested .....                              | 121 |
| Table 4-3 Level of Stabiliser Addition.....                     | 122 |
| Table 4-4 Change in Reflectance of the Spectra.....             | 132 |

## Chapter 6

|   |     |
|---|-----|
| Table 6-1 Additives used in PE.....         | 180 |
| Table 6-2 Levels of Additive Addition ..... | 180 |
| Table 6-3 Coating Removal Rate.....         | 198 |
| Table 6-4 Levels of UV Exposure .....       | 209 |

# **1 Introduction**



## 1.1 Pre-Finished Steel

Pre-finished steels are used in a variety of markets, all of which have unique service environments. For products that will be in outdoor environments for their entire service life, such as construction products which dominate half the strip steel market, or in environments such as marine constructions, coatings play an integral role in the product durability. If unprotected, the steel would be exposed to aggressive environments and would quickly oxidise and corrosion would rapidly propagate.

The primary purpose of the coating is therefore to provide a barrier between the steel substrate and the corrosion agents, water and oxygen and accelerating factors in the atmosphere such as irradiation and aggressive pollutants.

Strip steels coatings can take two forms; metallic or organic, often used alongside one another. Metallic coatings offer effective sacrificial protection over the exposed steel. Pre-coated organic steels are aesthetically pleasing and versatile, with varieties of colours and textures available. Their economic advantage has resulted in a rapid growth of use in industry. By eliminating the need for subsequent coating of a steel coil, this reduces labour, machinery and processing costs for the manufacturer.

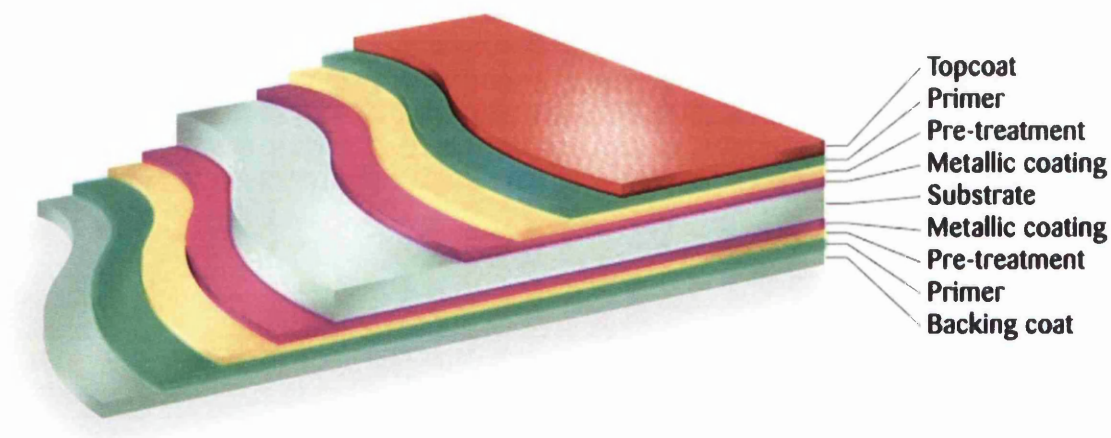


Figure 1-1 Coating Layers of an Organically Coated Steel Product

Investigations in this thesis concentrate on preventing the attack and degradation of the coating in applications prone to UV exposure. The wavelength of UV light is such that components of a coating can absorb it, inducing a photochemical reaction, ultimately leading to the breakdown of a coating. It is essential such an effect is kept to a minimum, not only for aesthetic reasons discussed later, but also the physical integrity of a coating. If delamination occurs or porosity develops, the substrate is exposed, increasing the risk of corrosion.

Similarly, the preparation of a coating and its substrate is essential for its longevity. Surface roughness and chipping can result in exposed substrate. Incomplete cleaning of the steel can induce a concentration gradient encouraging water diffusion resulting in bubbles under the paint surface, leading to blisters and pockets of concentrated solution. Such osmotic blistering can lead to corrosion. Incorrect paint preparation is a major cause of coating failure. Inclusions or incorrect additive levels also influence the integrity of the coating, whilst also acting as possible sites that induce UV degradation.

Organically coated steels used for cladding for example, are currently offered with guarantees for over 30 years (dependent on geographical location and positioning). So never before has the understanding and control of coating degradation been so important.

## **1.2 Constituents of Paint**

The top coat a coating system, often referred to as a paint, is made up of several key components as described in Table 1-1.

Table 1-1 Paint Components [1]

| <b>Component</b> | <b>Purpose</b>   |
|------------------|--|
| Solvent          | Disperse the constituents of the formulation and to reduce viscosity easing the application of the coating   |
| Binder/Resin     | Liquid polymeric or resinous materials used to hold the pigment and additives together providing adhesion.<br>Performance of the coating is dictated by the binder |
| Pigment          | Insoluble organic or inorganic particles dispersed in a coating colour and opacity to a substrate or to improve the substrate's environmental resistance           |
| Additives        | Additives or fillers are added to improve the properties of the coating e.g. flame retardants and plasticisers   |

There is a vast degree of difference in each of these components depending on the application method and product to be produced.

#### **1.2.1.1 The Coating System**

The resin component will have the greatest overall effect on the nature and performance of a paint. There are many different types of polymer that are used as the resin component, however for the purpose of coating strip steel products there are certain types of polymer that are more suitable than others. A list of some of the more common types used for coating steel substrates is given in Table 1.2.

Polyvinyl chloride (PVC) plastisol, PVDF, Polyurethane and Polyester are those which, given their properties, are particularly suited for the coating of construction strip steel.

Table 1-2 Selected Polymer Resin Types and Their Properties

| Polymer Type                   | Typical Coating Thicknesses | General Properties  |
|--------------------------------|-----------------------------|---|
| PVC Plastisol                  | 200-250 $\mu\text{m}$       | Good fabrication properties, high abrasion and damage resistance, excellent weathering properties, extensive colour range |
| Acrylic                        | 25 $\mu\text{m}$            | Good chemical and stain resistance, temperature resistant   |
| Polyester                      | 25 $\mu\text{m}$            | High gloss coating, good resistance to heat, stains and detergents, good flexibility                                      |
| Polyurethane                   | 20-100 $\mu\text{m}$        | Good chemical and mechanical resistance   |
| Epoxy                          | 5-125 $\mu\text{m}$         | Good flexibility, good resistance to chemical attack, not suitable for external use                                       |
| Polyvinylidene fluoride (PVDF) | 25 $\mu\text{m}$            | Excellent chemical resistance, good flexibility, highly weather resistant   |

### 1.2.1.2 Solvents

Producing a paint fluid enough to be applied on a continuous coating line as mentioned previously, means a solvent is necessary. After paint application, a proportion of the solvent is recycled (burned) through the oven burners whilst the rest of the solvent goes straight to the oxidiser and is burned. A solvent is typically selected based on its ability to dissolve resins and its evaporation rate. An interesting indirect effect of the solvent containing paints is their removal. Often strippers such as white spirit or Methyl Ethyl Ketone (MEK) are needed.

Despite the solvent adding versatility to a paint system, there are a variety of negative effects of its inclusion in paints. When a solvent releases vapours, they emit Volatile Organic Compounds (VOCs). These are a class of chemicals which evaporate readily at room temperature. VOCs have the ability to combine with nitrogen oxides, and in the presence of sunlight, low level ozone is produced, which is a precursor to smog pollution. Annual VOC emissions from the differing sources are shown below, in Table 1-3.

Table 1-3 Annual VOC Emissions [2]

| Method               | % of Annual VOC Emmisions |
|----------------------|---------------------------|
| Waste Management     | 1                         |
| Distrubution of Fuel | 5                         |
| Combustion Power     | 6                         |
| Product Processing   | 7                         |
| Vegetation           | 22                        |
| <b>Solvent Use</b>   | <b>24</b>                 |
| Tansportation        | 35                        |

The effects of the VOC emissions are believed to be both direct and indirect, all of which have an impact on the environment and human health. The bearing on human health ranges from irritation of eyes and the respiratory tract to the more deadly kidney damage and forms of cancer. Such an example is Formaldehyde; a paint additive that irritates mucous membranes, with carcinogenic effects.

It was clearly recognised by the government that VOC emissions needed to be controlled because of the effects they were having on human health and the environment, leading to the creating of the EC Directive;

EC Directive 1999/13/EC on "the limitation of emissions of volatile organic compounds due to the use of organic solvents in certain activities and installations" - known as the "Solvent Emissions Directive". [3]

The aim of the Solvents Emissions Directive (SED) is to prevent or reduce the effects of emissions of VOCs by providing measures and procedures to be implemented.

Because of the wide ranging uses of solvents, the SED applies to a cross-section of industry sectors from printing to dry cleaners. The scheme ultimately reduces solvent use nationwide, reducing any emissions. A threshold of solvent consumption is set, ensuring that industries meet an emission limit. Compliance with government regulation relies upon use of coatings containing less organic solvent as well as application methods that improve transfer efficiencies.

Industry as a whole will eventually need to consider developing a number of alternative coatings that not only reduce the use of potentially harmful chemicals, but eliminate them in their entirety. Three potential methods of paint application that can accommodate this are, spraying, dip and flow coating, using coating technologies that include:

- i. High-solids coatings
- ii. Waterborne coatings
- iii. Powder coatings
- iv. Radiation-cured coatings

These coating types can reduce emissions of VOCs and in so doing, reduce the generation of hazardous wastes. High transfer efficiency (percent material used that is not wasted) not only helps meet environmental regulations and cuts costs but also provides a safer work place.

Waterborne paints (sometimes referred to as 'latex paints') have the significant advantage of production with little or no VOCs. They are often used on wood furniture and building finishes and are easy to blend to produce a variety of colours in thick or thin coatings. The paints lend themselves to conventional brush applications and even electrostatic or electrodeposition. Unfortunately they do have their limitations. High temperature resistance is minimal as is their chemical resistance. Given the high content of water, corrosion can be a problem in many

ways. Firstly, the storage of the paint in cans, and secondly they can also corrode steel and some aluminium surfaces.

Powder coatings are by far more frequently used. Thermoplastic and thermoset resins are applied via numerous processes including electrostatic spraying and fluidised bed processes, to steel, aluminium and zinc/brass castings. They entail reduced costs as no solvent is needed as there is also efficient material use with no solid waste disposal. A good finish can be achieved enhancing durability and one application can produce a thick coat. However the limitations include powder clumping, difficulties including metal flake pigments and special equipment required to make colour changes. It is also hard to coat complex shapes and the process is only really efficient when coating large objects, as it is hard to make small paint batches.

### **1.2.2 Coil Coating Process**

The current process used in the continuous coil coating of steel is referred to as the 'reverse roll coating process' [4]. Organically coated steel products, comprise a variety of coating layers, all of which are applied individually by this particular coil coating process.

Prior to entrance within the coil coating process, the steel undergoes a metallic coating that offers sacrificial corrosion protection to the substrate such as the commonly used 99.85% Zinc 0.15 %Al [5]. The steel coils are fed off the reels and are passed through a pre-clean, with alkali and mechanical brushing. The steel then passes into the entrance accumulator which has the ability to vary its height, to allow the re-loading of new coils, whilst maintaining a continuous process speed. It undergoes a second cleansing and water rinse prior to the application of a pre-treatment layer. This consists of a 1  $\mu\text{m}$  thick conversion coating. This acts to provide additional corrosion protection, whilst also ensuring a high level of adhesion of any organic coatings. Historically, this has been a chromate based pre-treatment, but with tightening legislation, especially in markets such as domestic appliances, new product development is driving for chrome free alternative.

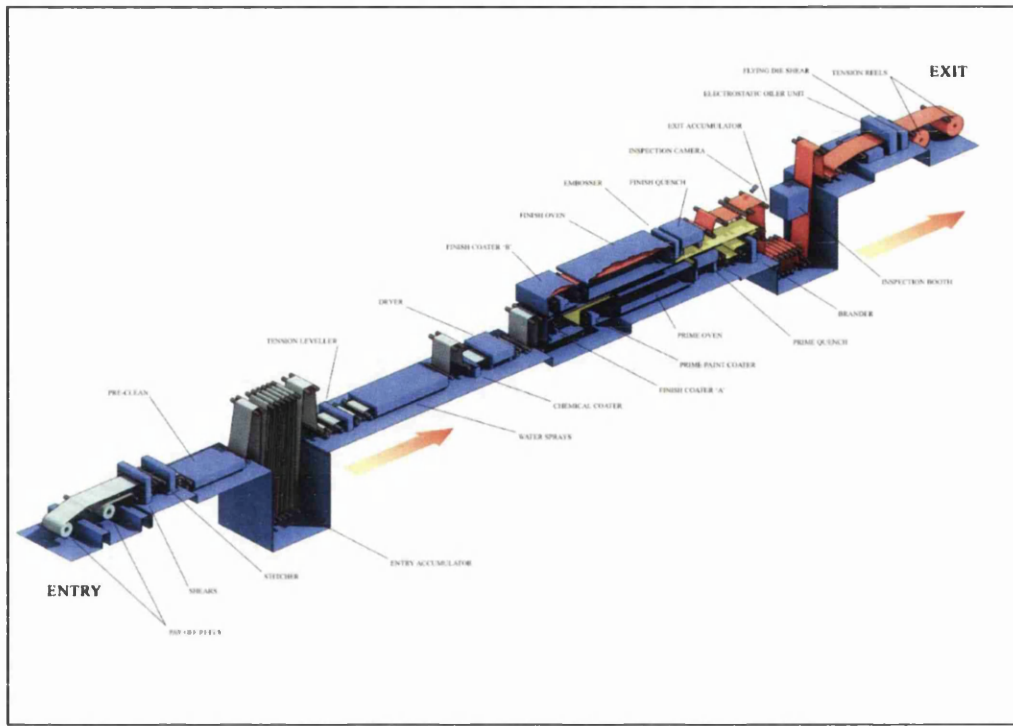


Figure 1-2 Coil Coating Line

During the subsequent priming stage, a 5-30  $\mu\text{m}$  thick layer is applied, providing additional corrosion protection and superior surface for the topcoat. The primers used are based on epoxy, polyester, polyurethane or acrylic resins, depending on the topcoat. The corrosion protection comes in the form of corrosion inhibiting pigments. Once again, a lot of research is being carried out to produce, an effective, chromate free corrosion inhibitors. An advance in this area of research can come in the form of 'smart pigments' [6-8]. They are ion exchanging pigments exhibiting the ability to remain insoluble in water (avoiding leaching and osmotic blistering) whilst only releasing inhibiting cations in the presence of an electrolyte. The primed steel passes through a primer oven to cure the coating, followed by quenching.

After drying using an air knife, the coil passes through a finish coater where the topcoat of between 25-200  $\mu\text{m}$  is applied via a roller coating process. The topcoat provides additional corrosion properties along with the aesthetics of the strip steels.



### **1.2.3 Polymer Coated Steels**

An alternative coating technique that could accommodate the high solid solvent free coating system, is already adopted in the steel industry, for packaging applications. Polymer coated steels for packaging applications comprise advanced steel grade substrates, an adhesion layer and polymer layers to achieve the range of desired properties. For example, polypropylene (PP) is widely used in the coating of steel for packaging applications because of: [9]

- i. Good chemical resistance
- ii. Highly formable
- iii. Heat sealable

Extrusion and laminating have clearly been identified by the packaging industries as safe, efficient and economical methods of coating steels. It similarly produces durable, safe (food safety) and environmentally acceptable polymer coatings. The latter is important as cans were traditionally lacquered with an extremely high VOC content coating.

There is in depth knowledge on the application and production of polymer coatings for 'indoor use' products and by taking this a step further, and applying such knowledge, with current photodegradation studies, emerges an opportunity to advance steels coated with polyolefins such as polypropylene (PP) and polyethylene (PE) into areas where PVC coatings currently dominate.

## **1.3 Mechanisms of Polymer Photodegradation**

### **1.3.1 Photochemistry**

Photochemistry is the study of chemical reactions of molecules or atoms that have been excited by the absorption of light. Knowing that coating degradation is often caused by exposure to UV irradiation, two possible modes of failure from photochemical excitation and induce coating failure are:

**Homogenous** : chromophores intrinsic to the polymer absorb UV light leading to a breakdown in its structure. The exact nature of chromophores is discussed in greater detail later (see section 1.61), but in essence it is a chemical group capable of selective light absorption.

**Heterogeneous** : where non-organic semi-conducting materials, usually metal oxides such as TiO<sub>2</sub> can absorb UV light forming excited states which destroy organic matter. Similarly, alternative pigments can have the same effect (e.g. ZnO).

These two very different mechanisms will be addressed individually

The energy in a photon of light is given by Equation 1-1. The energy of a photon is inversely proportional to its wavelength.

$$E = \frac{hc}{\lambda} \quad \text{(Equation 1-1)}$$

Where:

- E = Energy of the photon (kJmol<sup>-1</sup>)
- h = Planks constant (Js<sup>-1</sup>)
- c = Speed of light (ms<sup>-1</sup>)
- λ = Wavelength of the light (m)

The absorption of light provides activation energy sufficient to initiate photodegradation. The chromophore absorbs the UV promoting an electron from the ground state to a higher unoccupied orbital (as shown in Figure 1-3). However for this to occur the photon of light in question must have an amount of energy greater than or equal to the difference between the ground state and first excited singlet state (e.g. E<sub>1</sub>-E<sub>0</sub> in Figure 1-3), it results formation of an excited singlet state (S<sup>\*</sup>/S<sup>1</sup>).

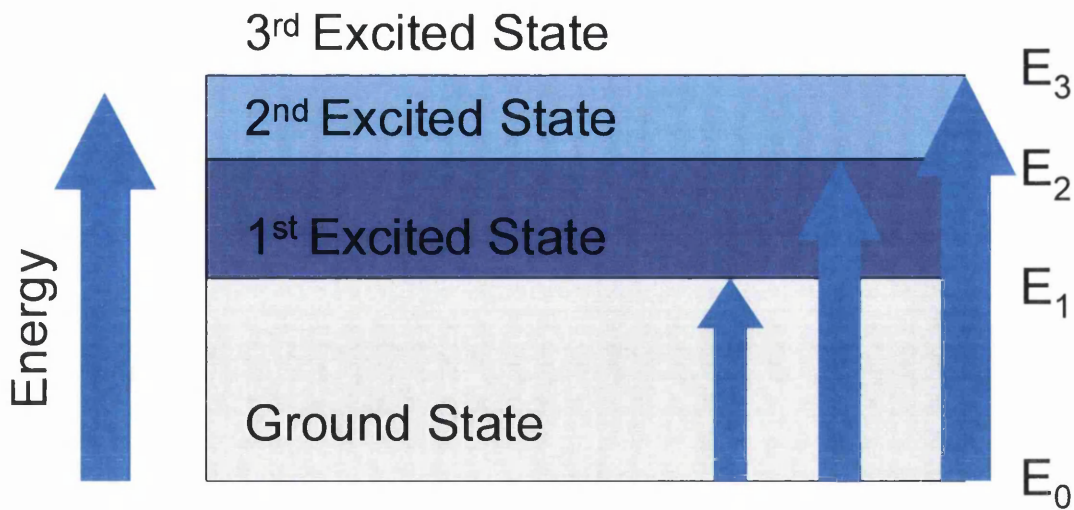


Figure 1-3 Energy Levels of Excited States

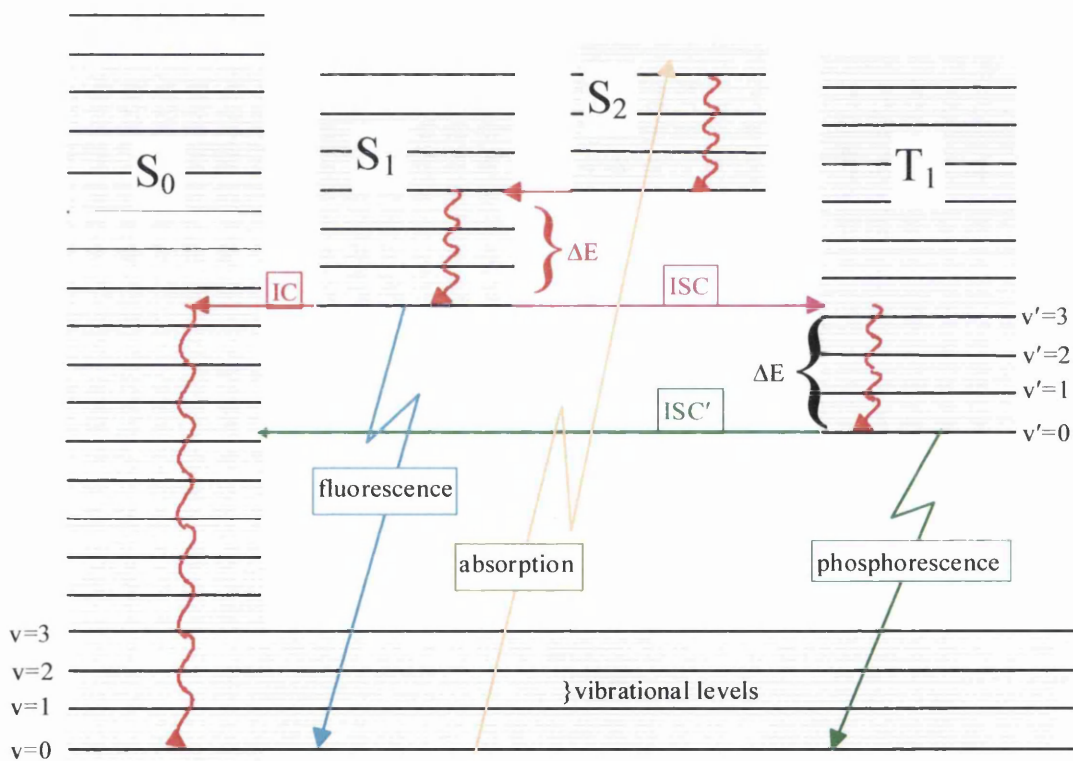


Figure 1-4 Deactivation Pathways Jablonski Diagram [10]

Any excess energy up to the amount required for the promotion to the next excited step is lost through vibration within the molecule.

Excited singlet molecules ( $S^*$ ) can lose their energy rapidly in a variety of ways (Figure 1-4). The various deactivation pathways are dictated by the absorbing chromophore present. Internal conversion (IC-catalysis) can occur back to the ground state occurs where energy is dissipated thermally. Carbonyl chromophores preferentially undergo IC.

More importantly however, the singlet state can undergo energy loss via inter-system crossing (ISC-recombination); this route occurs at many orders of magnitude less than IC. The inter-system crossing creates excited triplet states, which are much longer lived and can undergo bond cleavage (aromatic compounds undergo fluorescence emission). This can therefore result in molecular breakdown.

This is of particular interest given that it is this bond cleavage reaction that produces free radicals thus leading to photoactivity via a multitude of chemical reactions. Examples of such bond cleavage energies described in Table 1-4.

Table 1-4 Required Cleavage Energies for Bonds[11]

| <b>Bond broken</b> | <b>Bond dissociation<br/>(kJmol<sup>-1</sup>)</b> |
|--------------------|---|
| C-H                | 380 to 420  |
| O-H                | 420   |
| C-OH               | 380   |
| C-C                | 340   |
| C-O                | 320   |
| C-Cl               | 320   |
| RO-O               | 150   |
| RO-OR              | 140   |

## **The Quenching of Excited States**

It is often preferable to accelerate the decay process. This can be achieved via the addition of a quencher, decaying the excited singlet state to either to the ground state or to another low energy state (Equation 1-2).



Quenching can be achieved through many different routes, which include complex formation, heavy atom quenching, oxygen quenching and energy transfer [11-16].

## **Physical Aspects of Electronic Energy Transfer**

Energy transfers can occur either intra-molecularly (within the molecule) or inter-molecularly (between two molecules).

The degree of energy transfer is governed by a number of factors including; the distance between the donor and acceptor, the relative orientations of the donor, spectroscopic properties, optical properties of the matrix and the effect of collisions on the motion of the donor and the acceptor whilst the donor is excited. As energy transfer is never completely efficient, energy will be lost and thus the energy of the acceptor will be less than that of the original donor.

## **Radiative Energy Transfer**

This type of energy transfer is long range in comparison to the molecules involved and occurs when a photon is emitted by the donor molecule and then absorbed by the acceptor molecule. There is no direct interaction as transfer actually occurs by means of an intermediate photon. The overall efficiency of this transfer is dependent upon the amount of spectral overlap between the two molecules. Transfer of energy can only occur at similar wavelengths.

## **Non-Radiative Energy Transfer**

It can take one of two routes, the shorter in range works through the overlap of electron clouds, generally with a 1 to 1.5 nm gap between molecules and energy transfer occurs via electron exchange. The second route is slightly longer in range 5-

10nm between molecules and in this case the energy transfer is through dipole-dipole interactions.

### **Transfer in Polymer Matrices**

This can occur as intermolecular transfer or intramolecular transfer:

Intermolecular energy transfer can occur in one of three ways: By small molecules to molecular chromophores, polymeric chromophores to molecular chromophores or between polymeric chains. There are two types of intramolecular energy transfer:

The first being between localised chromophores (local). The local energy transfer (excitation) can travel in a chain like manner and thus is able to travel large distances. It is possible for this excitation to move along the chain until it becomes close enough to another excitation upon which annihilation will occur between two triplet or singlet states if two photons are absorbed on the same polymer chains.

The second occurs across loops in the polymer chain (long range).

As shown earlier the deactivation can occur either by luminescence or free radical formation (Figure 1-4).

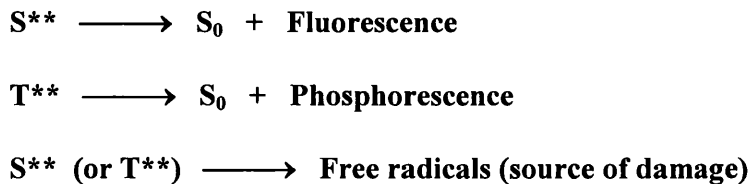


Figure 1-5 Radiative Deactivation of Excited States

### **1.3.2 General Mechanism of Polymer Degradation**

Polymers are relatively stable at normal atmospheric temperatures and do not undergo rapid degradation. However if under the same temperature conditions the sample is exposed to UV light then one might notice a significant degree of degradation. It is therefore not the oxidisability that is entirely responsible, but the

synergistic action of the factors<sup>[17]</sup>. Hence oxidation may be induced and accelerated by radiation.

Organic polymers cannot directly absorb sunlight because these hydrocarbons do not absorb sunlight wavelengths (>290nm) due to their ideal structure [17]. Degradation caused by UV irradiation can only occur when the polymer contains chromophores which absorb wavelengths of the sunlight spectrum on earth. These particular wavelengths then have sufficient energy to cause bond cleavage and degradation.

Chromophores that can absorb sunlight are: [18]

- i. Internal chain impurities-carbonyls or hydroperoxides that may originate from weathering, processing or even storage
- ii. External impurities- polymerisation catalyst residues or additives
- iii. Molecular structure of the polymer
- iv. Charge transfer complexes between oxygen and polymer chain

The manner in which they are present can divide the polymers into photoactive groups (Figure 1-6 and Figure 1-7) each with varying routes of degradation. To further illustrate the two alternative photo-reactive routes, the UV absorption spectra in Figure 1-8 show how a multitude of polymers absorb UV light. Type A polymers have absorption regions outside the normal spectra of sunlight, whilst polymer type B lie within it.

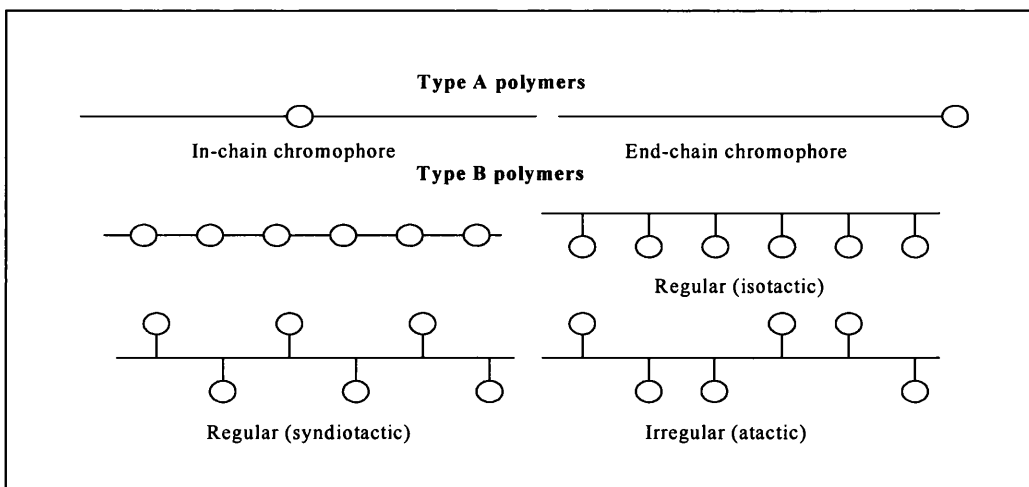


Figure 1-6 Formation of Chromophores in Type A and B Polymers

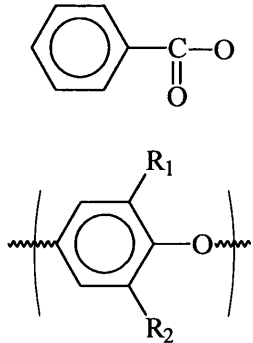
| Type A Polymers   | Example Chromophoric groups  | Example Polymers  |
|---|--|---|
| <p>In type A polymers the chromophores are impurities within the structure introduced during polymerisation or processing. They may even have been added as a separate component of the system.</p> | $\begin{array}{c} \text{---C=C---C=C---} \\ \text{---C---} \quad \text{---C=C---C---} \\ \parallel \quad \quad \quad \parallel \\ \text{O} \quad \quad \quad \text{O} \end{array}$ <p>POOH    <math>\text{Ti}^{+4}, \text{Al}^{+3}, \text{Fe}^{+3}</math></p> $\left[ \text{P---H}^{\oplus}\text{---O}_2^{-} \right] \left[ \begin{array}{c} \text{---C=C---} \\ \vdots \\ \text{O}_2 \end{array} \right]$ | <p>Poly(vinyl halides)</p> <p>Polyacrylics</p> <p>Poly(vinyl alcohols)</p> <p>Aliphatic esters</p> <p>Polyurethanes</p> |
| <p><b>Type B Polymers</b></p> <p>In type B polymers the chromophores are an integral part of the chemical structure. They can be part of, or as side groups attached to, the polymer backbone.</p>  |    | <p>Poly(ethyleneterephthalate)</p> <p>Poly(2,6-dialkyl-1,4-phenylene ether)</p> <p>Poly(ethersulphone)</p>              |

Figure 1-7 Chromophoric Groups in Type A and B polymers[19]

Regardless of which mechanism the degradation process may fall under, it is widely believed that all the above mechanisms involve free radical processes [11, 20]. It is also true that in most cases the degradation processes that occur are similar to those found in thermal degradation, the only significant difference being the initiation step and the nature of the degradation products.



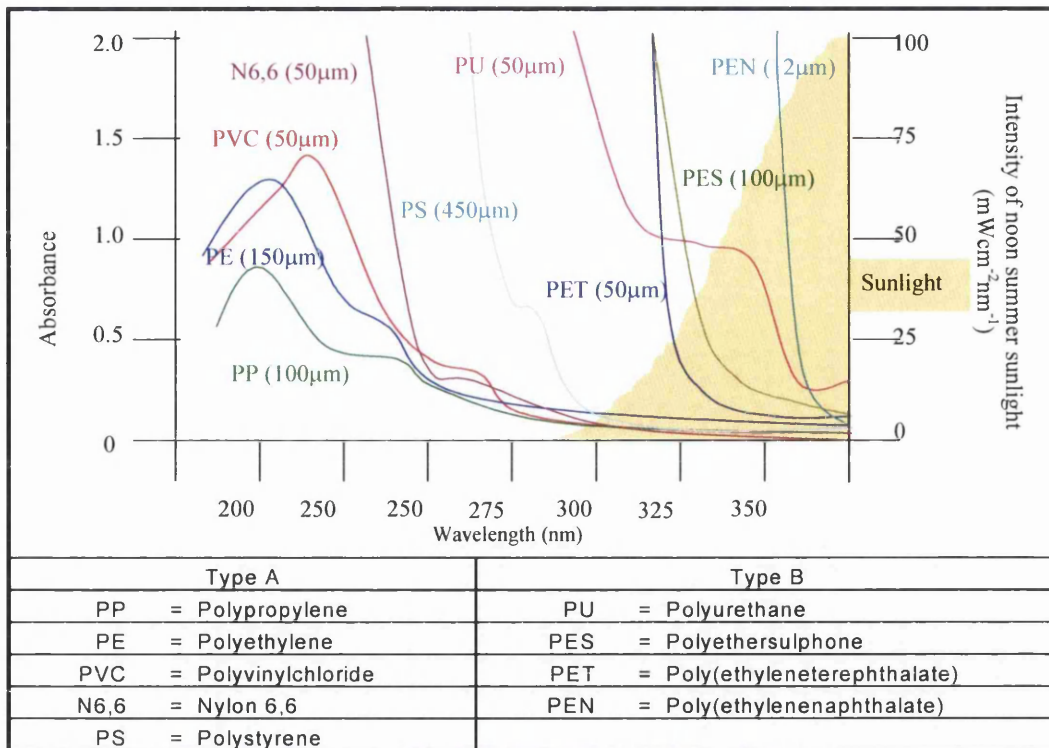


Figure 1-8 Absorption Spectra of Some Common Polymers (coating thickness shown in brackets) [21]

### 1.3.2.1 Photo-oxidation of Polymers

Photo-oxidative degradation is a combined photolysis and oxidative reaction, due to a radical-based autooxidative process, as outlined by Bolland and Gee (Figure 1-9). Hydrocarbon polymers and oxygen react in a chain reaction, initiated by the free radical mechanism. The three major steps involved in the free radical process (initiation, propagation and termination) are shown in Figure 1-10

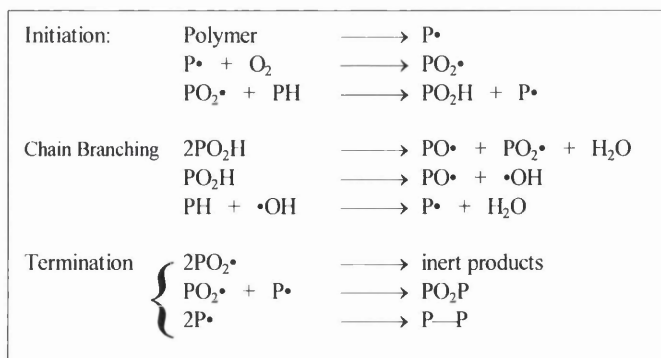


Figure 1-9 Bolland-Gee Auto-oxidation Mechanism [22]

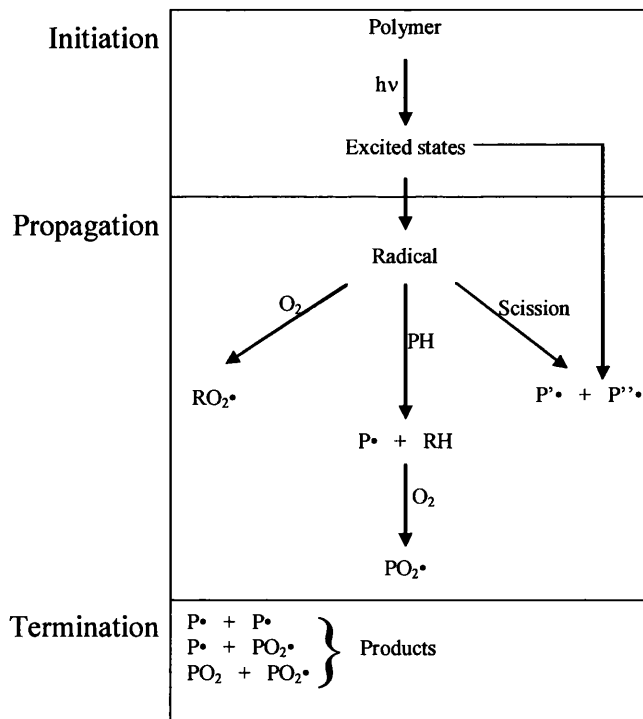


Figure 1-10 Overview of the Free Radical Degradation Mechanism [11].

### Initiation

During the initiation stage free radicals are produced. This is mainly a result of the photolysis reaction of chromophores present.

**Figure 1-11** Figure 1-11 shows some of the known chromophores along with their relevant process and also illustrates some of the chromophores that are present in type B polymers. In the case of type B polymers, the chromophore makes up part of the backbone of the polymer, when photo-cleavage occurs this will result in scission of the backbone. These reactions tend to develop very quickly, leading to the breakdown of the polymer backbone. Therefore a dramatic change in the mechanical properties of the polymer will occur. Thus type B polymers have very limited use for exterior applications.

| Functional Groups | Photochemical reaction   | Process   |
|-------------------|--|---|
| Hydroperoxides    | $\text{POOH} \xrightarrow{h\nu} \text{PO}\cdot + \cdot\text{OH}$   | Homolytic cleavage  |
| Peroxides         | $\text{POOP} \xrightarrow{h\nu} \text{PO}\cdot + \text{PO}\cdot$   |   |
| Carbonyl          | $\text{---CH}_3\text{---}\overset{\text{O}}{\parallel}\text{---CH}_2\text{---} \xrightarrow{h\nu} \text{---CH}_2\cdot + \cdot\overset{\text{O}}{\parallel}\text{---CH}_2\text{---}$  | Norrish Type I Photocleavage  |
|                   | $\text{---CH}_2\text{---CH}_2\text{---CH}_2\text{---}\overset{\text{O}}{\parallel}\text{---} \xrightarrow{h\nu} \text{CH}_3\text{---}\overset{\text{O}}{\parallel}\text{---} + \text{---CH=CH}_2$  | Norrish Type II Phorocleavage   |
|                   | $\text{---}\overset{\text{O}}{\parallel}\text{---C---CH}_2\text{---} \xrightarrow{h\nu} \text{---}\overset{\text{O}}{\parallel}\text{---}\overset{\cdot}{\text{C}}\text{---CH}_2\text{---} + \text{P}\cdot$                                    | Hydrogen abstraction  |
| Unsaturation      | $\text{---}(\text{CH}=\text{CH})_n\text{---}\overset{\text{Cl}}{\underset{ }{\text{C}}}\text{---} \xrightarrow{h\nu} \text{---}(\text{CH}=\text{CH})_n\text{---}\overset{\cdot}{\text{C}}\text{---} + \text{Cl}\cdot$                          | Allylic cleavage  |
| Metals            | $\text{M}^{n+}\text{X}^- \xrightarrow{h\nu} \text{M}^{(n-1)+} + \text{X}\cdot$   | Electron transfer   |
| Phenoxy           | $\text{---}\text{C}_6\text{H}_4\text{---O---CH}_2\text{---} \xrightarrow{h\nu} \text{---}\text{C}_6\text{H}_4\text{---O}\cdot + \cdot\text{CH}_2\text{---}$  | Cleavage  |
| Polyester         | $\text{---}\text{C}_6\text{H}_4\text{---}\overset{\text{O}}{\parallel}\text{---O---CH}_2\text{---} \xrightarrow{h\nu} \text{---}\text{C}_6\text{H}_4\text{---}\overset{\text{O}}{\parallel}\text{---O}\cdot + \cdot\text{CH}_2\text{---}$      |   |
| Polyamide         | $\text{---}\text{C}_6\text{H}_4\text{---}\overset{\text{O}}{\parallel}\text{---NH---CH}_2\text{---} \xrightarrow{h\nu} \text{---}\text{C}_6\text{H}_4\text{---}\overset{\text{O}}{\parallel}\text{---}\cdot + \cdot\text{NH---CH}_2\text{---}$ |   |
| Polyurethane      | $\text{---}\text{C}_6\text{H}_4\text{---NH---}\overset{\text{O}}{\parallel}\text{---O---CH}_2\text{---}$   | $\text{---}\text{C}_6\text{H}_4\text{---}\dot{\text{N}}\text{H} + \text{CO}_2 + \text{CH}_2\text{---}$                  |
|                   |  | $\text{---}\text{C}_6\text{H}_4\text{---NH}_2$<br>$\text{---}\overset{\text{O}}{\parallel}\text{---O---CH}_2\text{---}$ |

Figure 1-11 Chromophores and Photochemical Reactions[19]

Chain Initiation - Production of alkyl radical R $\cdot$ :



When polymers are in their solid state, the mobility of any radical formed is severely restricted thus leading to a relatively high recombination rate. This phenomenon is known as the Cage effect [20] and leads to a reduction in the efficiency in initiation.

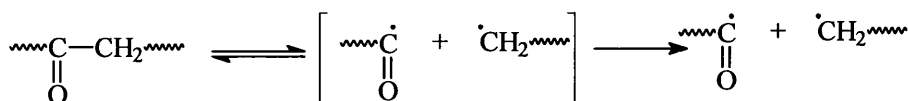


Figure 1-12 Cage recombination effect

## Propagation

The alkyl radical products are highly reactive and very quickly react with oxygen to form peroxy-radicals (Equation 1-4). These will in turn abstract hydrogen from the polymer backbone forming a hydroperoxide group (ROOH) (Equation 1-5).



The photodegradation can take on a further direction as via alkoxy or hydroxy hydrogen abstraction from the polymer. These processes are termed chain branching which is the main reason for the auto-accelerated kinetics often observed in the photo-oxidation of the polymers.

Ultimately, the hydroperoxide group is photolytically cleaved to produce highly reactive radicals continuing the cycle further. Photochemically hydroperoxides can decompose homolytically into alkoxy and hydroxyl radicals with a high quantum yield [23], giving rise to secondary reactions.



The polymer matrix will restrict diffusion and thus reduce the chain branching effect by favouring re-arrangement of alkoxy-hydroxy radical pairs formed by the ROOH photolysis [18]. This results in a cage reaction, which reduces the chain branching effect, but has the effect of producing ketone functions. These ketone functions are very effective chromophores, and thus potential photo- initiators [11, 18]

## Termination

Given that peroxy radicals have a high affinity for each other, the combination of them is the most likely source of termination. Combination of two ROO $\cdot$  radicals via a bio-molecular pathway creates an unstable tetra-oxide, which will rapidly lose its



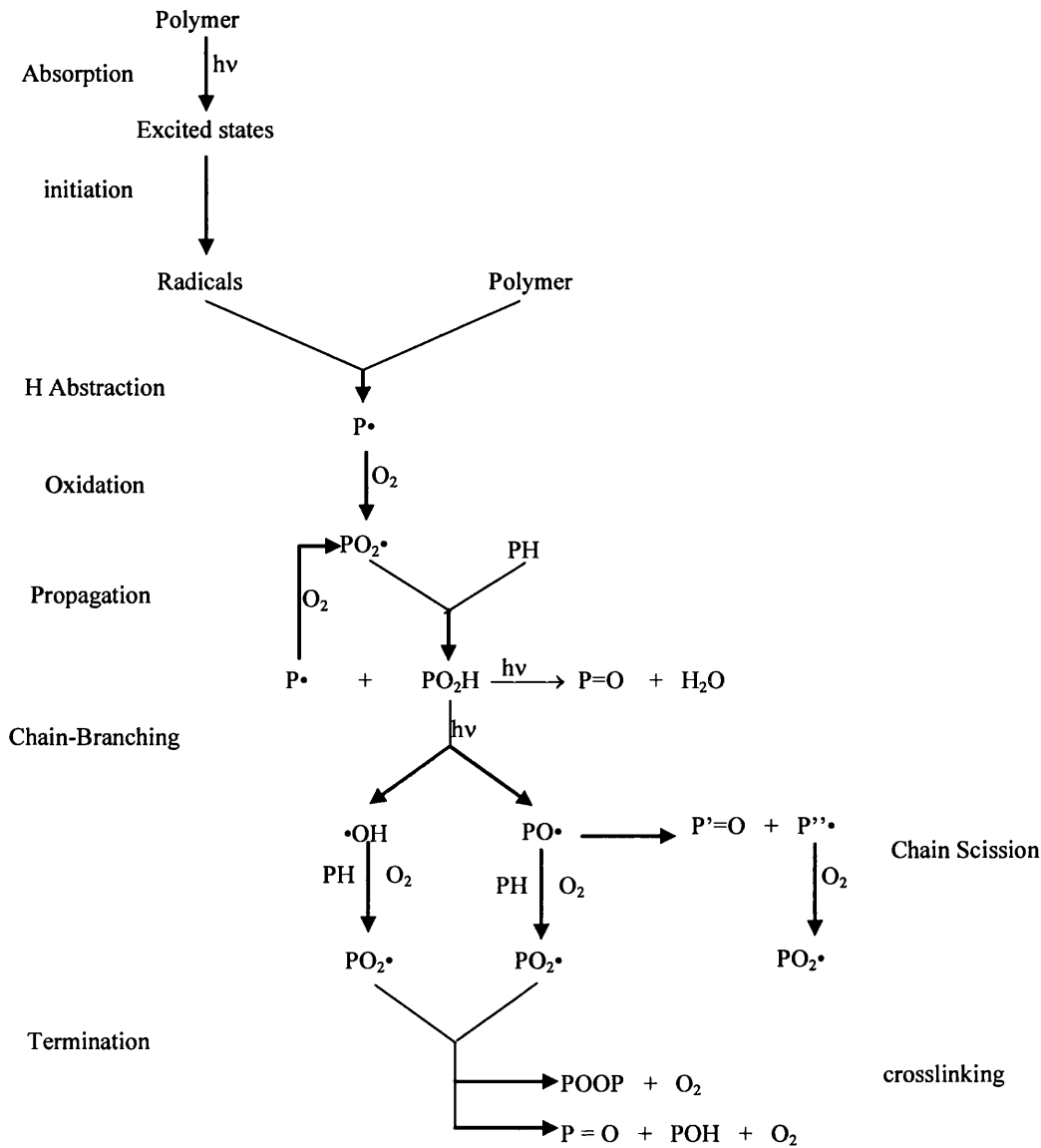


Figure 1-15 Flow diagram of Photo-Oxidation Reactions in Polymers [24]

### 1.3.3 Polyethylene and Poly (vinyl chloride)

Polyethylene (PE) is one of the most widely used and studied polymeric material, comprising as simple hydrogen and carbon structure. Essentially, the polyethylene molecule is a long chain of carbon atoms, with two hydrogen atoms attached to each carbon atom (Figure 1-16),

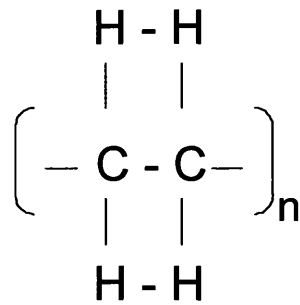


Figure 1-16 PE Structure

As discussed previously, photodegradation will only occur when the polyethylene contains chromophores that absorb the wavelengths present in the solar spectrum at the earth's surface. Therefore, in non-pigmented PE, the absorption by these chromophores (described in Table 1-4) of irradiation, is the enabler to photodegradation.

It is readily accepted in the literature, that similar to all other hydrocarbon polymers, polyethylene the 'typical' oxidation reaction scheme [11]; formation of free radicals, with subsequent formation of peroxy radical, cleavage of the oxygen bond and formation of carbonyl containing groups.

In addition to the oxidation kinetics, other aspects of the degradation have been discussed, including the depth of degradation in such polymers for example and whether it is merely limited to the polymer surface [25] and that the polymers resistant to photodegradation is also be governed by the morphology. [26, 27]

Poly (vinyl chloride) (PVC) is another commercial polymer that is present in a variety of products. As with PE, the structure of PVC (as in Figure 1-17) is not expected to absorb wavelengths above 220nm.

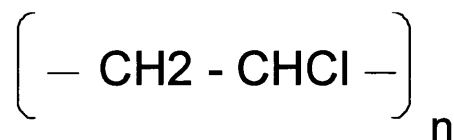


Figure 1-17 PVC Structure

With PVC photodegradation evident in many cases in the absence of any pigmentation, the PVC is clearly sensitive to UV irradiation. Referring back to 1.3.2, one such explanation could be reactive species present in the structure as a result of degradation caused during any processing.

## 1.4 Titanium Dioxide

A pigment is a particulate material used to colour and opacify a coating or film and on average, makes up 20% volume of a paint system [28]. Ideally it should be insoluble in the system, heat and light stable, non-toxic and chemically inert, whilst not imparting any unwanted characteristic (e.g. colour).

Pigments can be present in a variety of forms:

- i. Natural Earth compounds- Red Iron Oxide
- ii. Complex Organic Compounds – Blue/green Phthalocyanine
- iii. Titanium Dioxide- White
- iv. Carbon Black – Black

Titanium Dioxide ( $\text{TiO}_2$ ) is a white inorganic pigment dominating the inorganic pigment trade (~66%) [28]. It is used for its efficiency in scattering light (high reflective indices), imparting high opacity and whiteness.

It is almost always required on any coating to hide the substrate, referred to as its ‘hiding power’. This hiding power when incorporated into paint acts as to prevent any visible light passing through the coating. The hiding power of a coating can be quantified by its contrast ratio (CR):

$$\text{C.R.} = R_b/R_w \quad (\text{Equation 1-7})$$

Where  $R_w$  and  $R_b$  are the reflectances obtained over standard white and black backgrounds respectively. The hiding power is defined as the spreading rate of paint to give a contrast ratio of 0.98 [29].



Carbon black can produce a similar hiding ability, although this is achieved via the absorption of light energy.

Similarly, these scattering characteristics of  $\text{TiO}_2$  make it possible (given the correct level of addition) to offer some stability to weathering.

The extensive use of  $\text{TiO}_2$  is not merely limited to paints and coatings. Because of the availability of  $\text{TiO}_2$ , and properties it can also be incorporated into many other systems. For example in the production of some fast foods, such as chicken nuggets, the  $\text{TiO}_2$  imparts the white appearance, but is also considered safe because it is chemically inert. Other applications include sunscreen [30], toothpastes [31], tattoos [32] and lambda sensors [33].

#### 1.4.1 Structure of $\text{TiO}_2$

Titanium is abundant in many minerals, four of which such ores are:

- i. Rutile ( $\text{TiO}_2$ )
- ii. Anatase ( $\text{TiO}_2$ )
- iii. Ilmenite ( $\text{FeTiO}_3$ )
- iv. Brookite ( $\text{TiO}_2$ )
- v. Leucoxene ( $\text{TiO}_2 \cdot x\text{FeO} \cdot y\text{H}_2\text{O}$ )

Of these, Rutile, Anatase, and Brookite  $\text{TiO}_2$  are crystalline forms and Anatase and Rutile dominate the market. Given the greater refractive index of Rutile (2.73), the use of Anatase (2.55) is usually limited to paper and synthetics industries, whilst the greater light scattering ability of rutile lends itself to the plastics industry more. In general, the greater the difference between the pigments refractive index and that of the polymer matrix, the greater the degree of light scattering.

Commercial grades of  $\text{TiO}_2$  are rarely pure, and the degree of purity chosen depends on the service environment. Anatase is more photoreactive, hence when a lot of stability is required; its concentration is kept to a minimum.

Other than photoactivity and refractive indices, the Anatase and Rutile also differ in lattice structure and density, all of which impart on their performances within a coating system.

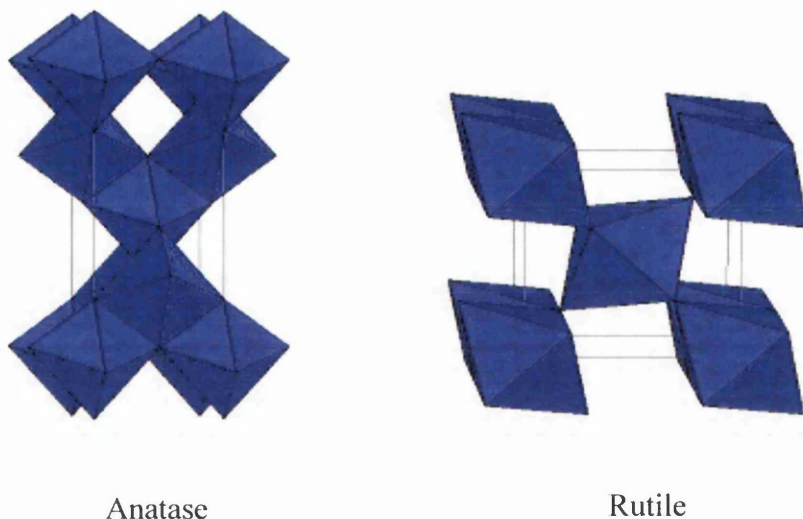


Figure 1-18 Crystal Structures of Anatase and Rutile [21]

Both structures are tetragonal (Figure 1-18), with the titanium atoms surrounded by six oxygen atoms of which each are surrounded by three titanium atoms. In both cases the bridging oxygen atoms are displaced towards one another, decreasing O-O distances, however this is greater for Rutile, explaining the differences in density and molar volume.

#### 1.4.2 Manufacture of TiO<sub>2</sub> [28]

TiO<sub>2</sub> pigments are produced from the ores by two processes, the sulphate and chloride process.

##### **The Sulphate Process**

Firstly the titanium rich ore (FeTiO<sub>3</sub>) is dissolved in hot concentrated sulphuric acid. It is considered beneficial to firstly grind the ore ensuring efficient sulphation. Scrap steel is then added to keep iron and other impurities in their more soluble oxidation states. Low iron content ores such as Rutile or Anatase are advantageous in terms of

waste disposal, but they dissolve too slowly in the acid. This results in a titanyl sulphate solution which can be thermally hydrolysed to precipitate out titanium oxyhydroxide, calcination of this will then yield Anatase. Alternatively the introduction of a Rutile seed crystal can be used during the hydrolysis stage to produce  $\text{TiO}_2$  in the Rutile phase.

To regulate the size of the  $\text{TiO}_2$  crystals phosphorous can be added. Phosphorous cannot penetrate the crystal lattice and thus remains on the surface of the crystal. So as the crystal grows the surface area of the crystal will decrease. The growth of the crystals will reach a critical point where by the phosphorous will inhibit further growth, ensuring homogeneous crystal sizes optimised for light scattering.

### **Chloride Process**

The chloride process was developed by DuPont in the early 1950's, and was an improvement on the sulphate process with less waste disposal, the higher quality and less energy input is required, is the common production method in the U.K.

The ore is mixed with a source of carbon and added into the chlorinator and fluidised at 900-1700°C. The reaction yields titanium tetrachloride ( $\text{TiCl}_4$ ). Hydrolysis of the  $\text{TiCl}_4$  follows, to form  $\text{TiO}_2$  particles. To gain the desired particle size the  $\text{TiCl}_4$  is vaporised and then flamed using a specifically designed reactor, which is optimised to prevent plugging and yield the desired crystal size. The flame reactor can also be used to introduce co-oxidants such as  $\text{AlCl}_3$ , which help to promote the formation of Rutile and minimise aggregation. Once cooled, the pigment particles are collected by passing a gas stream through the separator. The exothermic reaction also liberates chlorine which is recycled to the chlorination stage and any chlorine that remains within the solid  $\text{TiO}_2$  can then be removed using aqueous hydrolysis.

A schematic comparison of the two processes is shown in Figure 1-19

### **Surface Treatments**

Almost all commercially available  $\text{TiO}_2$  pigments have a surface treatment or coating for a number of reasons, including to reduce photoactivity, or to improve dispersion

in a system. All of which can affect the entire coating system in terms of durability. Commonly used are a variety of oxides and or oxy-hydrates.

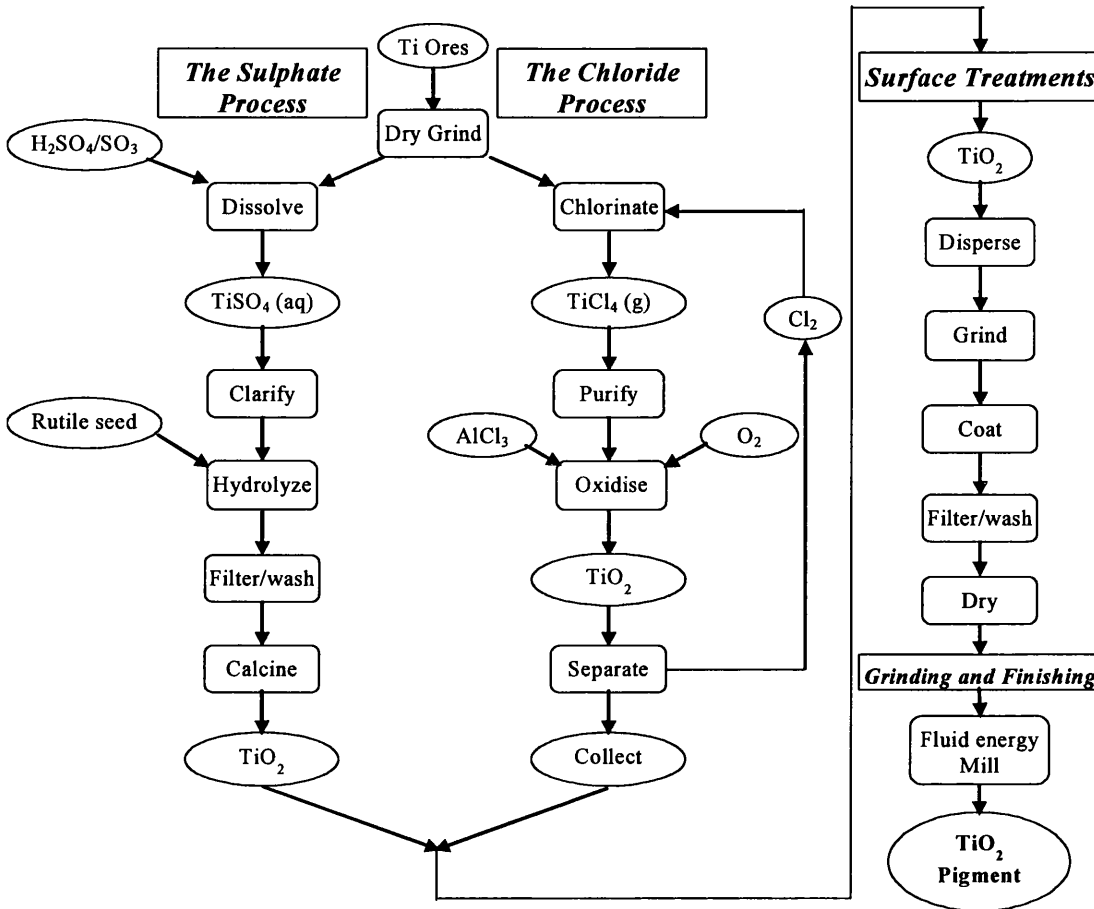


Figure 1-19 The Sulphate and Chloride Process

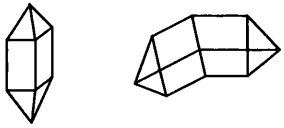
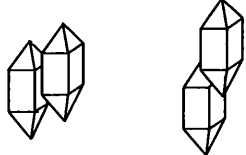
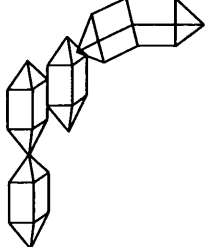
Depending on the service life of the polymer, the surface treatment can be one, or a combination of alumina, silica and zirconia. However it is known that there are potential problems regarding whether the coating (particularly silica) is deposited in amorphous or crystalline form. If the coating forms in a microcrystalline nature, this will allow penetration of oxygen and water vapour to the TiO<sub>2</sub> surface [34].

**Grinding and Finishing**

The bond strength and density of a single crystal of TiO<sub>2</sub> are so high that the crystals cannot be broken down by grinding. The crystals are grown to the correct size from

the beginning of the process, ensuring optimum light scattering properties. Despite this, during processing, the crystals can still form aggregates and agglomerates (Table 1-5), both of which need to be broken down to achieve a uniform particle size. The device used to break these agglomerates down is called a fluid energy mill (Figure 1-20).

Table 1-5 Typical Types of Particle Coagulation

|  |   |
|--|---|
|   | <p><b>Primary Particles:</b> These are single TiO<sub>2</sub> crystal or their crystallographic twins. (twins are two or more lattices intergrown to some deducible law of symmetry) They range in diameter from 0.1 to 0.3 μm.</p>   |
|   | <p><b>Aggregates:</b> These are primary particles that are connected via grain boundaries, they share crystal faces.</p>  |
|  | <p><b>Agglomerates:</b> These are assemblies of crystallites and aggregates that are bonded together via weak forces; they adhere together at edges and faces.</p>  |
| <p>Not Pictured</p>  | <p><b>Flocs:</b> these are associations of smaller particle assemblies that are bonded extremely weakly. They form spontaneously and disperse under modest shear. They are composed of crystallites, aggregates and agglomerates joined across corners or held together by short range attractive forces.</p> |

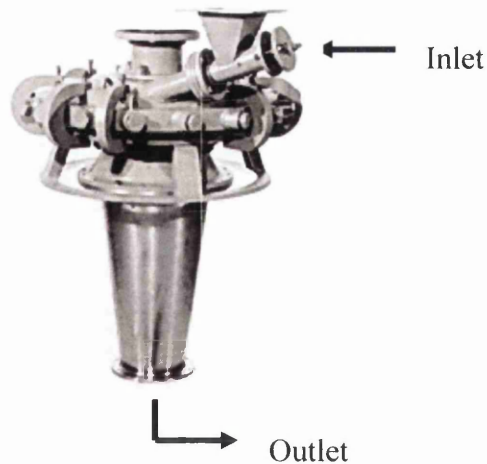


Figure 1-20 Typical Fluid Energy Mill

A fluid energy mill uses a fluid (usually in the form of steam) to accelerate the pigments to supersonic speeds. They are then injected into the cylinder causing the particles to collide and separate. Fragments lose speed and are then hit by other particles, which leads to further breakdown.

The exhaust from the fluid mill is channelled to a cyclone separator where the pigment is recovered. Although the fluid energy mills are very good at grinding small particles, they grind large particles very inefficiently thus where agglomerates are produced, they are pre-milled using a ball mill. This uses a drum half filled with ball bearings which fall under gravity to grind the particles. So once the large agglomerates have been broken down the particles are transferred to a fluid energy mill, and then once the desired size (approximately  $0.1\mu\text{m}$  to  $0.5\mu\text{m}$ ) has been reached the hot pigment is transferred to bags or transport containers and allowed to cool, although due to its excellent thermal insulating properties this can take some time.

### 1.4.3 Photoactivity of $\text{TiO}_2$

#### 1.4.3.1 Band Theory [35]

A band is a group of valence orbitals that are close in energy. Bands can be full, empty or partially occupied. The presence of a partially occupied band characterises a metal, hence because the energy states that make up the band are so close the

electrons can move between the energy states in the same band offering electrical conductivity.

In comparison, if there are no partially occupied bands, it is the band gap that dictates the electron movement. In the presence of a large energy gap, the material is an insulator, as shown in Figure 1-21. If the energy gap is significantly smaller, electron movement is permitted, and their movement from the filled 'valence' band to the unoccupied 'conduction' band. In the latter case, the material is a semiconductor.

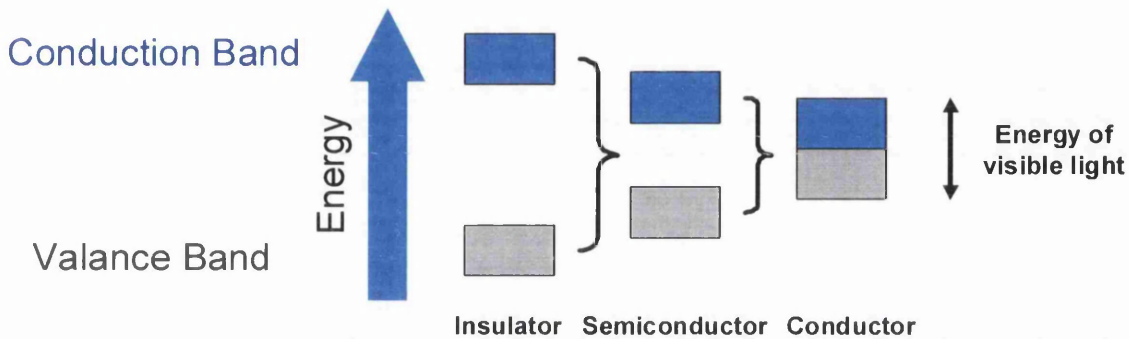


Figure 1-21 Valence and Conduction Bands, a) Partially -filled band, b) Large band gap, c) Smaller band gap

In either case, the excitation of electrons occurs as a result of light or heat. At low temperature and low levels of lighting semiconductors therefore act as insulators. The large band gap denotes the insulating material because the energy of visible light alone is too low to excite an electron from the conduction band. Similarly, the low electrical conduction capabilities is enhanced by the limited 'room' for the electrons to move around given the full valence band. Efficient conductors should ideally be dark in colour considering the absorption of light and heat promotes the electrons from the partially filled bands.

In the case of Rutile and Anatase  $\text{TiO}_2$  band gaps, they are 3.05eV and 3.29eV respectively. The white appearance is a result of the band gap being higher in energy than that of visible light with the energy gap in fact corresponding more closely to that of UV light. Therefore the radiation of UV light on a  $\text{TiO}_2$  crystal provides

sufficient energy to promote the electron from the valence band to the conduction band, thus leaving a vacancy (hole) of a positive charge, and a negatively charged mobile electron.

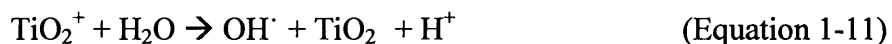
Due to the reactive nature of the species, in the absence of an electric field, the majority of the electron and vacancy pairs recombine, transforming 95% of the light energy as heat. However, some holes manage to diffuse apart and find their way to the surface.

#### 1.4.3.2 The Photocatalysis of TiO<sub>2</sub> [36]

The band gap of TiO<sub>2</sub> radiation corresponds with wavelength of UV light (360-380 nm) and thus an interaction will occur. There are however now two competing factors within the coating system; firstly the absorption of UV light prevents direct photochemical attack. Secondly, the absorption promotes free radicals by the following reactions, which can oxidise the polymer.



In the event that recombination does not occur, then the excited electron has the ability to combine with an oxygen atom and reduce it, thus forming a highly reactive oxygen radical. If this occurs, then the hole left by the electron is free to oxidise any adsorbed water or hydroxyl groups present.



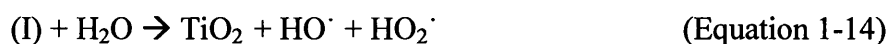
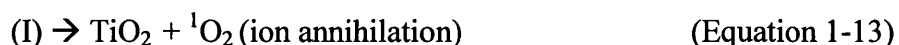
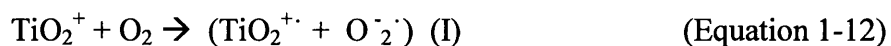
#### 1.4.3.3 Photodegradation in Polymers containing TiO<sub>2</sub>

As previously described, the photodegradation of a pigmented polymer is a result of two processes. Firstly, there is the homogeneous photochemical oxidation of the polymer, and secondly the photocatalytic oxidation induced by the titanium dioxide.



It has been suggested [37] that there are three mechanisms of photodegradation in TiO<sub>2</sub> pigment containing polymers. Similarly, this can also occur with other white pigments.

1. The electron transfer from photoexcited TiO<sub>2</sub> produces an oxygen radical anion. Ion annihilation forming a singlet oxygen can be considered which then attacks the polymer, modifying the reaction scheme as follows:



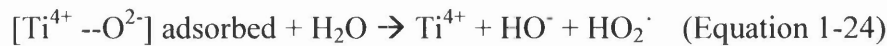
The presence of carbonyl groups in polyolefins could be attributed to this mechanism, via the attack on ethylenic double bonds by the singlet oxygen.

2. Electron transfer between water and photoexcited titanium dioxide has been suggested as a source of reactive hydroxyl radicals. The Ti<sup>3+</sup> ions are re-oxidised back to Ti<sup>4+</sup> to re start the cycle.



3. The production of hydroxyl radicals; vacancies react with surface hydroxyl groups to form hydroxyl radicals. Oxygen anions produced are absorbed onto the pigment particle surface, producing perhydroxyl radicals.





The  $\text{--OH}^\cdot$  and  $\text{HO}_2^\cdot$  radicals then cause oxidative degradation of the polymer substrate.

## 1.5 The Effect of Photodegradation on Coating Durability

The weathering of a pigmented polymer is going to be a combination of the homogeneous and heterogeneous mechanisms described. Photooxidation will impair mechanical properties of a polymer, whilst other effects specific to the inclusion of  $\text{TiO}_2$  will occur.

### 1.5.1 Gloss Loss and Chalking

Gloss is a measure of the amount of light reflected off a surface. The greater the reflection, the higher the gloss levels. As the film is photo-oxidised, it becomes pitted and gloss levels are reduced. After prolonged or especially intense exposure to UV irradiation, insoluble pigment particles can be seen as a chalky deposit on the coating surface. This phenomenon is depicted in Figure 1-22.

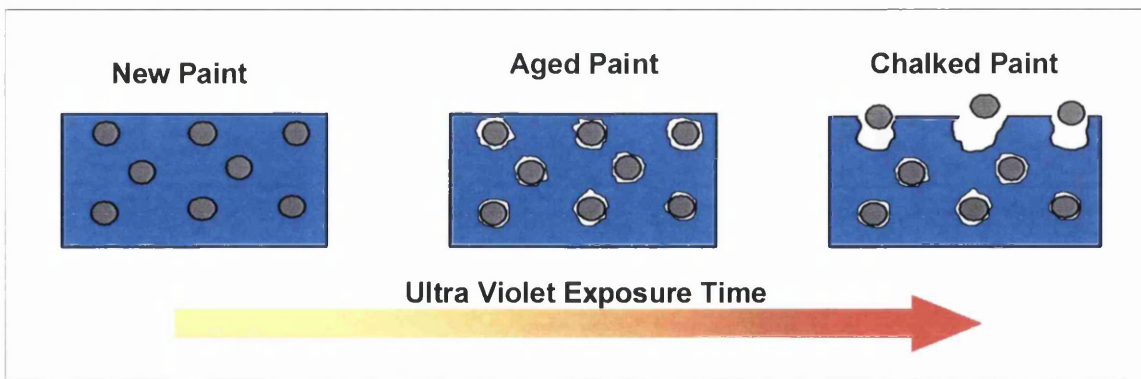


Figure 1-22 Chalking and its Effects

### 1.5.2 Colour Change

Colour fade and colour darkening are both representative of change induced by a chemical reaction. Not only is the deterioration in aesthetics undesirable, but this physical and chemical change is often an indication of irreversible gross failure of the coating.

An example of this, is the PVC ‘yellowing’ associated with white PVC products exposed to prolonged exposure to outdoor environments, such as PVC window frames. Weathering is the result of both thermal degradation during processing and photochemical degradation during exposure to solar radiation. Heat degradation that occurs during processing generates double bonds in the PVC and subsequently, molecules then absorb wavelengths from the solar spectrum during their in service life. Subsequently, dehydrochlorination of PVC leads to formation of conjugated double bonds [38]. When sufficient numbers form, the double bonds absorb the visible light which produces yellowing.

### 1.5.3 Delamination

The barrier properties of the coating are imperative for guaranteed protection of the substrate. UV degradation induces a breakdown in the structure of a coating, creating pinholes exposing the substrate. Although delamination can still occur with no pitting, corrosion of the substrate, cut edge corrosion and continuous UV degradation of the coating can lead to delamination.

### 1.5.4 Crazeing and Cracking

Weathering of a polymer results in chain scission of the longer, flexible polymer chains, changing to form shorter more brittle ones. This results in areas of stress on the coating will become less flexible and possibly crack and flake off.

### 1.5.5 Weight Loss and Film Thickness Change

As the polymer weathers there is a gradual loss of organic material and additives. This therefore actually enables the monitoring of degradation via measuring the film thickness or by the actual weight loss

In addition to the physical failure mechanism, Figure 1-23 outlines the micro-scale changes that can occur in polyolefins, some of which contribute to the macro-scale changes outlined above.

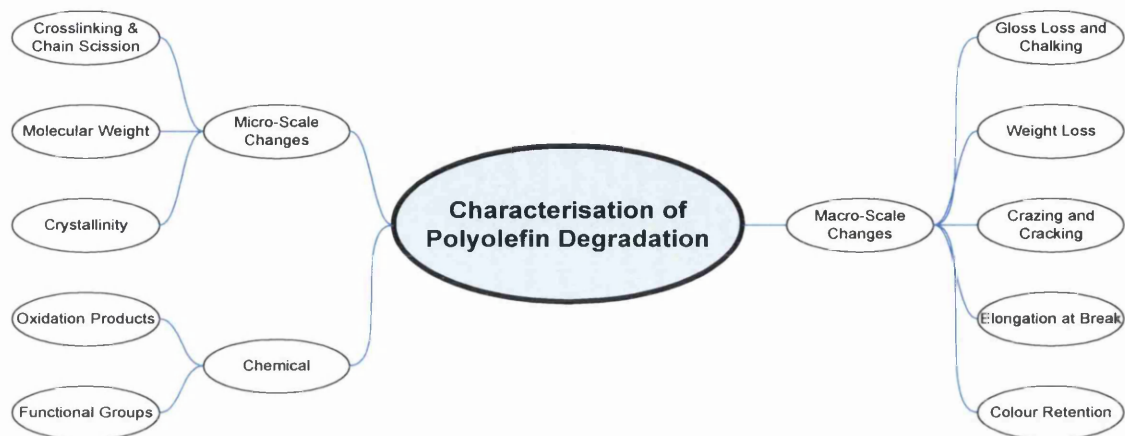


Figure 1-23 Influences and Effects of Photodegradation

## 1.6 Stabilisation against Photodegradation

Exposure to the natural environment has a significant effect on the useful lifetime of a polymer product. To counteract the damaging effects, a variety of stabilisers can be used. This protection can be achieved in 2 ways, physically or chemically.

### 1.6.1 Additives

There are a variety of mechanisms by which the photochemical reactions can be interrupted:

- i. Absorbing UV (UVAs)
- ii. UV Screening
- iii. Excited stated quenching
- iv. Free radical scavenging

There are a variety of stabilisers which achieve one or more of these mechanisms, and are in fact multifunctional in operation.

Additives designed to screen the polymer from photochemical reaction, do so by reflecting UV. It is imperative there is no internal scattering, and high enough concentrations in the surface area to provide sufficient screening. The screeners are added as pigments with high reflectance, but also often in a separate coating layer on the surface of the polymer. TiO<sub>2</sub> and other pigments with high reflective indices are popular, as other coloured pigments are generally poor UV reflectors. Excited state quenchers de-activate excited chromophores before they undergo chemical reactions.

#### 1.6.1.1 UVAs

UVAs slow the degradation process by preferentially absorbing UV radiation, and then dissipating the energy in a more harmless form, quite often heat. This is achieved via the non-radiative process as outlined previously. Such stabilisers function according to the Beer-Lambert Law, i.e. the amount of UV absorbed is a function of sample thickness and stabiliser concentration.

$$A = \epsilon cl \quad \text{(Equation 1-25)}$$

|            |   |                             |
|------------|---|-----------------------------|
| A          | = | Absorbance                  |
| $\epsilon$ | = | Molar absorbtivity constant |
| c          | = | Concentration               |
| l          | = | Pathlength                  |

High enough concentrations of stabilisers are needed and sufficient polymer thickness before enough absorption can take place to completely retard photodegradation. Given this, when choosing a UVA there are a number of consideration that need to be taken into account: [39]

- i. It must absorb harmful radiation, whilst dissipating it harmlessly
- ii. Should not impart colour (unless required)
- iii. Should be compatible over a range of concentrations (a careful degree of mobility of the stabiliser is favoured offering movement to photo-active regions-usually amorphous)
- iv. Good UV stability itself

- v. Withstand any processing conditions
- vi. Non-toxic and non-extractable under regular service conditions

The two main types of UVA are the hydroxy-benzophenones and hydroxy-phenyl-benzotriazoles. Hydroxy-benzophenones absorb UV light and convert it into harmless heat energy. They do this by forming reversible six-member hydrogen ring [40, 41]. This reversible reaction of UV absorption and heat dissipation leaves the absorber unchanged and thus it can undergo many cycles of UV absorbance so long as no other process interferes with the reaction (Figure 1-24). Benzotriazoles work in a slightly different way, in so much as they dissipate energy by a proton transfer reaction (heat) (Figure 1-25).

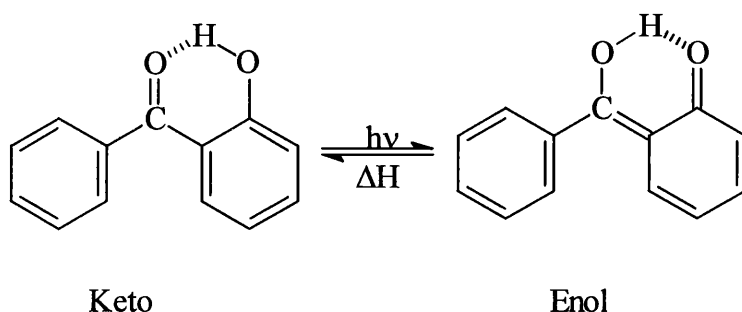


Figure 1-24 Keto/enol Tautomerism Energy Dissipation Mechanism in Hydroxyl-benzophenone

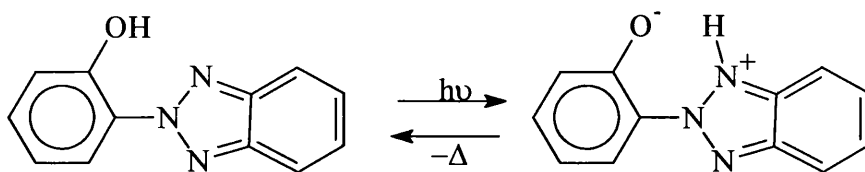


Figure 1-25 Benzotriazole Stabilisation Mechanism in Hydroxy-phenyl-benzotriazole

Carbon black is one of the most widely used pigments in the polymer industry and is recognised as being a popular stabiliser. It is a polycrystalline material and the chemical nature of its surface dictates the polymer matrix properties. Degradation in PP protected by Carbon black is more rapid at first but then proceeds more slowly[42].

Its stabilising mechanism reaches far further than the well known UVA property expected [43, 44]. It has been described that its stabilising characteristics even extend to quenching of excited states; donor/acceptor of free radicals in chain breaking reactions and hydroperoxide decomposition. However, the distinctive feature of any carbon black stabilised polymer, is its black colour, imparted by the carbon. This ultimately limits its use in a variety of applications, although it can still be very much utilised in products where black is considered a suitable colour. Similarly concerns arise with relation to the degree of heat that is actually dissipated within the (already black heat absorbing) polymer. Such an example is car bumpers.

However, complexities arise when the inclusion of a stabiliser may react with another necessary additive, such as a pigment. Unfortunately injection moulded poly(propylene-co-ethylene) car bumpers as investigated by Maia et al [45], also contain TiO<sub>2</sub>, as is the case for a variety of polymers products. It was suggested that the stabilising effects of the carbon black were in fact displaced by the photo-catalytic characteristic TiO<sub>2</sub> ageing the bumper imparting a white appearance. Efforts were made to re-stabilise the bumper via the addition of conducting carbon black. Although only a preliminary study, results showed a visually more stable car bumper was achievable, suggesting that the conducting carbon black deactivates the excited electron in the TiO<sub>2</sub> conduction band.

### **UVA distribution and Loss**

Given that a number of polymer products and coatings have a guaranteed outdoor life, then one would ideally like the product to regain its resistance to photodegradation. This can be achieved via the longevity of the stabilisers. Degradation at the coating/substrate interface can lead to delamination, which could be avoided if enough UVA remains present in the top coat.

UVAs have an effect on the degradation profile. Given that the UVA can ultimately be destroyed by a photochemical process, its loss rate will be dependent on the light absorbed by the irradiated coating. The top layer receives maximum light; consequently the stabiliser is likely to disappear more rapidly in this region.

In order to determine how the UVA was distributed within a film after exposure the effect of film thickness on UVA loss profile has been considered [16], showing that as the film thickness was increased, the UVA lifetime was found to drop.

Four processes were considered responsible for the loss of the UVA during photo-aging:

- i. Direct Photolysis of the UVA
- ii. Radical Induced Degradation
- iii. Migration of UVA towards surface
- iv. Erosion of coating

By setting up experimental conditions, that systematically eliminated the mechanisms, Decker et al attempted to quantify the degree to which the processes contribute to UVA loss. Results showed that 40% of loss was the result of exudation and 20% and 33% the result of direct photolysis and radical induced loss, respectively.

#### 1.6.1.2 Antioxidants [39]

Given that the weathering of coatings in an outdoor environment involves an oxidation route, antioxidants are often added to interfere with the chain process. Antioxidants are more frequently used in the prevention of thermal oxidation, although UV stable antioxidants can inhibit photochemical degradation by acting as radical acceptors suppressing reactions or by decomposing peroxides. The breakdown of a hydroperoxide causing chain scission can be inhibited by a stabiliser which will preferentially react with decomposition products (such as peroxide) without the formation of further reactive groups.

Phenolic antioxidants (AH), often used in polyolefins [46] have a labile hydrogen atom react in a similar manner to the hydrogen molecule, however in this case the radical formed (A $\cdot$ ) is not generally reactive.





The efficiency of antioxidants is determined by three processes, chemical reactivity, physical loss (evaporation and leaching) and physical loss of the stabiliser [47]. The loss of the stabiliser by physical processes is more significant than loss by chemical consumption. Highly mobile stabilisers are very reactive to degradation in polymers and can be rapidly present in degrading regions. On the other hand they can be so mobile they can leave the polymer without being activated. Ideally an optimum mobility and solubility needs to be addressed.

#### 1.6.1.3 Hindered Amine Light Stabilisers (HALS)

HALS are a more recent development in the world of stabilisation, and their introduction in the seventies had a significant effect on the amount of polyolefins used for outdoor applications.

HALS protect not by absorbing UV radiation, but by inhibiting the degradation mechanism. Therefore their efficiency is not dependent upon them being at a high concentration on the surface of a coating. They are effective and efficient, with high levels of stabilisation being achieved via smaller concentrations of the additive. They are not in fact consumed, but regenerated during a cyclic process (Figure 1-26), further improving their longevity. HALS in PP are highly effective for a long time but protection disappears quickly without warning [42].

Their exact influence is not entirely understood, but believed to be achieved via some of the following:

- i. Chain breaking donor/acceptor redox mechanism through the formation of nitroxyl radicals that terminate and deactivate alkyl and peroxy radicals.
- ii. Decomposition of hydroperoxides by the amine during processing.
- iii. Inhibition of the photoreaction of  $\alpha,\beta$ -unsaturated carbonyl groups in polyolefins.
- iv. Reduction in the quantum yield of hydroperoxide photolysis.
- v. Singlet oxygen quenching – only polydienes.
- vi. Complexion with hydroperoxides/oxygen.
- vii. Complexation with metal ions.
- viii. Excited state quenching via the nitroxyl radical.

With regard to products such as polypropylene fibres, due to the high surface to volume ratio, stabilisers with a low volatility and high extraction resistance are needed. A high molecular weight stabiliser such as the HALS, is ideal. Although there has been some concern regarding the influence of HALS on pigment dispersion and pigment agglomeration, a high molecular weight stabiliser with a narrow weight distribution is believed to overcome this problem [48].

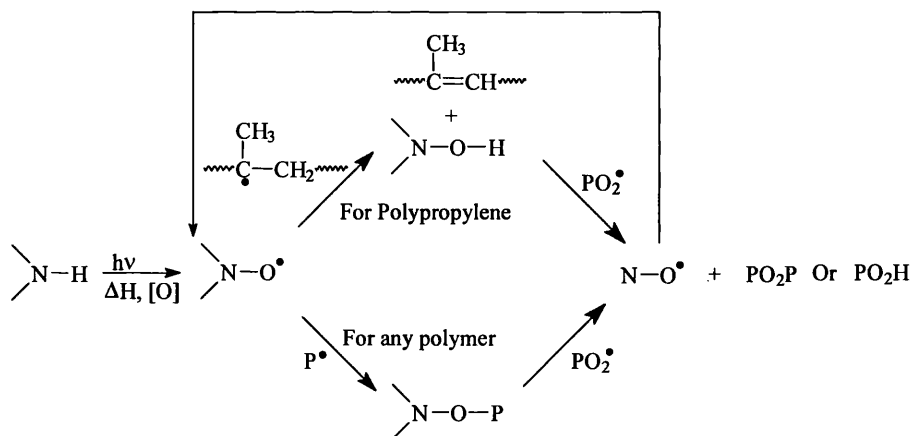


Figure 1-26 Cyclic Mechanism of HALS Stabilisation [20]

#### 1.6.1.4 Synergisms

A lot of literature has concentrated on the synergism of stabilisers, especially more recently HALS. The way in which additives work together is detrimental to the final stability of the polymer. HALS and UVAs have been shown to show a positive interaction [49]. Whilst the main role of HALS is to react with the free radicals formed and to therefore reduce the importance of oxidation in the polymer, they have been shown to actually slow down the disappearance of UVAs lost by exudation and radical induced processes.

#### 1.6.1.5 Novel Inhibitors

Hydrotalcite (HT),  $MgAl_2(OH)_6CO_3 \cdot 4H_2O$ , has been shown to have an effect on the degradation of PVC coatings [50]. The Mg/Al hydroxycarbonate is a commercially available white, low cost anionic mineral.

The ability of HT to behave as ion exchanger and the use of HT in plastisol coatings as a way of limiting the evolution of HCl was discussed[50]. The Cl ion exchanges with the carbonate to produce a weak carbonic acid which is unable to catalyse photodegradation. Part of this thesis extends on this study, investigating levels of addition and the influence of atmospheric conditions of TiO<sub>2</sub> pigmented PVC. The effectiveness of such inhibitor has also been investigated in other fields. [7]

### 1.6.2 Barrier Layers

UV irradiation, oxygen and water have all been shown to play a role in the photodegradation of polymers. To improve the durability of any coating system, each of those influencing factors can be reduced to control:

- i. UV penetration of the organic mater
- ii. Oxygen permeation
- iii. Water permeation

The stabilisers discussed previously primarily chemically control the actual or potential UV-polymer interaction, by absorbing, screening or interrupting the UV induced reactions. In addition to this technique, barrier layers also offer a physical barrier to oxygen and water permeation.

Clear coat lacquers are one such example, whereby the appearance of the base coating is still apparent whilst providing additional protection to degradation. One such example is the stabilization of polymers by acrylic top coats [51]. After QUVA weathering, the durability of PVC was noticeably higher with only a 50µm acrylic layer. In addition to this, the durability was further improved with the addition of UVAs and HALS into the acrylic. A clear coat such as this also provides additional properties; improved resistance to solvents, chemicals, abrasion and scratches.

Although more commonly considered an application for technologies such as that found in the semi-conductor or aerospace industries, this technique is finding wider uses that are associated with industries such as steel production [52, 53]. The ability

to coat using elements that are not possible via electroplating or dipping with improved efficiency, has led to a growth in this area of research.

More recently, the deposition of ceramic materials using physical vapour deposition (PVD) onto polymer substrates is a well known practise. The design and production of solarcells has seen a requirement for a thinly deposited layer that can prevent oxygen and water permeation. Due to the nature of the device, such encapsulation is necessary to maintain cell efficiency that, in the event of degradation, could reduce of components such as additives or electrolyte. A need for high optical transmission and careful control of UV transmission or reflectance has been highlighted [54-56].

## 1.7 Weathering and Accelerated Exposure

With product design and development, there needs to be the means of evaluating performance and benchmarking a product against others, giving an indication and even a definitive answer of which performs the best. The most accurate means of doing so would clearly be by exposing the polymer product to the expected service environment. However, given that such products are designed with durability in mind, this would take an unacceptable length of time.

It is necessary not only to give us information about the lifetime of a coating for aesthetic purposes, but also the ability for the polymer coating to act as a barrier for the substrate to weathering. With regard to a coating for outdoor application, major environmental influences are sunlight (UV exposure), water, oxygen, temperature, humidity and pollutants in the atmosphere.

Accelerated testing of a system uses equipment to artificially age a coating, often by exposing it to more aggressive conditions than those expected in service. It must however be taken into consideration that whilst this produces more rapid test results, that the conditions are not too severe as to interfere with the natural process being promoted.

Therefore a combination of both natural weathering and accelerated testing techniques is essential, including establishing a good correlation

### 1.7.1 Natural Exposure

Natural exposures are conducted under natural environmental conditions rather than inside a laboratory under artificial conditions. Commercial testing locations are available worldwide, each with varying environments that may or may not mimic the service environment expected.

Weathering conditions such as length of time of exposure, rainfall, temperatures, humidity and other possible pollutants must all be monitored and recorded. Some examples of outdoor weathering sites include:

- **Florida:** Sub tropical climate, high UV exposure, temperature and humidity. Provides a reproducible acceleration of European climates. Most popular site for outdoor natural weathering
- **Hook of Holland:** Marine location and area of industrial activity
- **Arizona:** High temperature (26°) low annual rainfall of only 200mm

The most accurate of all the exposure methods is obviously going to be a 'Full System Exposure'. This is designed to typically employ all or most of the end use system conditions. This type of method is especially popular with regard to automobiles, in particular, automotive interiors. Such material exposures in full systems provide engineers with information for benchmarking actual temperature performance, as well as offering the ability to characterise and compare full system exposure characteristics to those of other test methods.

However this is costly and space consuming and is more often usually used to benchmark other testing techniques. Sometimes it is merely a small component needing to be tested under a set of simple exposure conditions, giving rise to the use of a sample rack exposure technique. Simple alterations in location, backing and angle can significantly accelerate degradation effects. Any successful test programs must therefore insure that the same mechanisms occurring in end use conditions

occur at increased levels of critical weathering variables, and their relative interactions.

### 1.7.2 Artificial Exposure

There is always a need for a more rapid evaluation of a systems reaction to weathering, than can be achieved via the outdoor exposure methods described. Devices with artificial light sources can be used to accelerate the degradation. These methods are fully controlled and reproducible. However, great care must be taken to carefully monitor the particular photo-chemical mechanism. These could include Xenon arc lamps are a source of artificial light. Powered by electricity, they use ionized xenon gas to produce a bright white light that closely mimics natural daylight (Figure 1-27). Given the close simulation of natural light and degree of control over the source, this is a useful technique. Similarly, the ultraviolet source can be by way of either UV-A or UV-B lamps. UV-A lamps allow enhanced correlation with actual outdoor weathering whereas UV-B lamps emit UV below the normal sunlight cut-off and for most applications, therefore produce the fastest route degradation. This short wavelength UV can produce rapid degradation by mechanisms that do not occur when materials are exposed to sunlight. QUVB is therefore quick but not necessarily reliable.

Accelerated weathering is carried out in a QUV Weathering tester, which simulates the deterioration of coated materials caused by water and the ultraviolet energy. The method is intended to simulate the damaging effects of weathering, to permit prediction of the relative durability of materials exposed to an outside environment.

The effects of sunlight are simulated by means of fluorescent UV lamps and moisture is produced by means of a condensation system. Specimens are alternatively exposed to UV light alone, to condensation alone in a repetitive cycle. Exposure conditions may be varied by selection of; the fluorescent UV lamp, the timing of the UV and condensation exposure, the temperature of the UV exposure and the condensation

### 1.7.2.1 Accuracy of Accelerated Weathering

There is an extensive amount of research comparing the speculated accuracy of artificial exposure as a means of predicting outdoor weathering.

The results obtained from artificially accelerated tests should correlate with results of naturally weathering results of the same polymer. This is only theoretically true, because the reproducibility of the same samples exposed at different times is poor.

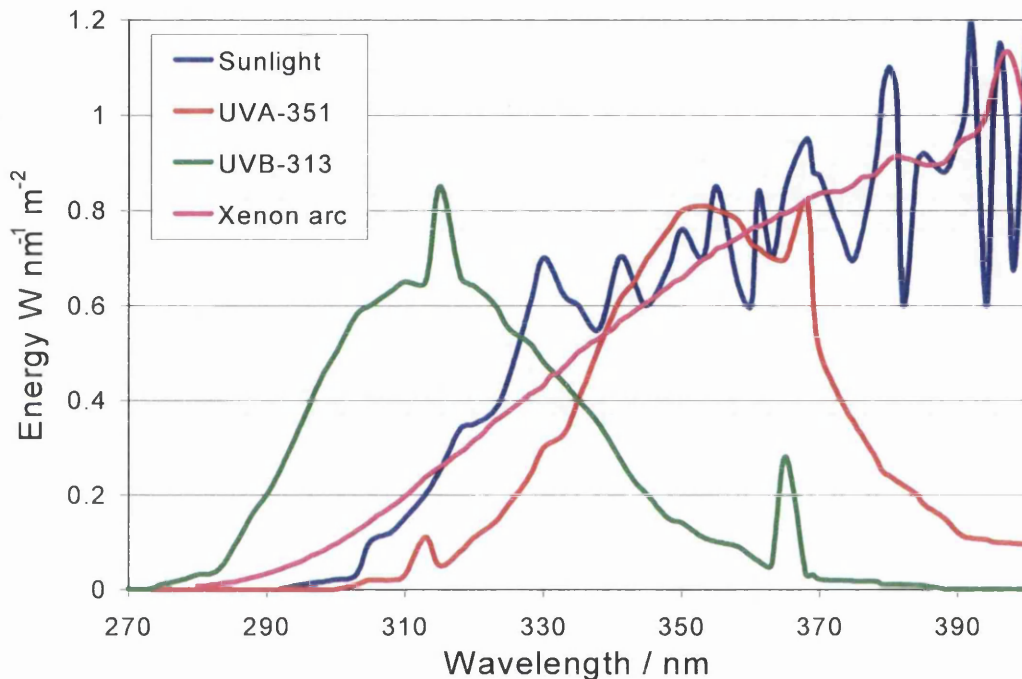


Figure 1-27 Spectrum of Different Light Sources

One of the major reasons for this may be the small consideration given to geographic climatologically data adopted in the accelerated test, and any such variations in natural weather with time.

Tests carried out in Geleen, Netherlands [49] highlight the severity of the accelerated testing and such possible explanations. Accelerated degradation was faster than outdoor degradation and led to a more rapid drop in elongation at break, higher oxygen uptake and faster changes in IR spectra. Environmental factors such as light intensity, spectral distribution and temperature have an influence on the degradation rate during the exposure of a polymer. Differences in these factors can lead to

difference in oxygen uptake and thus impairment on mechanical properties e.g. Outdoor ageing mainly took place in spring and summer. The acceleration rate depends on the degradation parameter measured. It was suspected differences between accelerated and outdoor weathering are probably due to a change of the mechanism leading to oxygen uptake. During accelerated weathering most of the oxygen is consumed through propagation reactions giving all the expected oxidation products such as carbonyls.

Efforts have been made to improve the accuracy of the prediction of outdoor weathering performance. Yang et al [57] suggest the answer may lie in looking carefully at factors other than just the above mentioned environmental factors. When considering PP in an outdoors environment, UV irradiation in addition to cumulative UV irradiation should be taken into account. Tests showed that by using low intensity of UV irradiation in accelerated weathering tests, weathering performance of polypropylene filaments under atmospheric conditions can be predicted following the 'energy equivalent method'. Once UV intensity in an accelerated test is so high, hydro peroxide decomposition of PP differs from that under actual service conditions. For a correct prediction UV intensity should be within the range resulting in the same kinetics of the main oxidation route to photooxidation of the material as that in its actual use outdoors.

## **1.8 Degradation Measurement Techniques**

### **1.8.1 Physical Testing Techniques**

#### **1.8.1.1 Gloss Loss and Chalking**

Gloss is a measure of the amount of light reflected off a surface. The more reflected, the higher the gloss. Gloss can be measured with photoelectric devices, which compare the reflected light versus the light originally falling on the surface at a given angle of reflection. As the film is photo-oxidised, it becomes pitted and gloss levels are reduced. After prolonged or especially intense exposure to UV irradiation, insoluble pigment particles can be seen as a chalky deposit on the coating surface.



### **1.8.1.2 Colour Retention**

A pigmented film is able to undergo colour changes in a number of ways e.g. colour fade and colour darkening. This is an undesirable aesthetic effect that great efforts should be made to avoid. Electronic colour sensors such as a spectrophotometer can be used to measure the colour of paint systems. The instrument is pre-calibrated, following which the test sample is compared against standard panels. The best method to determine the colour change is to record the full UV/Visible reflectance spectrum, which will show quantitatively how the colour is changing.

## **1.8.2 Chemical Test Methods to Quantify Degradation**

### **1.8.2.1 Infrared Spectroscopy [58]**

Infrared radiation (IR) lies in the Electromagnetic spectrum between the visible region and the microwave region. It is measured in units of frequency (Hz), wavenumber ( $\text{cm}^{-1}$ ) or wavelength (microns). Infrared can be further divided into three regions: Near, Mid and Far. The mid infrared red region (MIR) is by far the most widely used, especially looking wavelengths associated with inter-molecular vibrations found in organic molecules. The use of near infrared (NIR) has grown in recent years, particularly in the food and pharmaceutical industry for quantitative analysis of ingredients.

When a sample is exposed to infrared radiation, there are ultimately three possible interactions. It is either transmitted, absorbed or reflected by the sample. Thus all the available technology now allows one to obtain information on the molecular structure of an unknown molecule, by deducing how the observed maxima in a spectra relate to vibrational modes of a known molecule.

X-ray analysis looks at the inner electrons, UV the outer electrons and IR the bonds. The theory of IR spectroscopy ultimately deals with observation of simplified mass models which correspond in structure to natural molecules, and whose vibrational manner can be described by the classical principle of mechanics. Absorption of IR energy occurs because the frequency of molecular vibrations is the same as IR radiation frequency. Vibrations follow laws of simple mechanics e.g. Hooke's Law for harmonic motion. As a molecule vibrates, its dipole moment changes during the

vibration, and this is said to be “active” in the IR spectrum. If a dipole does not change during a vibration, it would not be observed. However, it must also be noted, that molecules that do not have a permanent dipole e.g. Carbon Dioxide, also absorb in the IR.

Within an IR spectrum, there are a variety of bands that can be identified:

- i. Fundamental group vibrations
- ii. Overtones
- iii. Combination Bands
- iv. Fingerprint region (skeleton vibrations)

Many vibration modes may be specifically associated with the movement of a few atoms, usually dependent on the rest of the molecule. There are ultimately four vibrations can arise in the form stretching (asymmetric or symmetric) and bending (in or out of plane). They are therefore known as group frequency vibrations, or characteristic group frequencies.

Table 1-6 Common Characteristic Group Frequencies

| Element  | Bond | Wavenumber (cm <sup>-1</sup> ) |
|----------|------|--------------------------------|
| Hydrogen | O-H  | 3300                           |
|          | N-H  | 3200                           |
|          | C-H  | 3000                           |
| Oxygen   | C=O  | 1700                           |
|          | C-O  | 1200                           |

An overtone corresponds to absorption of radiation corresponding to a change from e.g. a ground state to a 2<sup>nd</sup> vibrational energy level. A frequency of  $f_1$  may have an overtone at  $2f_1$ . They can be distinguished from their fundamentals because of their weak frequencies.

A combination band occurs when two frequencies  $f_1$  and  $f_2$ , may produce a combination,  $f_1 + f_2$  or  $f_1 - f_2$ . The fingerprint region corresponds to lower

wavenumbers  $1400$  to  $400\text{cm}^{-1}$ , which corresponds directly to the backbone stretches and vibrations influenced by the functional groups, and is unique to a specific molecule obtained.

A carbonyl group is a carbon oxygen double bond. If the carbonyl group is bonded to alkyl group the resulting compound is a ketone. If it is joined to at least one hydrogen bond, it forms an aldehyde. Carbonyl groups can be found in FTIR absorption spectra in the region of  $1700\text{ cm}^{-1}$ . As previously mentioned, monitoring the carbonyl groups after degradation is a popular method in quantifying degradation. With various absorption bands being attributed to specific vibrations e.g.  $1714\text{ cm}^{-1}$  is assigned to the C=O stretch

Hydroperoxides have also been considered key components in polyolefin degradation [59]. They can be identified by means IR spectroscopy, evident in the regions of  $3410$  to  $3600\text{cm}^{-1}$ .

### **1.8.2.2 Fourier Transform Infra Red Spectroscopy (FTIR)**

Traditional IR techniques acquire data examining discrete wavelengths sequentially in comparison to a reference sample beam. Fourier Transform Infra Red (FTIR) Spectroscopy is capable of scanning all the wavelengths of interest in a single scan. This makes it possible to scan the sample much quicker avoiding poor signal to noise ratios. Mathematical processing transforms the interferogram into transmittance against wavenumber, using Fourier transform mathematics. Techniques including baseline correction, scale expansion, plot modification and plot smoothing can all be used to improve the clarity of the final spectrum. Modern computer software offers an even greater array of features. These include the ability to store and later look up spectra, compiling a 'library' of information. Mathematical tools are also able to integrate a peak with a spectrum, quantitatively monitoring degradation products. Absorbance peaks at various wavenumbers identify the polymers and oxidation products.

Within the realms of the FTIR, there are numerous testing techniques to identify these oxidation products such as carbonyl groups and hydroperoxides.

## Transmission Testing

IR radiation is passed through a sample and the transmitted radiation is measured. The sample must therefore be sufficiently thin to allow the beam to pass through. In such an experiment, the transmitted radiation (T) is given by:

$$T = I/I_0 = \exp(-\alpha L) \quad (\text{Equation 1-27})$$

Where I is transmitted intensity

- $I_0$  is incident intensity
- $\alpha$  is the absorption co-efficient
- L is sample thickness

It must be noted however that the spectra observed will be symptomatic of the entire sample, as opposed to the surface properties for example. If investigative work is concentrating on the surface properties of the sample only, this method should be avoided and the following considered.

### 1.8.2.3 Flat Panel Reactor

As well as the regular IR spectroscopic techniques looking at the surface and transition characteristics of a polymer, novel methods to monitor the evolution of by-products to degradation have been developed. An analysis of the gas phase of irradiated polymers has proven to be a useful tool in the monitoring and prediction of polymer durability. The degradation of polymers such as PVC and PE results in the evolution of CO<sub>2</sub>. A sample is irradiated by UVA within the cell and the evolved CO<sub>2</sub> is circulated within the closed loop system. The gas passes through a pump and then a gas cell. The gas cell can have varying lengths depending on the level of detection required and is connected to a computer controlled FTIR which quantifies the CO<sub>2</sub> concentration. Carbon dioxide has an absorption at approximately 2360cm<sup>-1</sup> (measured component) and 2340cm<sup>-1</sup> and the change in CO<sub>2</sub> concentration within the closed loop system will influence the IR absorption at this wavenumber.

Using the apparatus in Figure 1-28, this method was used to implement rapid testing of TiO<sub>2</sub> photoactivity [60]. It was established as a means to rank TiO<sub>2</sub> pigment photoactivity in unplasticized PVC films pigmented with as shown in Figure 1-29.

This technique used and pioneered by Worsley et al, has been further used to measure the degradation of a variety of model and commercial coating systems [50, 60-63]

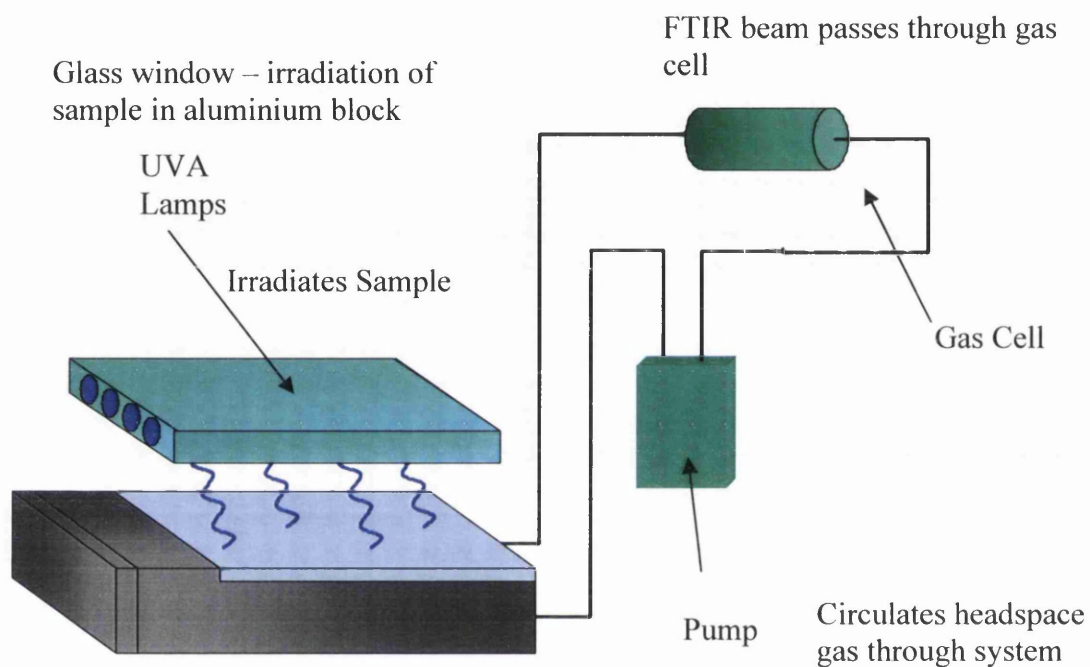


Figure 1-28 Flat Panel Irradiation Apparatus

It is essentially an aluminium cell, with a glass window. A sample is irradiated by UVA, within the cell, and the evolved CO<sub>2</sub> is circulated within the closed loop system. The gas passes through the pump and then a gas cell. It is connected to a computer controlled FTIR which quantifies the CO<sub>2</sub>.

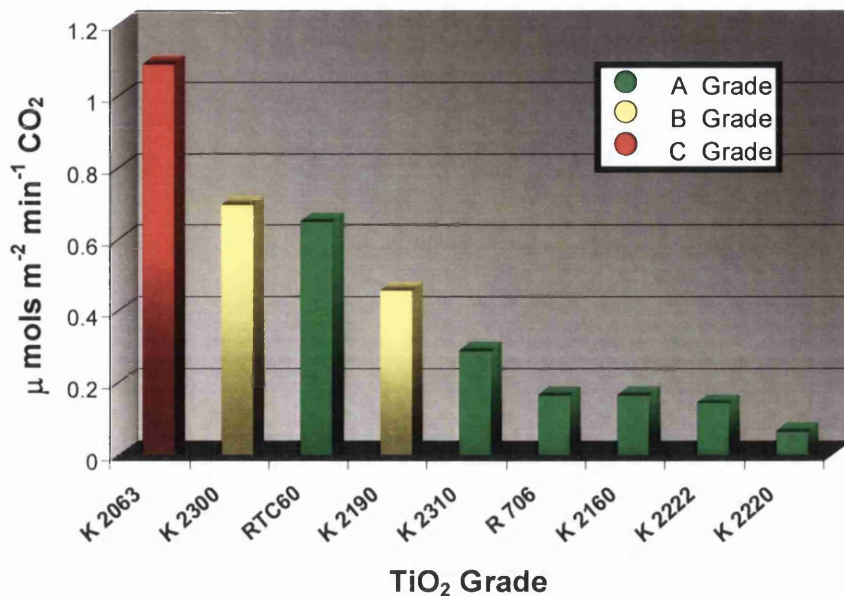


Figure 1-29 CO<sub>2</sub> Evolution Rate for Different Photoactive Grades of TiO<sub>2</sub> [19]

Similarly, Christensen, Egerton et al have studied the photodegradation of polymers at length [24, 64-73] and have developed a testing procedure similar to this. Although small differences in the apparatus and use of Xenon Arc exposure, the measure of CO<sub>2</sub> evolution is equally successful at providing an insight into polymer photodegradation; especially that of polymers such as PE and PP after short irradiation times of 200 minutes.

For degradation catalysed by TiO<sub>2</sub>, it is shown that the oxidation rate was influenced by UV intensity; the relationship being that of the square root of the intensity. Such a trend was also evident for PVC and acrylic paint films. It is also suggested, by the use of multiple films, that the oxidation of the film is not limited to the surface layer, as the oxidation of the film was not limited significantly by placing it behind a film of the same polymer. Also given that the top film has readily available access to oxygen, it was suggested that oxidation is not limited by oxygen diffusion. The induction time apparent for PP and not PE being a result of not O<sub>2</sub> diffusion in and CO<sub>2</sub> diffusion out, but instead a result of the two different oxidation routes of PP and PE.

### 1.8.3 Oxidation Induction Characteristics

Differential scanning calorimetry (DSC) is a thermoanalytical technique in which the difference in the amount of heat required to increase the temperature of a sample and reference are measured as a function of temperature.

Oxidative induction time/temperature (OIT) measurements provide a valuable characterisation parameter associated with the long term stabilities of polyolefins, particularly polyethylene. In order to ensure that the coatings will exhibit acceptable, long-term stability, test needs to be performed which will provide a reliable indication of the stability of the polyethylene coating. The effectiveness of any antioxidant and the longevity of them following weathering can be investigated, and also to give general indications of the polymers oxidative degradation characteristics.

Figure 1-30 shows a schematic of a typical OIT curve (heat flow vs time) with Sample A having less antioxidant present than sample B, and therefore having a smaller induction time.

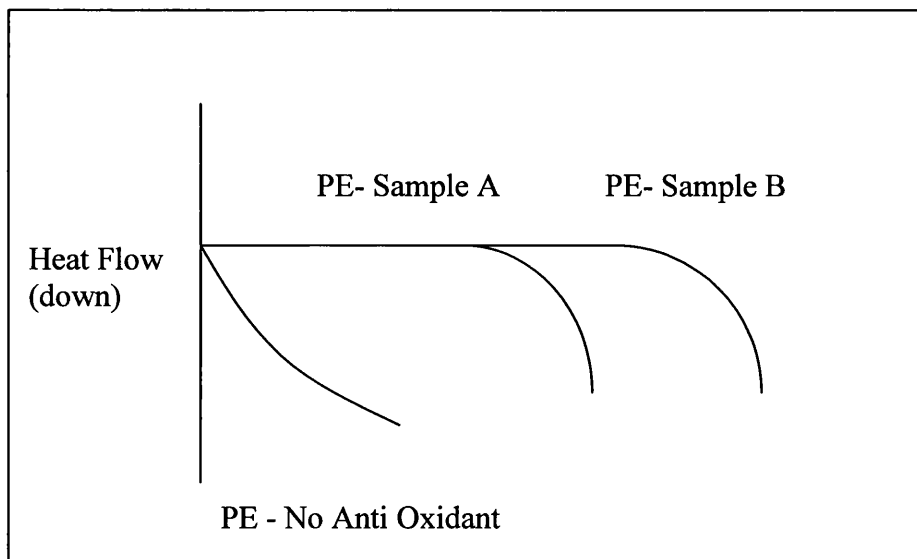


Figure 1-30 Typical Oxidation Induction Characteristics

## **1.9 Introduction to Investigation**

### **1.9.1 Motivation**

The steel industry has gone through some turbulent times recently and in addition, the supply of steel products has also changed in many sectors, where quality and reliability is now a fundamental prerequisite in the market place. The organic coated steel sector is not exempt from such difficulties.

The significant increase in raw material costs and other factors such as energy prices over the last few years, has not fully been passed onto the customer in terms of an increase in product cost, therefore, requiring the steel industry to absorb much of the impact themselves. As a result, greater pressures are put on the manufacturing processes to develop ever increasing quality at reduced process costs.

However, remaining competitive in such an economic climate is still extremely important, if not, more important than ever. An enabler to this is continued efforts in the area of research and development; a better understanding coupled with increasing product performance will enable the business to remain in the forefront of economic growth in the steel industry.

### **1.9.2 Structure of Thesis**

This thesis examines the effect the environment has on organic coated steel products in outdoor environments, and coating technologies to improve the coating resistance to weathering. The presence of UV irradiation and humidity has been examined as key factors influencing the coating quality, performance and longevity.

Chapter 1 introduces typical PVC plastisol paint products and application techniques, highlighting the components of a paint system, including an important pigment, TiO<sub>2</sub>. Another important component is the solvent and the requirement of a solvent in PVC plastisol paints solution is also highlighted. The associated environmental concerns of using a solvent are discussed and alternative solvent free coating systems are recognised as a potential alternative. With all differing coating systems, there are



advantages and limitations; by moving to a solvent free system, such as that of a solid film coating (for example such as a polyethylene film), the application process would need revising from that of a roller application with a solution paint formulation.

Following an overview of experimental procedures in Chapter 2, Chapter 3 investigates the effect of humidity of the photodegradation of TiO<sub>2</sub> pigmented PVC.

The inclusion of the pigment alone accelerates the photodegradation of the PVC coating. In addition to this, the presence of humidity also acts to influence the rate of photodegradation. The addition of a clay pigment 'hydrotalcite' was shown to reduce this rate of degradation and control the mechanisms and by-products of the degradation thus minimising the 'humidity-degradation' effect.

Chapters 4 and 5 assess techniques to stabilise a TiO<sub>2</sub> pigmented PVC coating system, firstly, the addition of a clear coat lacquer. The benefit of a clear coat top coat is that it should impart no change on the appearance of the pigmented base coat, merely acting as a protective layer rather than significantly affecting the appearance. Lacquers are often used in commercial systems to provide a scratch resistant barrier layer. The results discussed in this chapter show that there is significant benefit in the weathering performance of a TiO<sub>2</sub> pigment coating that is lacquered with a clear coat. In addition to this, commercially available stabilisers were concentrated in this clear coat to analyse whether any additional weathering resistance could be provided.

Chapter 5 builds upon the concept of a barrier layer, this time investigating the potential of a nano-scale system, as opposed to the 100 micron clear coats. A variety of materials were deposited on a TiO<sub>2</sub> pigmented PVC coating by physical vapour deposition (depositions ranging from 2nm to 100nm). The data discussed shows that the presence of even a nano-scale coating has a significant effect on the photodegradation of the PVC, namely improving the weathering resistance. The data highlights that any improvement of weathering resistance is very much dictated by deposition thickness and depositional material.

Having understood the influence UV and humidity have on the photodegradation of a coating system and investigated the potential opportunities to improve the weathering resistance, Chapter 6 revisits the discussion introduced in Chapter 1; a movement from solvent containing coating systems to a solvent free alternative. Polyethylene is identified as a suitable coating system to investigate as a material with potential for coil coating application.

Having already built up a wealth of degradation measurement techniques, including the novel flat panel reactor, the photodegradation of polyethylene was analysed in the same way. Building upon this, a new technique, often used to analyse the oxidation characteristics of a polymer, was designed and tested; the effects of in-situ UV irradiation on the oxidation characteristics of the samples. Whilst extremely important in terms of coupling the results of the regular oxidation induction experiment with other techniques such as the CO<sub>2</sub> evolution, the development of the in-situ UV oxidation experiment, showed how analysis of data was more difficult due to the combination of thermal and photo-oxidative processes occurring simultaneously. Despite this, the chapter highlights the careful consideration needed, and impact, when producing a coating via a thermal processing route, such as extrusion for example, and subsequently subjecting the sample to UV environments.

Chapter 7 summarises the conclusions from this work and considers some further work which could be proposed.

## 1.10 References

1. Lambourne, R. and Strivens, T.O., *Paint and Surface Coatings* ed. 1999, Cambridge: Woodhead Publishing.
2. European Solvents Industry Association (SIA) (1997) 'Solutions' - News from the Eu Solvents Industry.
3. Department of Environment, F.a.R.A., *Environmental Permitting Guidance the Solvent Emissions Directive for the Environmental Permitting (England and Wales) Regulations 2007, Directive, S.E., Editor. 2009 V.2.*
4. Graziano, F., *Metal Finishing*, 2000. **98**(6): p. 175-176.
5. Elvins, J., Spittle, J.A., and Worsley, D.A., *Corrosion Engineering, Science and Technology*, 2003. **38**(3): p. 197-204.
6. Williams, G. and McMurray, H.N., *Electrochemical and Solid State Letters*, 2003. **6**(3): p. B9-B11.
7. McMurray, H.N. and Williams, G., *Corrosion*, 2004. **60**(3): p. 219-228.
8. McMurray, H.N., Williams, D., Williams, G., and Worsley, D., *Corrosion Engineering Science and Technology*, 2003. **38**(2): p. 112-118.
9. CPP, *Corus Packaging Plus - Protact Information Booklet*, in Corus Publications.
10. Mills, A., *University of Wales Lecture Notes : Photochemistry*. 1996.
11. Allen, N.S. and Edge, M., *Fundamentals of Polymer Degradation and Stabilisation*. 1992, London: Elsevier Applied Science Publishers.
12. Allen, N.S., *Engineering Plastics*, 1995. **8**(4): p. 247-286.
13. George, G.A., *Materials Forum*, 1995. **19**: p. 145.
14. Braun, J.H., *Journal of Coatings Technology*, 1997. **69**(868): p. 59-72.
15. Rabek, J.F., *Photodegradation of Polymers, Physical Characteristics and Applications*. 1996, Berlin Springer Verlag.
16. Decker, C., Biry, S., and Zahouily, K., *Polymer Degradation and Stability*, 1995. **49**(1): p. 111-119.
17. Van Krevelen, D.W., *Properties of Polymers*. 1976: Elsevier. 465-467.
18. Gijsman, P., Meijers, G., and Vitarelli, G., *Polymer Degradation and Stability*, 1999. **65**(3): p. 433-441.

19. Robinson, A.J., The Development of Organic Coatings for Strip Steels with Improved Resistance to Photodegradation. 2005, Eng. D, University of Wales Swansea
20. Cheremisinoff, N.P., ed. Handbook of Polymer Science and Technology. Vol. 3. Applications and Processing Operation. 1989, Marcel Dekker Inc: New York.
21. Searle, J.R., Titanium Dioxide Pigment Photocatalysed Degradation of Pvc and Plasticised Pvc Coatings. 2002, Eng. D, University of Wales Swansea.
22. Mc Kellar, J.F. and Allen, N.S., Photochemistry of Man-Made Polymers. 1979, London: Applied Science Publishers.
23. Gugumus, F. and Agnew, Makromol Chem, 1990. **27**: p. 176.
24. Egerton, T.A. and Tooley, I.R., Journal of Physical Chemistry B, 2004. **108**(16): p. 5066-5072.
25. Turton, T.J. and White, J.R., Polymer Degradation and Stability, 2001. **74**(3): p. 559-568.
26. Rabello, M.S. and White, J.R., Polymer Degradation and Stability, 1997. **56**(1): p. 55-73.
27. Elvira, M., Tiemblo, P., and Gomez-Elvira, J.M., Polymer Degradation and Stability, 2004. **83**: p. 509-518.
28. Barksdale, J., Titanium and Its Occurrence, Chemistry and Technology. 1966: The Ronald Press Company.
29. Boxall, J. and Von Fraunhofer, J.A., Concise Paint Technology. 1977, London: Elek Science.
30. Brezova, V., Gabcova, S., Dvoranova, D., and Stasko, A., Photochemistry and Photobiology B: Biology, 2005. **79**(2): p. 121.
31. Colquitt, J.P., The Science of the Total Environment, 2002. **289**(1-3).
32. Gopee, N.V., Cui, Y., Olson, G., Warbritton, A.R., Miller, B.J., Couch, L.H., Wamer, W.G., and Howard, P.C., Toxicology and Applied Pharmacology, 2005. **2009**(2): p. 145.
33. Francioso, L., Presicce, A.M., Taurino, A.M., Rella, R., Scililiano, P., and Ficarella, A., Sensors and Actuators B: Chemical, 2003. **95**(1-3): p. 66.
34. Paint Research Association, Paint Technology Training Course Notes. 2001.
35. Housecroft, C. and Constable, E., Chemistry 2nd Edition. 1997: Longman Imprint. 289.

36. Marganski, R.E., Abstracts of Papers of the American Chemical Society, 1998. **216**: p. U608-U608.
37. Mc Kellar, J.F. and Allen, N.S., Photochemistry of Man-Made Polymers. 1979, London: Applied Science Publishers. 211-219.
38. Starnes Jr., W.H., Free Radicals in Thermal Dehydrochlorination of Poly(Vinyl Chloride), in Society of Plastics Engineers. 2011.
39. Ritchie, P., Plasticisers, Stabilisers and Fillers. 1972: Illiffe Book Ltd.
40. Cortolano, F.P., Vinyl Technology, 1993. **15(2)**: p. 69.
41. Scott, G., ed. Developments in Polymer Stabilisation Vol. 1. 1979, Elsevier Applied Science Publishers: London.
42. Qayyum, M.M. and White, J.R., Polymer Degradation and Stability, 1993. **41(2)**: p. 163-172.
43. Allen, N.S., Pena, J.M., Edge, M., and Liauw, C.M., Polymer Degradation and Stability, 2000. **67**: p. 563.
44. Pena, J.M., Allen, N.S., Edge, M., Liauw, C.M., Roberts, I., and Valange, N., Polymer Degradation and Stability, 2000. **70**: p. 437.
45. Maia, D.R.J., Balbinot, L., Poppi, R.J., and De Paoli, M.A., Polymer Degradation and Stability, 2003. **82(1)**: p. 89-98.
46. Lundback, M., Hedenqvist, M.S., Mattozzi, A., and Gedde, U.W., Polymer Degradation and Stability, 2006. **91(7)**: p. 1571-1580.
47. Boersma, A., Polymer Degradation and Stability, 2006. **91(3)**: p. 472-478.
48. CIBA, in Light Stabilisers for Polyolefins, Additive Booklet.
49. Gijsman, P., Hennekens, J., and Janssen, K., American Chemical Society, 1996. **33**: p. 9.
50. Martin, G.P., The Stabilisation of Pvc Using Hydrotalcite (Ht), in Swansea University School Of Engineering. 2008.
51. Decker, C. and Biry, S., Progress in Organic Coatings. **29(1-4)**: p. 81-87.
52. Zhang, J.T., Hu, J.M., Zhang, J.Q., and Cao, C.N., Progress in Organic Coatings, 2004(51): p. 145.
53. Warren, D.J., The Corrosion Behaviour of New Packaging Steel at Local Defects, in Swansea University School of Engineering. 2010, Swansea.
54. Kumar, A.P., Depan, D., Singh Tomer, N., and Singh, R.P., Progress in Polymer Science, 2009. **34(6)**: p. 479-515.

55. Fahlteich, J., Fahland, M., Schönberger, W., and Schiller, N., *Thin Solid Films*, 2009. **517**(10): p. 3075-3080.
56. Singh, B., Bouchet, J., Rochat, G., Letierrier, Y., Månson, J.A.E., and Fayet, P., *Surface and Coatings Technology*, 2007. **201**(16-17): p. 7107-7114.
57. Yang, X. and Ding, X., *Geotextiles and Geomembranes*, 2006. **24**: p. 103-109.
58. Perkin Elmer, *Introduction to Infrared Spectroscopy - Training Course Manual*. 2006.
59. Lemaire, J., Arnaud, R., and Gardette, J., *Pure and Applied Chemistry*, 1983. **55**(10): p. 1603-1614.
60. Worsley, D.A. and Searle, J.R., *Materials Science and Technology*, 2002. **18**(6): p. 681-684.
61. Robinson, A.J., Wray, J., and Worsley, D.A., *Materials Science and Technology*, 2006. **22**(12): p. 1503-1508.
62. Searle, J. and Worsley, D.A., *Plastics, Rubber and Composites*, 2002. **31**: p. 329.
63. Robinson, A.J., Searle, J.R., and Worsley, D.A., *Materials Science and Technology*, 2004. **20**(8): p. 1041-1048.
64. Christensen, P.A., Dilks, A., Egerton, E.J., and Lawson, E.J., *Journal of Material Science*, 2002. **37**: p. 4901-4909.
65. Christensen, P.A., Dilks, A., Egerton, T.A., and Temperley, J., *Journal of Materials Science*, 2000. **35**(21): p. 5353-5358.
66. Christensen, P.A., Dilks, A., Egerton, T.A., and Temperley, J., *Journal of Materials Science*, 1999. **34**(23): p. 5689-5700.
67. Christensen, P.A., Egerton, T.A., Fernando, S.S., and White, J.R., *Polymer Degradation and Stability*, 2009. **94**(11): p. 1999-2003.
68. Christensen, P.A., Egerton, T.A., Martins-Franchetti, S.M., Jin, C., and White, J.R., *Polymer Degradation and Stability*, 2008. **93**(1): p. 305-309.
69. Egerton, T.A. and King, C.J., *Journal of the Oil & Colour Chemists Association*, 1979. **62**(10): p. 386-391.
70. Fernando, S.S., Christensen, P.A., Egerton, T.A., Eveson, R., Franchetti, S.M.M., Voisin, D., and White, J.R., *Materials Science and Technology*, Pending Publication 2008.

71. Fernando, S.S., Christensen, P.A., Egerton, T.A., and White, J.R., *Polymer Degradation and Stability*, 2007. **92**(12): p. 2163-2172.
72. Jin, C., Christensen, P.A., Egerton, E.J., and J.R., W., *Journal of Materials Science and Technology*, 2006. **22**(8).
73. Jin, C.Q., Christensen, P.A., Egerton, T.A., Lawson, E.J., and White, J.R., *Polymer Degradation and Stability*, 2006. **91**(5): p. 1086-1096.
74. Robinson, A.J., Searle, J., and Worsley, D.A., *Materials Science and Technology*, 2004. **20**: p. 1041.
75. Singh, R.P., Tomer, N.S., and Bhadraiah, S.V., *Polymer Degradation and Stability*, 2001. **73**(3): p. 443-446.
76. O'Brien, F.E.M., *Journal of Scientific Instruments*, 1948. **25**(3): p. 73.
77. Worsley, D.A., Mills, A., Smith, K., and Hutchings, J., *Chemical Society, Chemical Communication*, 1995: p. 1119.
78. Martin, G.P., Robinson, A.J., and Worsley, D.A., *Materials Science and Technology*, 2006. **22**: p. 375.
79. Fernando, S.S., *Spectroscopic Studies of Polyalkene and Polyester Photo-Oxidation*, in School of Chemical Engineering and Advanced Materials Newcastle University. 2007, Newcastle University.
80. Wray, J., *The Degradation Studies of TiO<sub>2</sub> Pigmented Polyurethane Coating Systems*, in University of Swansea School of Engineering. 2009, Swansea University.
81. Jin, C.Q., *Ftir Studies of TiO<sub>2</sub> Pigmented Polymer Photodegradation*. 2004.
82. Henry, B.M., Assender, H.E., Eriat, A.G., and Grovenor, C.R.M., 2004: p. 609.
83. Henry, B.M., Eriat, A.G., McGuigan, A., and Grovenor, C.R.M., *Thin Solid Films*. **382**: p. 194.
84. Diebold, M.P. *Unconventional Effects of TiO<sub>2</sub> on Paint Durability*. in 5th Nürnberg Conference. 1999. Nuremberg, Germany
85. White, J.R., Shyichuk, A.V., Turton, T.J., and Syrotynska, I.D., *Polymer Degradation and Stability*, 2005: p. 1-6.

## **2 Experimental Procedures**



## **2.1 Coating Formulations**

### **2.1.1 PVC Paint Formulations**

#### **2.1.1.1 Standard Pigmented Model PVC Systems**

The model paint systems (unplasticised) consisted of the three basic paint components; a resin (Poly Vinyl Chloride (PVC)), a solvent (Tetrahydrofuran (THF)) and a pigment ( $\text{TiO}_2$ ). Various changes and additions were made to this paint to investigate the possible effects on photodegradation. These percentage additions relate to the total amount of resin contained within the paint on a weight for weight basis e.g. a 1g addition of  $\text{TiO}_2$  to a paint containing 10g of PVC resin would give a loading of 10 P.H.R = 10%. A model paint consisting of 100ml THF, 10g of PVC and 3g (30% (30 P.H.R)) of P25  $\text{TiO}_2$  is in these model coatings.

The  $\text{TiO}_2$  was dispersed in the 100mL THF and mixed using a high shear paint mixer until even dispersion of pigment particles was achieved. For studies using Hydrotalcite (HT) additions, the  $\text{TiO}_2$  addition was kept at 3g (30% loading) and a varying amount (g) of HT were now added. HT, a pigment grade double layered aluminium magnesium hydroxide, was obtained in a carbonate exchanged form from Aldrich Chemicals and used in as received form.

The 10g of PVC was added during the high shear mixing to ensure even mixing. Following a further 5 minutes of mixing, any remaining pigment agglomerates were removed with 15 minutes of sonication. Each of the paints was stirred continuously on a non-heated stirrer plate for a further 24 hours and then stored in darkness.

#### **2.1.1.2 Near Commercial White Plastisol Systems with Commercial Clear Top Coats**

The coatings were made in a commercial coating laboratory, where commercial base plastisol HPS200 formulations were made. Using a high shear mixer, the required amounts of base and  $\text{TiO}_2$  pigment was added. In this case, the conventional  $\text{TiO}_2$  pigment used was replaced by the more photoactive grade Kronos 1001, at a weight

percent loading of 20%. It is an untreated anatase unstable photoactive grade of TiO<sub>2</sub> with no surface treatment (>99% TiO<sub>2</sub>) produced via the sulphate process. It has a photoactivity in the order off 100 times greater than a stable coated grade such as K2220[19].

The plastisol was placed in a vacuum chamber and all the trapped air introduced during mixing was removed. Finally once chilled to room temperature, the viscosity of the plastisol was checked and adjusted if needed.

A number of different clear coats were chosen to trial the efficiency of the application of such a clear top coat to a PVC white plastisol:

- i. Clear HPS 200
- ii. High Performance Lacquer
- iii. Thermal Cure Polyurethane

Full details of these systems are covered by a commercial agreement with the supplying paint company.

### **2.1.1.3 Fully Formulated White Plastisol Systems with Stabilised Clear Top Coats**

Once again, the HPS200 plastisol formulation was used, with a loading of 20% K1001. In this instance, to test the true effectiveness of a clear coat as a protective barrier to photodegradation, all UVAs and HALS were removed from the HPS200 formulation.

The clear coat to be applied to the white plastisol was a non-pigmented HPS formulation again, to which a variety of UVAs and HALS were to be added in varying levels.

Table 2-1 Formulations of Clear Top Coats

|      | <b>Additive</b>           | <b>0%</b> | <b>0.1%</b> | <b>0.5%</b> | <b>1%</b> | <b>2%</b> | <b>5%</b> |
|------|---------------------------|-----------|-------------|-------------|-----------|-----------|-----------|
| UVA  | Chimisorb 81              | .         | .           | .           | .         | .         | .         |
|      | Hydroxybenzophenone (HBP) | .         | .           | .           | .         | .         | .         |
|      | Tinuvin 571               | .         | .           | .           | .         | .         | .         |
| HALS | Tinuvin 765               | .         | .           | .           | .         | .         | .         |
| Mix  | Tin Mix<br>(765 + 571)    | .         | .           | .           | .         | .         | .         |

Free films of the above formulations were also produced.

## 2.1.2 Polyethylene

### 2.1.2.1 Polymer Formulation

In comparison to the PVC paint formulation, a solid polyethylene pressed ‘sheet’ was produced to represent a solid film coating. Non pigmented virgin polyethylene (PE) was provided by Borealis, in conjunction with Corus Colors RD&T, in the form of beads. It is a commercially available non pigmented grade, with a stabilisation package for its processing, but not sold as being thermally or UV stabilised. TiO<sub>2</sub> grade K1001 was also used in the following work as a white pigment.

To assess the effect of humidity on PE photodegradation, virgin PE was mixed with K1001 at a weight percent loading of 30%. For all other experimentation looking at CO<sub>2</sub> and oxidation induction profiles and weathering, TiO<sub>2</sub> loadings used were 10% 30% and 50%. The remaining formulations were virgin PE and two stabilised non-pigmented alternatives. The two stabilisers chosen were an anti-oxidant (AO) and UV absorber (UVA); Irganox 1010 (AO) and Tinuvin 326 (UVA) respectively, both at the manufacturers recommended loading of 0.5%.

## 2.2 Sample Preparation

### 2.2.1 PVC

#### 2.2.1.1 Model PVC Systems

The flat cell can accommodate a maximum sample size of approximately 9.5cm x 22cm thus ensuring all the sample surface is exposed to the irradiating source. For PVC samples to be irradiated, the coating is cast onto a glass panel 22cm x 7cm.

By coating the edges of the glass slide with two layers of insulation tape (140 $\mu$ m), a constant height profile is formed, which upon drying provides a dried coating of approximately 20 $\mu$ m. The PVC is poured onto a secondary plate called a 'pouring plate' (at a right angle and positioned above the sample glass plate) then drawn down the panel using a glass bar as shown in Figure 2-1. Drawing down is performed in a single smooth motion so as to avoid defects in the coating. By using this method, excess PVC paint is drawn off the bottom of the sample plate and the coating remains one consistent thickness.

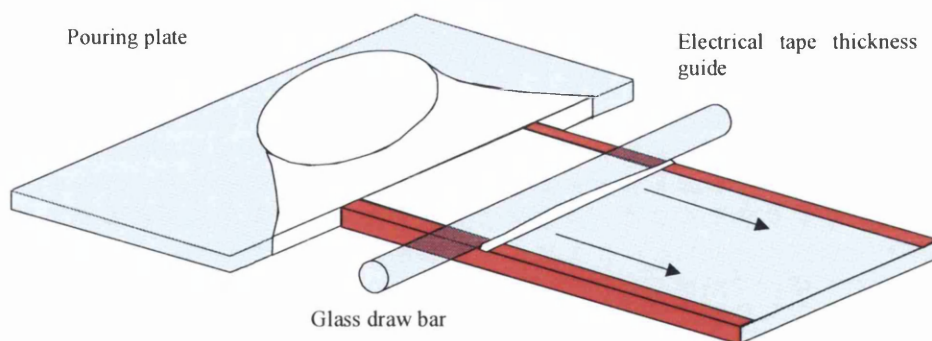


Figure 2-1 - 'Draw Down' Coating Technique

The panels were allowed to dry in a stable draught free environment so as to slow the rate of solvent evaporations, which in turn avoids pinholes developing in the film.

In order to remove any discrepancy in the area of panel coated incurred by the positioning of the insulation tape, or faults in the film when removing the tape, a glass template is used which has width of 7cm (meaning that the sample film size is always 7cm x 22cm). Finally all panels were stored in the dark for a minimum of seven days to insure that all THF had evaporated and thus negate any effect it may have on CO<sub>2</sub> evolution in the reactor.

### 2.2.1.2 Near Commercial White Plastisol Systems with Clear Coats

As shown in the schematic in Figure 2-2, A 200 micron 'K Bar' coating bar was used to cast a HPS200 pigmented plastisol, to a primed steel substrate. This was then semi-cured in an oven at 230 degrees for ten seconds, before the top coat was applied. The top coat systems listed Table 2-2 were applied on top of the white plastisol at the following thicknesses and then the entire panel was fully cured for a further 45 seconds at the same temperature, before being water quenched. Two samples of each coating were prepared for experimentation.

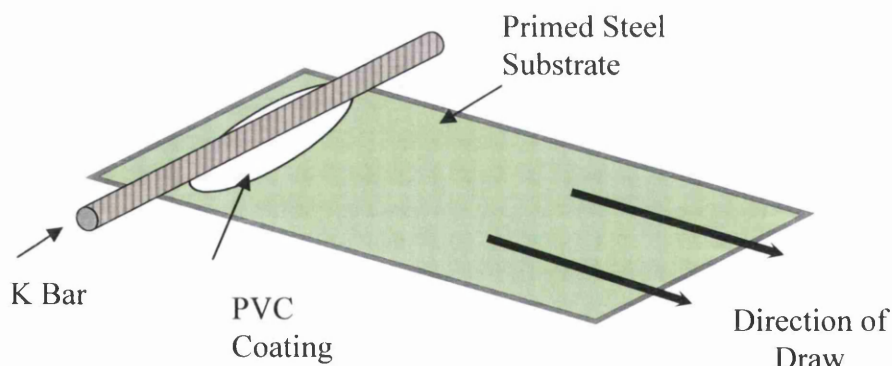


Figure 2-2 Coating of Primed Steel

Table 2-2 Clear Coat Lacquers Systems Compared

| Sample | Top Coat                   |
|--------|----------------------------|
| A      | None                       |
| B      | None                       |
| C      | HPS Clear 20 micron        |
| D      | HPS Clear 20 micron        |
| E      | HPS Clear 40 micron        |
| F      | HPS Clear 40 micron        |
| G      | High Performance 40 micron |
| H      | High Performance 40 micron |
| I      | Thermal Cure Polyurethane  |
| J      | Thermal Cure Polyurethane  |

### 2.2.1.3 Fully Formulated White Plastisol Systems with Stabilised Clear Coats

An automatic coating bar was used to cast the base pigmented HPS 200 plastisol. This was then also cured for ten seconds in an oven heated to 230°C to allow a semi-cure sufficient enough to apply the top coat. The combinations of HPS200 stabilised clear coats (as described in greater detail in 4.2.1) were applied and each panel was cured for a further 45 seconds and water quenched on removal from the oven. Two samples of each coating combination were prepared for experimentation.

### 2.2.1.4 Free Films

The stabilised clear coat formulations were applied to the steel substrate in the same manner using a draw down coater delivering a wet thickness of 200 microns. The non-primed steel panel was then cured for 45 seconds, quenched as before, and the clear coat was easily peeled off the substrate.

### 2.2.2 Polyethylene Coatings

In order to achieve the best possible dispersion as any additives, a Torque Rheometer (Figure 2-3) was used. This comprises a chamber with two mixing 'blades', a feed for material access and a ram to force material into the chamber. The chamber has a front and back head (heating elements), both of which can be heated independently. The speed at which the material is turned is dictated by the operator.

Preliminary trials have shown that the chamber can accommodate in the region of 35g of PE material, where thorough and successful mixing occurs.

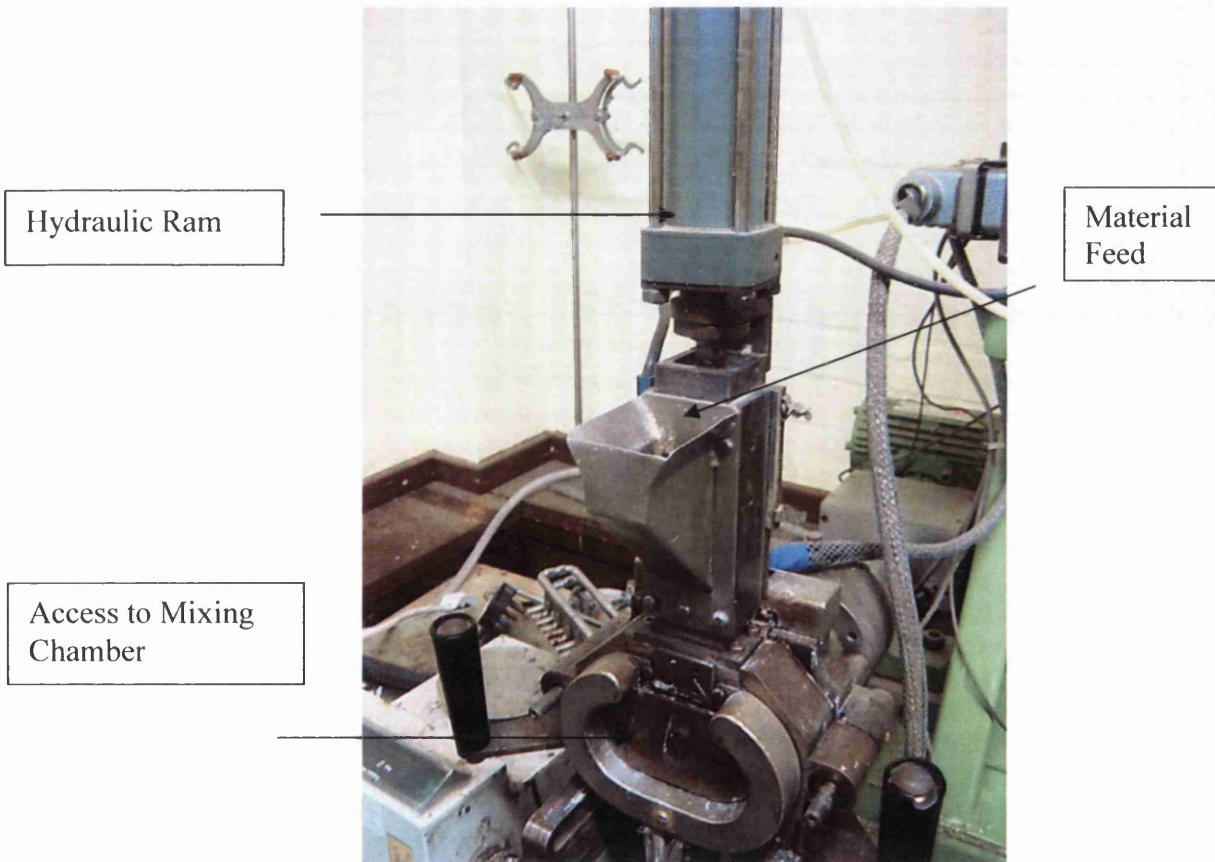


Figure 2-3 - Torque Rheometer

Firstly, the temperature was set to 160°C and the equipment was left to reach this temperature. Once again, initial trials found this was the optimum temperature for mixing without imparting any unnecessary thermal degradation. PE was added and

subsequently, the following levels of TiO<sub>2</sub> additions were added to the PE via the feed; 10%, 30%, 50%.

The hydraulic ram was then lowered to compact the mixture into the chamber and was left for five minutes to melt the polymer component sufficiently prior to mixing. Once the five minutes had elapsed, the turning screws were turned on and set to 45 revolutions per minute. After another 5 minutes, the polymer and TiO<sub>2</sub> are considered thoroughly mixed. The ram was lifted and the heating elements separated, to allow access for polymer removal. After every batch, the system must be purged with virgin polymer as to remove any contamination in the following batch.

The next stage of the sample making process was to produce plaques from which samples can be cut. It was important to expose all samples to the same potential level of thermal degradation during processing as to ensure reproducible results. In the case of the non-pigmented/non-stabilised PE, the virgin PE granules were also subjected to heating and mixing in the torque rheometer, to coincide with the production route of the other samples.

The compression mould consists of two hot plates (Figure 2-4), a hydraulic ram which raises the lower plate to compress, and an integrated water cooling system in the hot plates for cooling post-compression. Again, the equipment is heated to 160°C and left to reach temperature.





Figure 2-4 - Compression Moulder

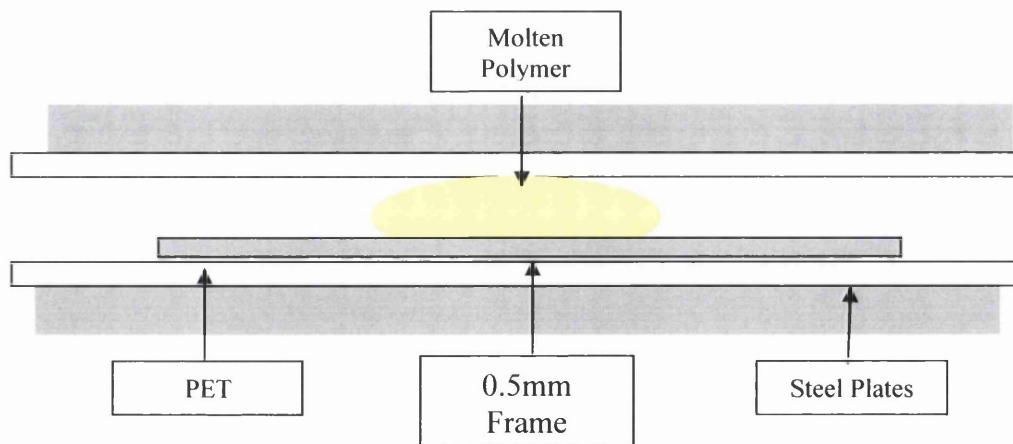


Figure 2-5 - 'Sandwich Like' Arrangement of Steel Plates, PET and Polymer

The polymer is placed in a sandwich like arrangement (Figure 2-5), comprising two metal plates and PET sheeting which gives a good surface finish and prevents contamination of molten polymer. Where a set thickness of approximately 0.5mm is needed here, a square metal frame can be used to maintaining a set distance of 0.5mm between the two metal plates.

The sandwich arrangement shown is then inserted between the hot plates, which were raised within touching distance of both metal plates. After ten minutes the polymer is suitably melted with no unnecessary degradation incurred, the plates are compressed to 25 Tonnes (as shown on the display). For removal, the equipment is set to 'cool' and the water supply turned on so the plates themselves cool. Once the equipment reaches room temperature, the sample can be removed and cut to size.

### 2.2.3 Plasma Vapour Deposition Coating of PVC Samples

PVC samples as described in 2.1.1.1 were made, however on smaller glass panels to allow for subsequent coating in the Lesker PVD75 equipment. All magnetron sputtering deposition was carried out in a vacuum of  $\sim 3 \times 10^{-3}$  Torr. An image of the PVD chamber can be seen in Figure 2-6.

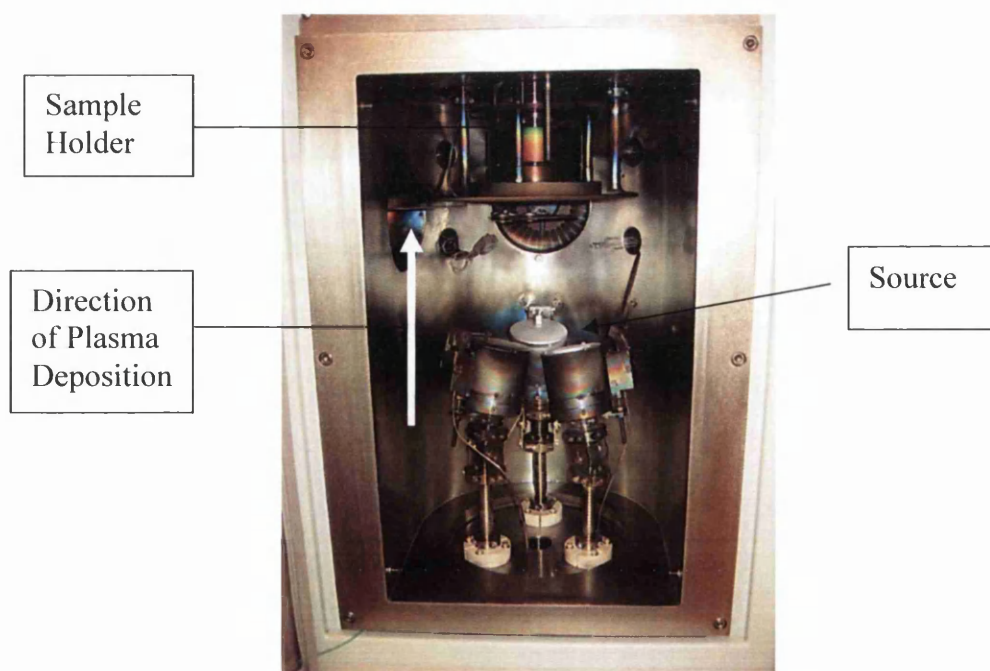


Figure 2-6 PVD Coating Chamber



Figure 2-7 Deposition Target

The following deposition targets were acquired from Kurt J. Lesker company and all at a minimum 99.2% purity and coating thicknesses of between 2nm and 1 $\mu$ m were applied to the PVC samples.

- i. Titanium
- ii. Aluminium
- iii. Copper
- iv. Zirconia
- v. Alumina
- vi. Indium Tin Oxide

For the deposition process the following conditions were used:

- i. Vacuum:  $3.68 \text{ E}^{-3}$  Torr
- ii. Applied Power: 100W
- iii. Gas Flow: 40 SCCM

## 2.3 Accelerated Weathering

### 2.3.1 Fourier Transform Infrared Spectrophotometer

Fourier Transform Infrared Spectroscopy (FTIR) is a technique which is used to obtain an infrared spectrum of absorption of a solid, liquid or gas. An FTIR spectrometer collects spectral data in a wide spectral range. This confers a significant advantage over a dispersive spectrometer which measures intensity over a narrow range of wavelengths at a time. The FTIR spectrum for CO<sub>2</sub> is comprises a double peak between 2300 and 2400 cm<sup>-1</sup>. Via use of a custom written program described shortly, it was possible to integrate the peak area between 2210 and 2480 cm<sup>-1</sup> and measure CO<sub>2</sub> concentration at timed intervals. The CO<sub>2</sub> concentration was measured using a Perkin Elmer Spectrum 100 FTIR Spectrometer controlled by automatic data collection software.

### 2.3.2 Carbon Dioxide Reactor

Using custom written software and equipment set up, it is possible to measure the amount of CO<sub>2</sub> evolved during degradation and thus deduce information about the level of degradation. The set up consists of irradiation apparatus, FTIR with gas cell and a pump.

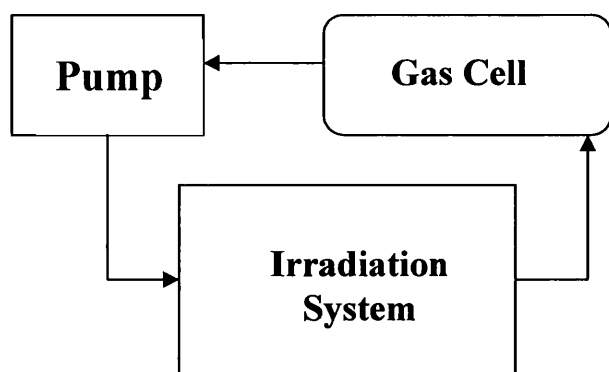


Figure 2-8 Schematic of Instrument Set Up

### 2.3.2.1 Apparatus

#### Irradiation Apparatus

A sample was irradiated in the flat panel cell reactor developed in previous work [74], which itself followed on from work using a tube style reactor [21]. The system is a closed loop, thus constantly measuring the CO<sub>2</sub> concentration as the gas is circulated through the gas cell, by a 6 litre per minute diaphragm pump. A bank of 6 x 8w Coast Wave Blacklight UVA lamps (Coast Air: irradiation  $\lambda_{\text{max}}$  355-365 nm, length 30cm intensity =  $4 \times 10^{17}$  photons s<sup>-1</sup>) are used to irradiate the flat panel sample.

#### IR Gas Cell

The gas cell is mounted within the FTIR; therefore the IR beam passes through the cell. The optical path length of the gas cells is variable from 10cm to 4m. The operator selects the cell path length based on the expected or previously seen CO<sub>2</sub> evolution, in that if very small quantities need to be detected, a longer path length cell is more suitable.

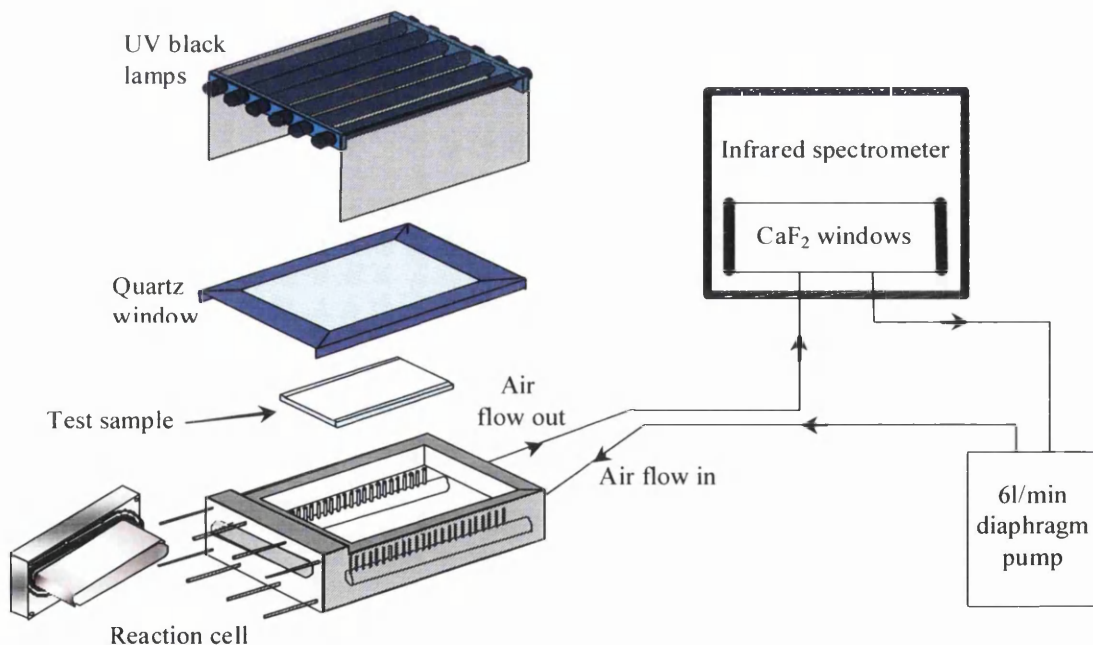


Figure 2-9 Schematic of Experimental Apparatus

### 2.3.2.2 Calibration of the FTIR Flat Panel Reactor

As a result of the evolution of CO<sub>2</sub> from the sample, there is a change in the chemistry of the headspace gas, which the FTIR records as a change in absorption units. By introducing known volumes of CO<sub>2</sub> gas into the apparatus prior to testing, and monitoring the response in absorption units with the known volumes, it is possible to equate the CO<sub>2</sub> evolved by photodegradation to an actual volume.

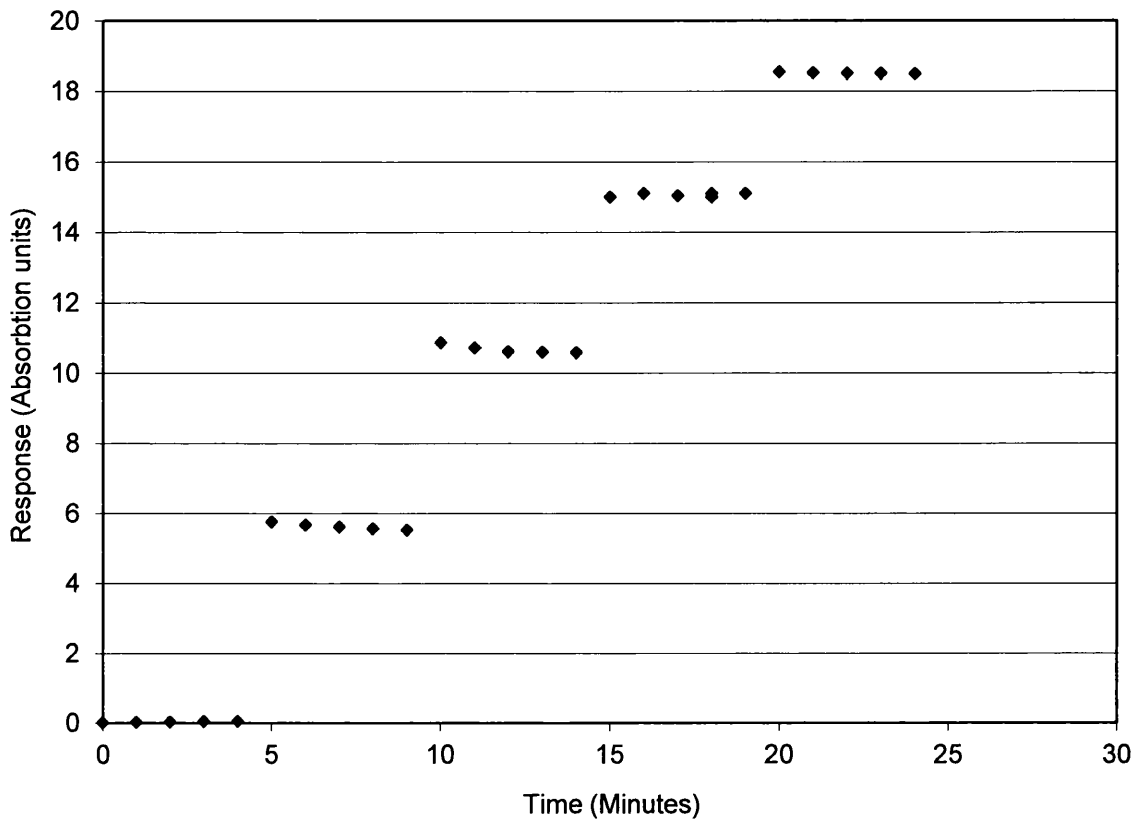


Figure 2-10 The Instantaneous Response of the System to Injections of 100microl CO<sub>2</sub>

Figure 2-10 shows the instantaneous response of the system to injections of 100ml CO<sub>2</sub>, which is summarised by Figure 2-11, showing the cumulative effect of the injections on the system in terms of microlitres of CO<sub>2</sub>. The gradient of 188.73 defines that for this set up, 1 absorption unit (abs) equates to 188.73 micro litres of CO<sub>2</sub> evolved. By taking the size of the sample into consideration, a calibration factor can be derived thus useful in converting data into the form micromols per metre squared of sample, in the following way;

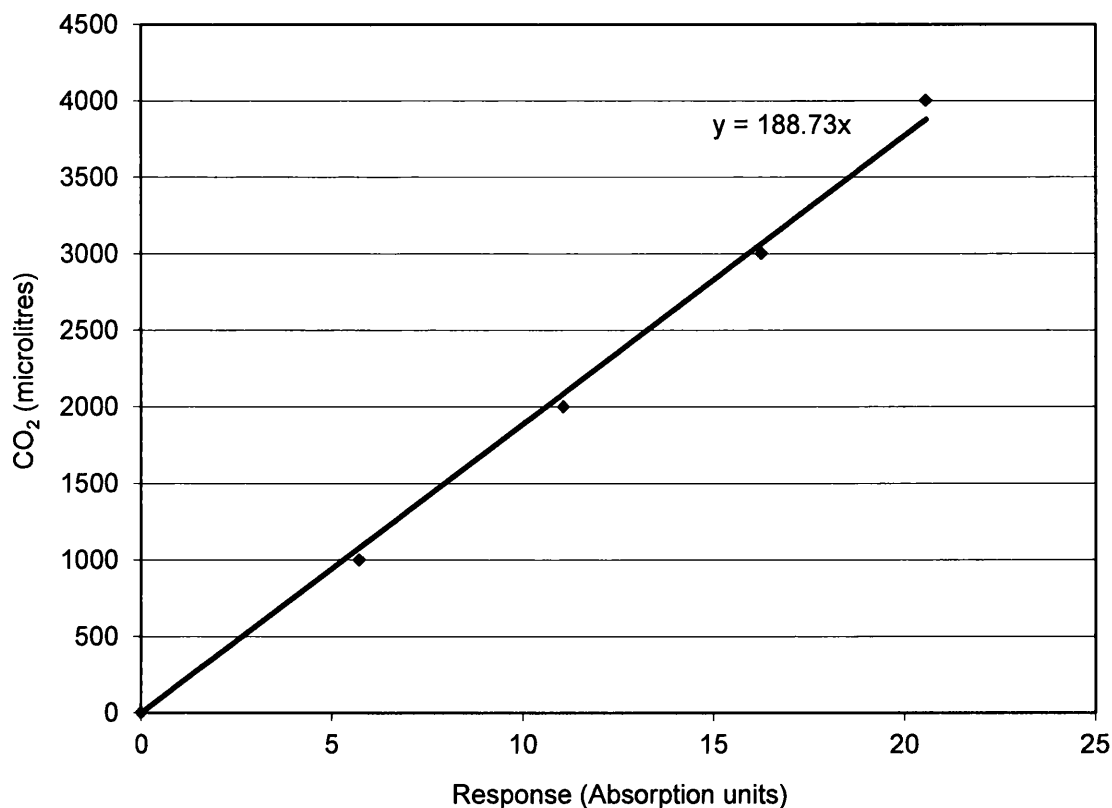


Figure 2-11 Cumulative Effect of the Injections

- i. Gradient = 188.73 microlitres CO<sub>2</sub>
- ii. 1 mole of CO<sub>2</sub> (at room temperature) = 24 Litres
- iii. 1 Abs =  $188.73 / 24 = 7.86$  micromols
- iv. Area of Panel = 8cm x 5cm = 0.004m<sup>2</sup>
- v. Therefore 250 panels per metered squared
- vi. Micromols per meter square =  $250 \times 7.86 = \underline{1965}$  (calibration factor)

The system was also purged with Nitrogen at 1 litre per minute.

### 2.3.3 Automatic Data Collection Programme (Evolgas)

The Evolgas software was developed with a full range of practical and data processing functions. This allowed fully automated data collection and definition of testing parameters prior to test initiation.

Scan Settings



The scan parameters chosen by the operator prior to the experiment are inputted in the Evolgas scan control interface, as seen in Figure 2-12. This includes the scan resolution, wavenumber and the number of scans performed per measurement. The parameters used can be seen below.

**Spectrum 100 FTIR**  
Swansea Corrosion Group - Faculty of Engineering

Select Resolution:  2 cm<sup>-1</sup>  4 cm<sup>-1</sup>  8 cm<sup>-1</sup>  16 cm<sup>-1</sup>

Enter Start of Range:   
Enter End of Range:

Select number of scans per measurement:  1  4  8  16

Time of single measurement: 16 seconds

Figure 2-12 The Evolgas Scan Control User Interface

### Timed Scan Control

**Spectrum 100 FTIR**  
Swansea Corrosion Group - Faculty of Engineering

|  |  |
|--|--|
| <p><b>First Stage</b></p> <p>Scan time: 16 seconds</p> <p>Select delay: <input type="text" value="1"/></p> <p>Time of 1 cycle: 1.00</p> <p>Enter number of cycles: <input type="text" value="11"/></p> | <p>Time now: 14:31 Wed, 14/06</p> <p>Total time to end of first stage: 11.00 minutes</p>                           |
| <p><b>Second Stage</b></p> <p>Select delay: <input type="text" value="10"/></p> <p>Time of 1 cycle: 10.00</p> <p>Enter number of cycles: <input type="text" value="1"/></p>                            | <p>Second stage will start at approx: 14:42 Wed, 14/06</p> <p>Total time to end of second stage: 21.00 minutes</p> |
| <p><b>Third Stage</b></p> <p>Select delay: <input type="text" value="10"/></p> <p>Time of 1 cycle: 10.00</p> <p>Enter number of cycles: <input type="text" value="1"/></p>                             | <p>Third stage will start at approx: 14:52 Wed, 14/06</p> <p>Total time to end of third stage: 31.00 minutes</p>   |
| <p><b>Fourth Stage</b></p> <p>Select delay: <input type="text" value="10"/></p> <p>Time of 1 cycle: 10.00</p>  | <p>Fourth stage will start at approx: 15:02 Wed, 14/06</p> <p>Fourth stage will continue until halted by user</p>  |

Figure 2-13 The Evolgas Timer Control User Interface



The timer control interface shown in Figure 2-12 allows for the operator to dictate the frequency of scans throughout the test duration. Because of the nature of some tests where particular time frames are of more importance, the software has been written in such a way it is possible to identify four testing stages, thus allowing more scans to be carried out at significant points which require a greater level of detail. Such an example would be the initial stages of photodegradation or during an equipment calibration.

### Processing Control

The ultimate purpose of the software was to monitor and measure the chemical change of a sample during irradiation. With every IR scan of the head space gas, a spectrum is produced, and given the irradiation is constant then the head space gas will continuously be changing, thus every spectrum will be different. Therefore, the software is designed to quantify this change by the integration of a given peak, thus a change in a particular chemical constituent. The processing options interface shown in Figure 2-14 allows multiple parameters to be defined. In this experimentation, the CO<sub>2</sub> peak was studied, thus the area of the CO<sub>2</sub> peak was integrated using the parameters as shown.

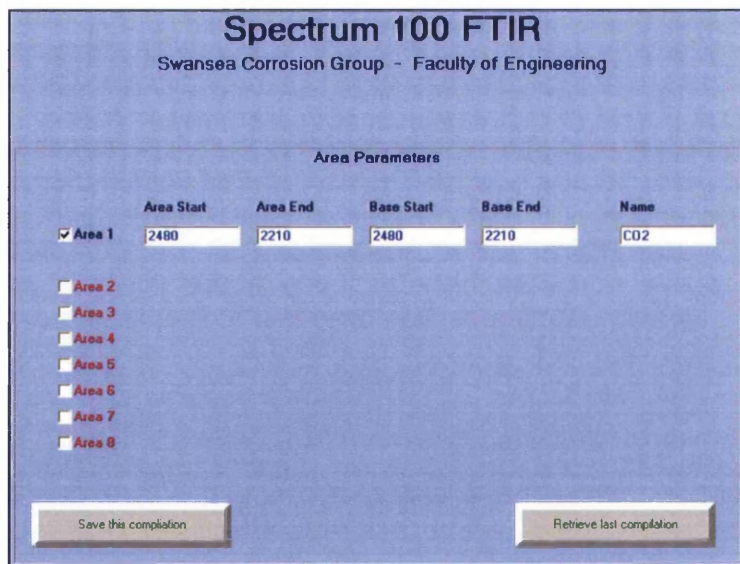


Figure 2-14 - Interface for Adjusting Area Parameters

## The Log File

The interface shown in Figure 2-15 displays test progress as a list of readings and a plot of measured CO<sub>2</sub> in absorption unit (Abs) alongside a plot of the results. The software also allows comments to be added to the log file allowing changes to the test to be recorded, for example injections of CO<sub>2</sub> during the calibration process or change of test sample.

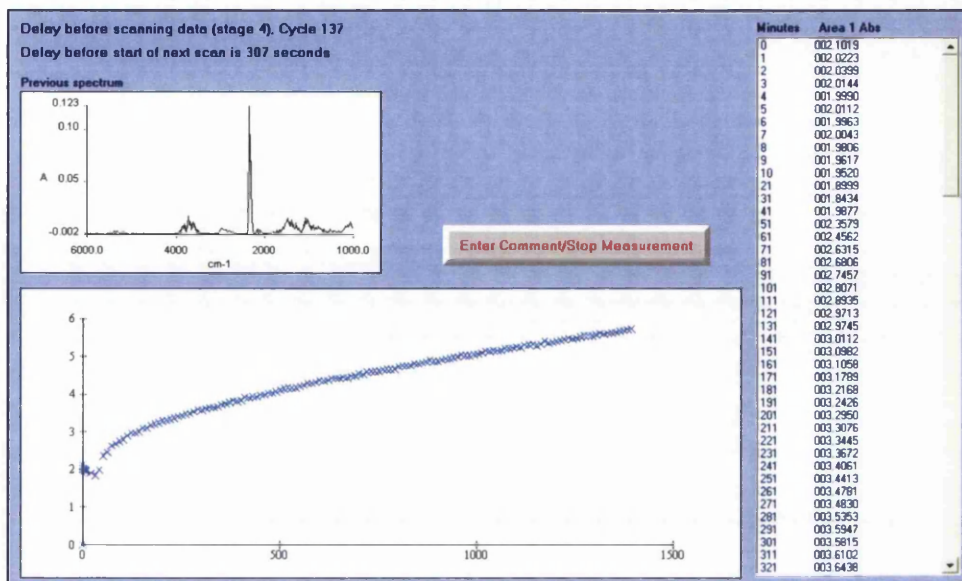


Figure 2-15 Screen Showing Test Progress and Log File

### 2.3.4 Atmospheric Condition Experimentation

The flat panel reactor described here was also utilised during experimentation whereby the effect of atmospheric conditions on photodegradation was measured. By introducing and controlling a relative humidity (RH) within the closed loop system, the CO<sub>2</sub> evolved during irradiation at the relative humidity was measured. The evolved gas was circulated through salt solutions and/or a drying agent, and re-circulated through the system, maintaining a set relative humidity. To avoid the dissolution of CO<sub>2</sub> gas into the salt solution (carbonic acid formation) the solution was adjusted to contain 2 μmol of nitric acid. More intricate details of this experiment are discussed in 3.2.4.

A schematic of the experimental set up can be seen in Figure 2-16.

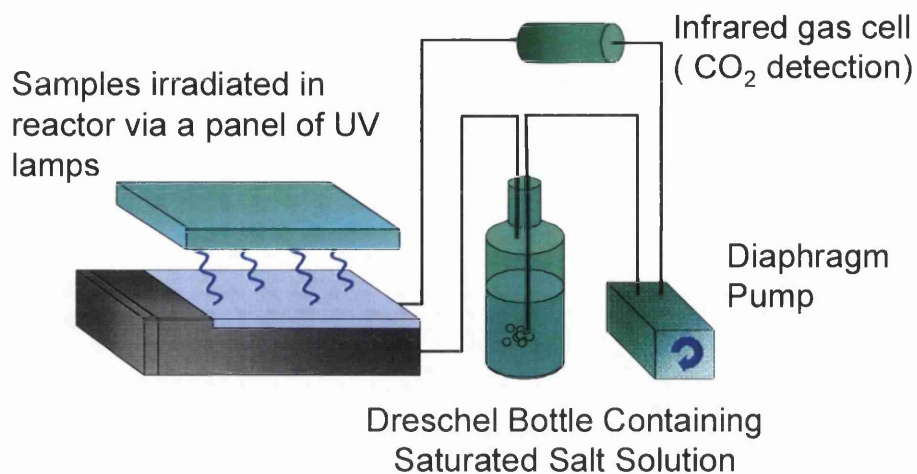


Figure 2-16 Schematic of Apparatus Used to Introduce and Measure the Effect of RH

## 2.4 DSC

The differential scanning calorimeter used was a Perkin Elmer Jade model DSC with Pyris software™. It consists of a disc-type heat flux design with low-mass aluminum furnace (alumina coated) and a sensor that is a machined disc of Chromel alloy (90% Nickel/10% Chromium). The DSC unit is connected to a water cooling system which is independently operated. Similarly it is connected to oxygen and nitrogen cylinders as it has an integrated gas flow control and switching option, with these features being controlled in the Pyris software.



Figure 2-17 - Jade DSC

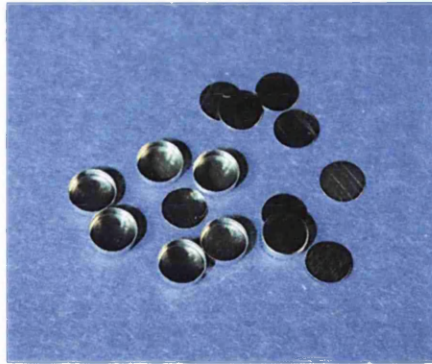


Figure 2-18 - Aluminium Sample Pans

Samples are put in aluminium pans and placed into the furnace on the relevant sensor disc, alongside the reference pan. For oxidation induction tests there is no need for the sample to be covered with a lid.

#### **2.4.1.1 Oxidation Induction Testing**

After the sample is cut to size, put in the furnace and all the test parameters inputted into the software, the nitrogen supply is turned on to 20mL/min. Upon reaching the experimental start temperature of 100°C it is held there for 5 minutes. At this point the atmosphere is changed to oxygen immediately and the furnace heats from 100°C to 230°C at a rate of 0.10°C/min. Once completed and oxidation has occurred, (evident by a rapid change in heat flow of the sample), the nitrogen atmosphere is re-introduced and the load temperature returned to 30°C. Typical oxidation profiles and experimental parameters are discussed in Chapter 6 in greater detail.

## **2.5 Commercial Accelerated Weathering**

### **2.5.1 QUVA**

PVC coated panels and polyethylene samples were irradiated in the QUVA (UV-340) chamber (Figure 2-19). The standard format was 8 hours UV-A exposure followed by 4 hours condensation at 40 degrees. This allows for two complete cycles in a 24 hour period. Studies on the lacquered PVC samples (section 4.2.1) were weathered for a total of 2100 QUV hours and PVD coated PVC wedges 100hours.



For the oxidation induction investigation, polyethylene samples pigmented with  $\text{TiO}_2$  showed signs of degradation at only 150 hours (chalking and colour change) and thus were removed at this time, along with the unpigmented and stabilised PE, tested and all returned for a further 300 hours.



Figure 2-19 QUVA Weatherometer

### 2.5.2 Gloss Measurement

Gloss is an optical property which can give an indication to the influences of photodegradation, which is dictated by the interaction of light with the physical characteristics of a surface. Materials with smooth surfaces appear glossy, while very rough surfaces reflect little or no light and therefore appear matt.

Coating gloss is a measure of the overall surface roughness and reflectivity. As degradation proceeds, there may be a break down in the coherent nature of a coating, with the formation of voids and defects in the organic matrix. As this occurs, the topography of the coating will alter, influencing the reflection of light and thus appear less glossy in nature.

The gloss was measured with a Minolta Multi Gloss 268. A tungsten filament lamp (2.5 V 60 mA) that emits a light flash which hits the surface of the coating at the pre-determined angle; the angle at which the gloss is measured can be selected manually

as either 30°, 60° or 90°. In this case, 60° was used. The measuring device was placed onto the coating, and when operated, light emitted is reflected by the coating at the same incident angle and measured by a silicon photo element. Each measurement was repeated five times for every sample, before being averaged.

### **2.5.3 Colour Measurement**

Complex reactions occurring during photodegradation are also known to alter the appearance of a coating in terms of colour. A more commonly known occurrence of this, is the 'yellowing' of some plastic products exposed to sunlight for prolonged periods [75].

The measurements before and after weathering were compared to assess the effects of degradation on coating colour. Colour was measured using a Gretag Macbeth Spectrolino spectrophotometer set at 45°/0° geometry. A D50 lens was used, which is a light source which closely imitates natural daylight. A beam of light illuminates the coating surface at a 45° angle with the surface normal (at a 90° angle to the surface of the coating) and the reflective response is captured by a standard observer set at a 2° angle with the surface normal.

Readings were taken five times for each sample (CIE-XYZ, CIE L\*a\*b measurements and the light reflectance spectrum between 380nm – 730nm) and averaged, before data was depicted in terms of Delta E. Colour measurements were only taken for samples described in 4.2.1.1 (commercial systems).

### **2.5.4 UV Vis Spectrophotometer**

Perkin Elmer Lambda 750S UV/Vis/NIR was used to take reflectance measurements of degrading coatings. The Lambda 750S spectrophotometer is capable of wavelengths between 200-3000nm<sup>-1</sup>

The 750S is equipped with a 60mm integrating sphere allowing reflectance and total solar reflectance measurements on coated steels as well as being well suited to transmission, total reflectance and diffuse reflectance of solids and powders. It is a

double beam double monochromator system, meaning that the sample beam is compared with a reference beam.

The diagram below (Figure 2-20) shows how both diffuse and specular components of total reflection are captured and is a good indication of the so named integrating sphere.

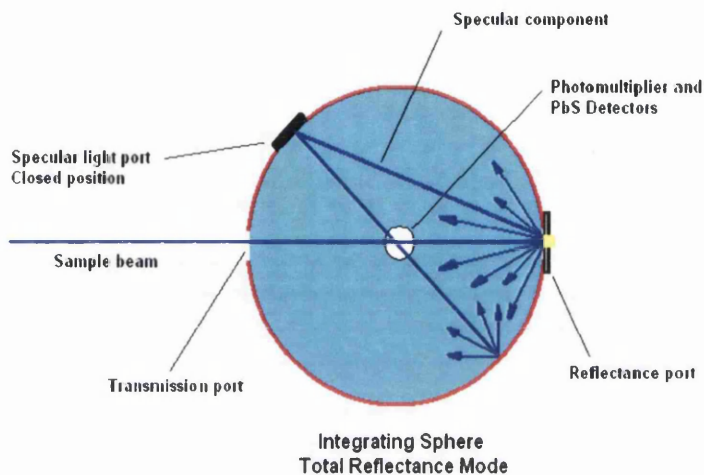


Figure 2-20 Integration Sphere of UV Vis Spectrophotometer

Looking at the absorption/reflectance of wavelengths of a coating can give a plethora of information. This could be an indication of how efficient a UV screening stabiliser works, or a stabilisers performance post weathering. In this experimental series, it was especially useful with regard to giving a representative view of chromophore absorptions, induced by colour change following photodegradation.

The reflectance spectra was collected at timed intervals, during the QUV accelerated weathering of the white plastisol coated steels and free films of the same clear top coats. The coated steels were measured every 300 QUV hours and the free films every 500 hours. This was the case given the free films did not contain a photoactive pigment, thus degradation was not expected to occur so rapidly. Reflectance measurements were taken at 5nm wavelength intervals.

### **2.5.5 Weight Loss Apparatus**

Whilst the combined effect of water and moisture on the fully formulated plastisol samples was being measured after weathering in the QUV, an overview of the stability of the clear coat alone (in the absence of the white plastisol coated steel) was investigated. One such aspect that was investigated was any weight loss during exposure to UVA alone. Along with other techniques, the weight loss was measured incrementally on a laboratory set of analytical scales.

The making of the clear coats free film samples is described in section 4.2.1.1. The free films were placed under a bank of 6 x 8w UVA lamps as used in 2.3.2.1.



## 2.6 References

1. Robinson, A.J., The Development of Organic Coatings for Strip Steels with Improved Resistance to Photodegradation. 2005, Eng. D, University of Wales Swansea
2. Robinson, A.J., Searle, J., and Worsley, D.A., Materials Science and Technology, 2004. **20**: p. 1041.
3. Searle, J.R., Titanium Dioxide Pigment Photocatalysed Degradation of Pvc and Plasticised Pvc Coatings. 2002, Eng. D, University of Wales Swansea.
4. Singh, R.P., Tomer, N.S., and Bhadraiah, S.V., Polymer Degradation and Stability, 2001. **73**(3): p. 443-446.

### **3 The Effects of Humidity on TiO<sub>2</sub> Photocatalysed Photodegradation**

## 3.1 Introduction

Poly(vinyl chloride) (PVC) is a frequent choice of material for a wide range of applications. In its plasticised form, PVC is extensively used for coated steel products due to its flexibility and resistance to damage during the forming process. It also provides an excellent barrier against oxidising elements, which would otherwise corrode the steel substrate. These products, both plasticised and un-plasticised, generally contain large amounts of Titanium Dioxide ( $\text{TiO}_2$ ) to optically enhance the product and in the case of coated steel products, act as a hiding (covering) agent to the steel substrate [28, 29]. However this band gap also means that  $\text{TiO}_2$  can be highly photoactive in nature leading to premature failure in certain high UV environments. Premature failure of both UPVC and PVC products can be caused by the  $\text{TiO}_2$  contained within the matrix. Via numerous complex reactions degradation of the PVC coating eventually results in the formation of Carbon Dioxide ( $\text{CO}_2$ ) Hydrogen Chloride (HCl) and Water ( $\text{H}_2\text{O}$ ).

In previous work [61, 62, 64, 71, 73, 74] it has been shown that the amount of  $\text{CO}_2$  evolved by the photo-catalysed degradation of PVC can be measured using Fourier Transform Infrared (FTIR) spectroscopy. It has also been shown that strong acidic species can have a catalytic effect upon  $\text{TiO}_2$ . HCl produced during photodegradation reacts with water (photo-generated or present in the atmosphere) creating hydrochloric acid which further catalyses the excited  $\text{TiO}_2$  reactions. It is therefore anticipated that variations in atmospheric relative humidity (RH) could affect the overall rate of PVC degradation.

### 3.1.1 Aims and Objectives

In this chapter, the closed loop flow reactor used previously to monitor  $\text{CO}_2$  evolution [19, 63] has been adapted so as to introduce a control on the RH of the system. The work investigates the effects of different RH conditions on the  $\text{TiO}_2$  photo-catalysed degradation of un-plasticised PVC. In addition, the stabilising effects of hydrotalcite mineral pigments within the film, which has the ability to remove chloride ions and release carbonate (making the photo-generated acid weaker) will be addressed.

In order to validate the results, the same experiment was carried out for an alternative polymer, polyethylene (PE) and compared to the literature, to ensure the phenomena seen was not symptomatic of the experimental procedure, and offer an insight into effect atmospheric conditions has on polymer photo-degradation.

## 3.2 Experimental Procedure

### 3.2.1 Model PVC Coatings

Degradation studies were carried out using a simple model UPVC paint system as outlined in 2.1.1.1 and Table 3-1. The formulation consisted of 3 grams of pigment (Degussa P25 TiO<sub>2</sub> which is highly photoactive, 10g of laboratory grade PVC (Aldrich MW ca 95000) and 100ml tetrahydrofuran (THF). This equated to a pigment loading of 30% weight for weight or 30 PHR (per hundred resin). For studies using Hydrotalcite (HT) additions, the TiO<sub>2</sub> addition was kept at 3 grams and a varying amount of HT was added prior to addition of the PVC. Glass panels of approximately 7.5cm x 7.5cm were used in the irradiation apparatus.

Table 3-1 Sample Matrix

| Experiment  | TiO <sub>2</sub> (%) | HT (%)       |
|---|----------------------|--------------|
| Varying RH  | 30                   | 0            |
| Effect of HT  | 30                   | 2,6,4,6,8,10 |
| Effect of RH on HT stabilised PVC                         | 30                   | 4            |
| Commercial Comparison (with removal of all HALS and UVAs) | 30                   | 4,10         |

### 3.2.2 Polyethylene Samples

The unpigmented PE (2.1.3) was pigmented with a loading of 30% weight for weight of TiO<sub>2</sub> (Kronos 1001) and samples were subjected to the mixing and pressing regime in the torque rheometer and compression moulder (outlined previously in Chapter 2). To ensure degradation occurred within the timescale of the experiment, it was decided to again use a highly photoactive grade of TiO<sub>2</sub>. In this instance, due

to the nature of sample preparation at elevated temperatures, Degussa P25 was deemed unsuitable; upon heating and mixing severe thermal degradation was evident by a severe colour change.

All polymer mixes were pressed to a thickness of 0.5mm. For testing in the flat panel reactor, two samples from each plaque were made measuring 7.5cm by 7.5cm.

### **3.2.3 Photodegradation Irradiation Apparatus and Data Collection**

The apparatus used, as shown in Chapter 2, irradiates a sample in a closed loop system. The headspace gases are circulated through an FTIR gas cell by a 6 litre per minute diaphragm pump. The FTIR gas cell used Calcium Fluoride ( $\text{CaF}_2$ ) windows which are resistant to the humidity conditions used and had a 10cm path length.  $\text{CO}_2$  concentration was then monitored via FTIR.

The custom written FTIR controller program was used to monitor all experiments. This allowed timed scans to be carried out on the headspace gases within the cell at 10 minute intervals. Using Perkin Elmer Spectrum 6 software, all spectra were scanned between  $6000\text{cm}^{-1}$  and  $1100\text{cm}^{-1}$  at a resolution of  $8\text{ cm}^{-1}$ .  $\text{CO}_2$  concentration calculations were carried out using an area range of  $2210 - 2480\text{ cm}^{-1}$ . The Spectrum software calculates  $\text{CO}_2$  absorbance units (from a known calibration point) with respect to time, giving a  $\text{CO}_2$  evolution plot, from which the rate of degradation can be calculated as seen in Figure 3-1. The apparatus was calibrated by injecting known quantities of  $\text{CO}_2$  and measuring the FTIR response.

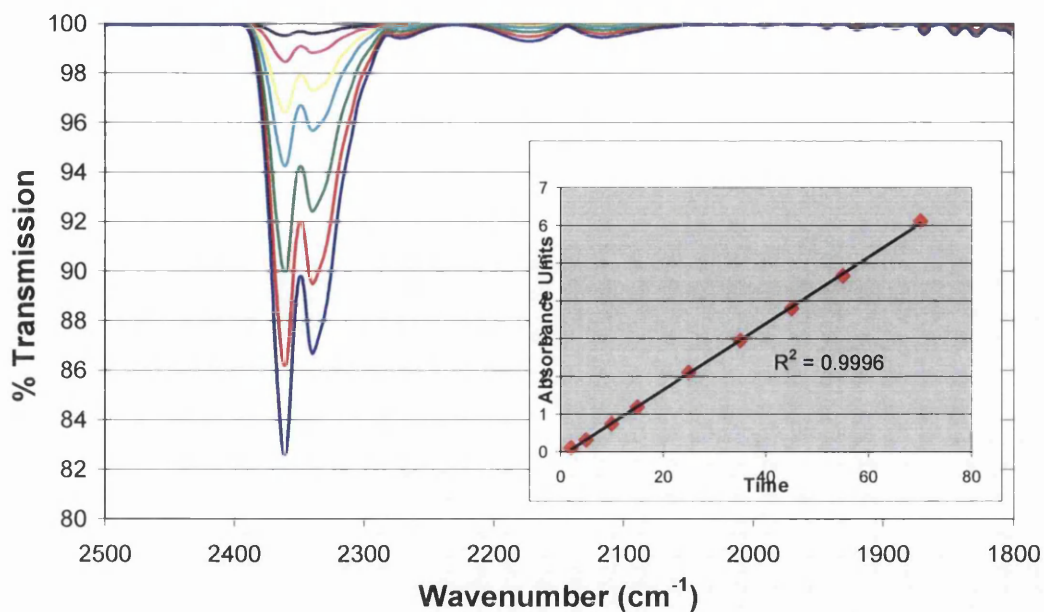


Figure 3-1 FTIR CO<sub>2</sub> Transmission Spectrum as a function of irradiation time for a model PVC/TiO<sub>2</sub> film.

### 3.2.4 Control of Relative Humidity above 32%

The RH within the system was controlled in one of two ways. Firstly, for RH above 32% saturated salt solutions were used where by the head space gas was circulated continuously through a particular saturated salt solution to give a desired RH. The various RH used were obtained using the particular salts shown in Table 3-2.

Relative humidities were obtained from particular saturated salt solutions at room temperatures [76].

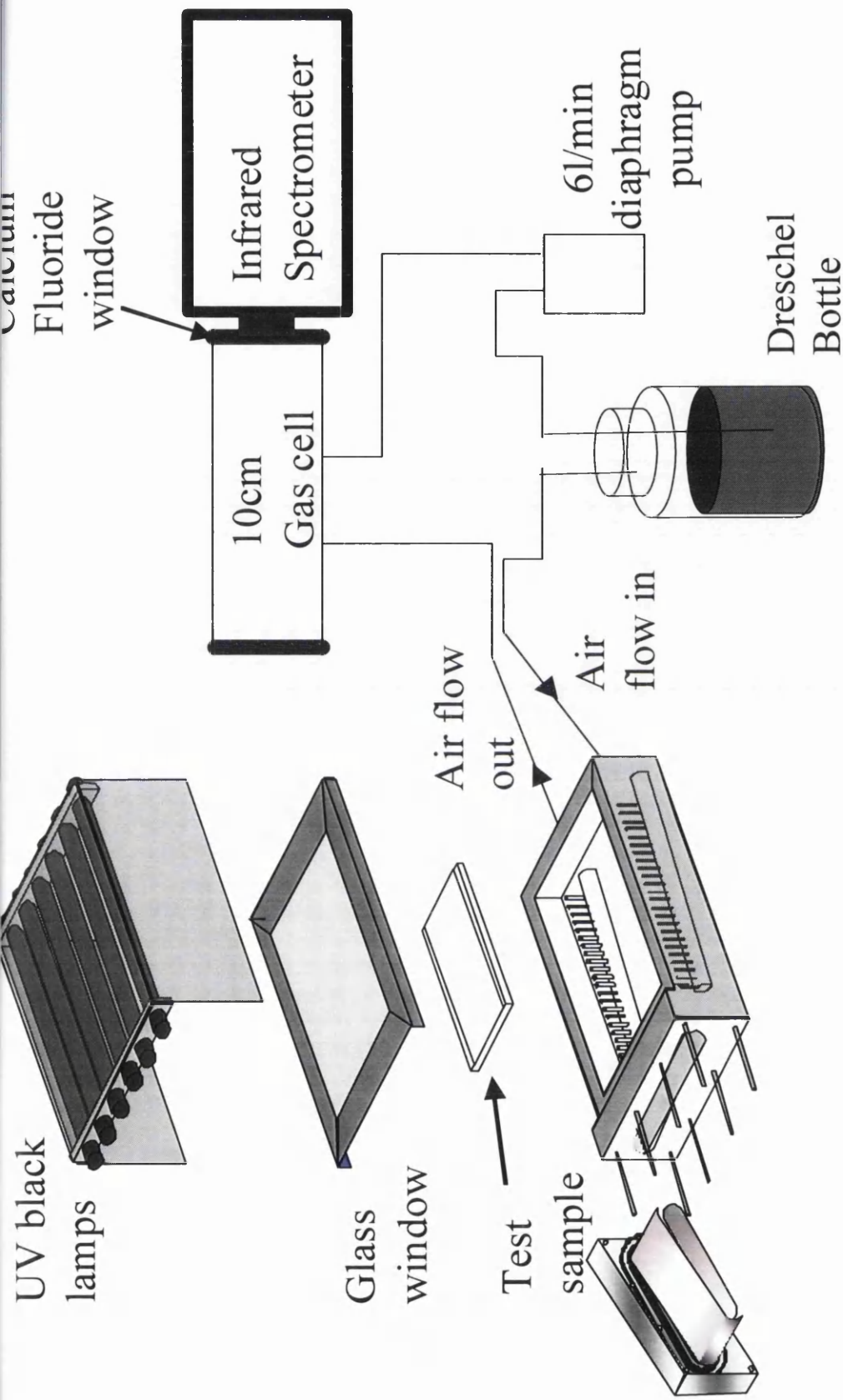


Figure 3-2 Apparatus for In-Situ Control of Relative Humidity above 32%

Table 3-2 Salt Solutions and Respective Achievable Relative Humidity

| Salt               |                      | Percentage R.H (%) |
|--------------------|----------------------|--------------------|
| Potassium Sulphate | $K_2SO_4$            | 98                 |
| Sodium Chloride    | NaCl                 | 77                 |
| Sodium Bromide     | $NaBr \cdot 2H_2O$   | 58                 |
| Calcium Chloride   | $CaCl_2 \cdot 6H_2O$ | 32                 |

Saturated salt solutions were formulated in 500ml Dreschel bottles, with a total volume of 300ml. To prevent the dissolution of  $CO_2$  in the salt solution (carbonic acid formation) the solution was adjusted to contain 2m.mol of nitric acid.

To achieve a zero percent humidity, i.e. complete moisture removal, magnesium perchlorate was used to dry the atmosphere within the system. Similarly, in this instance the head space volume within the Dreschel bottle remained the same at 200ml.

### 3.2.5 In-situ Assessment of Effect of Varying Humidity below 32% RH

When RH's below 32% were used a different technique was required. A humidity meter was placed within the system; this allowed for an accurate "live" RH reading. A bypass loop combined with the Dreschel bottle containing magnesium perchlorate was then used to systematically reduce the RH to the desired level. At desired humidity, the magnesium perchlorate was removed, and experimentation continued. This rapid testing procedure was repeated for a variety of RH. This technique allowed for testing at a wide range of humidities on any one single sample.



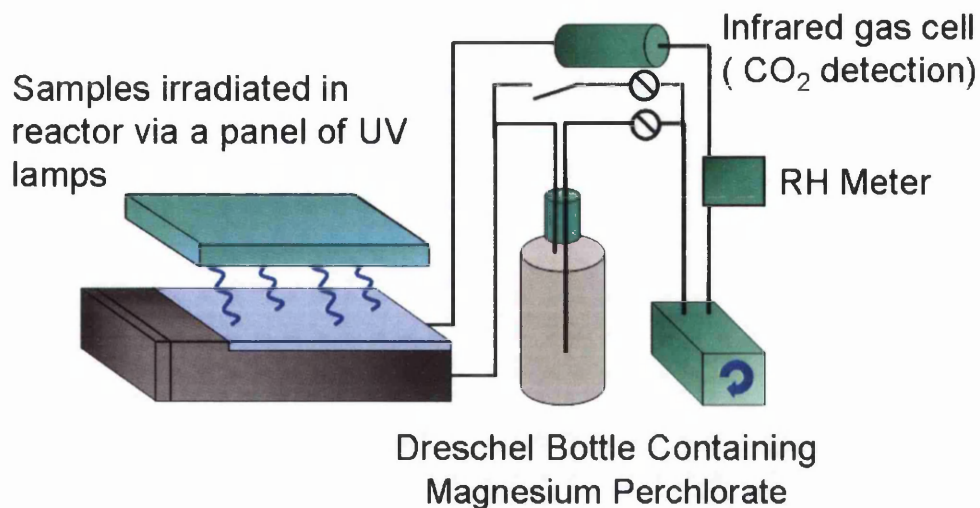


Figure 3-3 Apparatus for In-situ assessment of Effect of Varying Humidity below 32% RH

### 3.2.6 Gloss Retention during QUVA Weathering of Near Commercial HT Containing PVC Plastisol

30% TiO<sub>2</sub> model coating system as made here, with loadings of 4% and 10% HT were weathered and monitored for signs of degradation. In addition to this, they were compared to a commercial specification PVC plastisol sample with all UVAs and HALS removed.

The sample panels were irradiated using a QUVA accelerated weatherometer fitted with UVA lamps, as outlined in Chapter 2. Each sample was subject to a cyclic exposure of 8 hours UVA radiation and 4 hours condensation. In every 24 hour period this allows two complete cycles. The temperature for both cycles (UV and condensation) was set at 40 degrees and a light intensity of 0.68W/m<sup>2</sup>/nm.

Gloss was measured with the Minolta Multi-Gloss 268 at 60°, at 300 hour intervals.

### 3.3 Results and Discussion

#### 3.3.1 Effect of TiO<sub>2</sub> addition on PVC Photodegradation in Ambient Conditions

Figure 3-4 is typical CO<sub>2</sub> evolution profile for a UPVC film containing 30 PHR Degussa P25 TiO<sub>2</sub> and is typical for UPVC containing high photo-activity TiO<sub>2</sub>. This has been reported elsewhere and is believed to be related to HCl production [62] Figure 3-5 illustrates the mechanism of this formation.

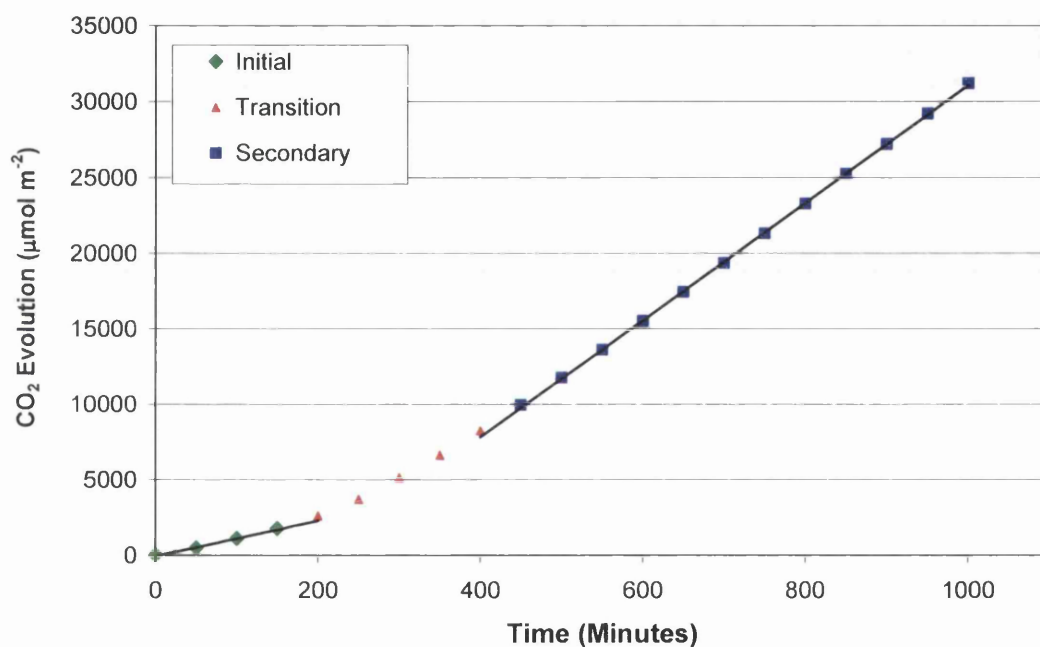


Figure 3-4 Typical CO<sub>2</sub> evolution kinetics from a 30PHR TiO<sub>2</sub> PVC film irradiated under typical lab conditions of ca 40% relative humidity.

It can be seen that for a control experiment (no stabiliser additions) there is an initial linear rate of CO<sub>2</sub> evolution over the first 200 minutes which then changes to a secondary much faster linear rate. In experiments reported [50], it has been found that strong acids, such as the proven evolution of HCl during TiO<sub>2</sub> pigmented PVC photodegradation, are capable of accelerating TiO<sub>2</sub> photo-catalysed reactions

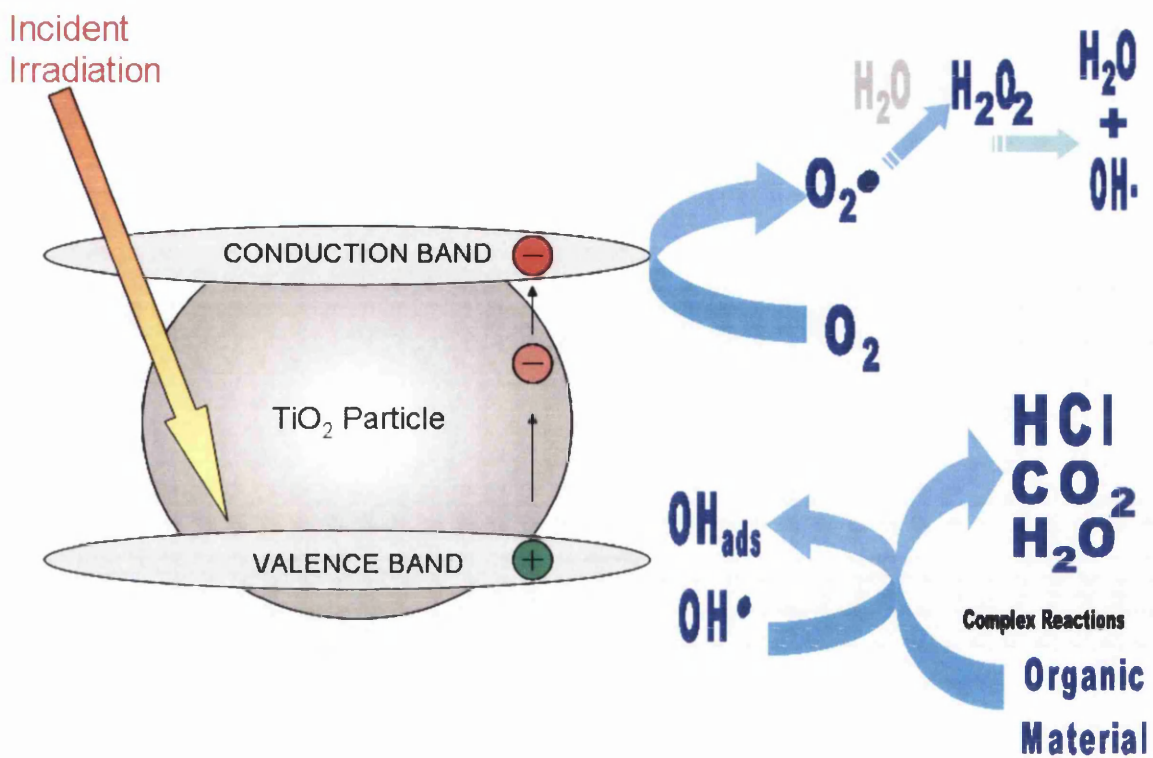


Figure 3-5 The Mechanism of  $\text{TiO}_2$  Catalysed PVC Photodegradation

The ratio between the secondary and initial rates for a 30 PHR  $\text{TiO}_2$  PVC film is approximately 3:1 under normal lab conditions (ca 40% RH). In other  $\text{TiO}_2$  containing organic systems it has been found that strong acids are capable of accelerating  $\text{TiO}_2$  photo-catalysed reactions [77] and it seems that this is the most likely explanation for the rate changes observed.

### 3.3.2 The Effect of Humidity on UPVC Photodegradation

As described earlier a Dreschel bottle containing saturated salt solutions was connected into the closed loop system causing the headspace within the system to maintain a set relative humidity. Figure 3-6 and Figure 3-7 shows the effect varying levels of relative humidity have on the secondary rate of CO<sub>2</sub> evolution.

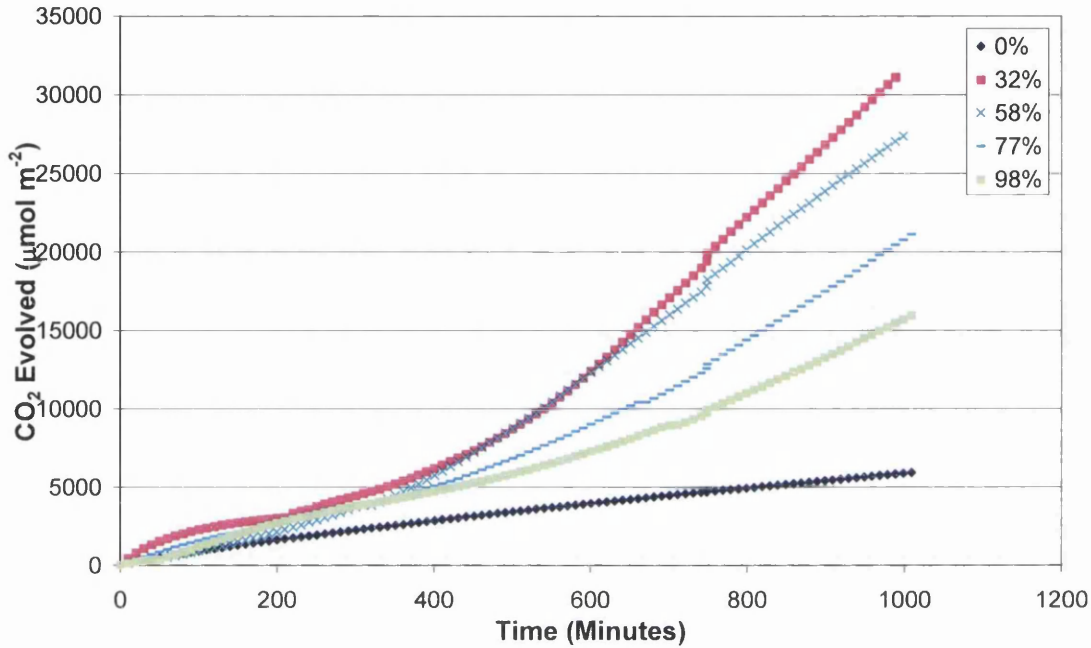


Figure 3-6 Typical CO<sub>2</sub> Evolution Profiles for UPVC in Varying Relative Humidities

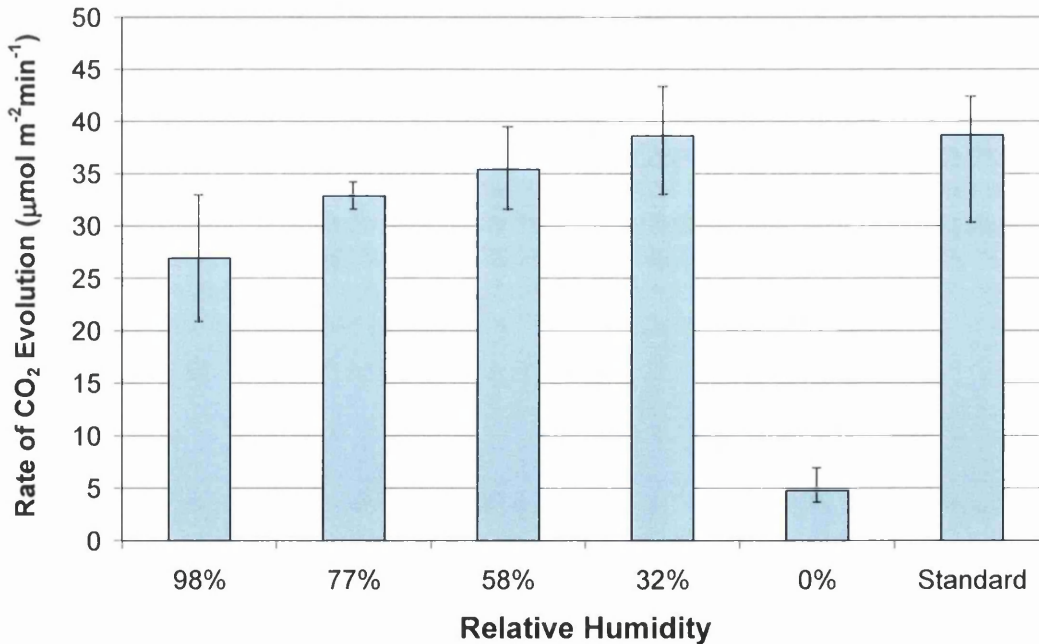


Figure 3-7 CO<sub>2</sub> Evolution Rates for UPVC at Varying Relative Humidities Controlled Using Saturated Salt Solutions

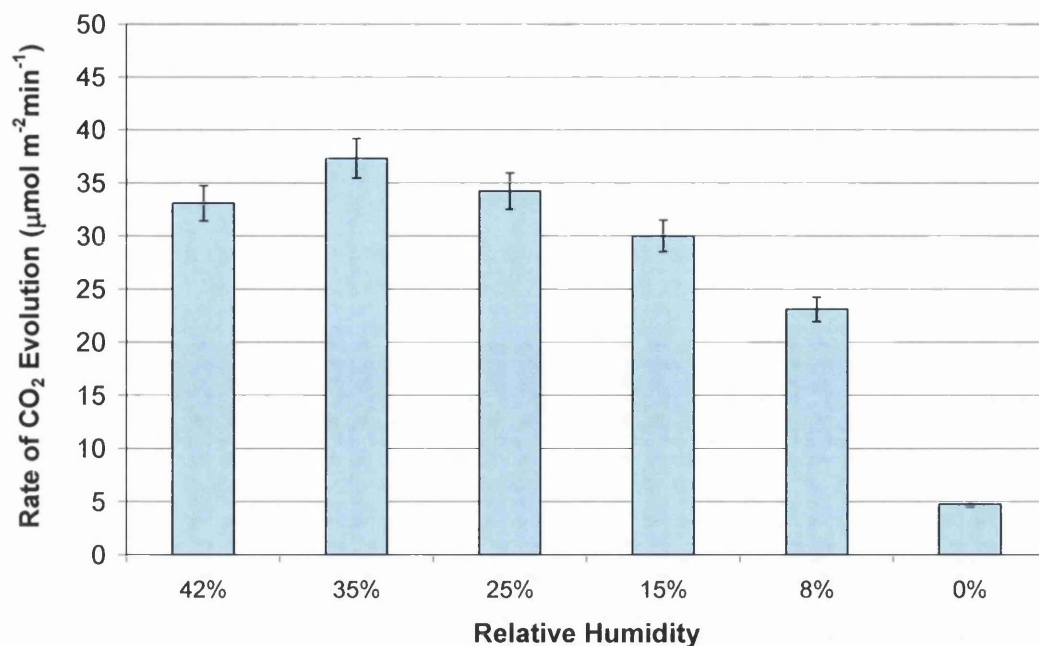


Figure 3-8 CO<sub>2</sub> Evolution Rates for UPVC at Relative Humidities Less Than 43%

The 'standard' result is that of a normal laboratory air set up, with no salt solution present meaning the RH within the apparatus is initially at the same level as the ambient laboratory ca 40% as shown in Figure 3-4. Decreasing the RH from 98% to 32% increases the secondary photodegradation rate. However, reducing the RH to 0% with the use of the magnesium perchlorate lowers the secondary rate of CO<sub>2</sub> evolution and thus the rate photodegradation very significantly.

As the RH is increased (between 32% and 98% RH), the ability of the H<sub>2</sub>O formed in the degradation of the PVC to evaporate decreases, increasing the H<sub>2</sub>O concentration within the paint film. HCl is one of the main photodegradation products and the effective increase in water within the film as RH increases appears to reduce the concentration of hydrochloric acid which reduced the catalytic effect. Obviously at 0% RH there is no water present and so HCl gas cannot form hydrochloric acid and is simply lost to the headspace.

In the second series of experiments the RH was controlled precisely between 0% and 42% (Figure 3-8) by including an in-situ humidity meter and a drying tube which could be switched in and out of the flow system. This enabled very accurate control of the RH values and the effects on the secondary rate of CO<sub>2</sub> evolution.

Again this data shows that the highest degradation rate occurs at around 35% RH. Once the RH is reduced further, the rate of CO<sub>2</sub> evolution and thus photodegradation appears to be less severe. In this instance, at lower levels of RH there appears to be insufficient H<sub>2</sub>O present in the system for hydrochloric acid to form, reducing any possible catalytic effect on the TiO<sub>2</sub>. In addition, it is likely that water in itself is important in the photo-catalytic process in terms of regenerating surface bound hydroxyl radicals that initiate the photodegradation of the PVC.

### **3.3.3 The Effect of Hydrotalcite Addition on UPVC Photodegradation**

As previously reported [50, 78], preventing the acid catalysis by including HT (an ion exchange pigment) within a UPVC paint reduces the rate of TiO<sub>2</sub> photo-catalysed oxidation. In a typical CO<sub>2</sub> evolution profile for a model UPVC film (in a standard experimental set up) containing 5% HT, the initial rate is similar to the secondary rate and there is no acid catalysis effect as can be seen in Figure 3-9.

The HT is a magnesium aluminium double layer hydroxide, with exchangeable ions in the interlayer spacing. The HT is able to exchange carbonate from its structure for chloride produced as hydrochloric acid in the film (Figure 3-10). The resulting carbonic acid is a much weaker acid and cannot catalyse the TiO<sub>2</sub> as effectively.



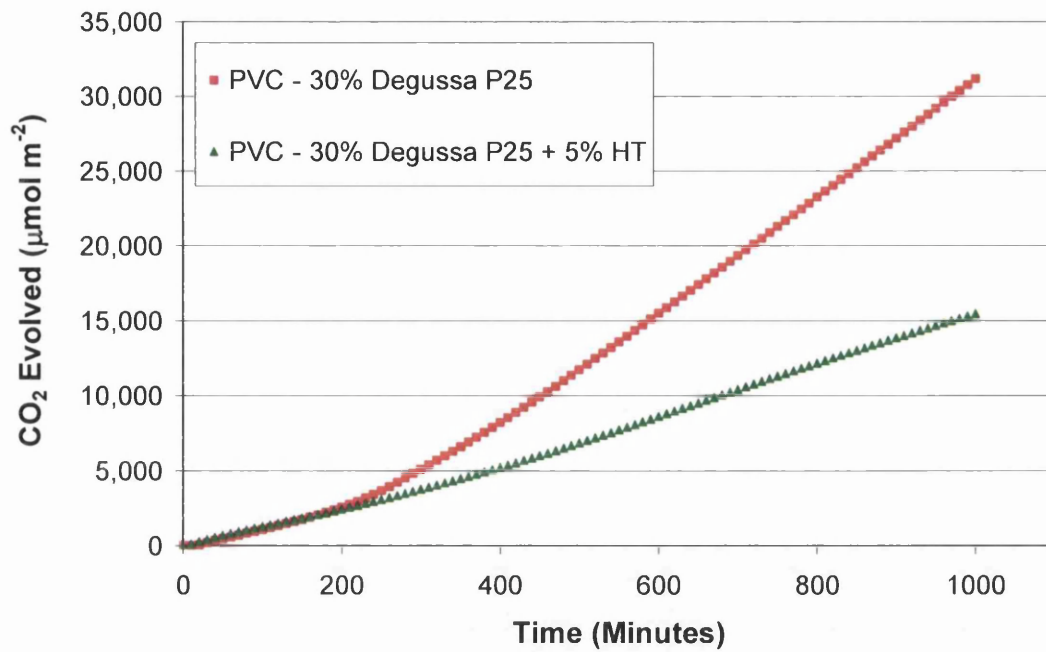


Figure 3-9 Typical CO<sub>2</sub> evolution Kinetic Effects of a 5% (PHR) HT Addition on of a 30PHR TiO<sub>2</sub>/PVC film

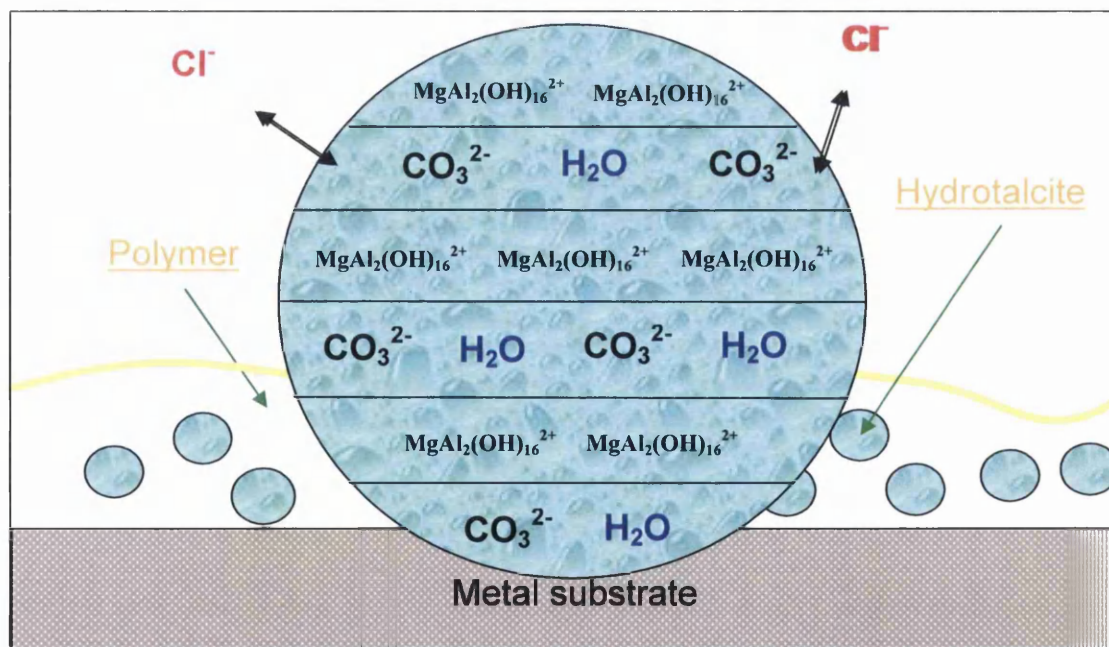


Figure 3-10 Schematic of Ion Exchange Mechanism [50]

### 3.3.4 The Influence of Varying Levels of HT Addition

The UPVC was pigmented with 2, 4, 6, 8 and 10% weight for weight loadings and irradiated in the flat panel reactor at a RH of 32%. The scale of CO<sub>2</sub> volume is significantly reduced and now more comparable to that of a non TiO<sub>2</sub> pigmented polymer, indicating that indeed the HT is effective in counteracting the acid catalysis that was previously occurring.

As seen in Figure 3-9, the extent of the acid catalysis can be seen by the change in initial rate to the secondary rate. In the presence of HT, as it effects this transition in degradation rate, there is little or no change in the rate of CO<sub>2</sub> is evolved. Figure 3-12 shows the rate ratio which illustrates the effectiveness of the HT in removing the catalytic effect of HCl since a rate ratio of 1 will indicate no acceleration in rate as a result of photodecomposition products interacting with the TiO<sub>2</sub>.

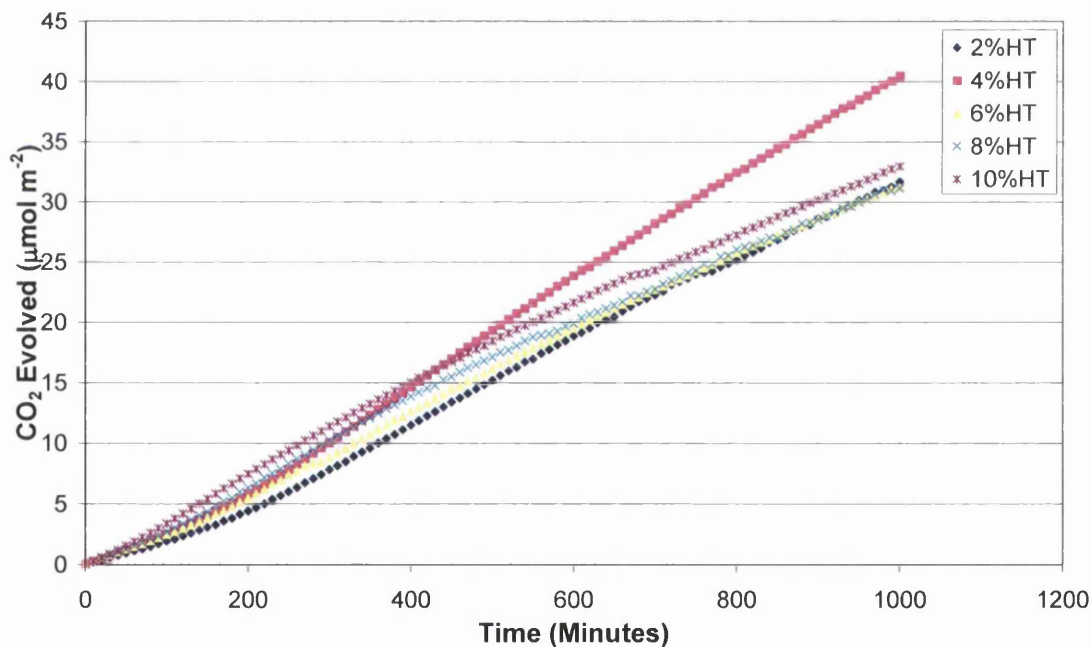


Figure 3-11 Typical CO<sub>2</sub> Evolution Profiles for HT Pigmented UPVC



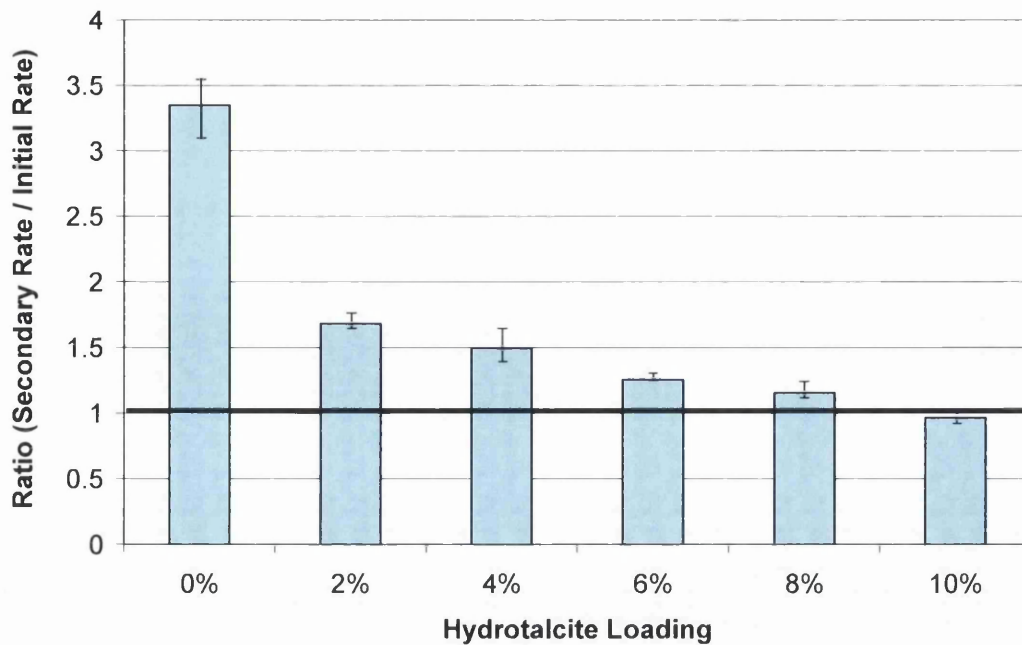


Figure 3-12 CO<sub>2</sub> Evolution Rates for HT Pigmented UPVC at 32%RH

Figure 3-12 shows the effectiveness of varying levels HT additions at the most aggressive humidity condition, found in this work, of 32% RH. This clearly illustrates that the HT has a powerful effect in reducing the acid catalysis effect in UPVC paint, with increasing amounts of HT reducing the extent of degradation.

Interestingly, at this RH, HT only becomes truly effective at eliminating acid catalysis at additions of at least 10%. Despite this, it is still a powerful stabiliser, as seen by the reduction in rate ratio, with only a 2% addition. In addition, it should be noted that at loadings of around 5% it is effective under standard lab humidity levels of around 40% as shown in Figure 3-9.

### 3.3.5 Influence of Humidity on the HT Stabilised System

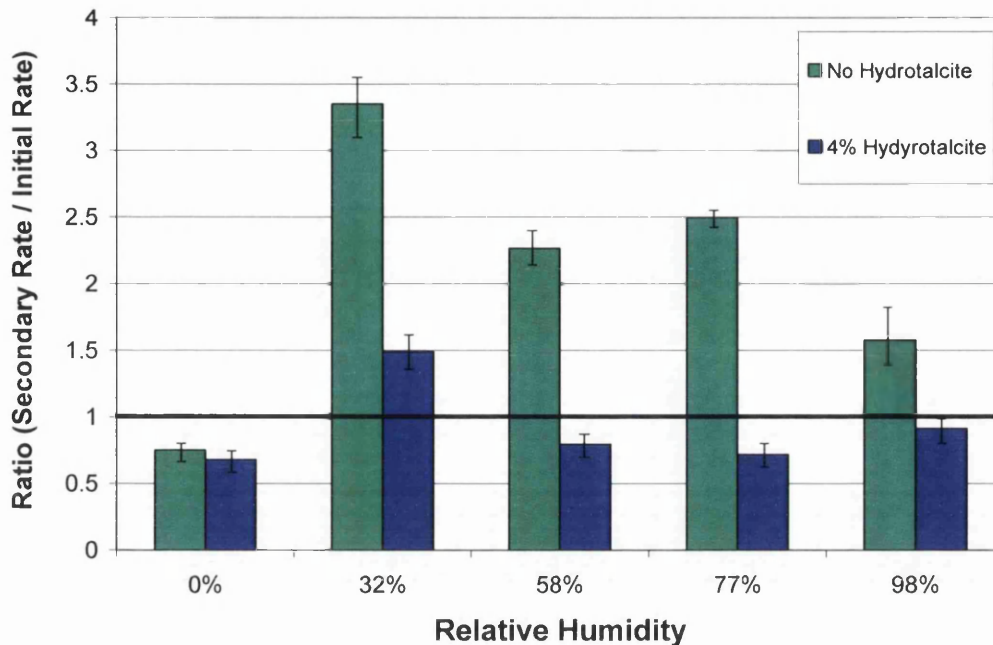


Figure 3-13 The Effect Of Varying RH on 4%HT UPVC CO<sub>2</sub> Evolution Rates

To illustrate the effects of HT additions concentrations at different humidities, a 4% HT sample was irradiated. Figure 3-13 shows the influence of a 4% HT addition to 30PHR TiO<sub>2</sub> UPVC films at a variety of RH values. Again the data is presented as a secondary to initial rate ratio since a value greater than 1 indicates catalysis by the photo-generated hydrochloric acid. At all RH, the HT is successful at reducing the rate ratio.

Here it can be seen that it is only at the RH values of around 30% that the HT is ineffective at lower loadings. This work however is of course of significance in that in any drying phase in full sun, the coating or pigmented PVC would experience changing levels of moisture and this work indicates that the highest rates of degradation for TiO<sub>2</sub> pigmented PVC will occur in full sun conditions when the RH passes through ca 30%.

Interestingly, even at 0% RH the HT is still effective at marginally reducing the rate ratio indicating that despite efforts, complete moisture removal from the system was unlikely.

### 3.3.6 The Effect of HT Addition on Gloss Performance of Weathered PVC Samples

Whilst the data described in this chapter clearly identifies HT as a suitable additive to assist in reducing the extent to which photocatalysis occurs, additional measurements were taken to monitor the influence it has on other indicators of premature coating failure, such as reduction in gloss. Similarly, the process also gave an indication as to whether using HT would be commercially viable in terms of the production process.

A commercial plastisol PVC (HPS 200) pigmented with 20% TiO<sub>2</sub> (Kronos 1001) was formulated in the absence of any HALS or UVAs (usually included in such a formulation). The gloss values during QUVA weathering were measured for such samples and in addition samples with a 4% and 10% HT addition. The change in gloss after weathering can be seen in Figure 3-14

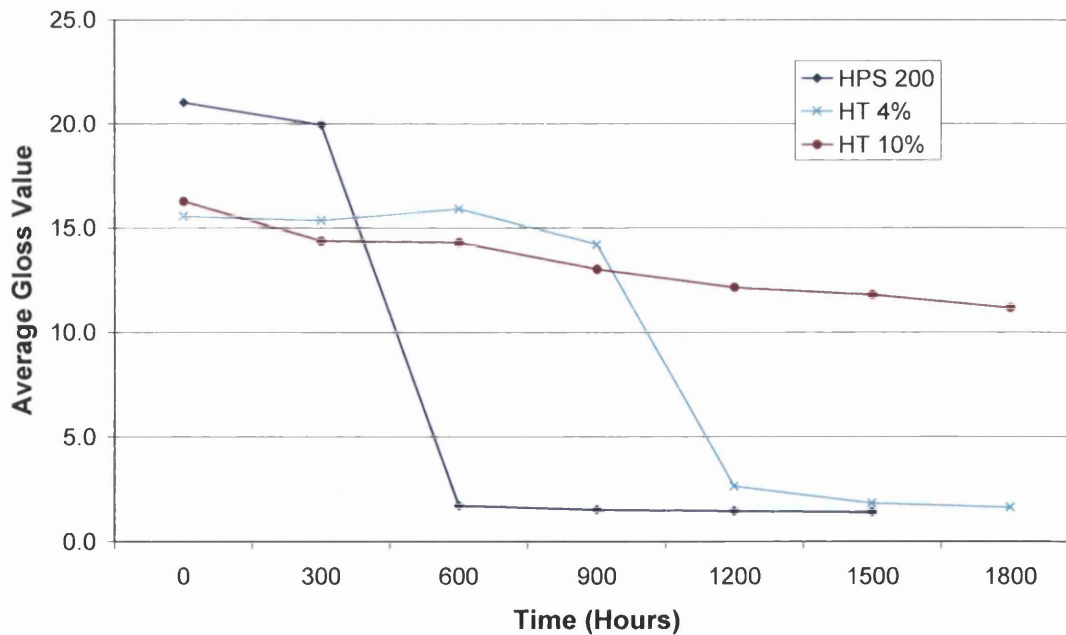


Figure 3-14 The Change in Gloss Level After QUVA Weathering

Although appearing to reduce the initial gloss value of the HPS200 prior to weathering, the success of HT as a stabiliser during weathering is very clear. After just 300 hours of weathering, the gloss of HPS200 reduced significantly and chalking was evident and similarly at a 4% loading of HT, at approximately 900 hours of weathering the integrity of the sample begins to become impaired with significant chalking apparent. This is a significant improvement with only a low level addition of 4%. At a higher addition of 10%, after 1800 hours of weathering, the gloss level has only fallen by 15% when both other samples were considered failed.

### **3.4 The Effect of Humidity on Polyethylene**

#### **Photodegradation**

30% (PHR) TiO<sub>2</sub> pigmented PE samples were subjected the same testing regime, irradiated in the flat panel reactor at different RH controlled by salt solutions and CO<sub>2</sub> profiles were collected.

Results shown here confirm that the phenomena seen with PVC photodegradation and differing RH is in fact a result of the degradation mechanisms occurring, not an artifact of the experimental process. The evolution profiles seen in Figure 3-15 allow for a comparison of evolution rates as before (Figure 3-16).

In contrast to the previous results with PVC, in the presence of increasing humidity, the rate of degradation increases also. The most significant increase is between 0% RH and 32% RH and smaller incremental increases thereafter, up to 98% RH.

Despite being considered a photo-stable polymer Figure 3-17 shows greater rates of degradation of PE than PVC. This is likely to be attributed to a greater degree of reactive species evident as a result of the high temperature sample making process, in the absence of any heat stabilising additives.

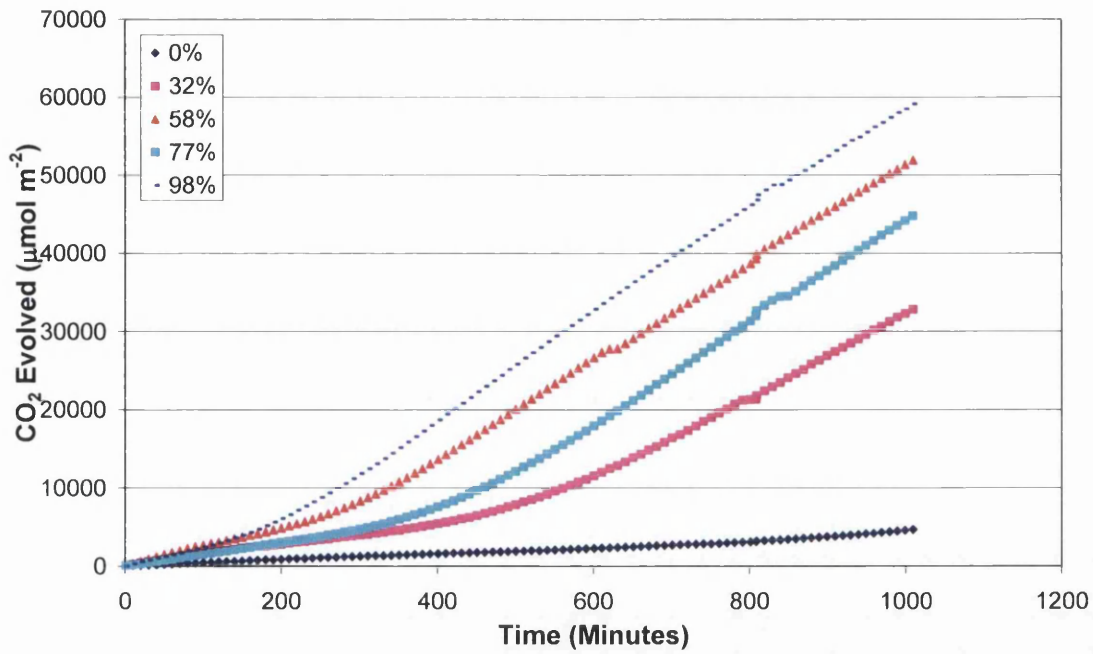


Figure 3-15 Typical CO<sub>2</sub> Evolution Profiles for PE at Varying RH

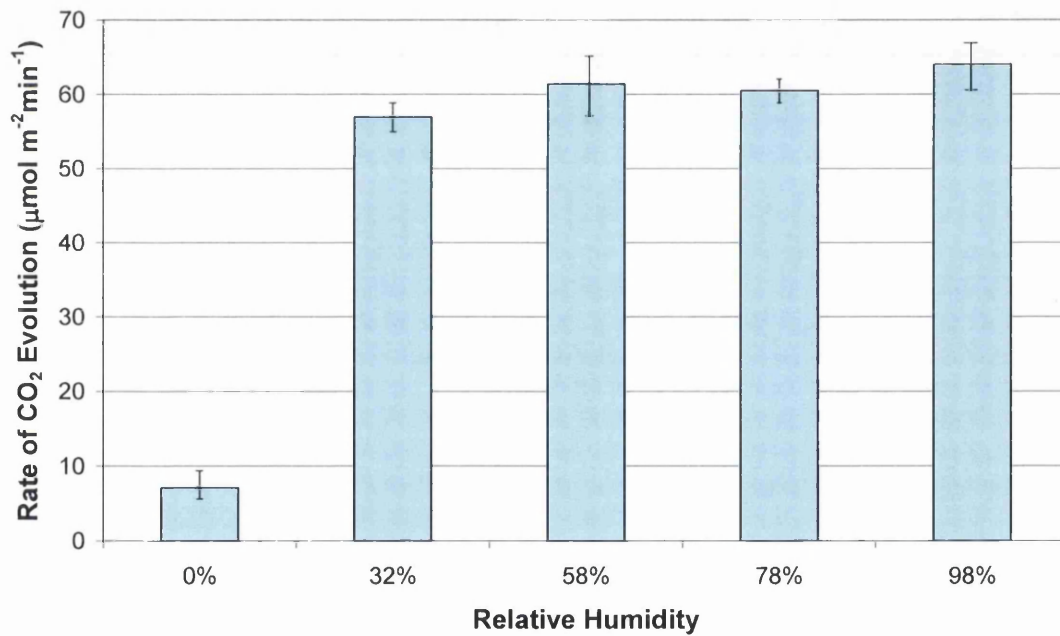


Figure 3-16 CO<sub>2</sub> Evolution Rates for TiO<sub>2</sub> Pigmented PE at Varying RH

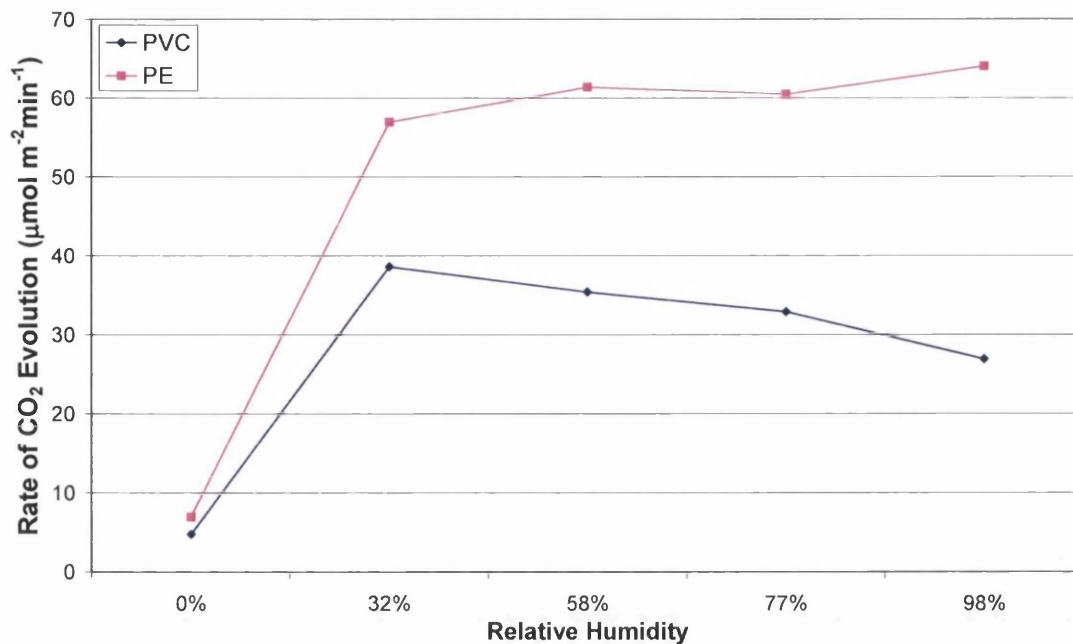
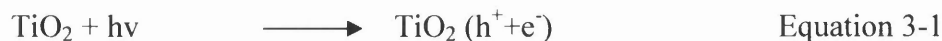


Figure 3-17 Comparison of the CO<sub>2</sub> Evolution Rates for TiO<sub>2</sub> Pigmented PE and PVC at Varying RH

The increase in degradation of PE seen here with increasing humidity is consistent with evidence seen in literature [79] whereby the intensity of the CO<sub>2</sub> band was used to measure degradation in a similar technique. In this instance both Anatase and Rutile pigments were used to investigate if the TiO<sub>2</sub> particle would influence the photodegradation. The difference that was noted helps to outline that TiO<sub>2</sub> plays a role in the degradation of pigmented PE at varying humidities; the Anatase pigmented PE responding more sensitively to humidity than Rutile pigmented PE.

Hydroxyl radical (OH•) is the primary oxidant in TiO<sub>2</sub> catalysis and after excitation of band gap OH• is produced by reaction of photogenerated hole and adsorbed water.

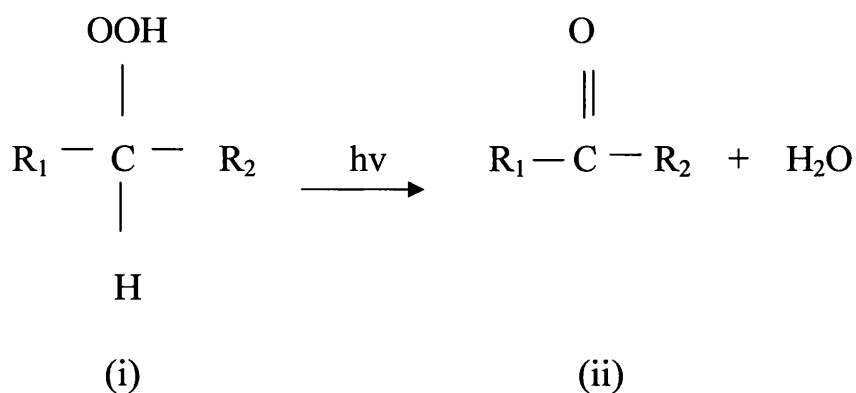


The reaction of the electron hole with water adsorbed on the TiO<sub>2</sub> surface results in the formation of the primary oxidant OH, as is the case with electron hole reaction

with hydroxyl anions. The highly active radical species present then has the potential to attack organic molecules.

However, although not shown in this thesis, this does not explain the increase in CO<sub>2</sub> evolution seen in the investigations of Fernando and Egerton et.al [79], whereby unpigmented PE was investigated in the same experiment and showed the same phenomena, indicating that an additional mechanism must be occurring within the bulk polymer to account for the increase in degradation seen. Egerton et.al. explored the theory discussed by N.S.Allen et.al[11] who attributed a similar phenomenon in polyesters to hydrolysis. Given polyesters are a product of the photodegradation of PE (see Eq 3-4 to 3-6) hydrolysis is possible with the formation of smaller ester molecules that are susceptible to photodegradation.

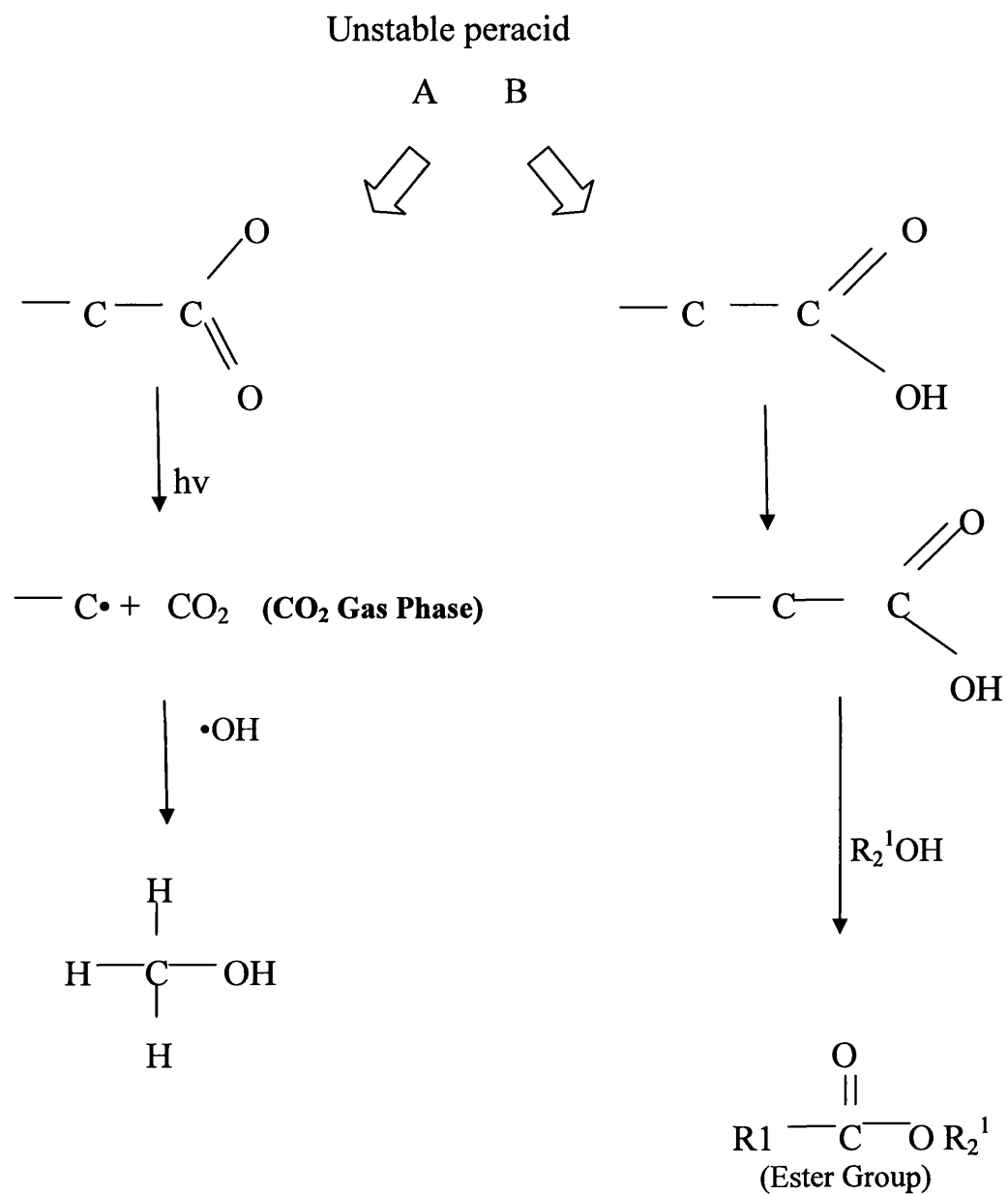
In the presence of UV, the hydroperoxides (i) undergo reactions resulting in the formation of a ketone (ii) and subsequently an alcohol species (iii) and unstable radical transition (iv to v). The resultant unstable peracid will result in the formation these ester groups (vi):



Equation 3-4: Hydroperoxides undergo reaction resulting in the formation of a ketone







Equation 3-7: Reaction scheme showing formation of CO<sub>2</sub> and ester groups

### 3.5 Conclusions

The data presented in this chapter shows the extent to which atmospheric humidity conditions, in addition to UV irradiation play a role in the photo-catalysed degradation of UPVC. The photo-mineralisation of UPVC containing  $\text{TiO}_2$ , in the presence of UV irradiation, is known to produce HCl, and the conversion of this to hydrochloric acid increases the rate of degradation within the UPVC. This is clearly shown since the rate of  $\text{CO}_2$  evolution increases dramatically under normal conditions but not at all when either in conditions of 0% humidity or when an additive is included which removes chloride ions (in this case hydrotalcite).

The highest rate of photodegradation occurs at RH values of 32-35%. At higher levels there is a successive decrease in the rate of  $\text{CO}_2$  evolution and this appears to relate to an effective dilution of hydrochloric acid within the film. At lower RH values it seems that HCl gas can leave the film but it is also likely that water itself is important in the surface hydroxyl radical regeneration mechanisms and this leads to the situation where there is a maximum in photoactivity at around 32-35%.

To control the effects of hydrochloric acid generation in the PVC films which is accelerating photodegradation an ion exchange mineral hydrotalcite (HT) has been used. This removes chloride ions and replaces them with carbonate and the resultant carbonic acid is clearly a weaker acid and unable to catalyse the  $\text{TiO}_2$ . HT is an inert easily handled mineral pigment which is non-toxic and does not present any health risk, and therefore an ideal candidate for incorporation within UPVC matrices and products that might be subject to high UV environments. The data shows that even the most severe cases of degradation, such as at moderate RH values of 32%, HT inclusion has a profound effect on stabilisation. Inclusion of HT at levels of 10% reduces hydrochloric acid catalysis to zero even though a highly photoactive  $\text{TiO}_2$  was used.

In addition, the technique was verified by using an alternative polymer, polyethylene, whereby it was discovered that increasing RH in the presence of UV irradiation increases the rate of photo-oxidation of  $\text{TiO}_2$  pigmented PE. The potential

adsorption of water on the  $\text{TiO}_2$  surface, results in the formation of highly active radical species that have the potential to attack organic molecules, and similarly hydrolysis.

### 3.6 References

1. Barksdale, J., Titanium and Its Occurrence, Chemistry and Technology. 1966: The Ronald Press Company.
2. Boxall, J. and Von Fraunhofer, J.A., Concise Paint Technology. 1977, London: Elek Science.
3. Robinson, A.J., Searle, J., and Worsley, D.A., Materials Science and Technology, 2004. **20**: p. 1041.
4. Robinson, A.J., Wray, J., and Worsley, D.A., Materials Science and Technology, 2006. **22**(12): p. 1503-1508.
5. Searle, J. and Worsley, D.A., Plastics, Rubber and Composites, 2002. **31**: p. 329.
6. Jin, C.Q., Christensen, P.A., Egerton, T.A., Lawson, E.J., and White, J.R., Polymer Degradation and Stability, 2006. **91**(5): p. 1086-1096.
7. Christensen, P.A., Dilks, A., Egerton, E.J., and Lawson, E.J., Journal of Material Science, 2002. **37**: p. 4901-4909.
8. Fernando, S.S., Christensen, P.A., Egerton, T.A., and White, J.R., Polymer Degradation and Stability, 2007. **92**(12): p. 2163-2172.
9. Robinson, A.J., Searle, J.R., and Worsley, D.A., Materials Science and Technology, 2004. **20**(8): p. 1041-1048.
10. Robinson, A.J., The Development of Organic Coatings for Strip Steels with Improved Resistance to Photodegradation. 2005, Eng. D, University of Wales Swansea
11. O'Brien, F.E.M., Journal of Scientific Instruments, 1948. **25**(3): p. 73.
12. Martin, G.P., The Stabilisation of Pvc Using Hydrotalcite (Ht), in Swansea University School Of Engineering. 2008.
13. Worsley, D.A., Mills, A., Smith, K., and Hutchings, J., Chemical Society, Chemical Communication, 1995: p. 1119.
14. Martin, G.P., Robinson, A.J., and Worsley, D.A., Materials Science and Technology, 2006. **22**: p. 375.

15. Fernando, S.S., Spectroscopic Studies of Polyalkene and Polyester Photo-Oxidation, in School of Chemical Engineering and Advanced Materials Newcastle University. 2007, Newcastle University.
16. Allen, N.S. and Edge, M., Fundamentals of Polymer Degradation and Stabilisation. 1992, London: Elsevier Applied Science Publishers.

## **4 The Effect of Clear Top Coats on Improving the Weathering Resistance of PVC Systems**

## **4.1 Introduction**

PVC plastisol products are a popular option for outdoor applications and as outlined in Chapter 1, are susceptible to environmental degradation. Top-coats or clear coat lacquers are one technique of further enhancing the performance of a product in an aggressive environment. However, the balance between cost and performance is an important one.

Top coats are used in a variety of coating systems to improve its performance and lifetime expectancy for that particular application, whether it is ornaments or flat roofing membranes. The benefits of such lacquers can include improved scratch resistance, superior gloss properties and hydrophobic properties for self cleaning. In addition, for outdoor applications they may include a barrier to oxygen and water and provide superior UV resistance.

### **4.1.1 Aims and Objectives**

Where products are succeeding in a market place and there is a high level of demand, there is still a drive to maintain or even improve on market share. This can be via product improvements; e.g. greater product warranties, or cost reduction; lowering the price of the product without sacrificing performance.

This work investigates the potential to improve the weathering resistance of PVC coated steel via the application of PVC clear coats. Series 1 of experimentation has encompassed a brief comparison of how a PVC clear coat performs in comparison to some sophisticated lacquer systems.

Following this, a more comprehensive series of experimentation investigated stabilisation systems intrinsic to the clear coat. Investigations focussed on the removal of stabilisers from the bulk PVC and integrating them into the PVC clear coat and effects on early onset degradation were investigated.

## 4.2 Experimental Techniques

To investigate the effectiveness of clear top coats, commercial lacquer systems were compared. During this preliminary investigation, clear formulations of the HPS200 base system were also applied in the form of the top coat. The base formulation in all cases was applied to pre-primed steel substrate.

### 4.2.1 Sample Preparation

#### 4.2.1.1 Commercial Systems

Commercial specification HPS200 formulations were made pigmented with photoactive grade Kronos 1001, at a weight percent loading of 20%. It is an untreated Anatase unstable photoactive grade of TiO<sub>2</sub>. This base formulation sample alone was produced and tested. For the case of the HPS clear coat sample, a top coat of the same HPS formulation minus the TiO<sub>2</sub> was applied. Further to this, two commercially available lacquers were also applied to the HPS200 base formulation; a high performance clear coat used in the automotive industry and a thermal curing polyurethane. Full details of these systems are covered by a commercial agreement with the supplying paint company.

Table 4-1 Sample Matrix for Commercial Lacquer Comparison

| Sample ID | System                | Thickness (µm) |
|-----------|-----------------------|----------------|
| A & B     | No Top Coat           | -              |
| C & D     | HPS Clear Coat        | 20             |
| E & F     | HPS Clear Coat        | 40             |
| G & H     | BASF High Performance | 40             |
| I & J     | Thermal Cure PU       | 40             |

A 'K Bar' coating bar was used to cast a HPS200 pigmented plastisol which was then semi-cured in the oven at 230°C for ten seconds, before the top coat was applied. The top coat systems were applied on top of the white plastisol and then the entire panel was fully cured for a further 45 seconds at the same temperature, before being water quenched.



#### 4.2.1.2 Fully Formulated Systems

Once again, the HPS200 plastisol formulation was used, with a loading of 20% K1001. In this instance, to test the true effectiveness of a clear coat as a protective barrier to photodegradation, all UVAs and HALS were removed from the bulk HPS200 formulation.

The clear coat applied to the white plastisol was a non-pigmented HPS200 formulation again, to which a variety of UVAs and HALS were to be added in varying levels.

Table 4-2 Stabilisers Tested

| <b>Stabiliser</b>                      | <b>Type</b> |
|--|-------------|
| 2-Hydroxy-4-(octyloxy)<br>benzophenone | UVA         |
| Chimasorb 81                           | UVA         |
| Tinuvin 571                            | UVA         |
| Tinuvin765                             | HALS        |

Table 4-3 Level of Stabiliser Addition

|      | <b>Additive</b>           | <b>0%</b> | <b>0.1%</b> | <b>0.5% *</b> | <b>1%</b> | <b>2%</b> | <b>5%</b> |
|------|---------------------------|-----------|-------------|---------------|-----------|-----------|-----------|
| UVA  | Chimasorb 81              | .         | .           | .             | .         | .         | .         |
|      | Hydroxybenzophenone (HBP) | .         | .           | .             | .         | .         | .         |
|      | Tinuvin 571               | .         | .           | .             | .         | .         | .         |
| HALS | Tinuvin 765               | .         | .           | .             | .         | .         | .         |
| Mix  | Tin Mix<br>(765 + 571)    | .         | .           | .             | .         | .         | .         |

\*Recommended commercial level of addition

An automatic coating bar was used to cast the base pigmented HPS 200 plastisol and this was cured for ten seconds in an oven heated to 230°C to allow a semi-cure sufficient enough to apply the top coat. The combinations of clear coats were applied and each panel was cured for a further 45 seconds and water quenched on removal from the oven. Two samples of each coating combination were prepared for experimentation. Free films of the above formulations were also produced. The formulations were applied to the steel substrate in the same manner using a draw down coater and the non-primed steel panel was then cured for 45 seconds, quenched as before, and the clear coat was easily peeled off the substrate.

## 4.2.2 Accelerated Weathering

### 4.2.2.1 Artificial Weathering QUVA

Both the initial set of samples produced to compare the effectiveness of a variety of commercial lacquers, and the matrix of stabilised clear coats, were subjected to weathering in the QUVA weatherometer (2.5.1)

Each panel was subject to weathering cycles consisting of 8 hours UVA radiation and 4 hours condensation. The panel temperatures for both cycles (UV and condensation) were set at 40°C and a light intensity of 0.68 W/m<sup>2</sup>/nm at 340nm. The light intensity was calibrated every 2 weeks. The panels were weathered for a total of 2100 hrs at which point the HPS200 control sample had failed completely.

#### **4.2.2.2 CO<sub>2</sub> Evolution in the Flat Panel Irradiation Apparatus**

The flat panel reactor used to quantify the photoactivity is outlined in section 2.3.2. The near commercial lacquered samples described in 2.1.1.2 were irradiated in the close loop flow system for typically 20 hours. The CO<sub>2</sub> levels contained by the system were measured via a computer controlled FTIR using a 10cm path length gas cell incorporated in the flow system apparatus. The volume of the CO<sub>2</sub> evolved was calculated via calibration of the equipment with known quantities of CO<sub>2</sub> system.

#### **4.2.3 Gloss and Colour Change**

All the panels were measured for gloss loss with a Minolta Multi-Gloss 268 using the 60° angle setting as described in 2.5.2. Each panel was measured at 5 separate points and the average value recorded. The gloss loss measurements are given as a gloss retention to take into consideration any variance in gloss of repeat samples of the same coating. This is mainly due to the small differences in the curing process so hence the gloss value of a weathered panel needs to be relative to the initial gloss before weathering of that specific panel. The gloss retention is calculated with the following:

$$\text{Gloss Retention (\%)} = (\text{Gloss Weathered} / \text{Gloss un-weathered}) * 100$$

#### **4.2.4 Colour Change Measurements**

Colour was measured in the form of a reflectance spectrum and the difference in reflectance spectrum after total weathering was calculated. The colour reflectance was completed by using a Gretag-Macbeth measuring reflectance over the range 370nm-730nm, but this was not capable of measuring the reflectance spectrum including the gloss component.

In addition to this, the UV visible reflectance spectra was collected at timed intervals on the Perkin Elmer Lambda 750S UV/Vis/NIR, during the QUV accelerated weathering of the coated steels and free films (2.1.1.3) of the same clear top coats every 300 QUV hours. This was also able to give an indication of colour change due to the chromophore absorptions, induced by colour change following photodegradation.

#### **4.2.5 Weight loss**

The weight loss experiments were carried out as detailed in section 2.5.5. Free films of all the clear coat systems described in 2.1.1.3, measuring 8cm by 4cm were placed under UVA lamps for 24 hours each day and the weight was measured every 200 hours for a total test duration of 1400 hours.

#### **4.2.6 Imaging**

To monitor changes to the appearance of the near commercial samples lacquered with a variety of clear coats, the samples were all scanned using a Canon Pixma 870 scanner at 600dpi.

## 4.3 Results and Discussion

### 4.3.1 Commercial Systems

In initial stages of investigating the effect of clear coat lacquers concentrated of comparing 5 systems; a base HPS200 formulation and that of the same base system with a clear HPS200 top coat (20 and 40 microns), a commercially available high performance lacquer and also a commercially available thermal cure PU system. The gloss was measured at 300 hour weathering intervals and gloss retention was calculated as shown below.

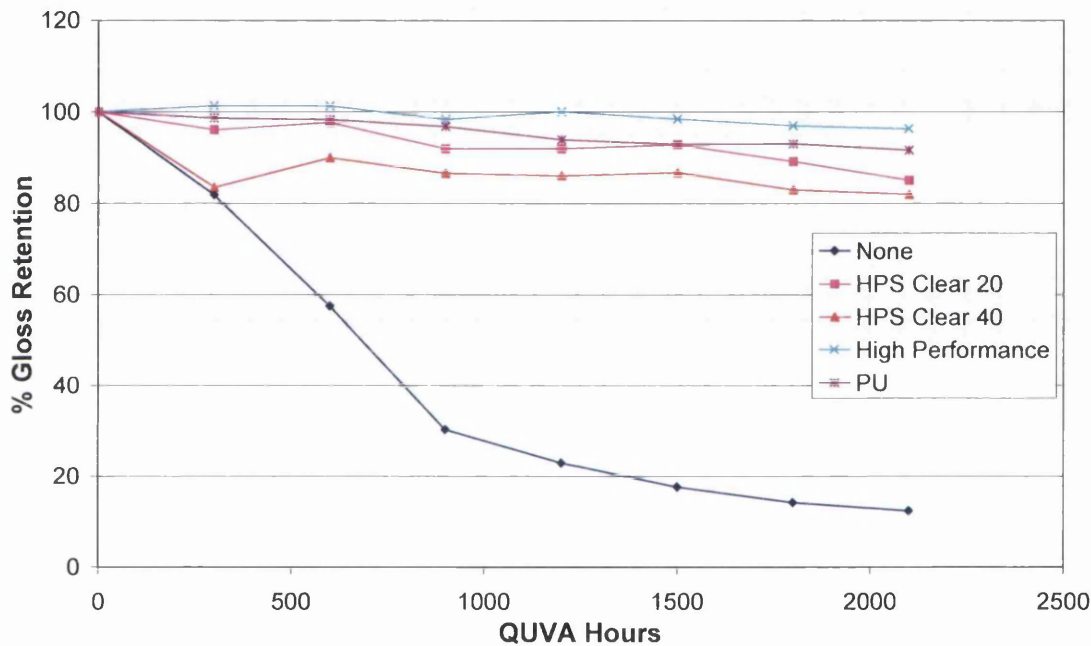


Figure 4-1 Change in Gloss Retention of Near Commercial Lacquered HPS200

The presence of a lacquer system alone has a significant effect of the level of gloss retained. All lacquered systems after 2100 hours weathering still sustain a gloss retention of above 80% whereas the un-coated HPS200 sample exhibits rapid gloss loss after the initial 300 hours weathering. Severe chalking and loss of organic matter was evident, typical of  $\text{TiO}_2$  catalysed photodegradation. The lesser extent of degradation that occurs in the non- $\text{TiO}_2$  pigmented clear coats over this duration means that the reduced level of organic degradation, sustains a coherent top surface layer and thus an improved level of gloss.

As anticipated, the commercially available clear coat systems out perform all others. However, the performance of the HPS clear top coat is promising, with it only performing marginally less well than the commercial ones. Of the HPS clear coats, the 40 micron top coat has a greater reduction in gloss than the 20 micron top coat.

In addition to gloss, the colour change in these samples was also measured. Using the Gretag-Macbeth, Figure 4-2 shows the colour change, shown as  $\Delta E$  after 2100 hours, with positive  $\Delta E$  values indicating darkening of the surface colour.

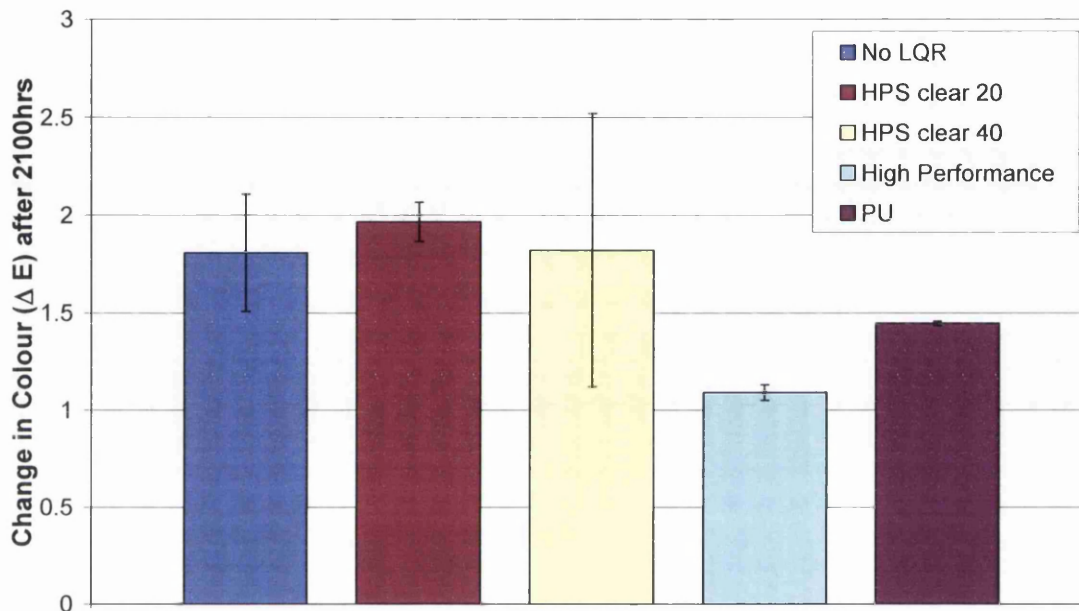


Figure 4-2 Change in Colour of Near Commercial Lacquered HPS200 after 2100hrs Weathering

Colour changes were measured in all samples, however  $\Delta E$  values this small are in fact considered extremely small, with a value around 1 being considered hardly noticeable to the human eye. As anticipated, the high performance and PU commercial systems exhibit the smallest change in colour and of all samples and the colour change across the sample was consistent. With the three HPS200 systems, the colour change was greater and the values similar, despite there being a clear coat in two cases. As the colour change measured is a purely surface concentrated technique, the colour change indicated here is the yellowing of the PVC as a result of UV irradiation that is shown here. As this technique does not taking into account

the gloss component of colour change, it is of little surprise the non-lacquered sample does not differ too greatly, as despite chalking occurring, there will still ultimately be some darkening of the bulk PVC too.

As previously discussed, the reflectance spectra collected on the Lambda 750S UV/Vis/NIR can also indicate the extent and nature of colour change as a result of weathering. The total reflectance was measured between 380nm and 750nm (visible region) for all samples throughout weathering and the change in total reflectance after 2100 hours is calculated.

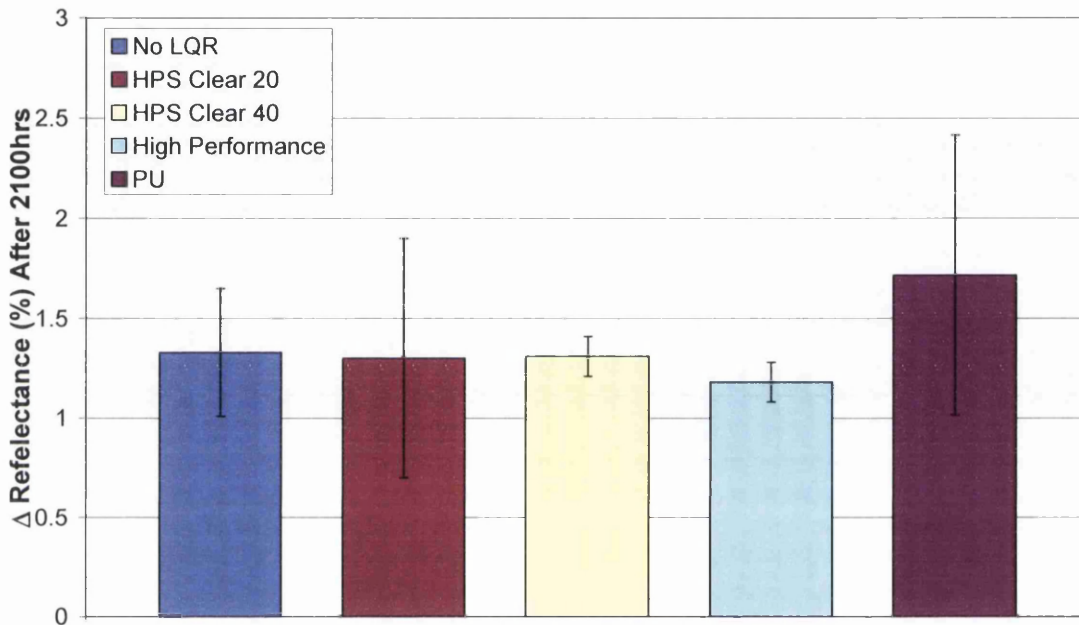


Figure 4-3 Change in Total Reflectance between 350nm and 780nm after 2100hrs Weathering

As with the data collected on colour change from using the Gretag, the colour change in all samples is to the same scale. The non-lacquered sample and clear HPS200 are similar once again, and the high performance lacquer offers the greatest resistance to colour change. However in this instance, the PU lacquer does not appear to perform as well, with the greatest change in colour measured. Rather than being attributed to the degradation of the lacquer, a likely explanation for this lies more closely with the measurement used to measure the colour change. The UV spectrophotometer measurement process to measure colour, also includes the gloss component of colour. It has been reported [80] that during the photodegradation of PU coatings a

phenomena whereby gloss values increase and then fluctuate with weathering. This was attributed to changing polymer properties during initial irradiation symptomatic with  $T_g$  effects and relaxation of the microstructure was suggested. Given the scatter in this result, it is therefore likely that the sample surface has localised fluctuations in gloss. Although the gloss values measured shown in this section still show an overall loss in gloss retention, sample specific increases were also evident (Figure 4-4). Due to the number of repeat measurements taken of gloss value, this ‘increase in gloss’ phenomenon was not apparent in the averaged data for gloss retention.

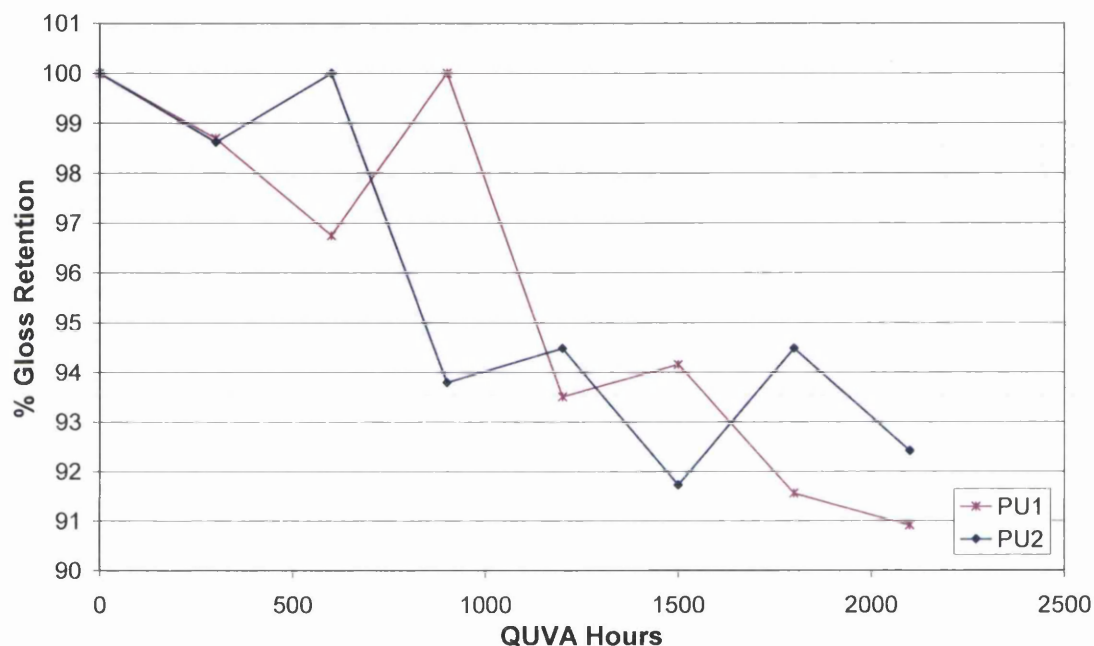


Figure 4-4 Average Gloss Retention Values for 2 PU Lacquered Samples

Looking more closely at the reflectance spectra themselves, Figure 4-6 to Figure 4-10, the regions of colour change can be identified. The superimposed graph (as in Figure 4-5) also shows the wavelengths at which the greatest average change has occurred after weathering, with a positive value indicating an increase in absorbance of a particular wavelength.



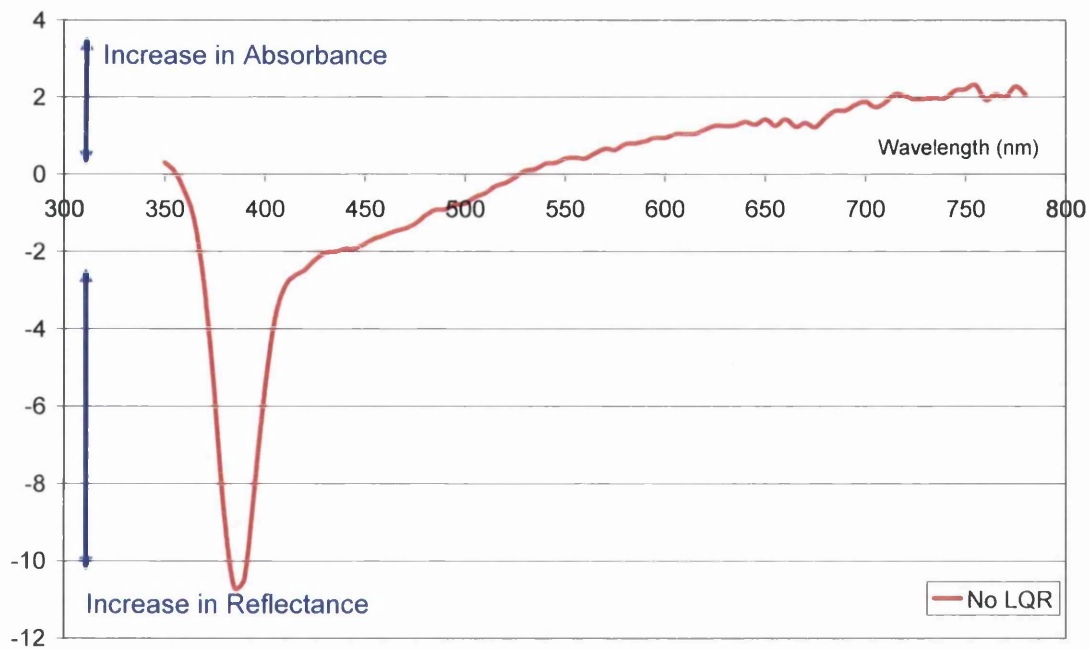


Figure 4-5 The Change in Reflectance at the Respective Wavelength

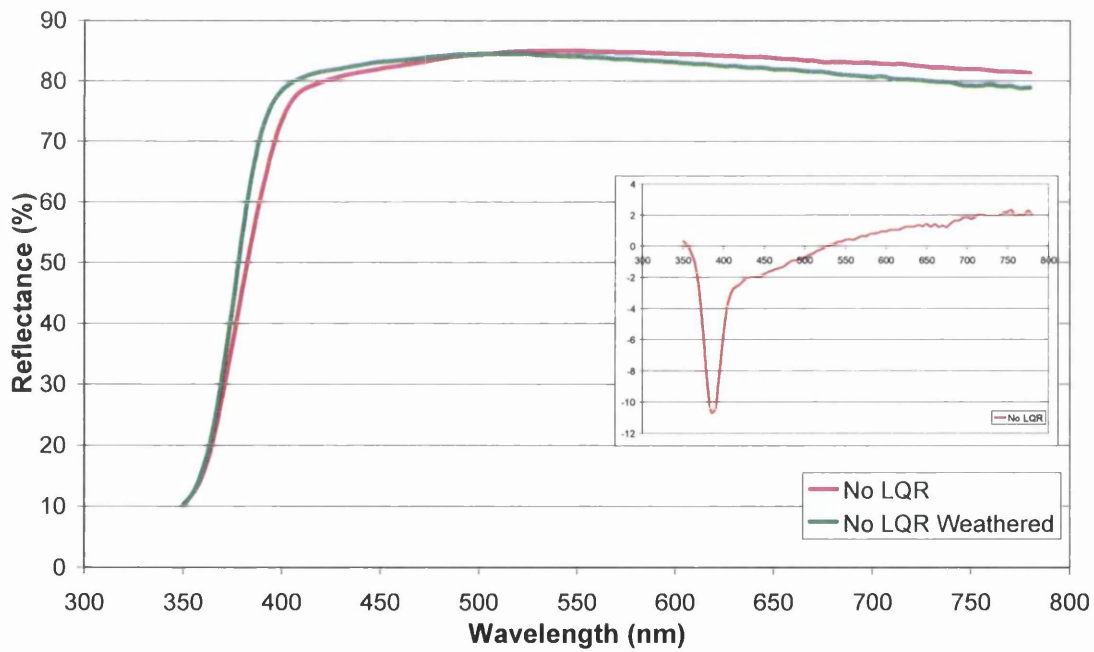


Figure 4-6 Reflectance Spectra between 350nm and 780nm for a Non-Lacquered HPS200 Before and After Weathering

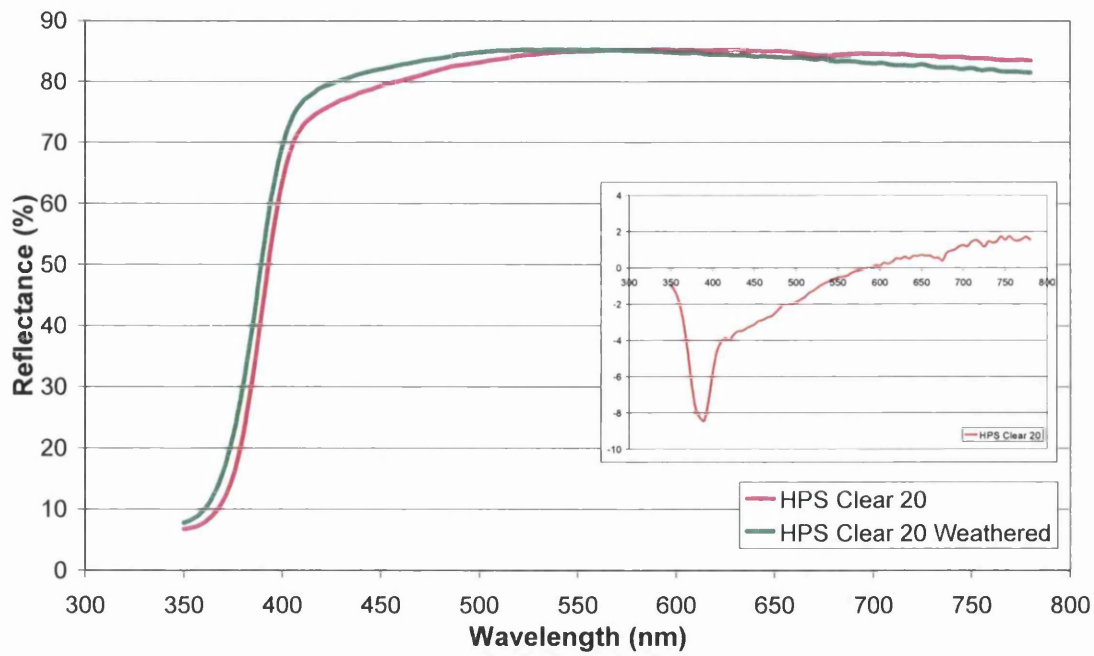


Figure 4-7 Reflectance Spectra between 350nm and 780nm for a 20 Micron Clear HPS200 Lacquered Sample Before and After Weathering

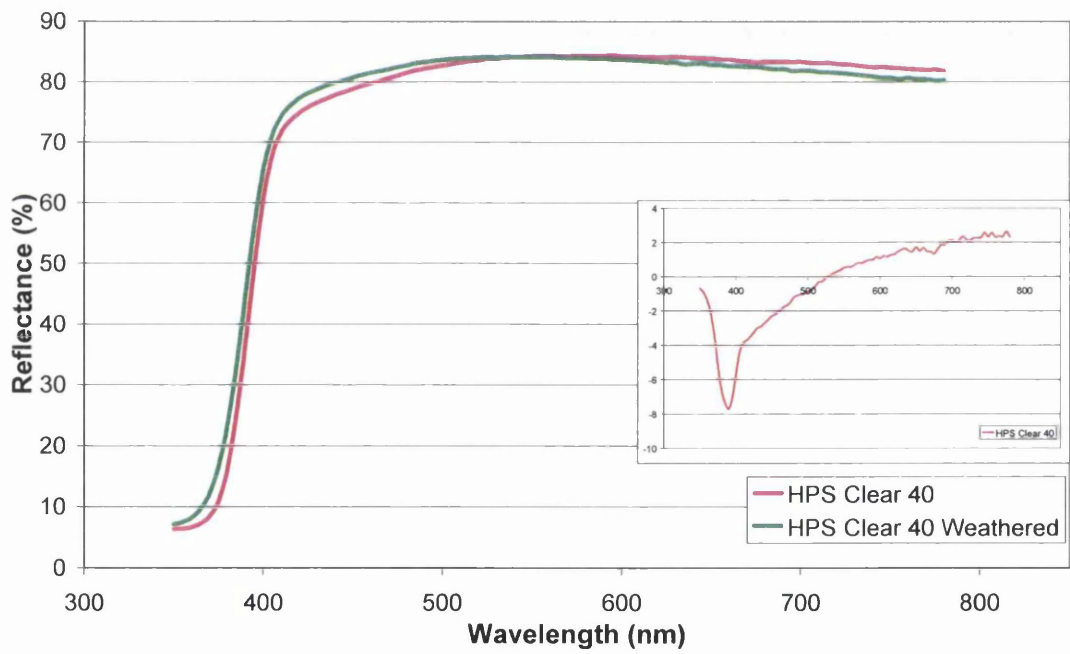


Figure 4-8 Reflectance Spectra between 350nm and 780nm for a 40 Micron Clear HPS200 Lacquered Sample Before and After Weathering

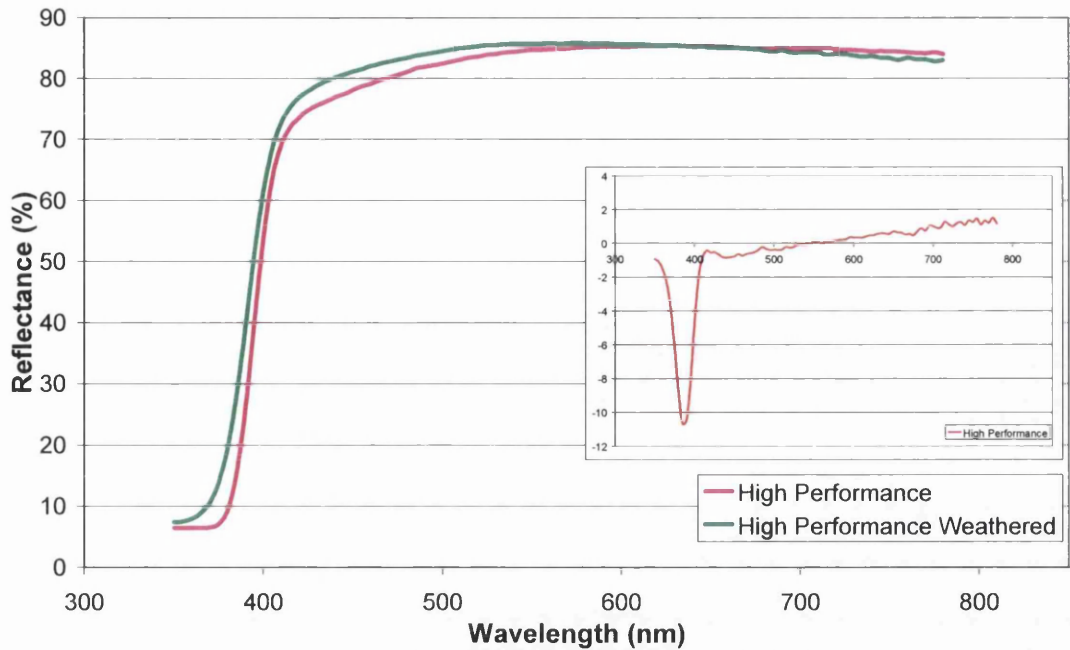


Figure 4-9 Reflectance Spectra between 350nm and 780nm for a High Performance Lacquered Sample Before and After Weathering

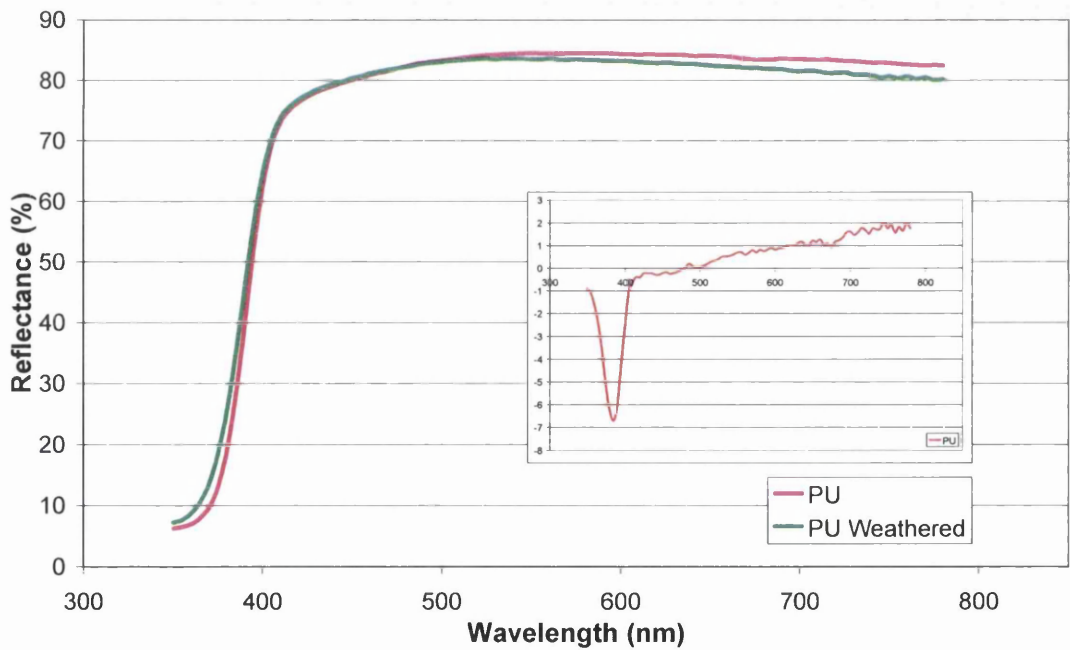


Figure 4-10 Reflectance Spectra between 350nm and 780nm for a PU Lacquered Sample Before and After Weathering

In the case of all samples, after weathering, there is an increase in absorbance above the point of intercept on the superimposed graphs and increase in reflectance below that. The corresponding wavelengths can be seen in Table 4-4.

Table 4-4 Change in Reflectance of the Spectra

|                  | <b>Greatest Change in Reflectance (nm)</b> | <b>Intercept (nm)</b> |
|------------------|--|-----------------------|
| No LQR           | 385  | 525                   |
| HPS Clear 20     | 390  | 580                   |
| HPS Clear 40     | 390  | 525                   |
| High Performance | 385  | 560                   |
| PU               | 385  | 475                   |

All samples absorb greater in the region of wavelengths that correspond with the colours yellow to red in the visible spectrum (~500nm and above) resulting in a darkening of the surface, symptomatic of a greater reflectance in colours such as the violets and blues. The greatest change in reflectance noted in this data is wavelengths encroaching on that of UV excitation of TiO<sub>2</sub>, with weathering appearing to increase the reflectance and thus potentially, resistance of the lacquer to UV penetration. The non-lacquered sample exhibited the greatest degree of reflectance improvement in this region after weathering, which is typical of the screening mechanism offered by TiO<sub>2</sub>, as was the case prior to weathering.

### 4.3.2 Fully Formulated Clear Coat Systems

The previous comparison of the performance of commercially available clear coats highlighted some interesting potential in the use of HPS200 clear coats for lacquering systems, as a cost effective alternative to the more expensive high performance lacquers, for PVC plastisol coatings.

A clear HPS200 formulation was again used as a top coat with a variety of potentially stabilising additives at different levels. The purpose of this was to evaluate if there was any benefit in a stabilising the top coat. This evaluation summarises if stabilising the lacquer has significant benefits over a non-stabilised lacquer, and would potentially allow for the simplification of a pigmented PVC plastisol systems by removal of bulk stabilisation (from pigmented base coat).

Once again, the HPS200 plastisol formulation was used, with a loading of 20% K1001. In this instance, to test the true effectiveness of a clear coat as a protective barrier to photodegradation, all UVAs and HALS were removed from the HPS200 base coat formulation.

#### 4.3.2.1 Gloss Retention

The gloss retention of all formulations was measured after 2100 hours weathering. Figure 4-11 The Gloss Retention after 2100hrs Weathering of HBP Stabilised Lacquer Figure 4-15 illustrates the significant benefit achieved with the lacquering of a TiO<sub>2</sub> pigmented PVC plastisol with regard to gloss retention.

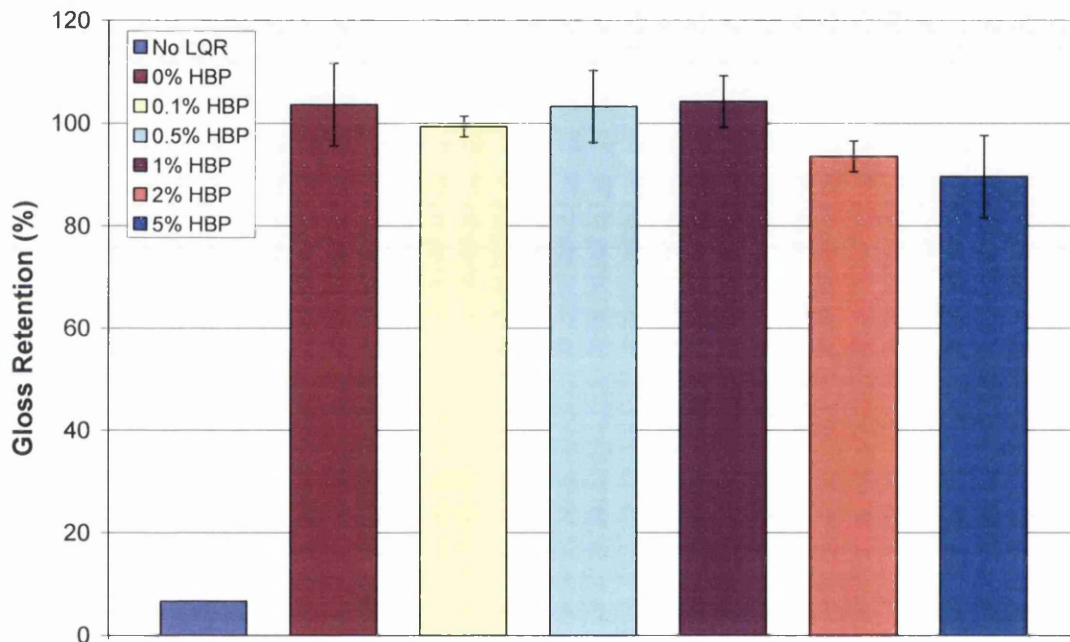


Figure 4-11 The Gloss Retention after 2100hrs Weathering of HBP Stabilised Lacquer

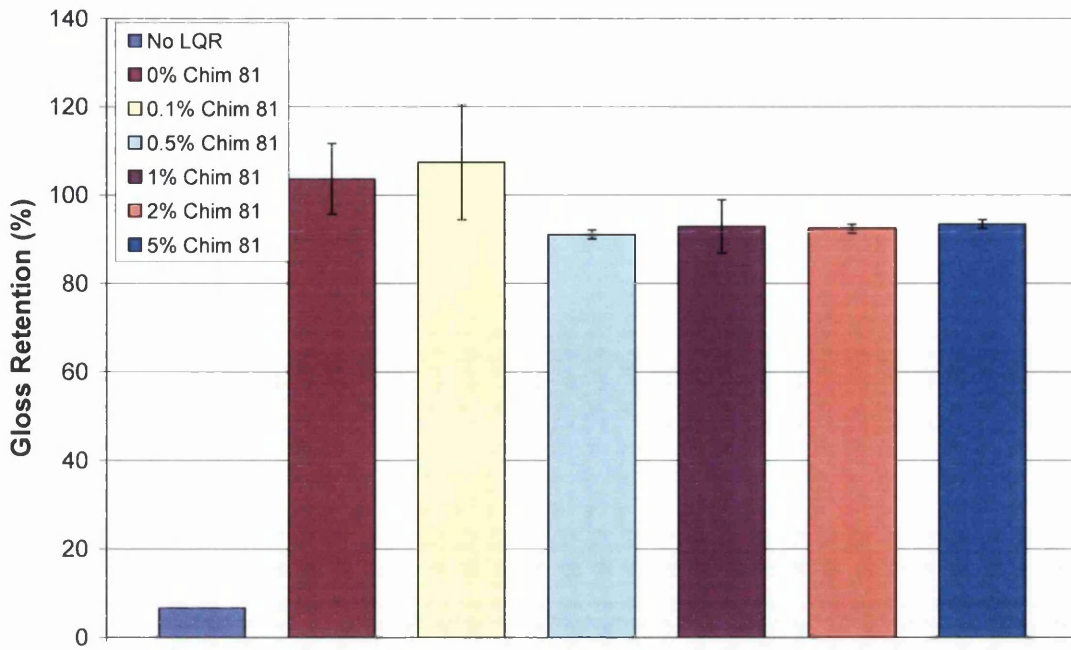


Figure 4-12 The Gloss Retention after 2100hrs Weathering of Chimisorb 81 Stabilised Lacquer

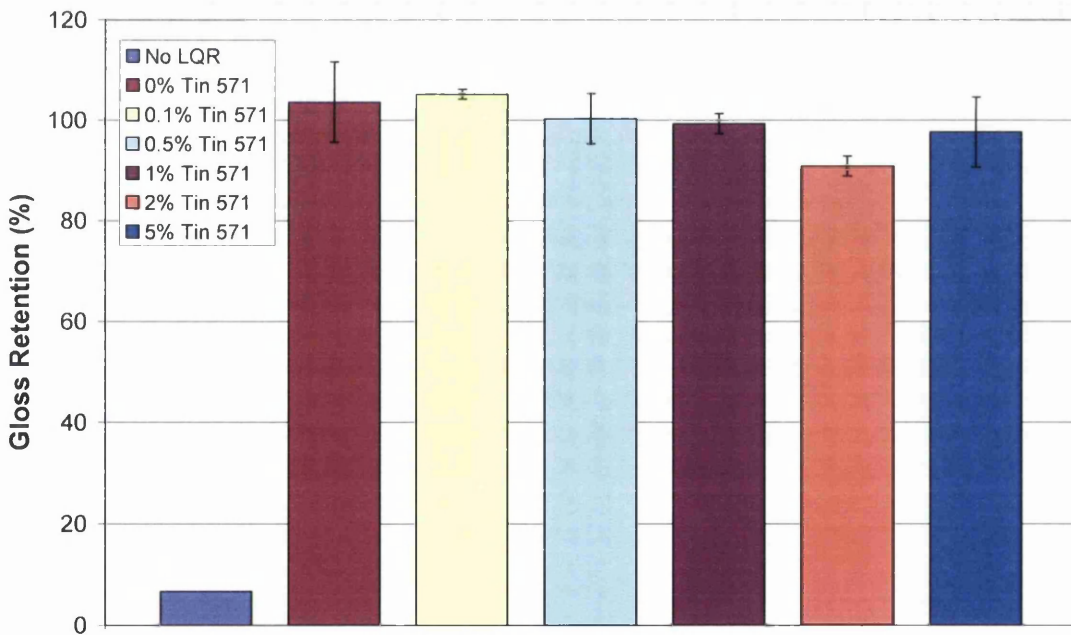


Figure 4-13 The Gloss Retention after 2100hrs Weathering of Tinuvin 571 Stabilised Lacquer

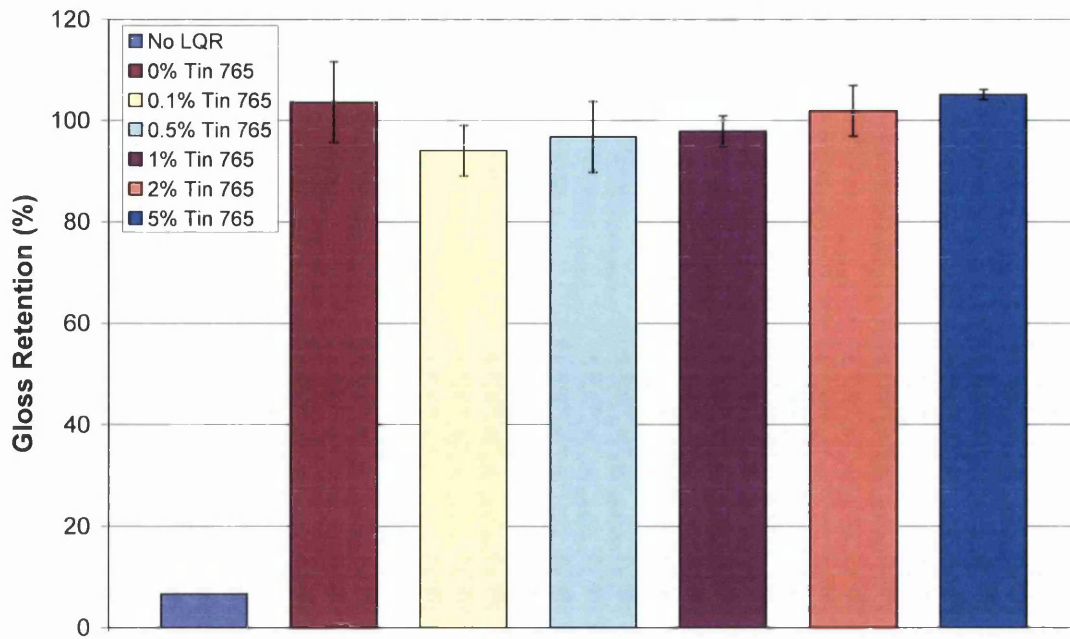


Figure 4-14 The Gloss Retention after 2100hrs Weathering of Tinuvin 765 Stabilised Lacquer

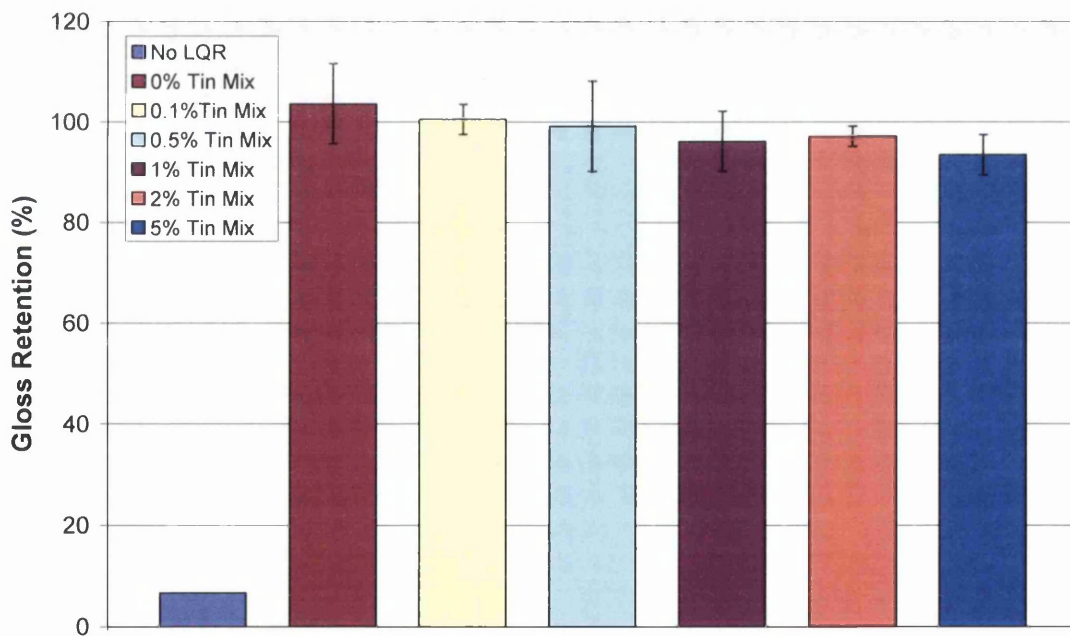


Figure 4-15 The Gloss Retention after 2100hrs Weathering of Tinuvin Mix Stabilised Lacquer



The addition of HBP appears to have little effect on the gloss retention performance as opposed to the non-stabilised lacquer. In fact, at addition levels of 2% and above it appears to have a detrimental effect. This is also mirrored with the addition of UVA Chimisorb 81, whereby a small increase in gloss is apparent at a low loading of 0.1% and a subsequent drop in gloss retention in the region of 10% for all loadings above this. At such loadings of 0.1% and above, no worsening in the performance is evident. For UVA Tinuvin 571, decreasing gloss retention is of the same order with increasing UVA addition. In contrast, the initial addition of HALS Tinuvin 575 worsens the gloss retention, and only at increasing loadings to 5% is the performance equivalent to that of the non-stabilised lacquer. The resultant effect of combining UVA Tinuvin 571 and Tinuvin 575 is a decrease in gloss retention with increased loading.

#### 4.3.2.2 CO<sub>2</sub> Evolution

As previously shown, the CO<sub>2</sub> evolution can prove a useful tool in indicating the rate at which samples will photodegrade. The matrix of samples was irradiated in the flat panel reactor for 1200 minutes, and as before the secondary rates were calculated and compared.

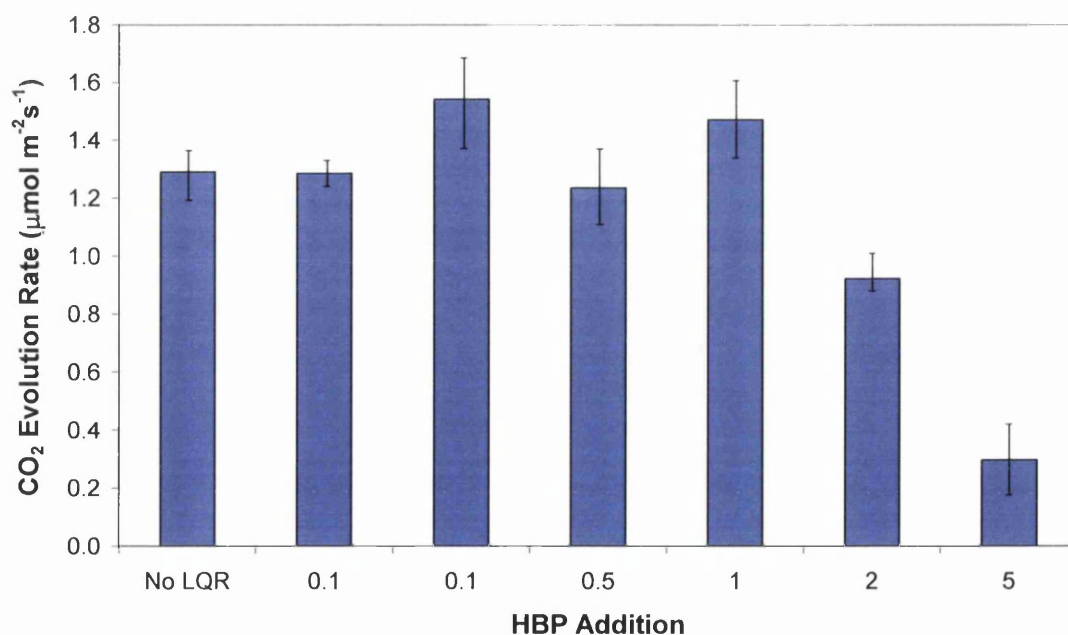


Figure 4-16 CO<sub>2</sub> Evolution Rates for HBP



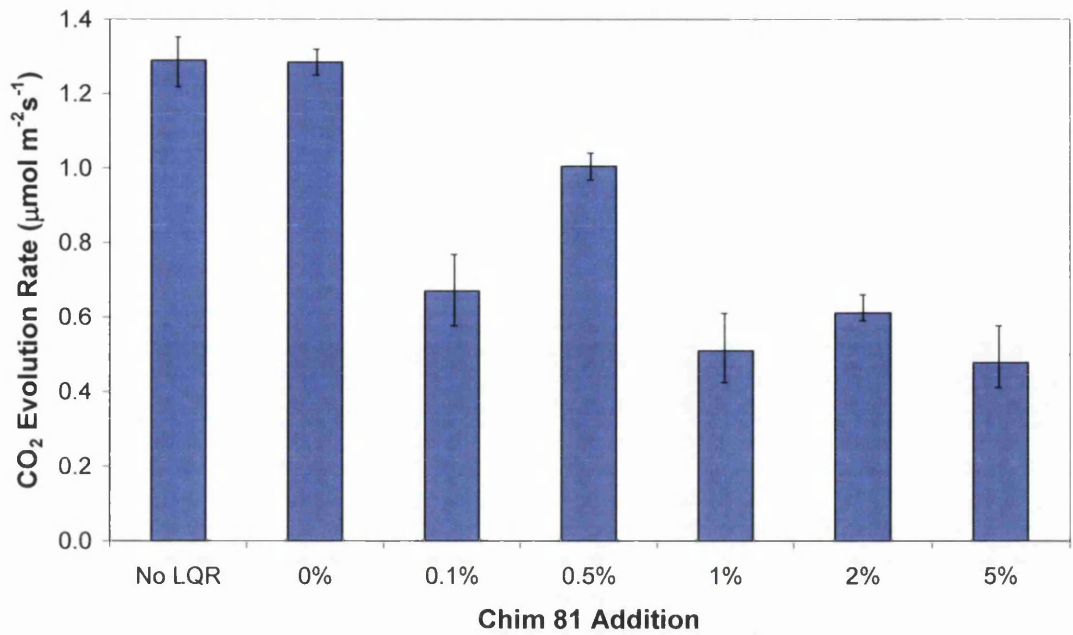


Figure 4-17 CO<sub>2</sub> Evolution Rates for Chimasorb 81

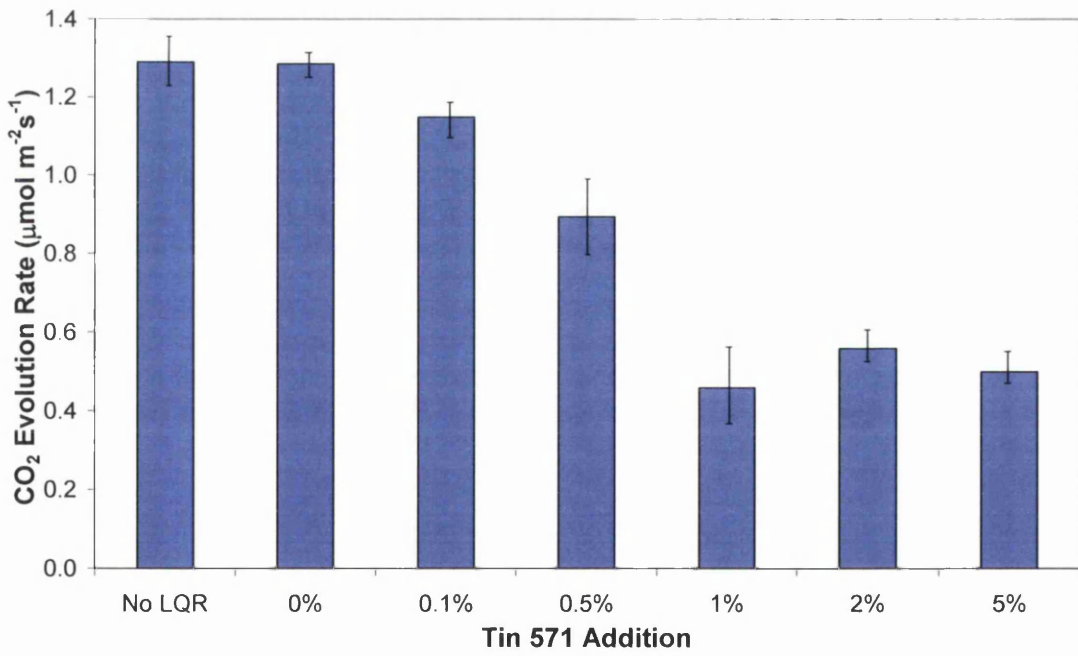


Figure 4-18 CO<sub>2</sub> Evolution Rates for Tinuvin 571

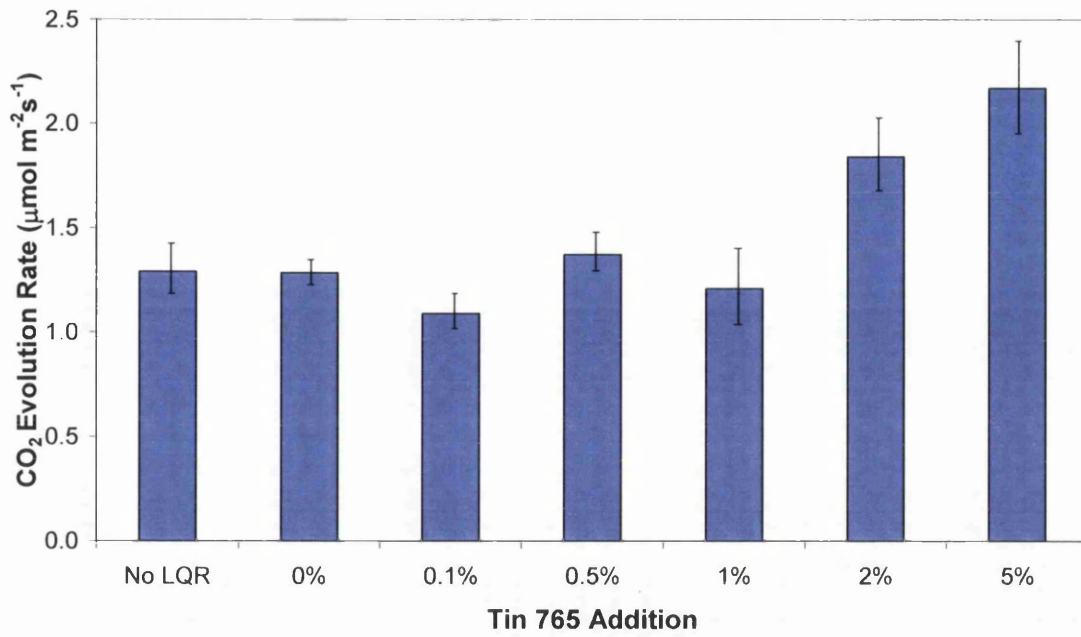


Figure 4-19 CO<sub>2</sub> Evolution Rates for Tinuvin 765

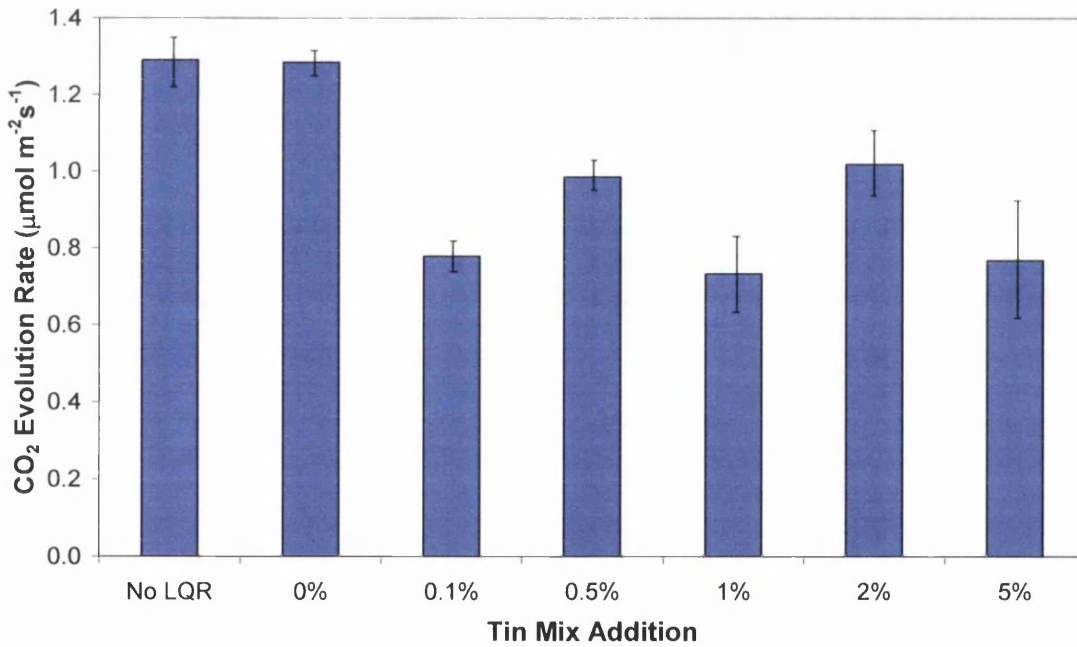


Figure 4-20 CO<sub>2</sub> Evolution Rates for Tinuvin Mix

The rate at which the CO<sub>2</sub> is evolved is the same for the sample without a lacquer, as the equivalent with a clear coat lacquer. Given the exposed TiO<sub>2</sub> pigmented surface layer in the non-lacquered sample, this is a surprising result, but indicates that during the test duration severe TiO<sub>2</sub> photo-catalysis is not apparent. These samples are not weathered, so the likelihood is during the test duration, penetration of the bulk PVC is not significant enough to activate the TiO<sub>2</sub>.

With UVAs, an increase in addition level does act to reduce the CO<sub>2</sub> evolution rate. With HBP the effect is not noticeable until higher loadings of 2% and above. However, with Chimasorb 81 and Tinuvin 571, with loading of 1% and above, the CO<sub>2</sub> evolution rates are more than halved. In contrast, with the addition of HALS Tinuvin 575, no significant stabilisation effect is evident and at loadings of 2% and more the degradation rate dramatically increases. The additive itself potentially acting as chromophore and degrading. It is therefore of little surprise, that when combining the UVA and HALS, the effects counteract each other, and a marginal decrease in evolution rate is evident with any level of addition, and not dependent on loading.

Commercially available additives such as Chimasorb 81, Tinuvin 765 and 571 are all formulated to be efficient at low addition levels, with manufacturers recommending loadings of ~0.5%. Taking into consideration the cost implications of increasing the level of addition Figure 4-21 summarises how the degree of additive loading effects the degradation resistance, as measured by CO<sub>2</sub> evolution, UVA Chimasorb 81 is demonstrated to be very effective at low levels of addition.

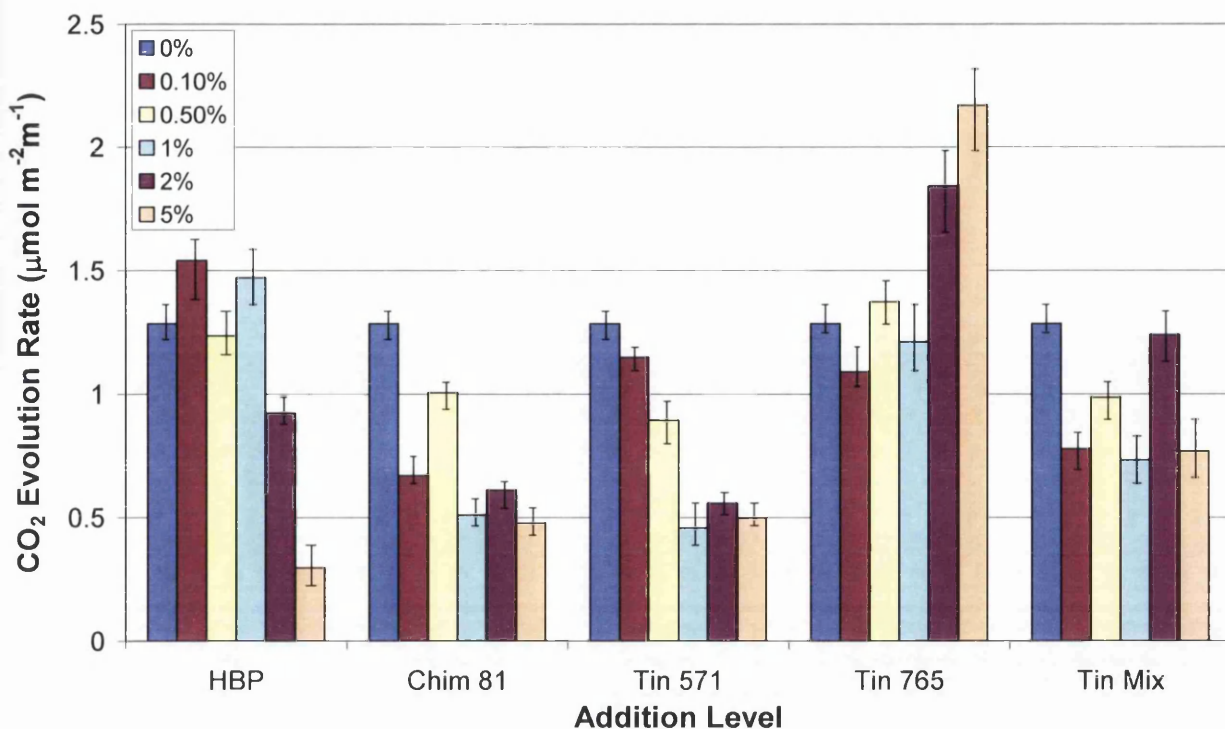


Figure 4-21 Average CO<sub>2</sub> Evolution Rate for Various Loading Levels of Additives

#### 4.3.2.3 Colour Change and Visual Inspection

As with the commercial grade clear coats, colour change was measured. Collecting UV spectra of the samples before and after weathering, the colour change was measured by calculating the change in reflectance as measured in the visible light spectrum. The larger the change in reflectance the greater the colour change measured.

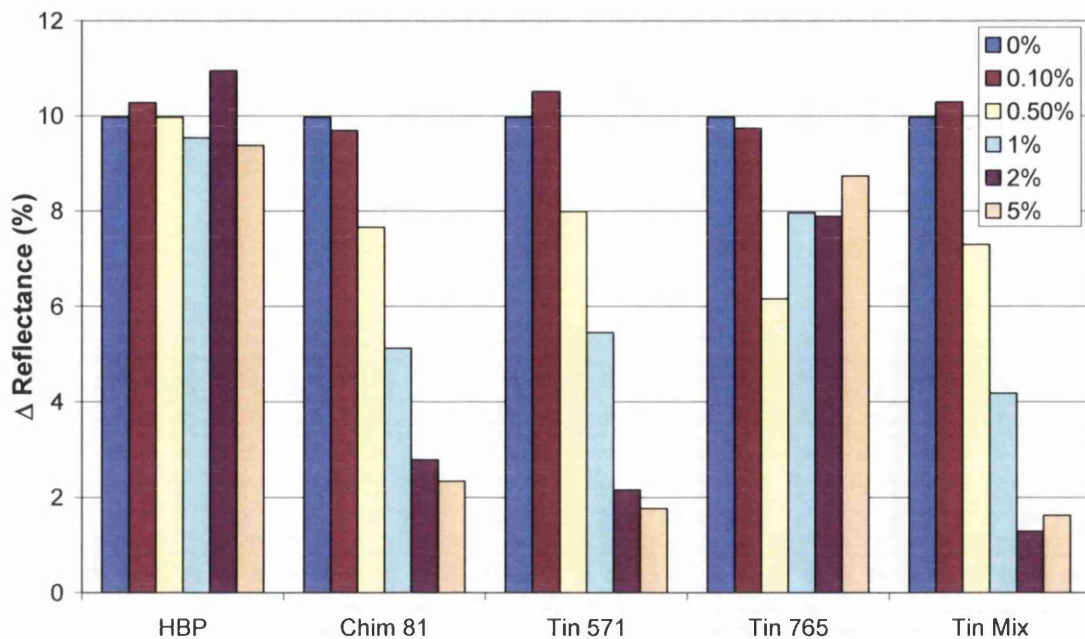


Figure 4-22 Change in Reflectance Spectrum after 1200hrs

After only 1200 hours weathering, significant colour change is evident in the lacquers stabilised with HBP and the level of addition has minimal influence on the colour stability of the system. In contrast, the alternative UVAs had a greater influence on the colour change measured and increasing the level of addition broadly reducing the colour change. The addition of HALS stabiliser Tinuvin 765 is also effective at reducing the colour change and is measured as being the most effective at reducing the colour change at a loading of 0.5%. At loadings of 2% and more, the combination of UVA Tinuvin 571 and HALS Tinuvin 765, proves to be more effective than the stabilisers in their separate form and at the higher loadings the performance is never worse than either of them.

*These findings support that of the visual inspection. Figure 4-23*

*Figure 4-23 shows the extent of colour change and Figure 4-24 illustrates the most and least severe of the colour changes as measured by change in reflectance.*



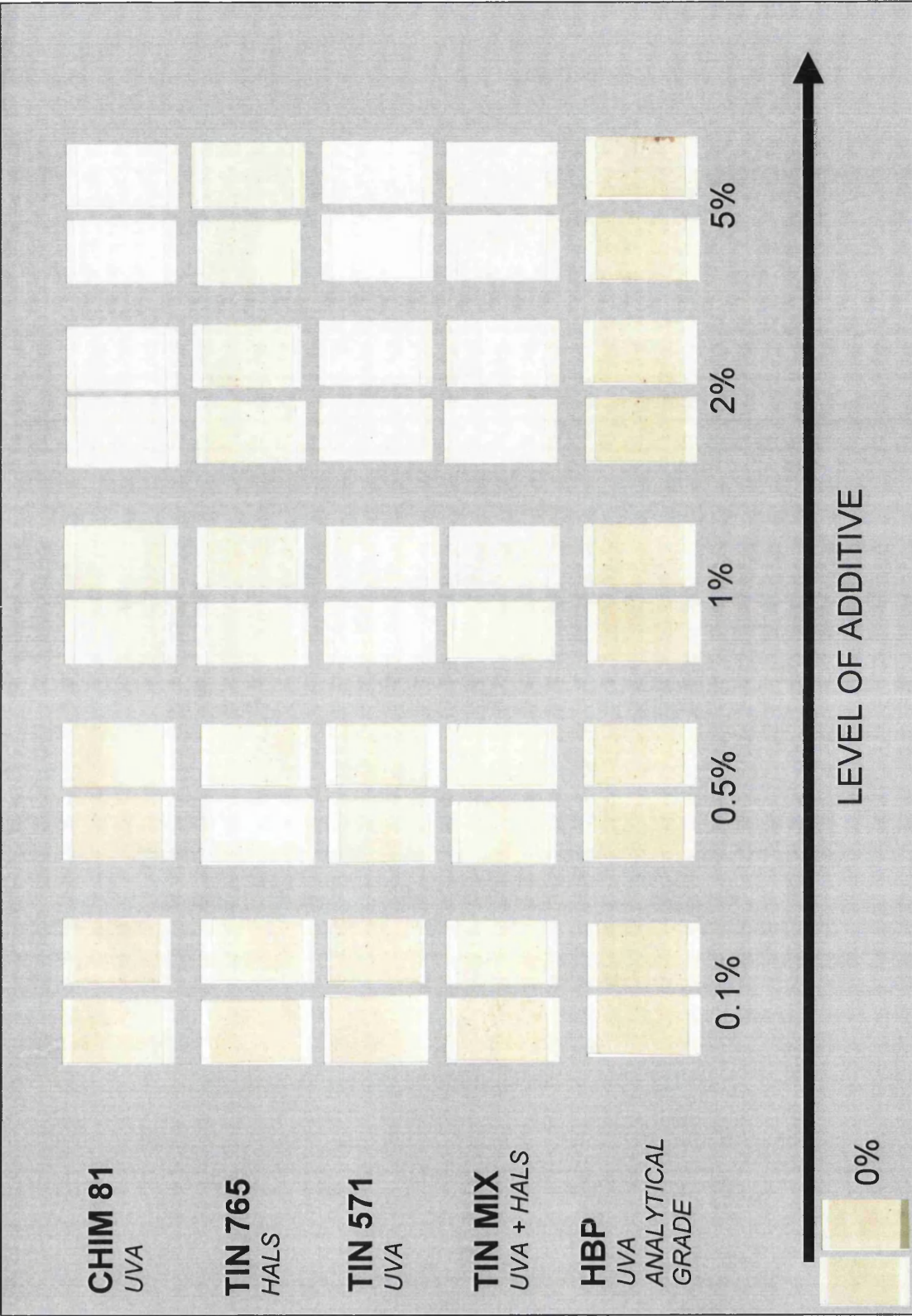


Figure 4-23 Sample Matrix after 2100hrs QUV Weathering

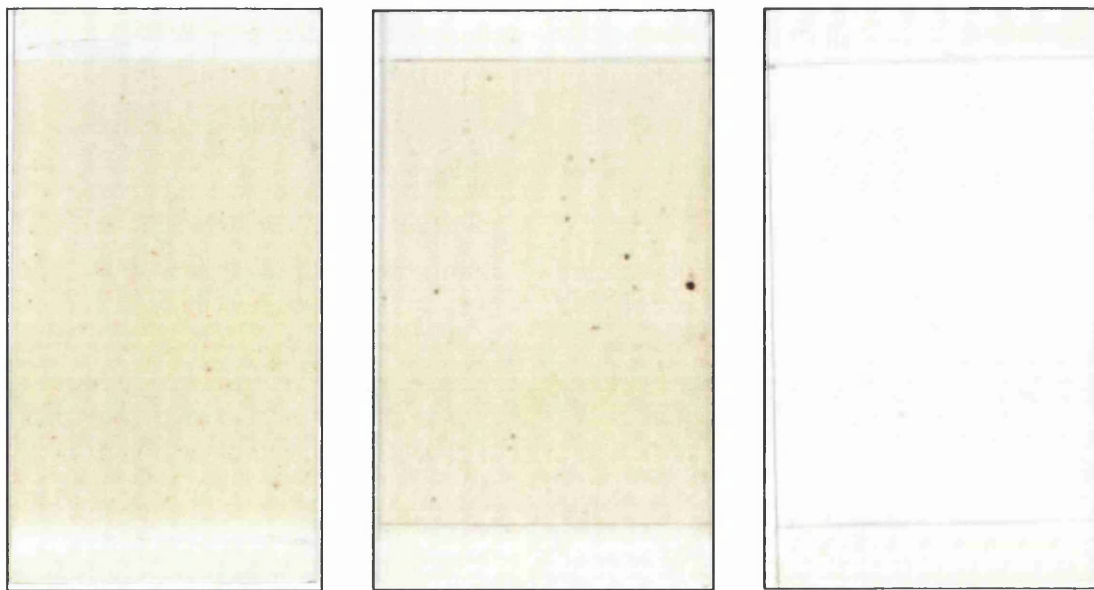


Figure 4-24 Lacquer- NoAdditive, 2% HBP & 5% Tinuvin 571 Images after Weathering

Severe colour change and localised darkening is evident in most samples. There is no visible loss in the clear top coat integrity and no evidence of severe loss of organic matter from the exposed surface also, and the colour change is not rectified by gentle attempt at passing a piece of fabric across the surface. This therefore indicates that the degradation leading to such colour change is occurring in either the bulk clear coat or at the interface of the basecoat and clear coat.

To analyse the likelihood of either of these potential explanations, a few key experiments were carried out to identify how photo-stable the clear coats are themselves.

#### **4.3.2.4 Clear Coat Free Films**

Free films of all the clear coat top coats were produced and irradiated under UVA lamps as described in 4.2.1.2.

After 1400hrs UVA irradiation time (equivalent to the UVA irradiation time in the QUVA weatherometer) the mass loss was measured and shown in Figure 4-25 as a percentage of original mass.

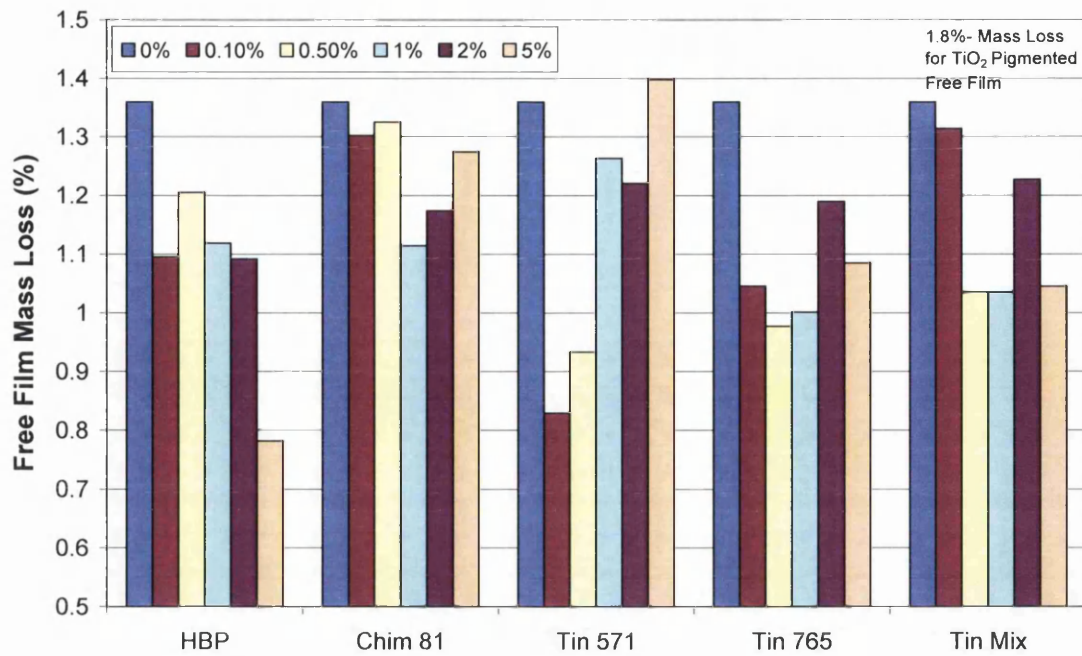


Figure 4-25 Mass Loss of Free Film Clear Top Coats after UVA Exposure

The mass loss for a TiO<sub>2</sub> pigmented free film is 1.8% compared to only 1.35% for a non-TiO<sub>2</sub> containing film, highlighting the effect that TiO<sub>2</sub> presence has on accelerating the photo-oxidation and loss of mass. In all cases apart from 5% Tinuvin 571, the addition of any of the stabilisers to the clear free film acts to reduce the degree of mass loss measured. This highlights, in the absence of TiO<sub>2</sub>, that the free films are inherently stable.

As with the weathered steel coated sample, the gloss change of the free films has been measured.



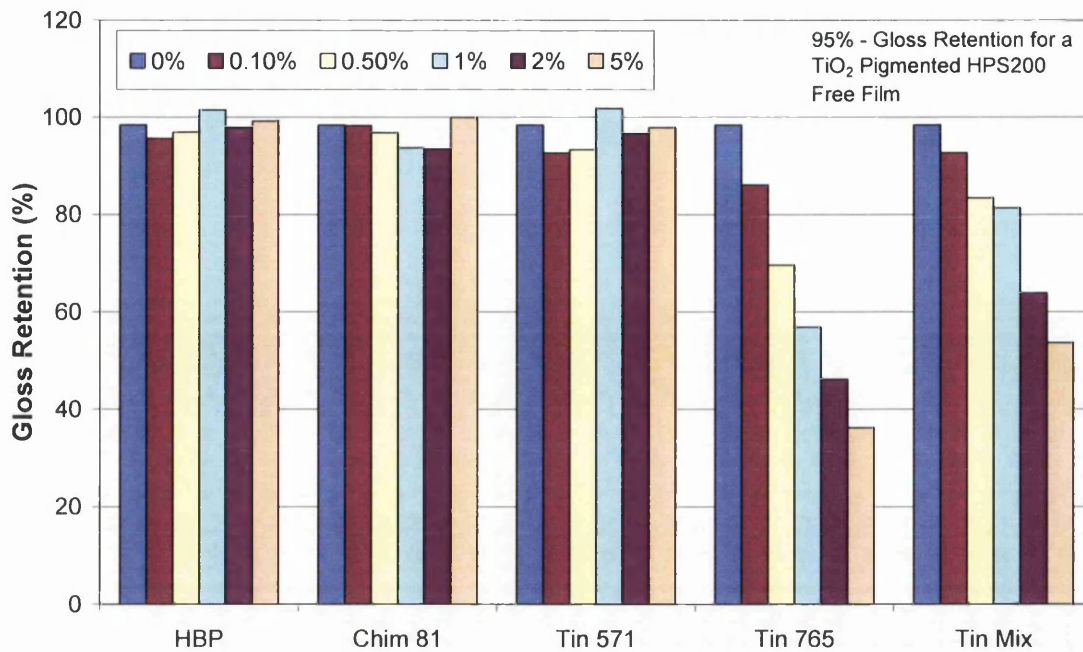


Figure 4-26 Gloss Retention of Free Films after 1400hrs QUV Exposure

The addition of UVAs into the free film has a varying effect on the gloss values measured. The relationship between the level of addition of HBP and Tinuvin 571 is minimal, as was seen with the steel coated samples. For Chimasorb 81, increasing the addition level decreases gloss retention measured until loading of 5% shown here, whereby 100% gloss retention is evident after 1400 hours. However, the greatest difference noted between these results and that of the clear coated TiO<sub>2</sub> pigmented HPS200, is the effect the addition of HALS has. Increasing the level of HALS dramatically reduces the gloss retention after weathering, indicating the unstable nature of the Tinuvin 765.

The expected protection offered by the free films over the base coat system to UV attack, could be predicted by the analysis of the UV spectra of the free film. Given the base HPS200 is pigmented with TiO<sub>2</sub>, wavelengths in the region of 385nm are significant in the acceleration of photodegradation as a result of TiO<sub>2</sub> activation and photocatalysis [60, 81]. The reflectance at a wavelength of 385nm is shown below.

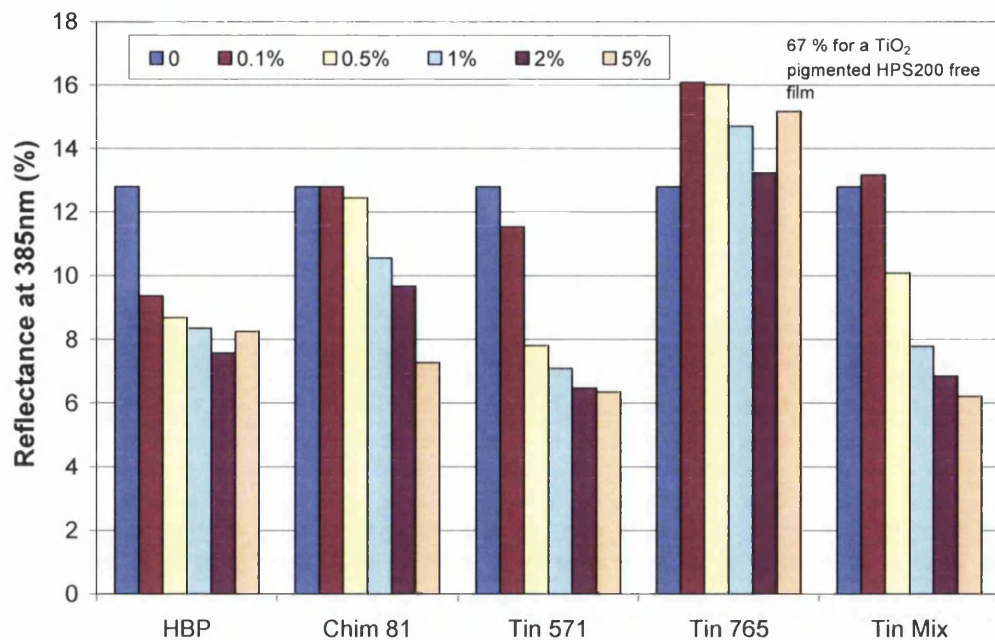


Figure 4-27 UV Vis Reflectance of Free Films at 385nm

UVAs preferentially absorb the UV component of light over the polymer, then allow it to dissipate in a more harmless form of energy, e.g. heat whilst still allowing the transmission of visible light not imparting any significant colour change. They are therefore considered more effective when a greater amount of UV is absorbed. The increasing levels of UVA addition in the free films show a lessening amount of UV reflectance which one would expect, hopefully providing increasing resistance to photodegradation.

As discussed previously in Chapter 1, in contrast, HALS work by interrupting the degradative free radical reactions (for example those initiated by the TiO<sub>2</sub> particles). The big advantage with HALS is that they do not rely on physical absorption of UV light and as a result their efficiency is not necessarily dependent upon them being at a high concentration in the surface of the paint film preventing UV penetration. Therefore, the reflectance values seen above in Figure 4-27 are not a true reflection of the ability of the additive to stabilise against degradation, moreover a measurement of the influence of another medium in the bulk PVC.

This data indicates that the non-pigmented free films themselves are considered inherently stable. After UVA exposure, no colour change was visible to the eye,

mass loss is negligible and can be further reduced with the inclusion of stabilisers. The inclusion of UVAs sustains high gloss levels and an increase in addition level has a significant effect of UV absorption. However, a reduction in gloss is evident with HALS stabilised free films which was not seen when the clear coated were lacquered over the pigmented base coat.

All this evidence supports the theory that the extreme colour change seen and severe localised dark spots are a result of degradation at the interface of the TiO<sub>2</sub> containing basecoat and clear coat. No such phenomenon was noted in the weathering of the near commercial samples in 4.3.1, where stabilisers were still present in the basecoat plastisol.

The formation of HCl in the TiO<sub>2</sub> pigmented base coat is acting as an accelerant to the degradation mechanism and encapsulation of the acidic species under the top coat is going to accelerate the effect and colour change seen. Another explanation for the very localised dark spots seen, is that the lacquer is inhomogeneous and thus leads to concentrated areas of water and oxygen permeation and more severe localised degradation.

### **4.3.3 Photodegradation of TiO<sub>2</sub> Pigmented HPS 200 with Clear Coat Lacquers**

The coating systems were assigned a performance ranking in each weathering experiment, colour change, CO<sub>2</sub> evolution rate and gloss retention. CO<sub>2</sub> evolution rate was expressed as a percent of the largest CO<sub>2</sub> rate measured, as was percent change in colour reflectance. Gloss was illustrated as a percent gloss reduction measured. Thus a smaller area of a graph would indicate less change after weathering and less reactivity of the sample, providing an opportunity to compare the durability of the various samples.

Figure 4-28 illustrates the influence of HBP addition on durability. In this instance, the data is normalised and shown relative to a coating system with no lacquer and the dramatic increase in the durability of the system by including any clear coat is visible.

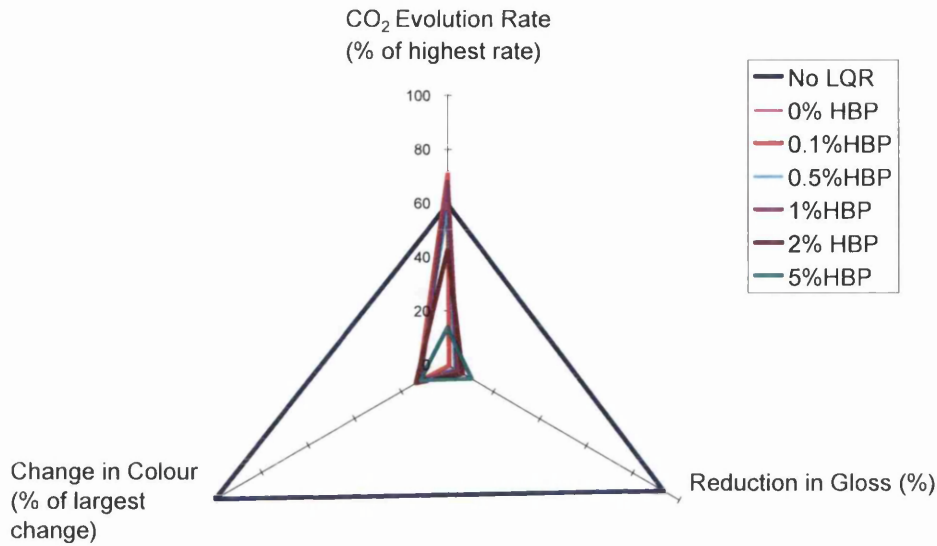


Figure 4-28 Ranking of Durability Characteristics of a HBP Stabilised Clear Coat

Ignoring the system with no lacquer, data was again normalised to all the types and level of additions, now more clearly showing the effect. The areas of all graphs were collated, and photoactivity was ranked relative to a lacquer with no stabiliser. Therefore, if the photoactivity index is greater than 1, the stabiliser has a detrimental effect on the durability, increasing the extent of degradation, whereas if the index is less than one, durability is improved.

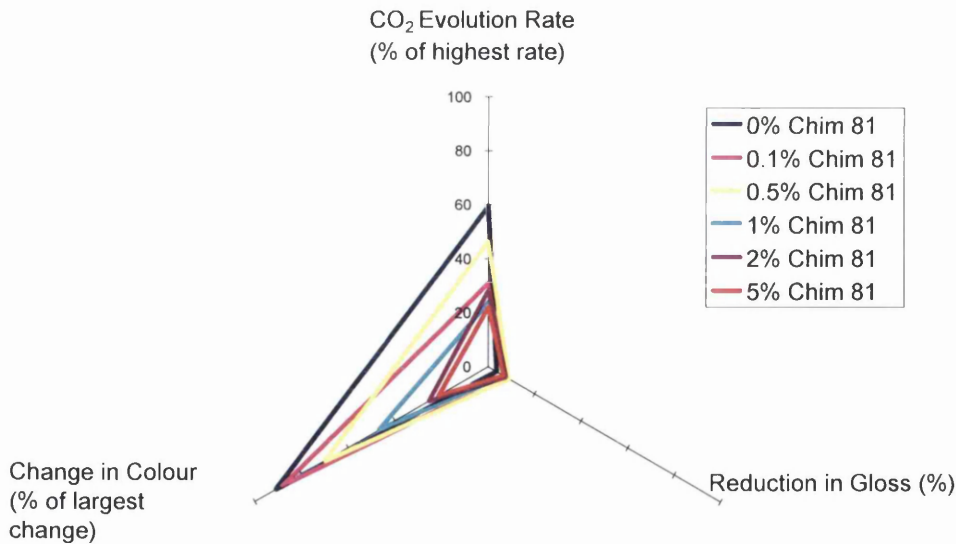


Figure 4-29 Ranking of Durability Characteristics of Chimasorb 81 Stabilised Clear Coat

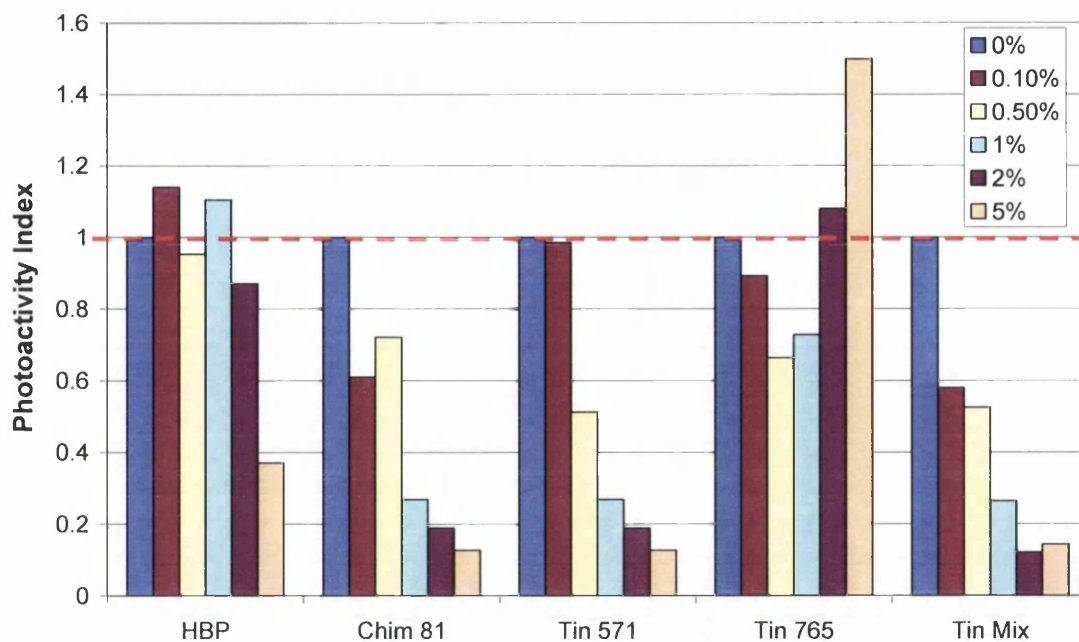


Figure 4-30 Photoactivity Ranking of All Clear Coats

HBP and Tinuvin 765 both have reactivity indices above 1, indicating that durability is reduced, at loadings of 0.15 and 1% and 2 and 5% respectively. However, the remaining commercially available stabilisers all show a positive effect on the coating durability, with Tin Mix, the combination of UVA and HALS performing the best, reducing the photoactivity at every level of addition the most. This combination of UVA and HALS stabiliser is commonly seen in commercial coating formulations, combining the better of the two different stabilisation techniques. The general trend is with increasing UVA addition the durability also increases, as indicated by the UV reflectance spectra of the free films. As also indicated by the spectra, gloss and mass loss of the and free films, the combination of additive level and extent of degradation is more complex. The photoactivity ranking indicates an addition level of 0.5% HBP is preferential.

## 4.4 Conclusions

All data discussed here shows that a barrier layer is very efficient at reducing the extent of coating failure induced by photodegradation, as measured by gloss, colour change and CO<sub>2</sub> evolution.

During the initial investigation, the potential benefits of using a PVC clear coat lacquer were obvious. Comparing it to commercially available systems, clear HPS200 top coats were proving to be a potentially viable low cost alternative to some more sophisticated systems.

Some level of stabilisation is essential in a coating for outdoor applications and in this instance; it was concentrated in the top clear coat. The efficiency of varying loadings of UVAs, HALS and both combined, to reduce photodegradation was analysed.

Although, at first glance the improvement in potential weathering resistance provided by including such stabilisers in the clear coat is minimal (compared to the clear coat without them in), visual inspection of the sample strongly indicates that they are all playing a key role.

It is highly likely that at the clear coat-basecoat interface, where HCl production is concentrated, the extent of degradation and colour change is dictated by the stabiliser. Alternatively, given these samples were produced on non-galvanised steel substrate, there is a possibility that due to severe localised degradation, or a concentration of reactive species, the 'brown spots' is in fact iron oxide leaching through the coating.

With further investigation into the exact nature of the severe and localised colour change, concentrating the stabilisers in the top coat is a feasible option and there is potential to offer increased performance at reduced costs.

## 4.5 References

1. Wray, J., The Degradation Studies of TiO<sub>2</sub> Pigmented Polyurethane Coating Systems, in University of Swansea School of Engineering. Eng D 2009, Swansea University
2. Jin, C.Q., FTIR Studies of TiO<sub>2</sub> Pigmented Polymer Photodegradation. 2004.
3. Worsley, D.A. and J.R. Searle, Photoactivity Test for TiO<sub>2</sub> Pigment Photocatalysed Polymer Degradation. *Materials Science and Technology*, 2002. **18**(6): p. 681-684.

## **5 Nano-scale Coatings for the Improved Weathering Resistance of PVC**



## **5.1 Introduction**

As shown in this thesis, a barrier layer on a potentially reactive substrate has the potential to increase its durability, whether it is to protect from water or oxygen permeation, or even acidic attack in some packaging applications.

Physical Vapour Deposition (PVD) barrier layers are commonly being used in solar cell applications [55], such as ‘dye sensitised’ solar cells. This development has been driven by the need to encapsulate all the functional components of the flexible ‘cells’. Limiting the permeation of water for example is of great interest in the fight to reduce any degradation of the cell electrolyte and additives. Similarly, whilst wanting the cells to operate efficiently, stringent control over UV penetration is also of importance to also allow for control over operation of the cell components.

Recent work has highlighted [55, 56] the influence nano-scale coatings have on controlling oxygen and water permeation. With both such factors, combined with UV, playing a significant role in the photodegradation of PVC, the same is considered here, assessing a potential change in material performance following the application of a nano-metric coating.

### **5.1.1 Aims and Objective**

This chapter is an introduction to using the technique of Magnetron Sputtering PVD to deposit coatings of differing composition and thicknesses, to assess the potential for the production of a coating with improved weathering resistance.

The extent of photo-oxidation is measured using the flat panel reactor, measuring the volume of CO<sub>2</sub> evolved. In addition to this, wedged coatings have been produced and weathered in a QUVA weatherometer, to evaluate the effect of deposition thickness on appearance, durability and also give an insight into the barrier mechanisms offered by the deposited coating.

## 5.2 Experimental

### 5.2.1 Barrier Coatings for Improved PVC Photodegradation

To assess the influence of PVD coatings on PVC photodegradation, a model PVC coating was formulated (as described in 2.1). The formulation was pigmented with 30% weight for weight Degussa P25 TiO<sub>2</sub> (highly photoactive) and cast onto glass panels measuring 6cm by 8cm.

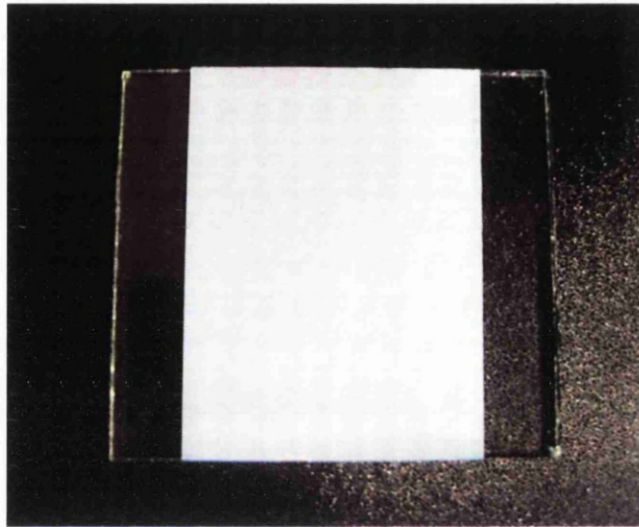


Figure 5-1 Model PVC Coated Sample for PVD Coating

Subsequently, these samples were coated with the following, in the Lesker PVD75, at 2nm, 5nm, 20nm and 200nm:

- i. Indium Tin Oxide (ITO)
- ii. Zirconia (ZrO<sub>2</sub>)
- iii. Alumina (Al<sub>2</sub>O<sub>3</sub>)
- iv. Aluminium (Al)
- v. Copper (Cu)
- vi. Titanium (Ti)

## 5.2.2 Wedge Coated Fully Formulated Model PVC Coating

To investigate the potential durability of nano-scale coatings to weathering, a wedged deposition was production.

As in Chapter 2 a fully formulated HPS200 plastisol was used, with a pigment loading of 20% K1001 grade  $\text{TiO}_2$ . Again, to test the effectiveness of this barrier coating as a protective barrier to photodegradation rapidly, all UVAs and HALS were removed from the HPS200 formulation. The coatings were drawn onto primed steel, cured and cut into coupons measuring 10cm by 4cm.

Wedged coatings were produced through the use of a sliding shutter within the coating chamber. Through control of the rate at which the shutter retracts and exposes the substrate (and ensuring a steadily maintained deposition rate), a coating of varying thickness can be produced. A schematic of this procedure can be seen in Figure 5-2, The shutter speed used was calculated from the following equation 4.1, where  $w$  is the width of sample to be coated,  $t$  is the desired maximum thickness of deposition and  $R_d$  is the rate of deposition.

$$\text{Shutter Speed} = \frac{W}{(t/R_d)} \quad (\text{Equation 5.1})$$

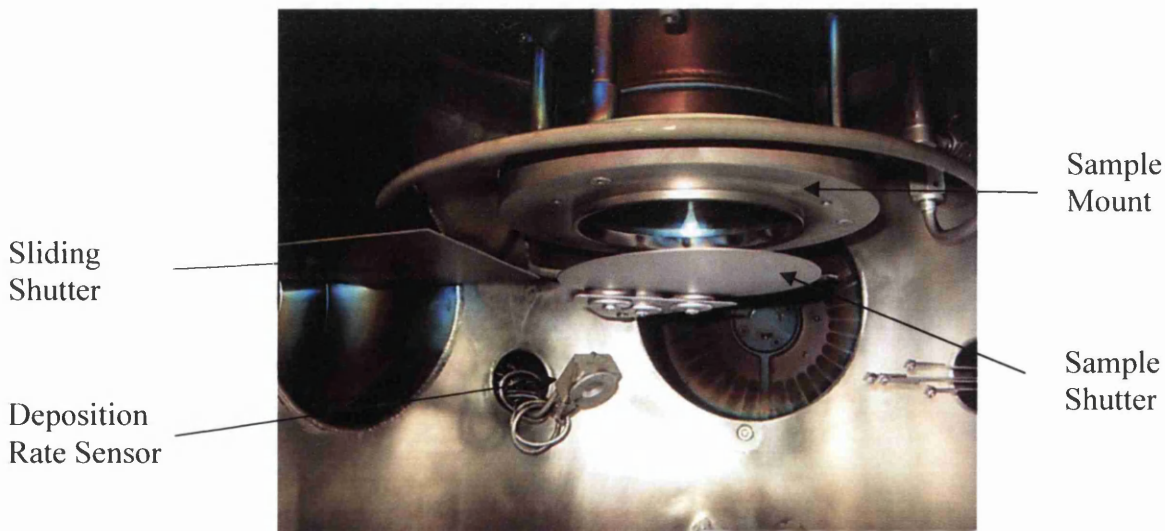


Figure 5-2 Deposition Coating Chamber

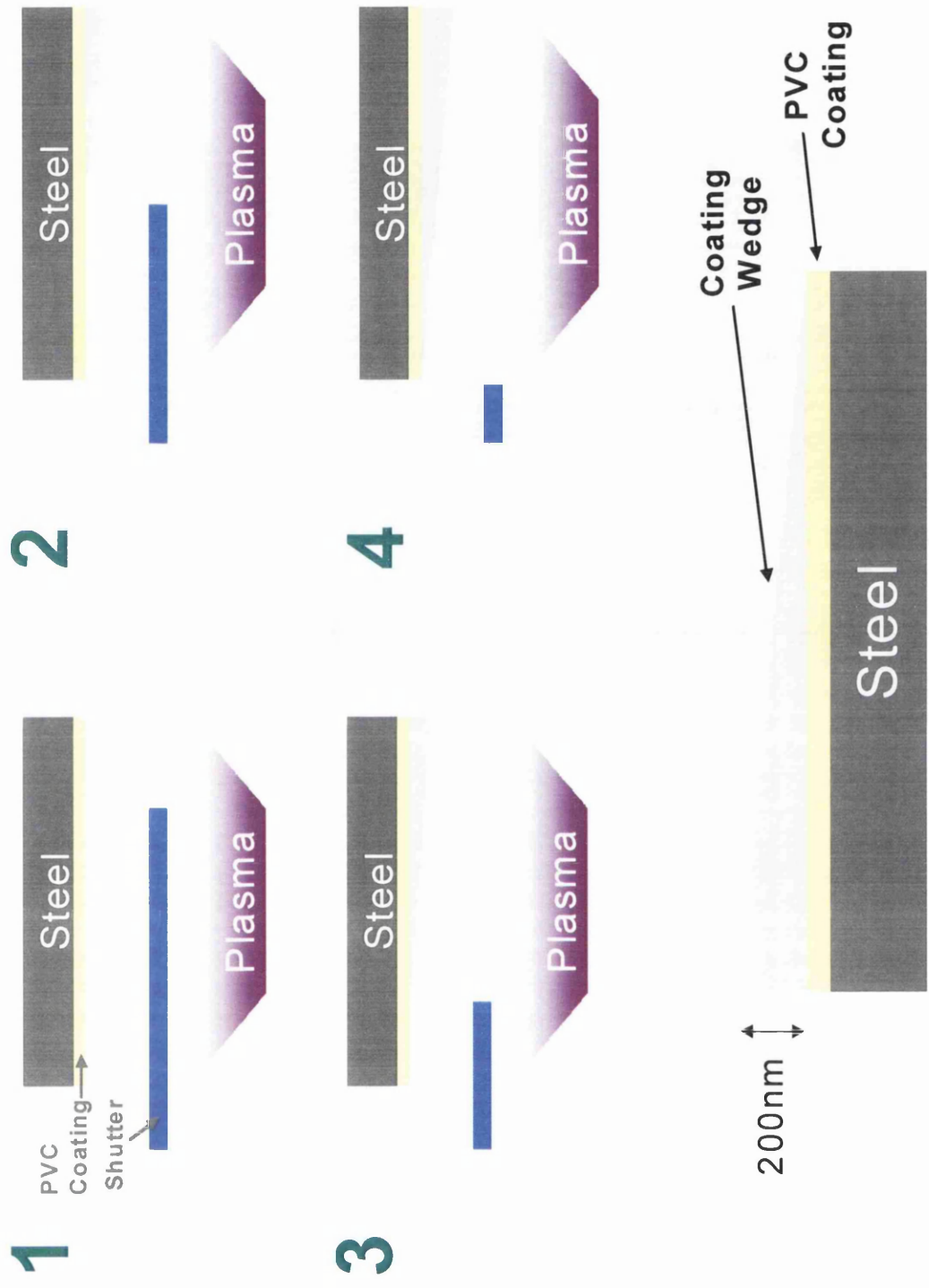


Figure 5-3 Schematic of Technique Used to Produce the Aluminium Wedge Coated PVC Sample

## **5.2.3 Accelerated Weathering**

### **5.2.3.1 CO<sub>2</sub> Evolution Profiles**

Two model PVC coated glass samples for each PVD coating sample were cast and subsequently coated at 2nm, 5nm, 20nm and 200nm for each of the metallic coatings. Each sample was irradiated in the flat panel reactor and the data collected was calibrated and graphed as displayed as volume of CO<sub>2</sub> evolved.

### **5.2.3.2 QUVA Weathering**

The aluminum and titanium wedge coated fully formulated PVC sample was exposed to QUVA weathering for a test duration of 1000 hours. Samples were removed at 200 hour intervals, and images scanned on Canon Pixma MX870. Weathering cycles consisting of 8 hours UVA radiation and 4 hours condensation were employed. The panel temperature for both cycles was set at 40°C and a light intensity of 0.68/m<sup>2</sup>/nm.

## 5.3 Results and Discussion

### 5.3.1 CO<sub>2</sub> Evolution

In order to measure the potential of a nano-scale deposited coating in reducing the photodegradation of PVC, the flat panel apparatus were used. Evolved CO<sub>2</sub> was measured as an indicator of the degree of photo-oxidation occurring.

In order to investigate the level of deposition to be applied, a preliminary experiment was carried out. A 1 $\mu$ m, 200nm and 20nm ITO layer was deposited onto the model PVC sample and irradiated in the flat panel reactor and the CO<sub>2</sub> evolved was measured. Figure 5-4 shows the effect the varying levels of deposition has, with CO<sub>2</sub> evolution evident in all cases.

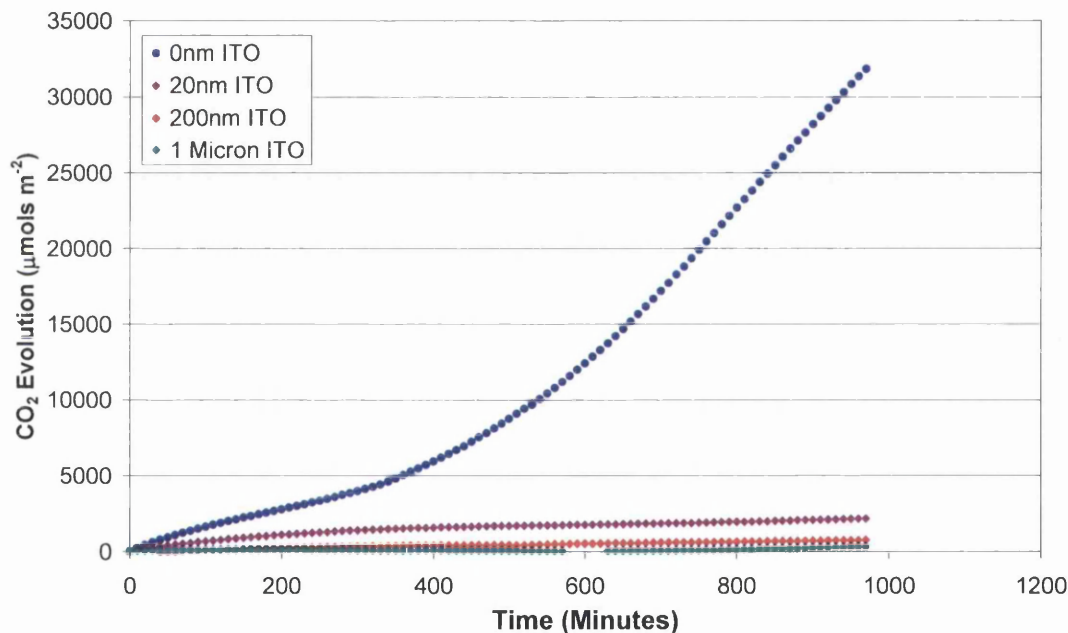


Figure 5-4 Typical CO<sub>2</sub> Evolution Profile for ITO Coated PVC Samples

Clearly, the addition of an additional coating to the surface of the PVC sample has a dramatic influence on reducing the volume of CO<sub>2</sub> evolved. At only a 20nm deposition, the amount of CO<sub>2</sub> evolved is reduced by almost 90%. Taking into consideration the time taken to apply the 1 $\mu$ m coating and cost associated with consumption of target material, along with the promising results shown above, further experimentation was limited to the testing of depositions 0nm to 200nm. The evolution plots for the remaining deposition materials are shown in Figure 5-5 to Figure 5-10.

# ITO Deposition

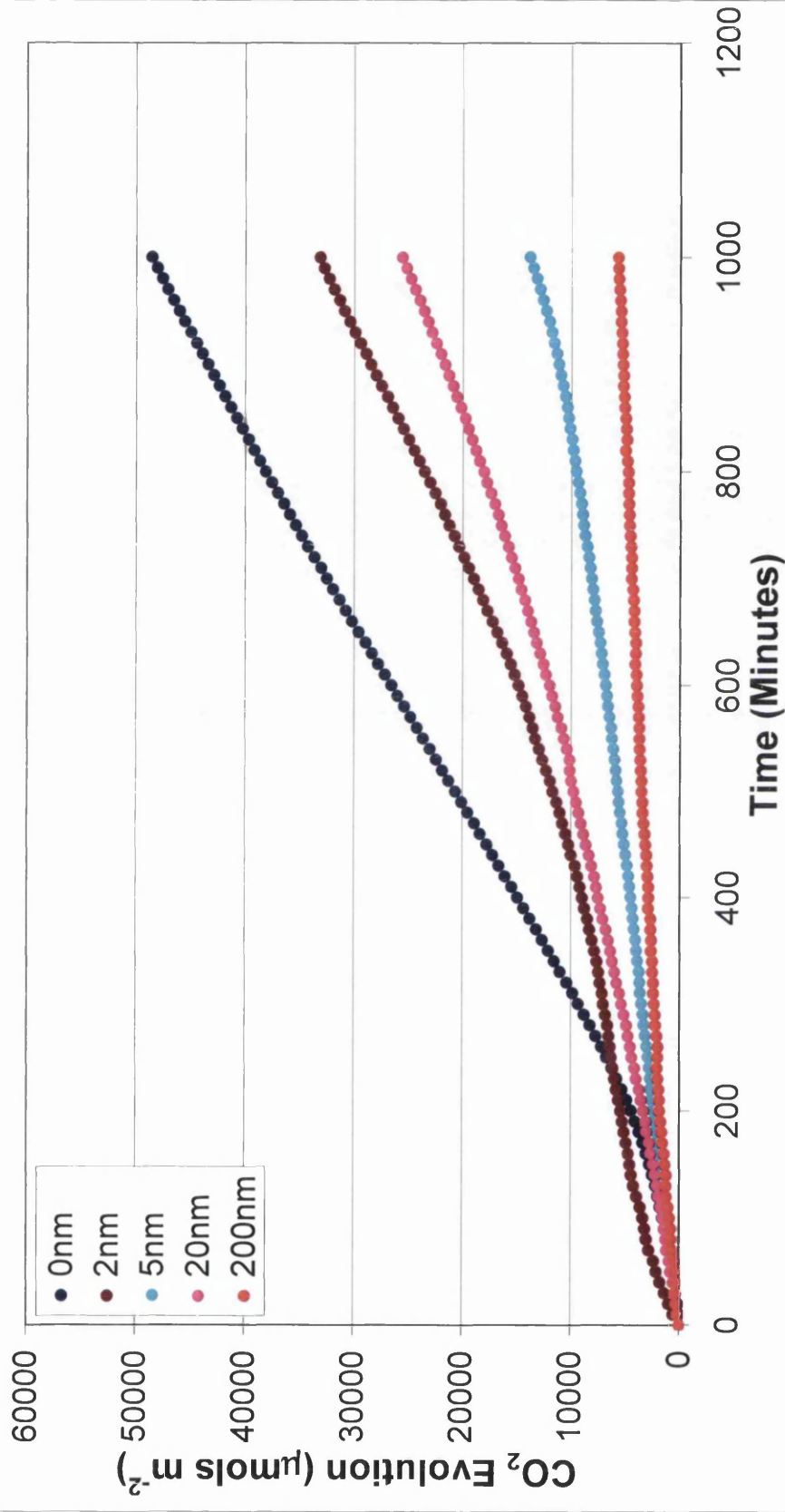


Figure 5-5 CO<sub>2</sub> Evolution Profiles for ITO Coated PVC



# Al Deposition

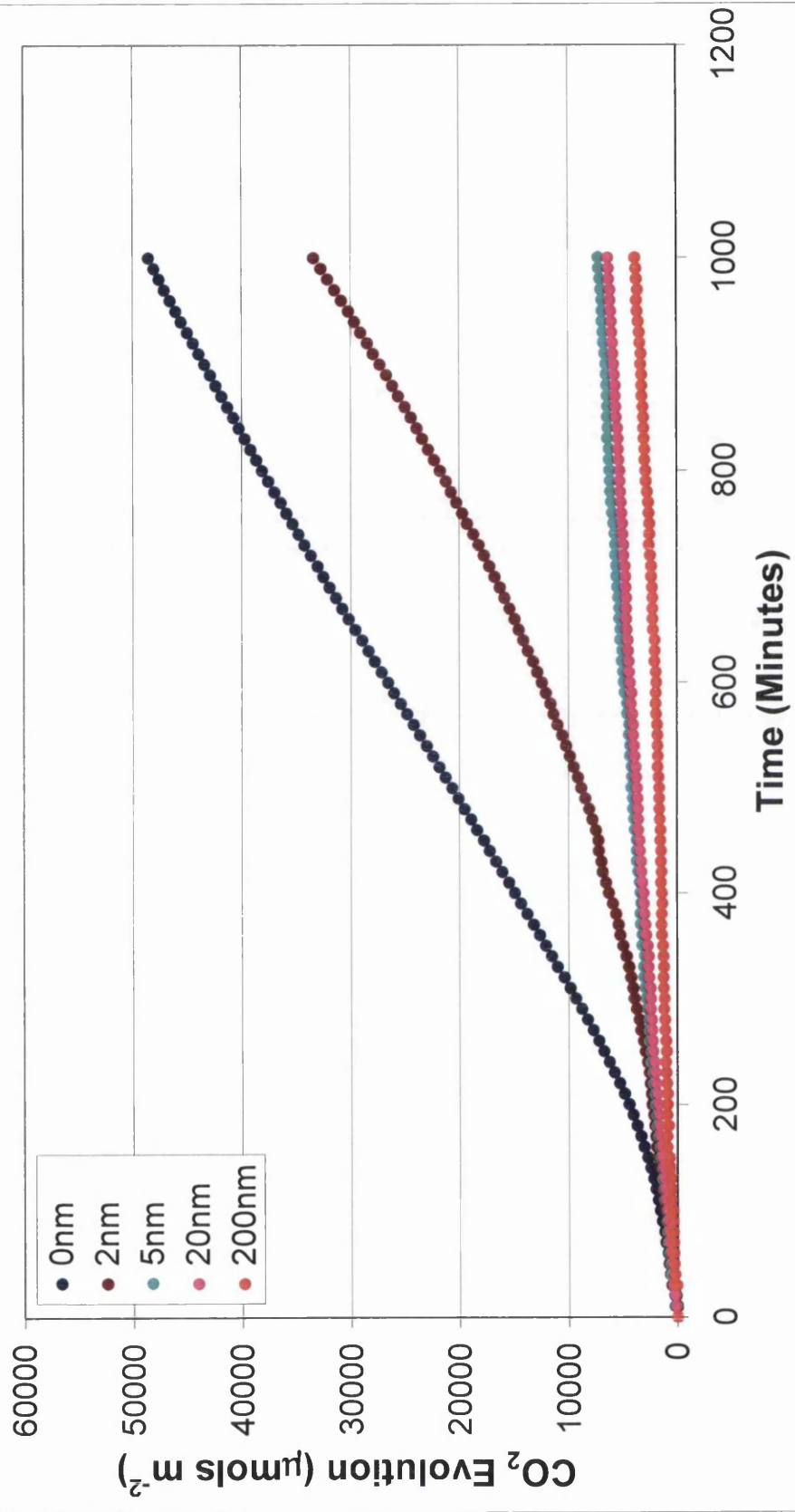


Figure 5-6 CO<sub>2</sub> Evolution Profiles for Aluminium Coated PVC



# Cu Deposition

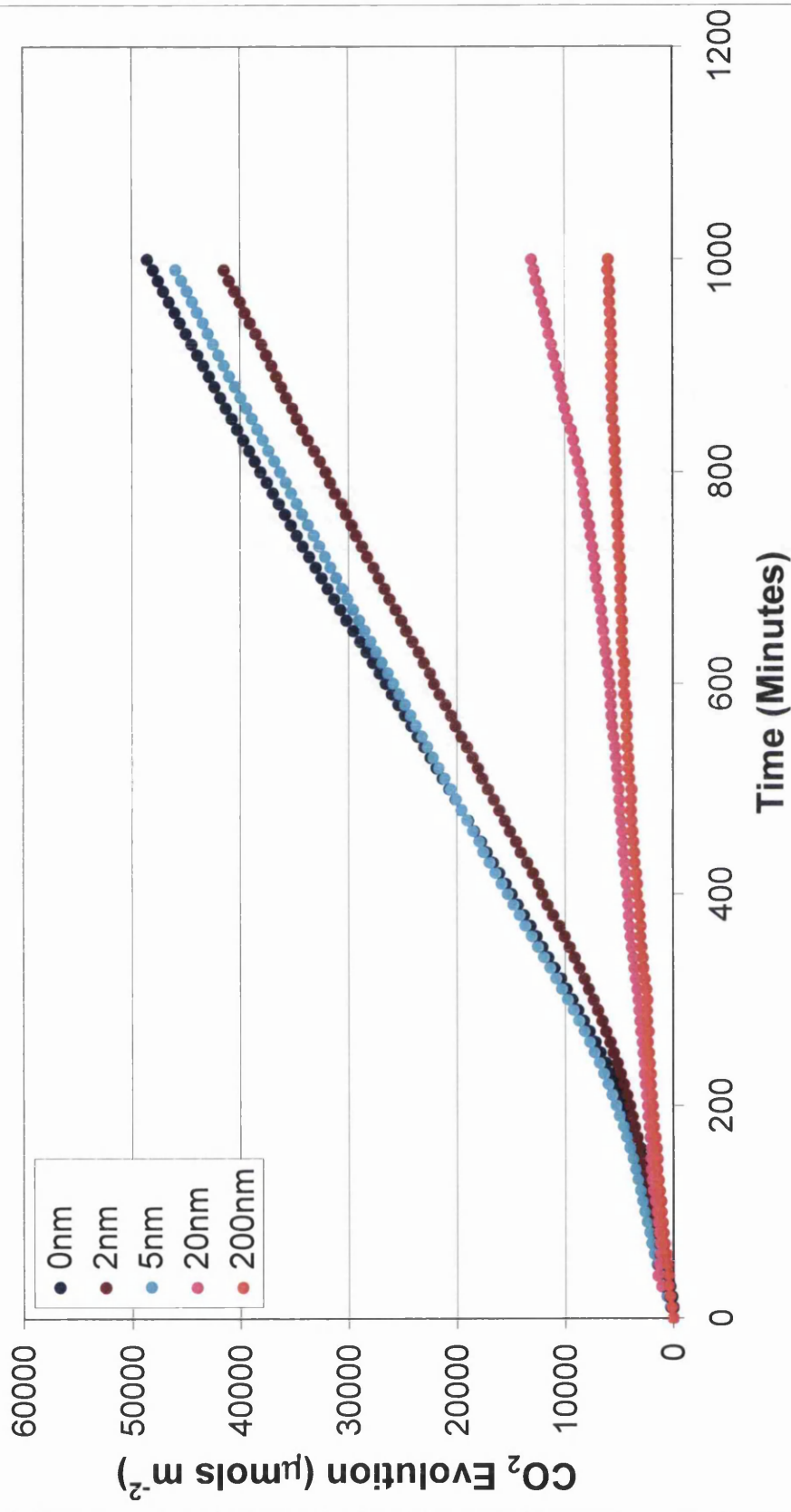


Figure 5-7 CO<sub>2</sub> Evolution Profiles for Copper Coated PVC

# Al<sub>2</sub>O<sub>3</sub> Deposition

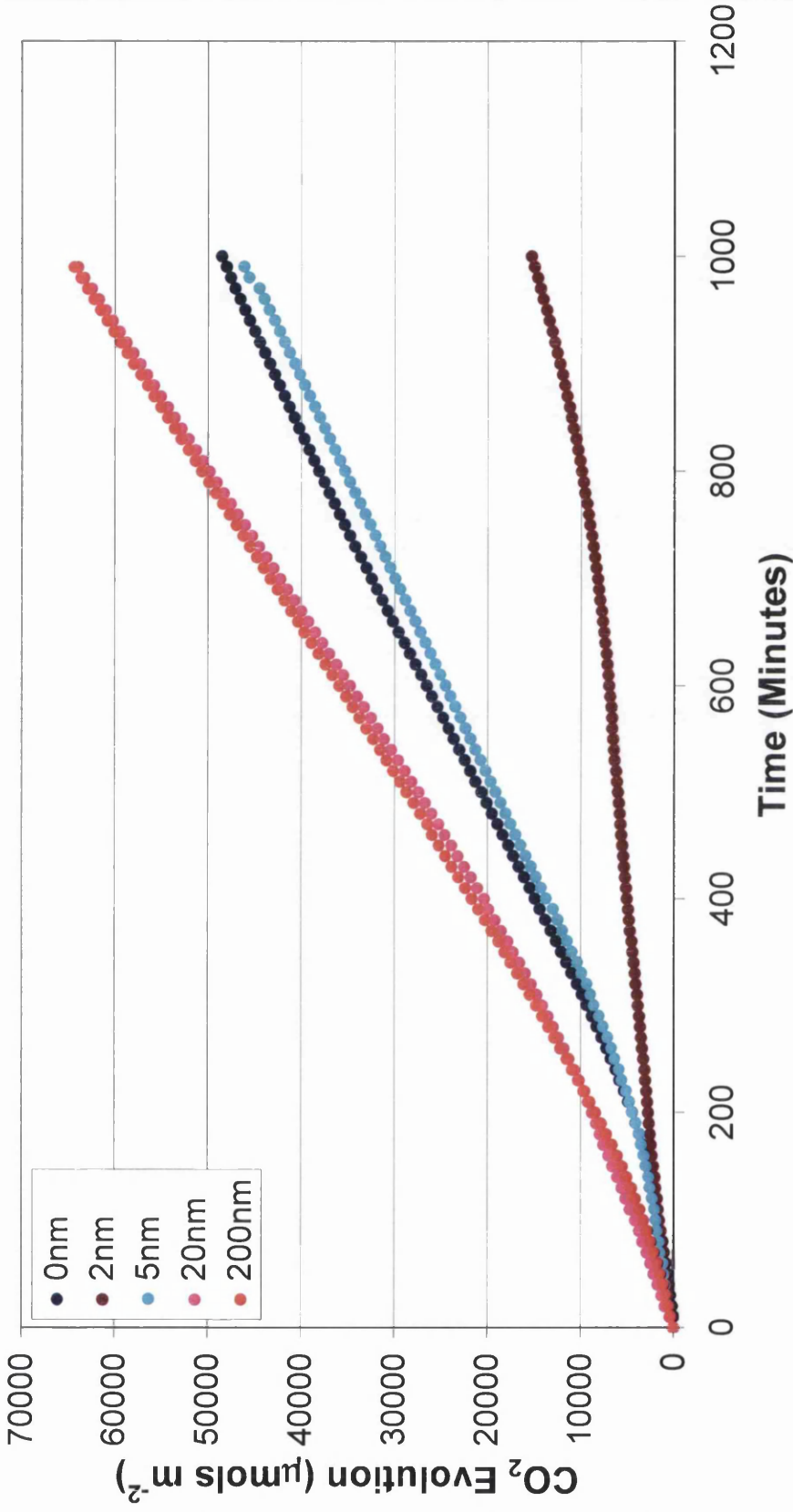


Figure 5-8 CO<sub>2</sub> Evolution Profiles for Alumina Coated PVC

# ZrO<sub>2</sub> Deposition

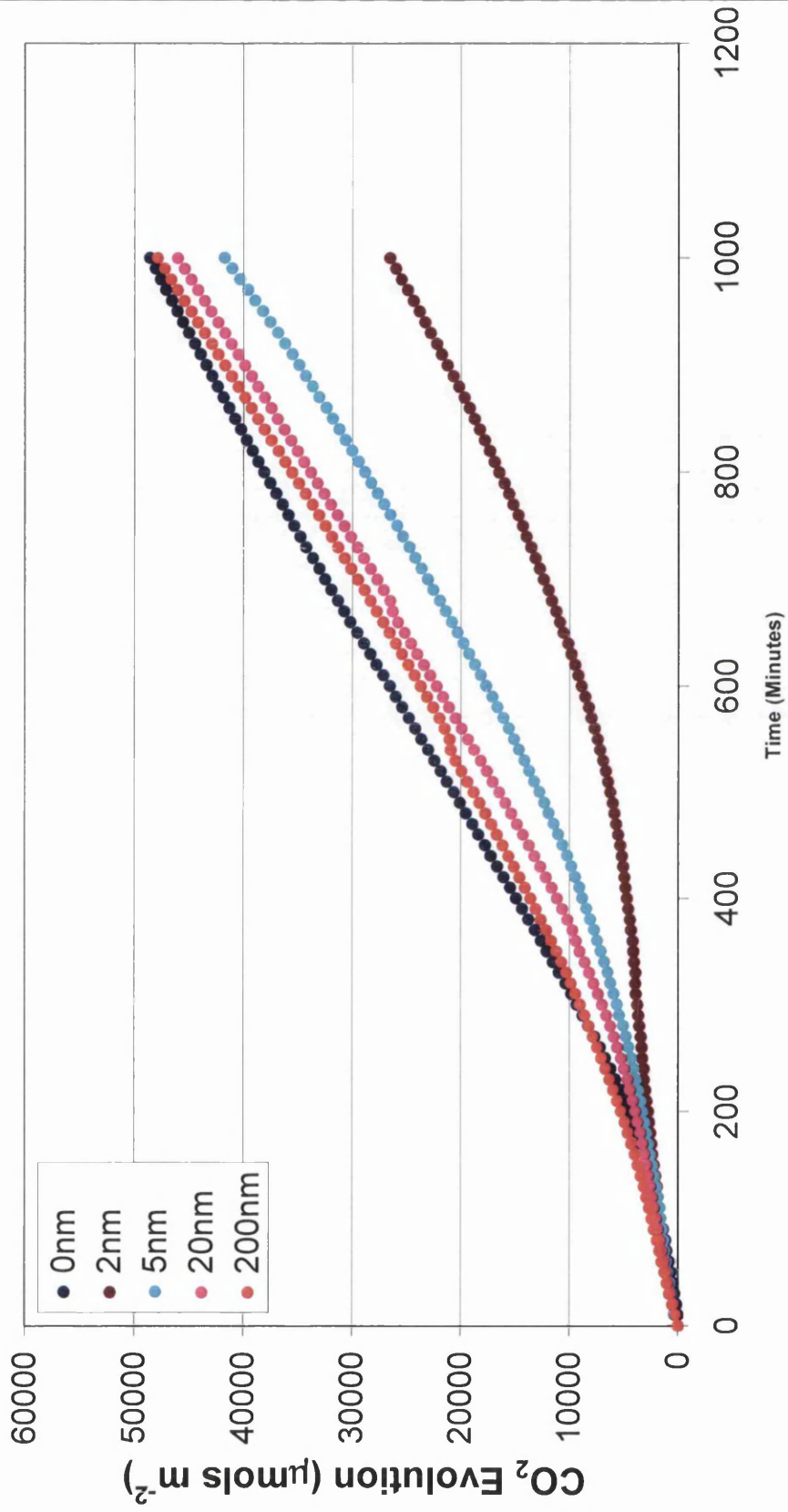


Figure 5-9 CO<sub>2</sub> Evolution Profiles for Zirconia Coated PVC

# Ti Deposition

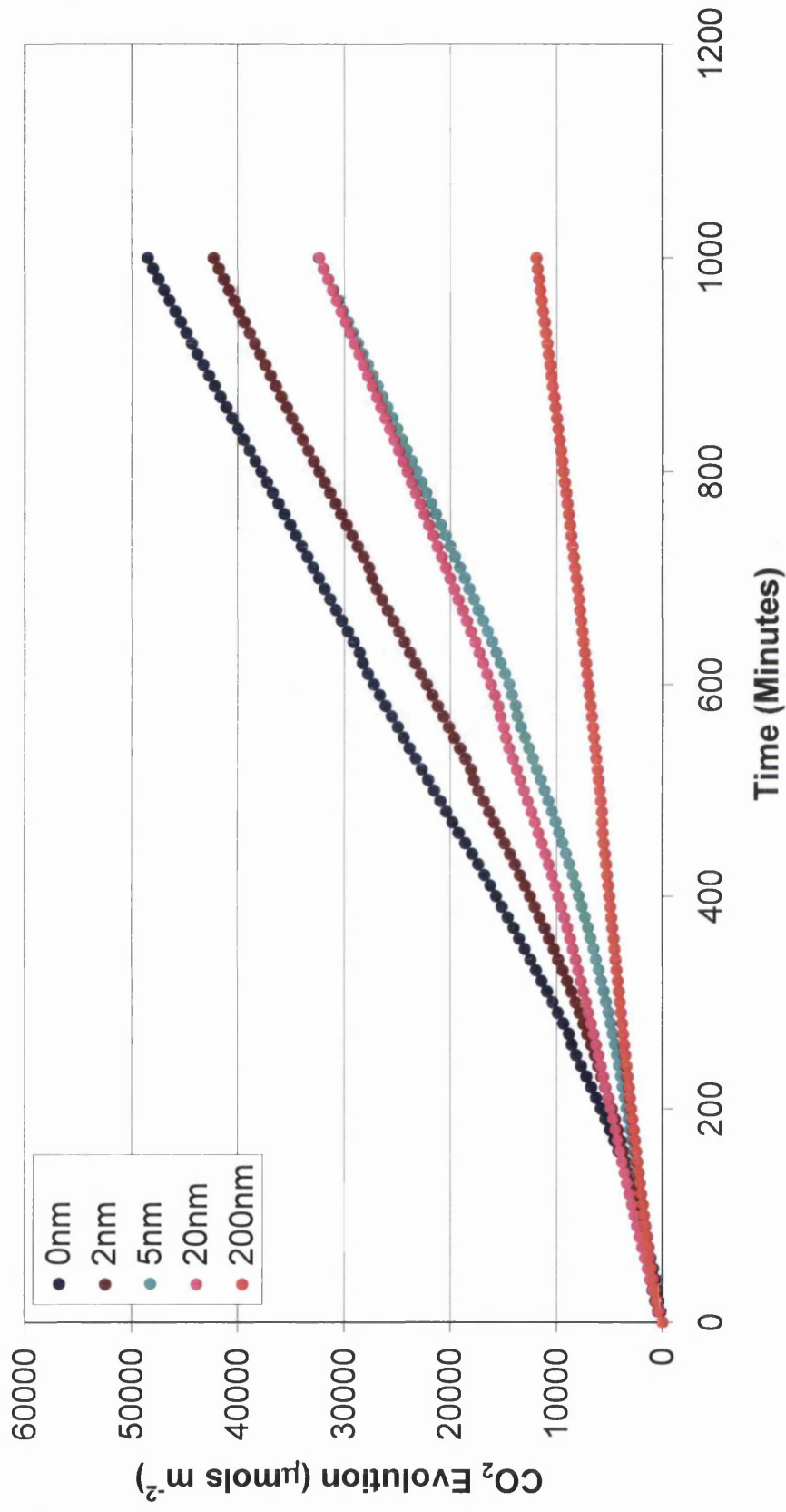


Figure 5-10 CO<sub>2</sub> Evolution Profiles for Titanium Coated PVC

Looking closely at the evolution plots, it is apparent that the characteristics of the evolution plots differ, both in terms of deposition material and coating thickness. As previously shown in 3.3.1, the evolution profile for a TiO<sub>2</sub> pigmented model PVC coating, there is a transition rate between that on the more linear initial and secondary rate, as evident in Figure 5-11.

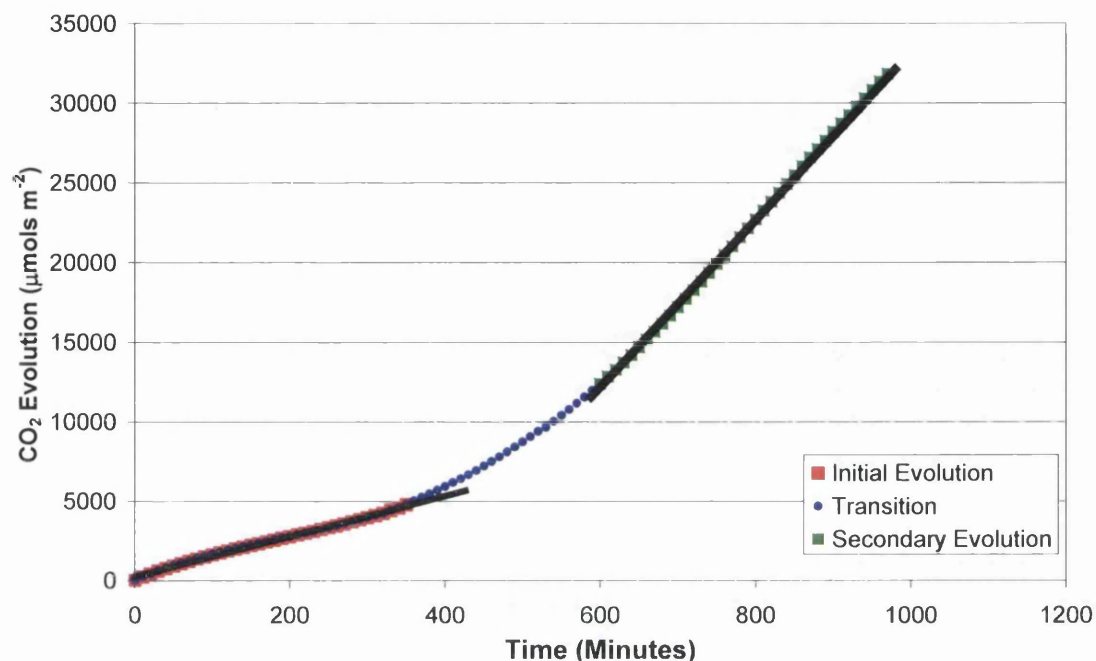


Figure 5-11 CO<sub>2</sub> Evolution Profile for Model PVC in the Absence of a Barrier Layer

This was attributed to acid catalysis. The band gap of TiO<sub>2</sub> means that TiO<sub>2</sub> can be highly photoactive in nature leading to premature failure in certain high UV environments. Via numerous complex reactions, degradation of the TiO<sub>2</sub> pigmented PVC coating, results in the formation of CO<sub>2</sub>, HCl and water and as discussed previously, strong acidic species are known [77] to have a catalytic effect upon TiO<sub>2</sub>. Hence the acceleration in rate observed. In the case here, the presence of an additional surface coating is affecting such a phenomenon.

On removal from irradiation apparatus, there was no visible sign of change in the appearance of the samples.

In the case of ITO, for the 2nm coating, the transition of rate is no longer definitive, as it steadily occurs over approximately 200 minutes, reaching a secondary linear

rate at 800 minutes. For the 200nm coating, no 'kick-off' is actually visible. This phenomenon is also mirrored with the aluminium and titanium deposition.

For the case of the copper deposited coating, the addition at thicknesses of 2nm and 5nm is not as efficient at reducing the evolution, and at 20nm although dramatically reduced, the transition followed by an accelerated evolution is still evident. Although reducing the volume of CO<sub>2</sub> evolved in all instances, the Zirconia coating is also not as efficient and even at 200nm and transition in the rate is clearly visible followed by CO<sub>2</sub> evolution at an accelerated rate. The thickness of the coating (2nm to 200nm) is also inversely proportional to the volume of CO<sub>2</sub> evolved after 1000 minutes.

Perhaps the most interesting of the results is that of the Alumina deposition. At coating thickness of 20nm and 200nm, the volume of CO<sub>2</sub> evolved is actually greater than that on the control with no PVD coating. Rapid CO<sub>2</sub> evolution from onset is evident as is a rapid linear rate after 200 minutes with no definitive transition point. The 5nm alumina coating performs similarly to the control and again the 2nm coating is the most efficient at reducing the CO<sub>2</sub> evolved.

This therefore makes the comparison of plots by means of secondary rates more complicated, given in some case at test durations of 800 minutes the transition is only just occurring and the rate is not linear and steady state. The data was compared in terms of total volume of CO<sub>2</sub> evolved at 1000 minutes, reflecting the total level of photo-oxidation that occurred.

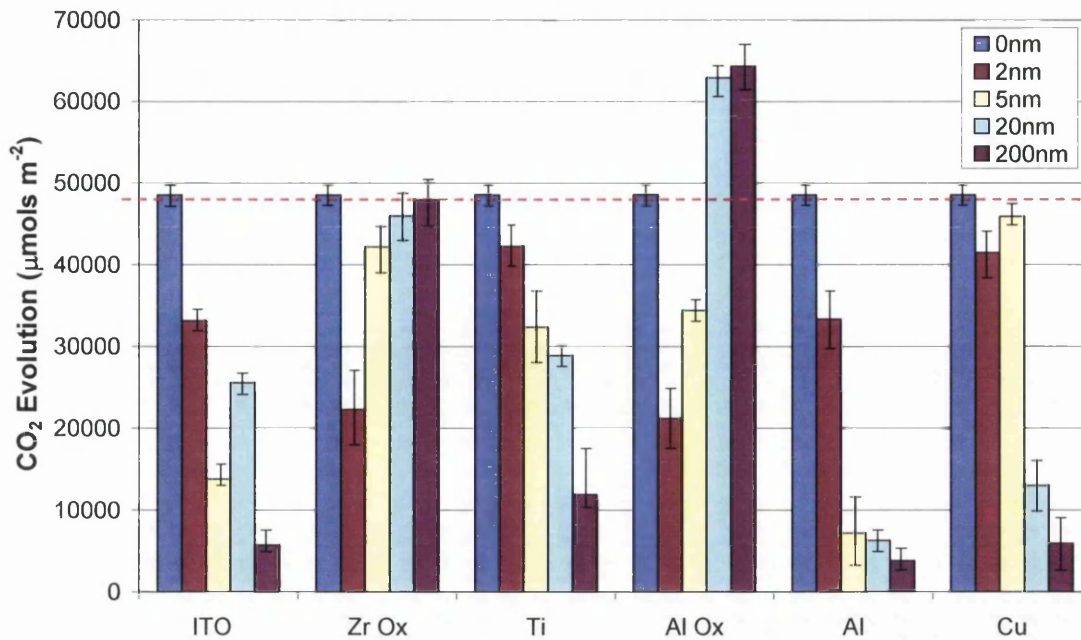


Figure 5-12 CO<sub>2</sub> Evolution Volumes at 1000 Minutes

Figure 5-12 clearly illustrates that the only case whereby the deposition of a thin inorganic coating is detrimental to the reactivity of the PVC coating is the application of alumina at thicknesses of greater than 20nm. For ITO, aluminium, titanium and copper, the trend in data is increasing the thickness of deposition will reduce the volume of CO<sub>2</sub> evolved, thus indication is that the extent of photo-oxidation is also reduced. Interestingly, Zirconia, although offering resistance to oxidation, increasing the thickness of the coating is actually at the detriment of the oxidative stability of the sample. Evidently, a similar phenomenon occurs with alumina, but this time more severely, acting as an aid to the oxidative degradation of the PVC sample beyond that seen in the absence of a deposited coating.

In commercial coating systems, PVD coatings are often used to provide a barrier against the permeation of water and oxygen, usually allowing transmission in visible region (as not to impart any significant colour change) whilst protecting the underlying system from UV attack. In advanced systems, the concept of inter layer between barrier layers is utilised [55]. The effectiveness of such systems is often measured using oxygen and water permeation experiments, as this gives an indication to the most suitable coating selection, for example [82] Alumina exhibits



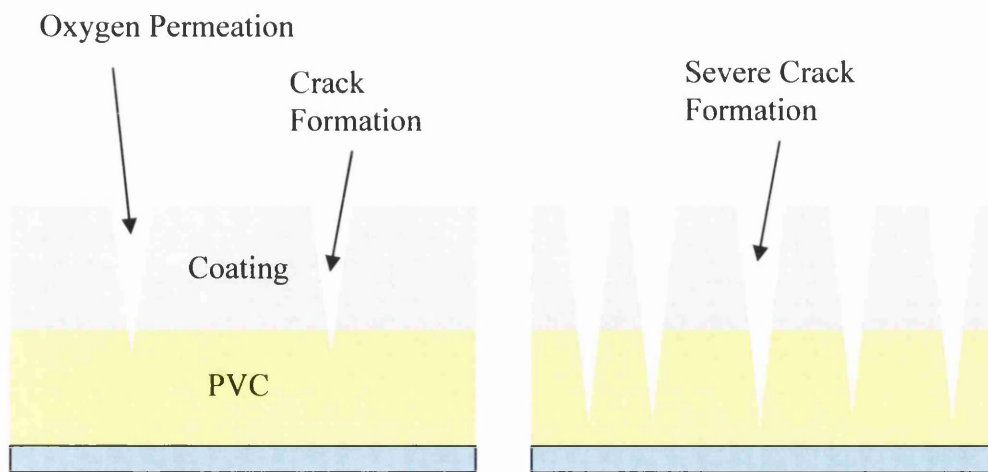
low levels of water vapour permeation, and ITO is shown to be the most impermeable to oxygen.

Gas permeation through a solid is considered a temperature dependent process and Henry et al. [83] have shown with  $\text{Al}_2\text{O}_3$  and ITO coatings on PET, between 10 and 40 degrees, only small increases in oxygen permeation are resulting at the higher temperatures. The temperature recorded with the flat panel irradiation apparatus was measured at constant  $40^\circ\text{C}$ , therefore no temperature related phenomena is expected to play a role in the results seen here. Interestingly in this literature, the type of deposition coating played little significance in the activation energy required for oxygen permeation measured [55], indicating that the rate determining factor is in fact defects in the coating itself and not the choice of coating material. In the case of the results discussed in this chapter, the difference in oxidation characteristics shown is likely to therefore be due to differing levels of defects in the coating.

For the Alumina and Zirconia coatings, increasing the thickness from 2nm to 200nm increases the oxidation measured ( $\text{CO}_2$  evolved). These results indicate a reduction in the coating integrity with increasing thickness. This can be attributed to the compatibility of the PVC and metallic surface, perhaps the formation of microcracks due to a change in surface tension with increasing thickness. As the formation of surface defects increases, the amount of exposed PVC could potentially increase as well as ease of oxygen permeation essential for photo-oxidation. This increase in degradation then becomes especially evident at 20nm and 200nm in alumina. The amount of  $\text{CO}_2$  evolved is greater than that of the non-coated PVC. For this increase to occur, there is going to be some degree of irreversible degradation occurring to the PVC coating itself.

One such explanation would be the theory of severe microcrack formation. Increasing thickness and thus altering surface tensions and potentially changing thermal conductivity, could all contribute to the extent to which microcracks form. Where severe microcrack formation may result in the failure of the integrity of the PVC coating, additional  $\text{TiO}_2$  pigmented surface layer may be exposed, not only increasing the surface area prone to  $\text{TiO}_2$  excitation and but also facilitating the ease of oxygen permeation to this surface area.





n.b. not to scale

Figure 5-13 Formation on Microcracks in Deposited Coating  
 a) microcrack formation b) severe microcrack formation that may result in the increase in PVC degradation rate

Similarly, in the event of such crack formation, there is potential for the entrapment of water and/or HCl in the crack, causing catalysis over and above the non-coated PVC, resulting in extremely localised degradation.

Although thermal degradation of the PVC is also a possibility, the CO<sub>2</sub> evolution experiment only takes place at 40°C and there appears to be no trend in power used to deposit the coatings and CO<sub>2</sub> evolved relative to thickness. Further analysis of the coating structure at every stage on the experiment process using SEM analysis could assist in validating this, as well as identifying if the grain boundaries of the coating are also playing a role in the resistance to degradation.

On the contrary, the CO<sub>2</sub> evolved (trend) decreases with increasing ITO, Al, Ti and Cu thickness. In this instance, a more coherent barrier level is achieved at all thickness with much smaller volumes of CO<sub>2</sub> evolving indicating a greater resistance to oxygen and photodegradation.

In addition to this theory of limiting the oxygen permeability, the UV screening provided by the coating itself is also likely to also be a determining factor. Scope for this is evident, merely in looking at the different appearances of the coatings. For

example, the metallic appearance of the aluminium deposited surface is more likely to reflect UV irradiation, compared to the matt, yellow appearance of the titanium coated PVC, or the more translucent aluminium oxide.

Taking into consideration the cost and time implications of such an application technique with regard to how feasible such a coating system may be on a commercial scale, Figure 5-14 summarises the potential.

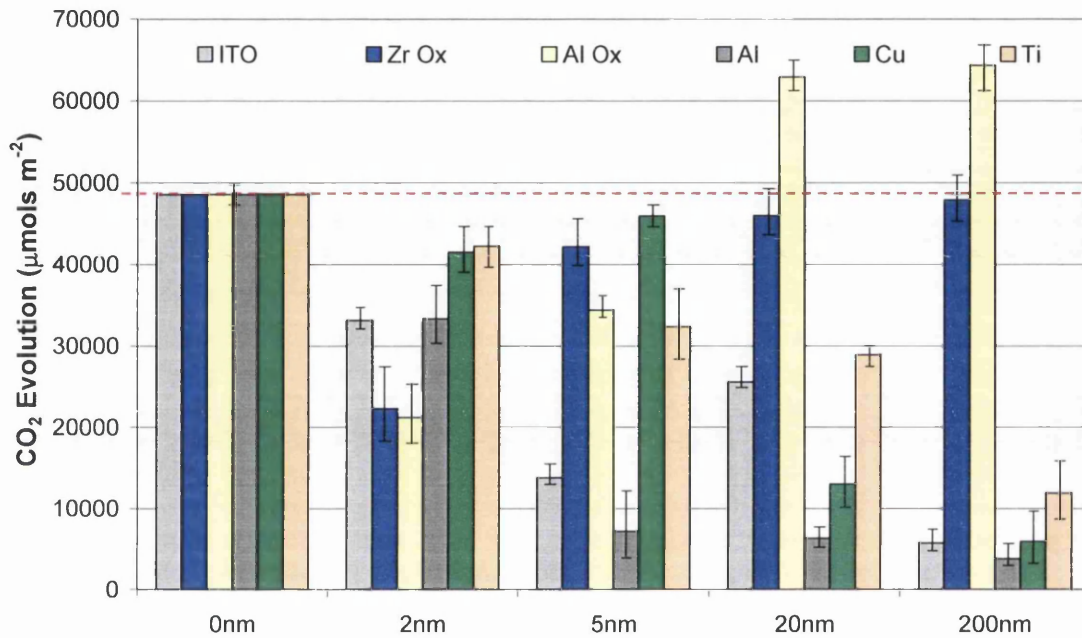


Figure 5-14 CO<sub>2</sub> Evolution Volumes at 1000 Minutes

At small coating thicknesses of only 2nm, alumina outperforms all other coatings in terms of oxidation characteristics. However, given the dramatic decrease in protection offered when reaching thicknesses or near 20nm, this choice of coating would best be avoided. At an additional deposition of only 3nm, aluminium is clearly very efficient at offering a superior level of resistance to photo-oxidation, comparable to ITO and 200nm. Increasing the thickness of the aluminium appears to provide only a marginal improvement in reducing CO<sub>2</sub> evolved, so therefore a likely candidate for material selection at low levels of deposition.

### 5.3.2 Aluminum and Titanium Wedge Coated PVC

Having highlighted aluminium as a potentially efficient barrier deposition layer to increase the photo-stability of PVC (and the effect of coating thickness of its ability to inhibit such degradation), an aluminum wedge coated PVC sample was produced. A titanium wedge was also produced to compare whether the slightly inferior protection offered as shown in the CO<sub>2</sub> evolution results, would also be apparent here. Both show that an increase in thickness is preferential for increased protection.

Once again, the HPS200 plastisol formulation was used, with a loading of 20% K1001 grade TiO<sub>2</sub>, with all UVAs and HALS removed from the HPS200 formulation. The PVC was coated with an a wedge, with thickness changing from 200nm to 0nm along its length, as seen in Figure 5-15 and Figure 5-16

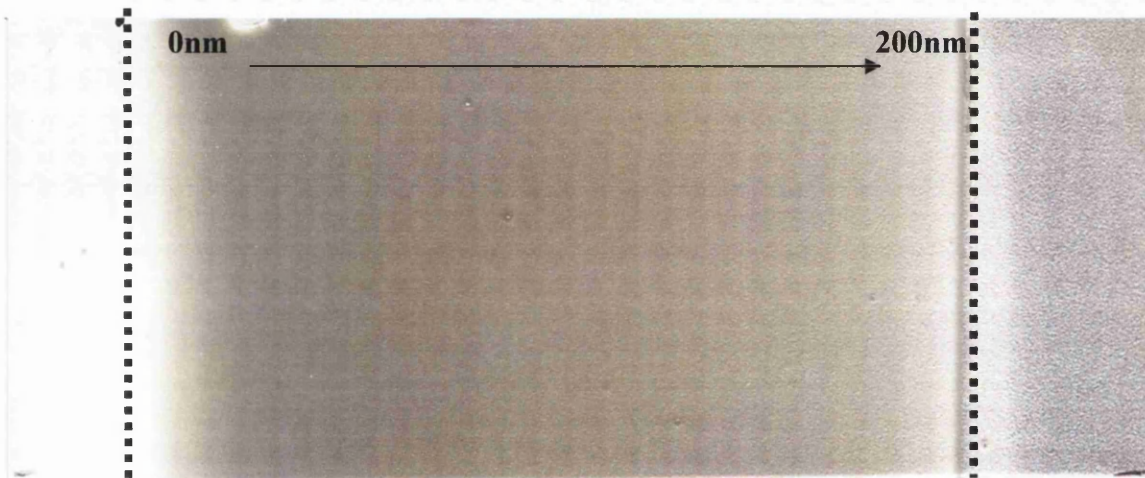


Figure 5-15 Aluminium Wedge Coated PVC

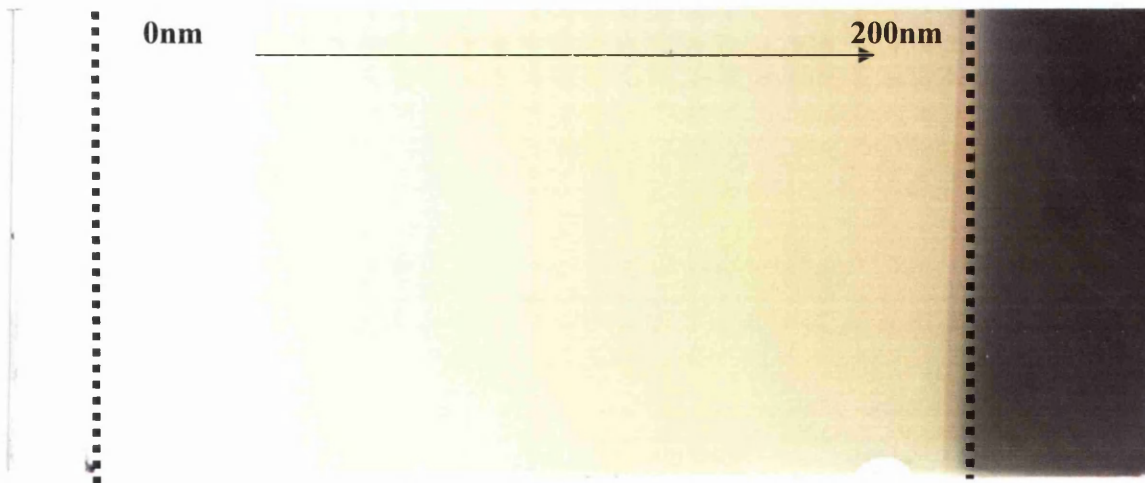


Figure 5-16 Titanium Wedge Coated PVC

The effect of increasing thickness is clearly visible, with an increasingly silver and yellow appearance at higher thicknesses of the Al and Ti respectively. Only at thickness of approximately 15nm in both cases is the white appearance of the PVC clearly visible. The wedge sample was then weathered in the QUVA weatherometer for 1000 hours.

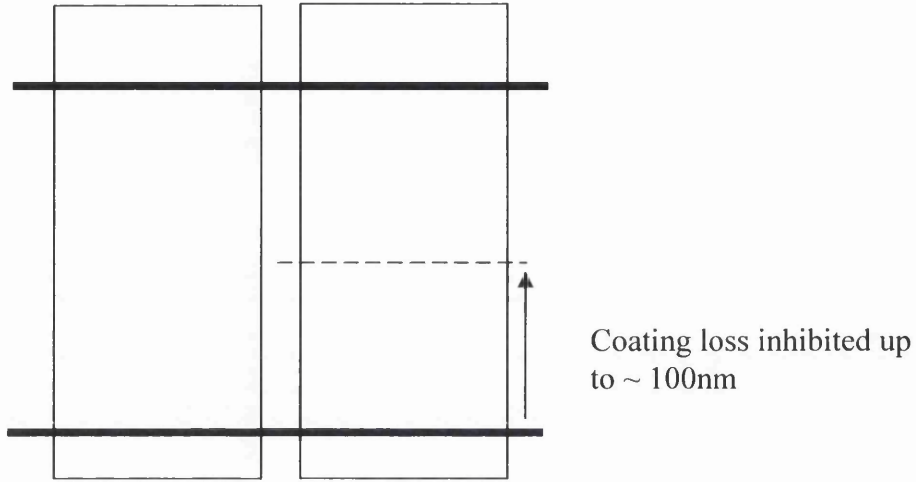


Figure 5-17 Aluminium Wedge Coated PVC Before and after 1000h hours QUVA Weathering

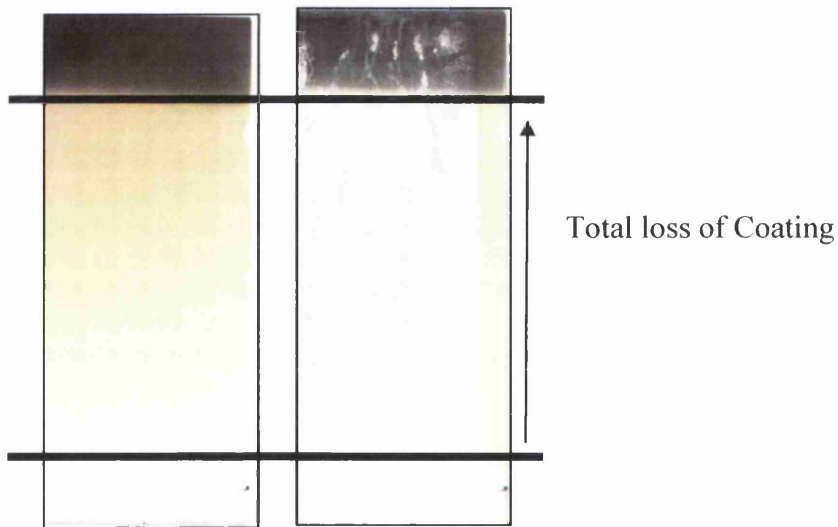


Figure 5-18 Titanium Wedge Coated PVC Before and after 1000h hours QUVA Weathering



**Aluminium Deposition**

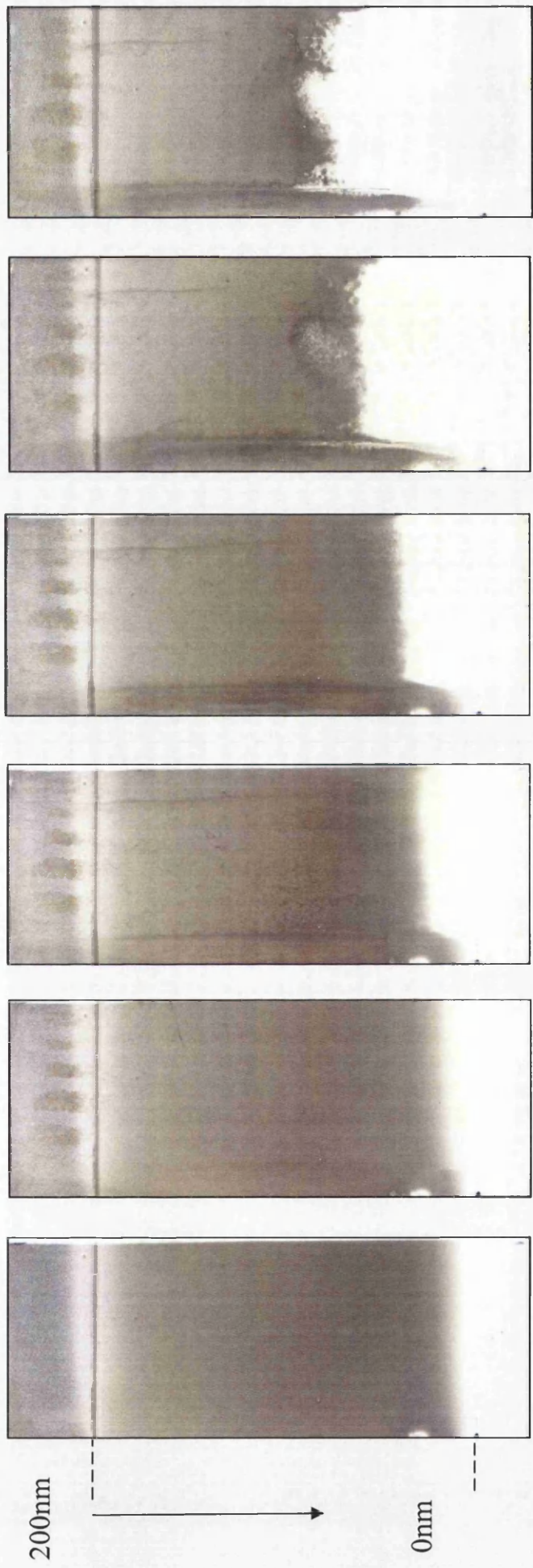
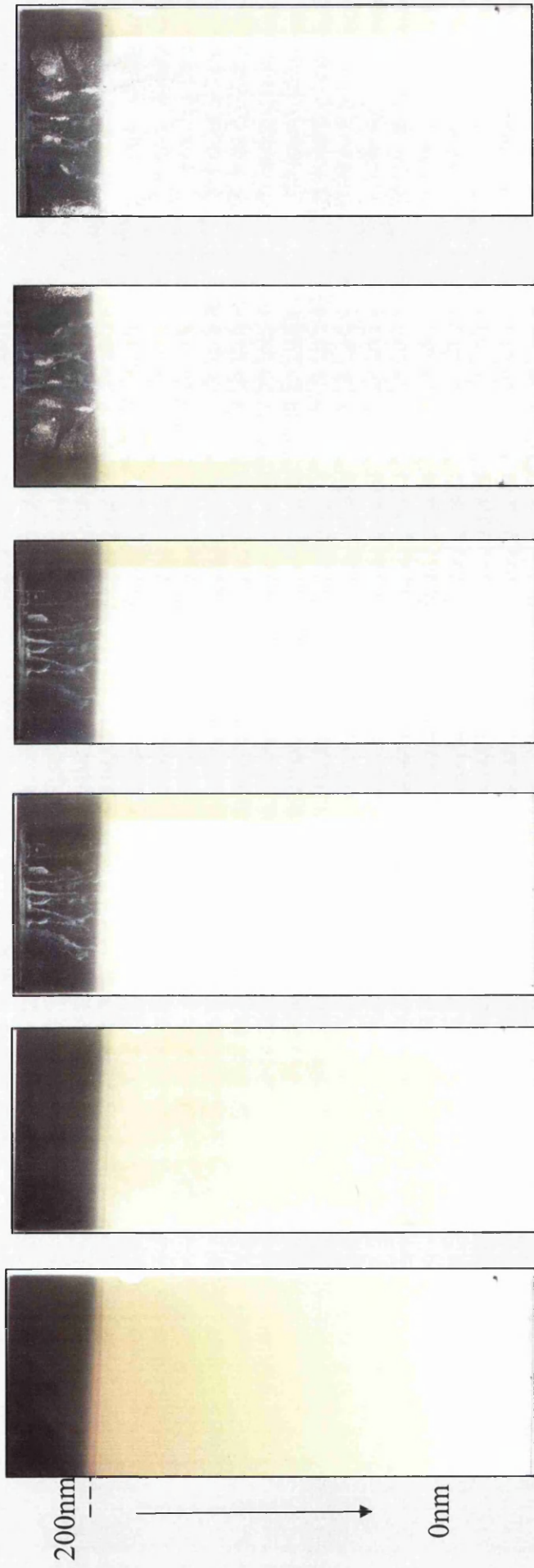


Figure 5-19 Scanned Images of Aluminum Wedge Coated PVC Sample During QUVA Weathering

# Titanium Deposition



0 hrs QUVA  
Weathering



1000 hrs QUVA  
Weathering

Figure 5-20 Scanned Images of Titanium Wedge Coated PVC Sample During QUVA Weathering

Where PVC was exposed to weathering, chalking was visible and loss of organic material also.

After 1000 hours QUVA, the furthest point at which the coating had receded to and PVC was exposed was measured. Therefore, after 1000 hours weathering, at aluminium coating thicknesses of approximately 100nm, the deposited aluminum coating was still intact; however total coating failure of the titanium coated PVC had occurred.

This experiment also reflects the results seen for the CO<sub>2</sub> evolution experiment; the removal of aluminum and titanium coating during weathering is likely to be heavily influenced by the thickness of coating applied. Where it was previously shown that the oxidation can be reduced with only 5nm scale depositions, in reality, as shown here the fragile nature of such a coating is not likely to withstand manual and coil handling procedures, encountered during the coil coating process.

## 5.4 Conclusions

The efficiency of various nano-scale coatings has been illustrated, highlighting the potential for improved resistance to weathering. The CO<sub>2</sub> evolution data was used as a tool to quantify and compare how the coating choice and thickness affected the rate of oxidation. Although only being an introductory study, what is obvious is that although great potential has been shown there is a tradeoff between appearance, performance and the cost associated with the deposition material and process.

To illustrate the fantastic scale of potential increase in PVC coating durability, Figure 5-21 compares the average CO<sub>2</sub> evolution rates for a deposition coating in this study using a 'U grade' photoactive grade TiO<sub>2</sub> model PVC, an 'A grade' TiO<sub>2</sub> pigmented PVC and commercial standard durability PU [80]

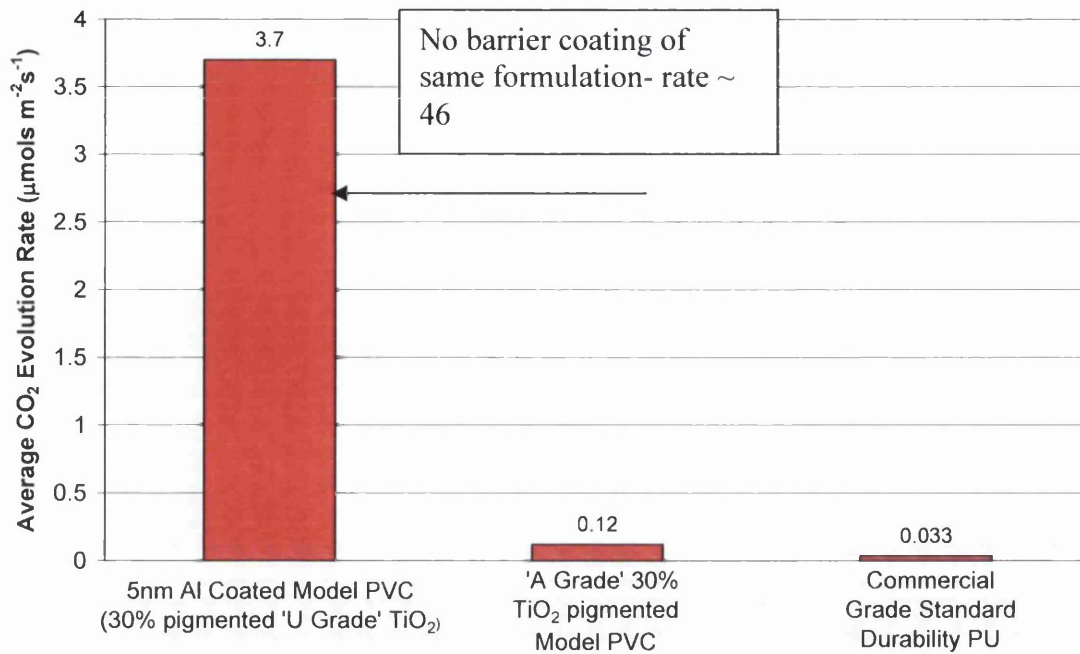


Figure 5-21 CO<sub>2</sub> Evolution Rates for Various Coatings

Where it was previously shown that the oxidation can be reduced with only 5nm scale depositions, in reality, as shown in 5.3.2, the fragile nature of such a coating is not likely to withstand manual and coil handling procedures, encountered during the coil coating process; something which could be overcome with the use of clear coat lacquers.

Such a system may be considered too sophisticated or costly, for the current applications of PVC plastisols, such as external cladding; however, the mechanisms of improving a coatings resistance to photodegradation have been illustrated in this chapter. For an application whereby a 'metallic-style' finish is desirable, on a low grade substrate and base coating, coupled with a clear coat lacquer for protection against physical damage, there is the potential for a visually attractive, durable novel coating system to be produced.



## 5.5 References

1. Fahlteich, J., Fahland, M., Schönberger, W., and Schiller, N., *Thin Solid Films*, 2009. **517**(10): p. 3075-3080.
2. Singh, B., Bouchet, J., Rochat, G., Leterrier, Y., Manson, J.A.E., and Fayet, P., *Surface and Coatings Technology*, 2007. **201**(16-17): p. 7107-7114.
3. Worsley, D.A., Mills, A., Smith, K., and Hutchings, J., *Chemical Society, Chemical Communication*, 1995: p. 1119.
4. Henry, B.M., Assender, H.E., Eriat, A.G., and Grovenor, C.R.M., 2004: p. 609.
5. Henry, B.M., Erlat, A.G., McGuigan, A., and Grovenor, C.R.M., *Thin Solid Films*. **382**: p. 194.
6. Wray, J., *The Degradation Studies of TiO<sub>2</sub> Pigmented Polyurethane Coating Systems*, in University of Swansea School of Engineering. 2009, Swansea University.

## **6 Polyethylene Photodegradation & Development of Accelerated Testing Techniques**

## **6.1 Introduction**

Having addressed a potential increase in the use of polymers such as polyethylene in coating applications as a result of more stringent environmental requirements, it is of importance to generate knowledge on its performance. The basis of polyethylene degradation has been discussed in the literature (1.3.3), also including techniques used to investigate it. In these cases, previously discussed more established testing techniques have coupled with new testing techniques to verify the data.

With increasing pressure to bring newly developed products to the market, rapid and accelerated testing techniques are favourable. However, the true representation of this data to lifetime prediction is questionable. A balance between a variety of testing techniques is the most likely way to indicate the performance of the component, with each technique offering an alternative measure of its longevity.

With every differing test method, another insight into the nature of its degradation and performance is gained and this itself is invaluable in the effort to improve (or even reduce) the lifetime of a product.

### **6.1.1 Aims and Objectives**

The success of measuring the evolution of CO<sub>2</sub> under normal irradiation conditions and atmospheric changes has been shown in this thesis, results being indicative of the severity of degradation and thus a comparison on product longevity can be drawn.

This chapter looks to extend on the above mentioned experimentation, with a more comprehensive sample matrix including commercially available stabilisers and pigments known to accelerate photodegradation, noting the effect of the various additives.

In addition to CO<sub>2</sub> profiles, a technique that measures the oxidation stability of the material has been carried out, and further to this, an experimental system has been devised to accommodate in situ oxidation profile in the presence of UV light. The

aim of this work is to verify the new technique and gain a greater understanding of the degradation mechanisms and accuracy of the testing techniques.

## 6.2 Experimental

### 6.2.1 Pigments and Stabilisers

In order to explore both the nature of the polyethylene photodegradation and the effectiveness of newly developed accelerated techniques, a variety of sample coatings were produced. As previously mentioned, TiO<sub>2</sub> is a widely used pigment that is also known to potentially act as a ‘pro-degradant’. The un-pigmented virgin polyethylene (as described in chapter 2) was stabilised with the addition of an anti-oxidant (AO) and UV absorber (UVA). It must be noted, these samples were not pigmented with TiO<sub>2</sub> in addition to the AO and UVA.

Table 6-1 Additives used in PE

| Name         | Type  |
|--------------|---|
| Kronos 1001  | TiO <sub>2</sub><br>(Anatase-TiO <sub>2</sub> content 99%<br>Photoactivity grade C) |
| Irganox 1010 | Phenolic Anti-oxidant   |
| Tinuvin 326  | UVA   |

Table 6-2 Levels of Additive Addition

| Sample ID | Additive     | % Addition |
|-----------|--------------|------------|
| 1         | No Additive  | 0          |
| 2         | K1001        | 10*        |
| 3         | K1001        | 30         |
| 4         | K1001        | 50         |
| 5         | Irganox 1010 | 0.5**      |
| 6         | Tinuvin 326  | 0.5*       |

\* Likely commercial level of addition

\*\* As recommended by manufacturer

(Insufficient mixing of 70% TiO<sub>2</sub> in PE hindered any higher levels of pigmentation)

### **6.2.2 Sample Preparation**

All samples were subjected to the mixing and pressing regime outlined previously 2.2.2 using virgin PE.

It was important to expose all samples to the same potential level of thermal degradation during processing so as to ensure reproducible results. In the case of the non-pigmented/non-stabilised PE, the virgin PE granules were also subjected to heating and mixing in the torque rheometer, to coincide with the production route of the other samples. The importance of this will be evident later, where thermal decomposition is touched upon.

All polymer mixes were pressed to a thickness of 0.5mm. For testing in the flat panel reactor, two samples from each plaque were made measuring 15cm by 7.5cm. For weathering, four samples from each plaque were cut for mounting in the QUVA weatherometer, measuring 7.5cm by 7.5cm. A hole punch was used to press a circular sample of suitable size that measured the size of the aluminium pans to contain the DSC samples.

### **6.2.3 Accelerated Weathering**

The sample panels were irradiated using a QUVA accelerated weatherometer fitted with UVA lamps, as outlined in Chapter 2. Each sample was subject to a cyclic exposure of 8 hours UVA radiation and 4 hours condensation. The temperature for both cycles (UV and condensation) was set at 40°C and a light intensity of 0.8W/m<sup>2</sup>/nm. Samples were exposed for 150 hours initially, to measure early onset photodegradation (TiO<sub>2</sub> samples especially) and then further exposed for 300 hours (450 hours in total) to investigate more aggressive levels of degradation.

### **6.2.4 CO<sub>2</sub> Reactor**

The flat panel reactor previously used [63], was now used to assess the photostability of these various coatings. The samples were irradiated in the closed loop flow system for typically 1200 minutes (20 hours) with experiments carried out at lab humidity. Because the samples were run in the flat panel reactor, then further

weathered and subsequently tested again, a timing device was used to ensure that all the samples were irradiated for 1200 minutes exactly.

Due to the stable nature of the non-pigmented samples, a longer gas path length cell (2.3.2) was used to detect the smaller volumes of CO<sub>2</sub> being evolved. Samples 1 to 6 were tested.

### **6.2.5 Differential Scanning Calorimetry (DSC)**

Oxidation induction experiments can take two forms, oxidation induction temperatures (OITemp) or oxidation induction times (OITime). Whilst OITimes are more regularly referred to in literature, they are somewhat more complex to engineer; for an oxidation induction time, a set temperature is maintained and the time taken until oxidation is considered the OITime. However, when using this technique on a variety of different samples, a suitable temperature has to be chosen for all experiments, in order to ensure that the OITime is actually measurable and comparable on all the samples. For example, if a temperature too high is chosen, oxidation may occur in a matter of seconds rather than minutes and this will be difficult to differentiate between samples. In the case of this work, an OITemp was the chosen route of experimentation (which shall now be referred to as OIT throughout this thesis).

As with all DSC experimentation, the following procedure was followed:

- i. Turn on cooler
- ii. Turn on DSC, nitrogen equilibrium
- iii. Input software data
- iv. Weigh for normalising
- v. Sample into chamber (no lid)
- vi. Set experimental parameters

The following testing parameters were used for the oxidation induction testing:

- i. Action Occurs Immediately: Turn nitrogen on 20mL/min
- ii. Initial Temperature : 100°C

- iii. Hold for 5 minutes at 100°C
- iv. Switch gas to oxygen immediately
- v. Heat from 100° C to 230°C at 0.10°C/min
- vi. Hold for 5 minutes at 230°C
- vii. Switch to nitrogen immediately
- viii. Return to load temperature of 30°C
- ix. Turn gas off

Data is recorded, normalised and heat flow is plotted against temperature. Tangents of the heat flow curve in the region of oxidation are used to locate the oxidation temperature.

### **6.2.6 Development of Technique for In-situ Oxidation Induction Profiles**

In order to measure the influence of UV on the oxidation induction characteristics, an in-situ technique was designed. The DSC equipment was adapted to irradiate the sample whilst the oxidation experiment was in progress, measuring the combined effect of UV and an oxidative environment on the oxidation induction temperature.

Given the closed controlled atmosphere of the furnace that the sample sits within, the DSC furnace lid was replaced with a transparent one to allow for the UV to irradiate the sample.

Figure 6-1 illustrates the effect that the choice of new furnace lid has on the transmission. Two, 2mm quartz circular furnace lids were manufactured to replace the regularly used lids between the lamp and the closed furnace.

An adjustable lamp containing a 'ProlitePlus 25 W Compact Fluorescent Bulb' (intensity 1 W/m<sup>2</sup>/nm) was erected alongside the DSC and could be manoeuvred into position easily. Protective foil covered the DSC unit and a metal unit was manufactured to surround the experimental set up to protect against over exposure to other lab users.

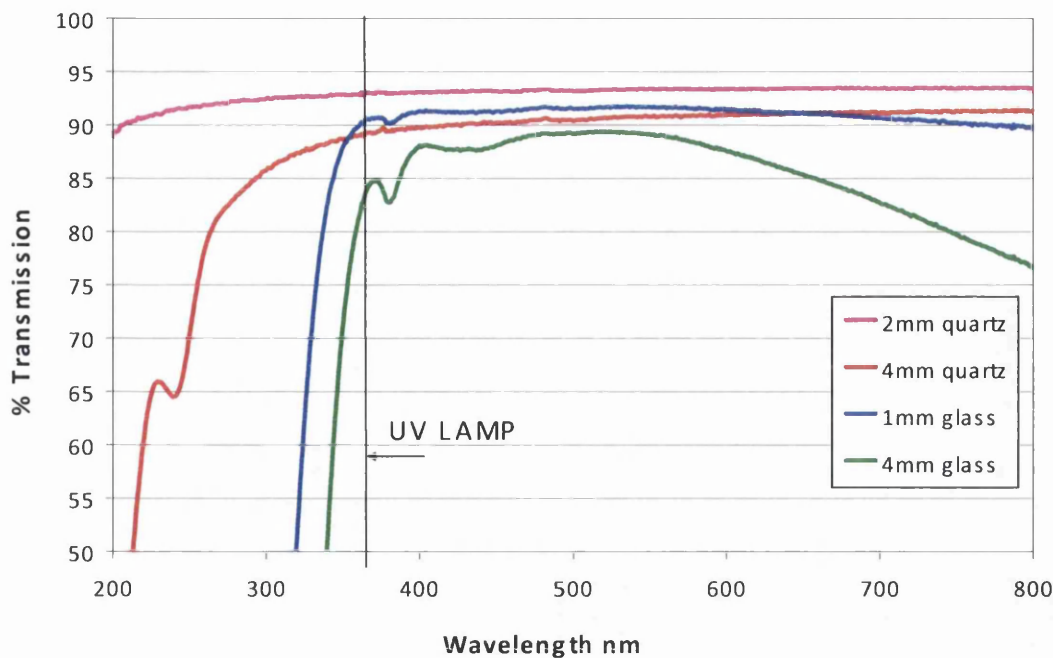


Figure 6-1 UV Vis. Spectrum of Various Options for Furnace Lid

In this instance, the test technique is now adapted, with the lamp being turned on as soon as the system has equilibrated and the oxygen atmosphere is introduced.

- i. Action Occurs Immediately: Turn nitrogen on 20mL/min
- ii. Initial Temperature : 100°C
- iii. Hold for 5 minutes at 100°C
- iv. Switch gas to oxygen immediately
- v. Turn on lamp
- vi. Heat from 100°C to 230°C at 0.10°C/min
- vii. Hold for 5 minutes at 230°C
- viii. Switch to nitrogen immediately
- ix. Return to load temperature of 30°C
- x. Turn gas off



## 6.3 Results and Discussion

### 6.3.1 In-situ CO<sub>2</sub> Evolution Profiles of PE

The FTIR flat panel irradiation apparatus was used to record the volume of CO<sub>2</sub> evolved during the test duration. Figure 6-2 and Figure 6-3 illustrate the CO<sub>2</sub> evolution profiles of polyethylene under regular test conditions. Evolution was instantaneous and no CO<sub>2</sub> evolution was evident in the absence of UV.

The evolution of the TiO<sub>2</sub> pigmented PE was significantly greater than that of the virgin and stabilised PE; with the scale of the evolutions of the above graphs illustrating this. The influence of the photo-active pigment is very evident, although relative to this, the impact of varying levels of TiO<sub>2</sub> addition is small. As expected, Tinuvin reduces the level of CO<sub>2</sub> evolution, whilst on the contrary Irganox actually increases it.

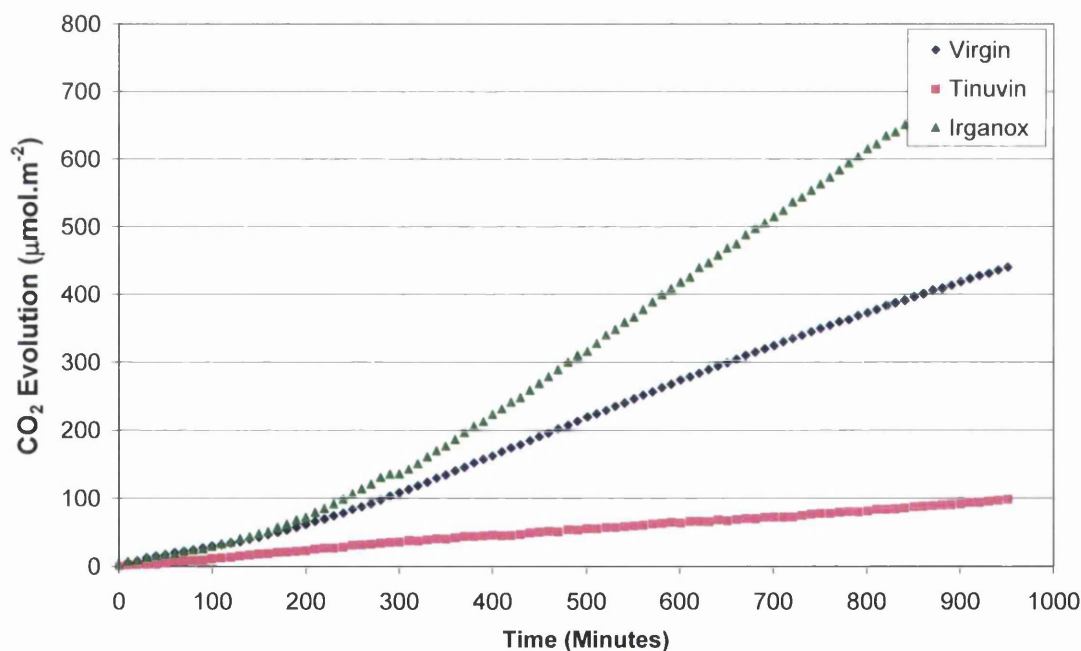


Figure 6-2 CO<sub>2</sub> Evolution Curve for Virgin and Stabilised PE

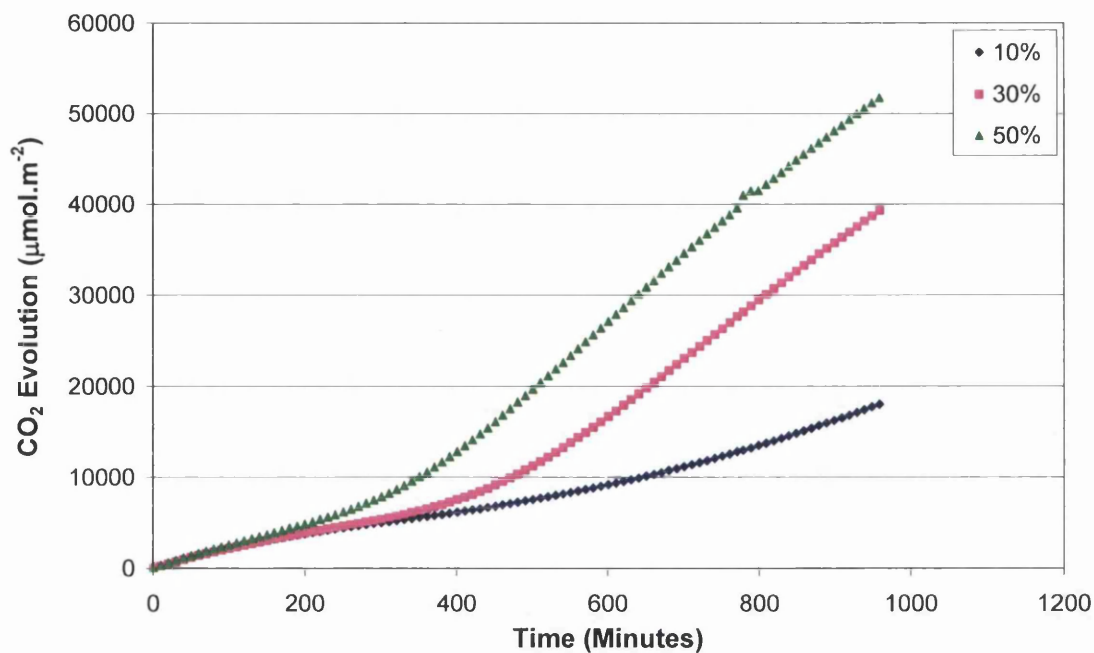


Figure 6-3 CO<sub>2</sub> Evolution Curve for TiO<sub>2</sub> Pigmented PE

The gradient of the plot between 600 and 900 minutes was used to calculate the rate of CO<sub>2</sub> evolution and give a quantitative measure of coating degradation.

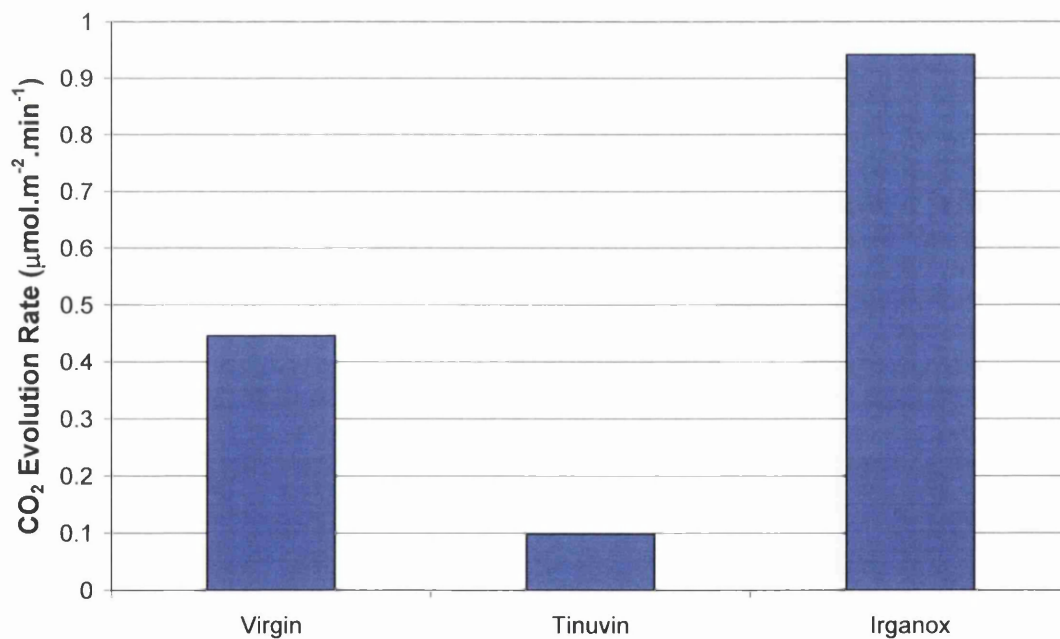


Figure 6-4 CO<sub>2</sub> Evolution Rates for Virgin and Stabilised PE

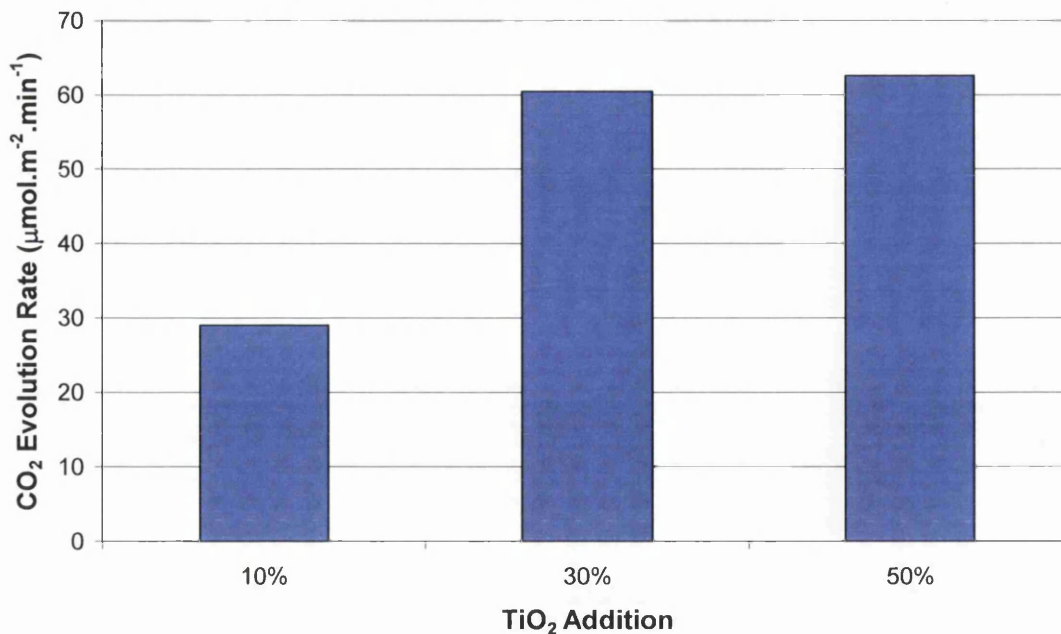


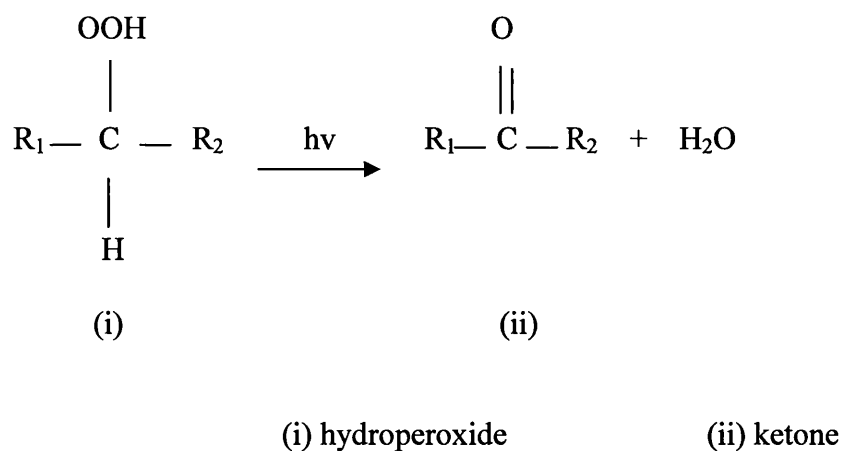
Figure 6-5 CO<sub>2</sub> Evolution Rates for TiO<sub>2</sub> Pigmented PE

The addition of a photoactive TiO<sub>2</sub> pigment causes significant photocatalysis and coating degradation. On average, the TiO<sub>2</sub> pigmented PE samples are in the region of 100 times more photoactive than virgin PE. This effect is also widely evident in PVC coating systems pigmented with TiO<sub>2</sub> [60, 81, 84].

Following a sequence of complex reactions, CO<sub>2</sub> is produced as a by-product of the photo-oxidation of PE, making it an ideal parameter to measure the extent and rate to which degradation is occurring, even in stable systems like this. As described in the introduction, a radical (R) present within the polymer can react with oxygen to give a peroxy polymer radical, which can further react with PE molecules to give a polymer hydro-peroxide. Such a sequence of reactions can be initiated UV irradiation.



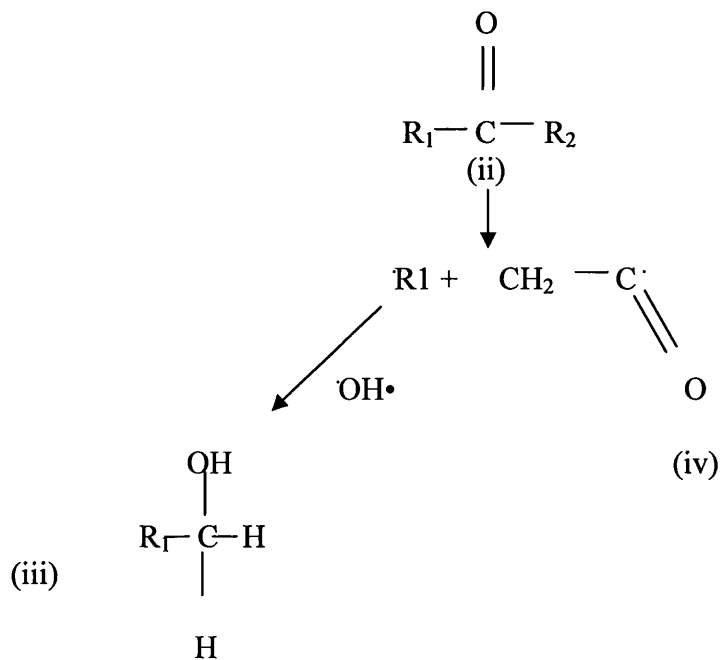
In the presence of UV, the hydroperoxides can then undergo further reactions, resulting in the formation of a ketone (Equation 6-4).



(Equation 6-4)

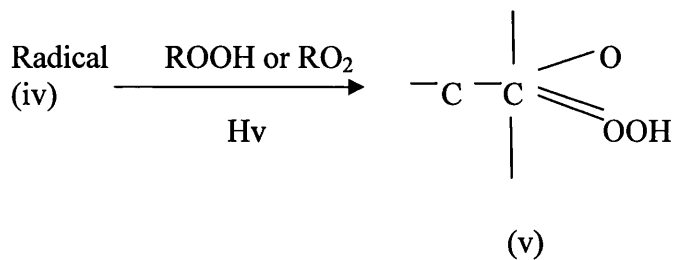
The ketone can then subsequently undergo further Norrish I and II reactions:

Norrish I: The formation of radical species which then further react to produce unstable peracids. Subsequent reaction of the peracids is discussed shortly.



(iii) alcohol species  
(iv) radical

(Equation 6-5)

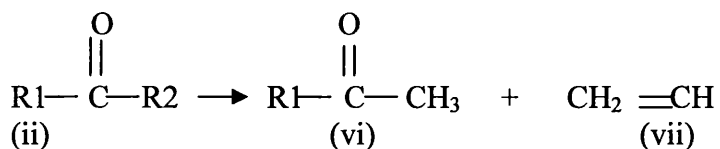


(v) unstable peracids

(Equation 6-6)

Norrish II: reaction of the ketone (ii) to a methyl ketone (vi) and vinyl groups (vii).

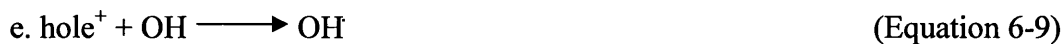
The methyl ketones may react further to generate an aldehyde (Equation 6-7).



Equation (6-7)

The peracids formed during the Norrish I reaction, can further react, by 2 different routes as seen in Figure 6-6. It is the reaction via Path A that results in the formation of CO<sub>2</sub>, as measured during this experiment.

In PE pigmented TiO<sub>2</sub>, the degradation rate is far more rapid. The oxidation sequence is induced by UV light, and the degradation is attributed to the UV activation of the TiO<sub>2</sub>. The generation of OH radicals will react with PE molecules encroaching on the TiO<sub>2</sub> surface causing oxidation of the polymer.



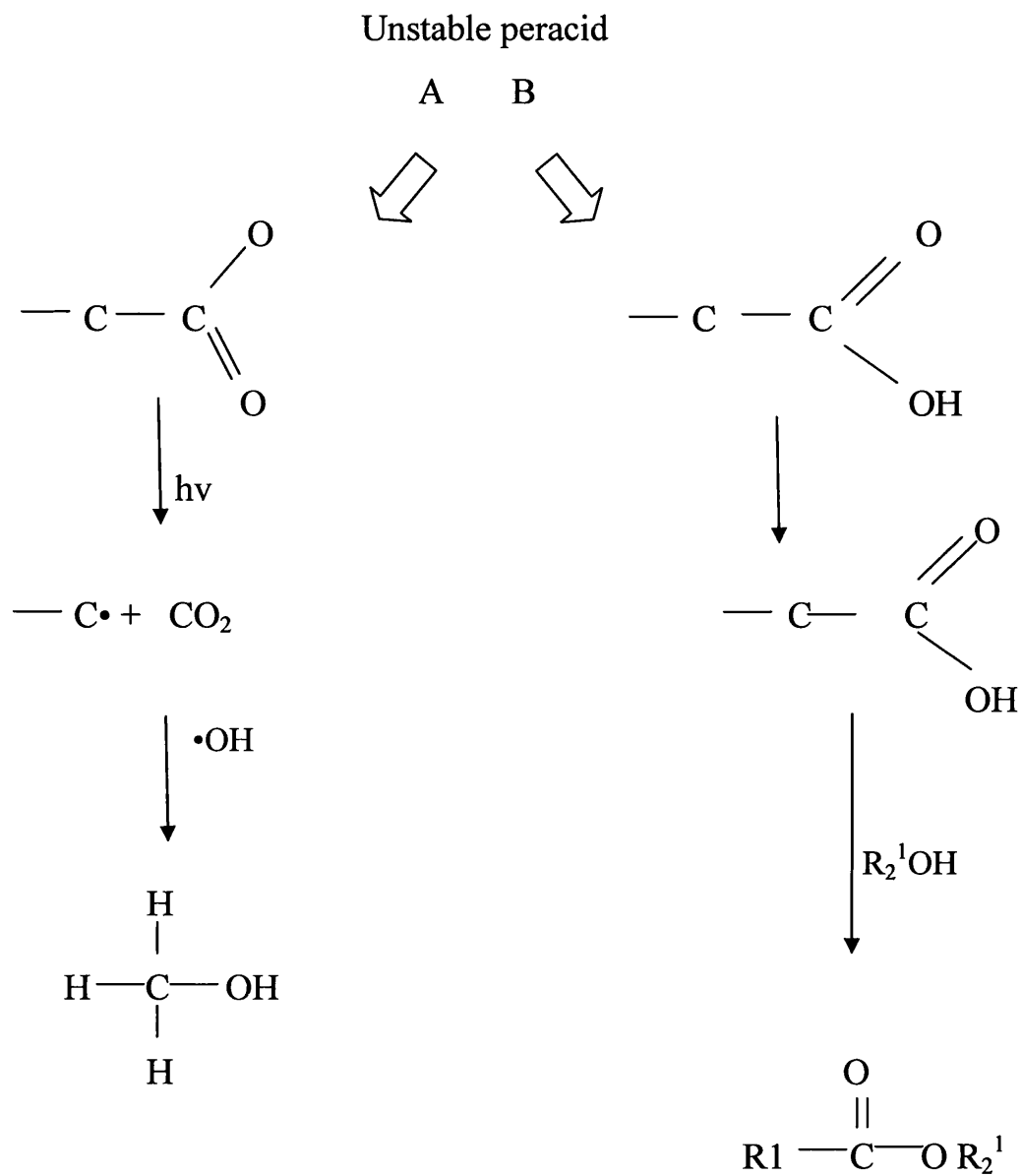


Figure 6-6 Formation of  $\text{CO}_2$  during oxidation of PE

The addition of 30% TiO<sub>2</sub> compared to 10%, has a significant influence, doubling the rate of CO<sub>2</sub> evolution. At this level of addition, an increase in photocatalysis is substantial. In comparison to this, a 50% addition level has only a marginal effect on the rate of degradation. Due to the high refractive index of TiO<sub>2</sub> and inherently stable nature of PE, it can be considered that at such a high loading, the screening effect of the pigment in fact starts to infringe on the photocatalysis that occurs. The similar rates of CO<sub>2</sub> evolved by these pigment loadings is a result of the TiO<sub>2</sub> reducing light penetration into the PE sample and hindering the efficiency of the pigment coating in reducing photocatalysis.

With regard to stabilisers, the use of UVA Tinuvin reduces the rate of CO<sub>2</sub> evolution by a factor of 4 and therefore photo-oxidation does not occur so rapidly. As expected the UVA successfully preferentially absorbs the UV radiation, dissipating the energy in a harmless manner such as heat.

In comparison to the stabilising effect of the Tinuvin, the addition of Irganox (a widely used thermal anti-oxidant stabiliser) in fact appears to promote CO<sub>2</sub> evolution and therefore can be considered to accelerate the degree of photo-oxidation. This form of stabiliser is more commonly used as a heat stabiliser for thermal degradation. It is evident that the inherently stable virgin PE, in the presence of such an additive, in fact undergoes a greater degree of photo-oxidation. Phenolic anti-oxidants (AH) such as this work by directly trapping peroxy radicals formed during degradation to break the auto-oxidation chain reaction. In fact, in some instances, UV stable thermal antioxidants can potentially inhibit photochemical degradation by acting as radical acceptors suppressing reactions or by decomposing peroxides, however in this case this is clearly not occurring. [46]

The likely explanation for this is that despite being an AO itself, in high UV conditions the Irganox itself begins to breakdown and the reactive species that are a by-product to this degradation then act to promote oxidation in the polymer matrix. In this instance, the normally non-reactive radical species formed during the reaction, is in fact an enabler of photocatalysis.



### 6.3.2 In-situ CO<sub>2</sub> Evolution of Artificially Weathered PE

The above experimentation was repeated, this time with periodic artificial weathering in a QUV weatherometer. After testing in the flat panel reactor they were returned to the QUV cabinet for further exposure. Figure 6-7 and Figure 6-8 show the CO<sub>2</sub> evolution profiles for the virgin, stabilised and pigmented PE at various stages of artificial weathering. 150hrs was firstly measured to monitor early onset degradation in the more photo-active samples. At this stage, degradation phenomenon such as chalking was already evident in the TiO<sub>2</sub> pigmented samples, whereas little degradation was evident in the remaining samples, so all were therefore exposed to an additional 300 hrs to encourage degradation in the more stable samples. As before, due to the orders of magnitude difference in CO<sub>2</sub> evolved, evolution profiles are shown on 2 graphs.

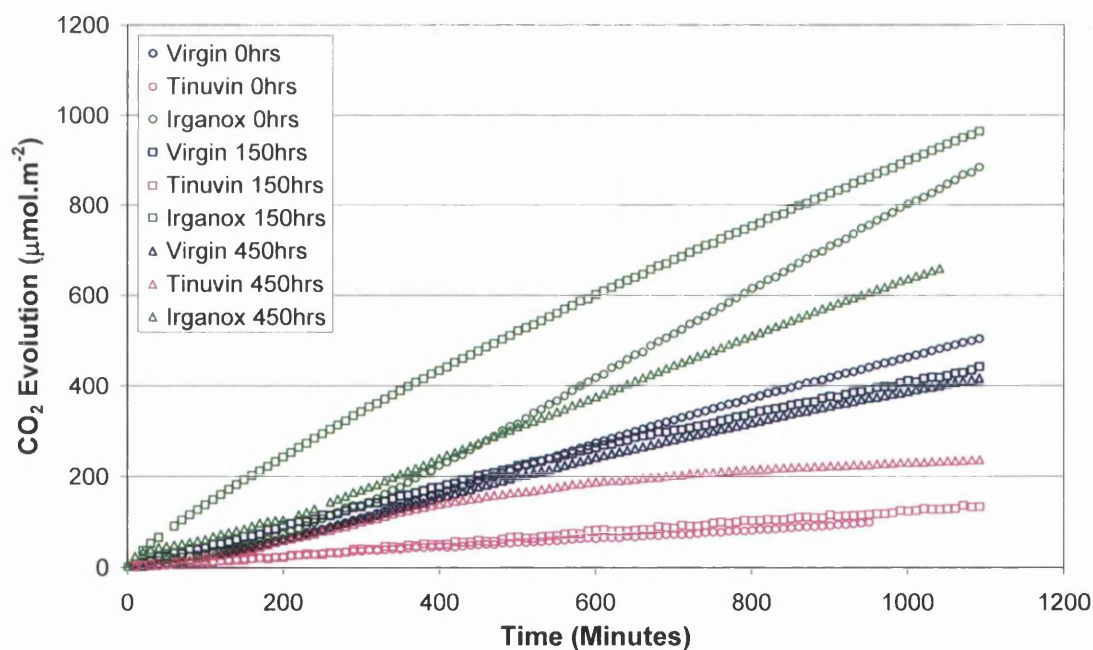


Figure 6-7 CO<sub>2</sub> Profiles for Virgin and Stabilised PE after Varying QUV Exposure



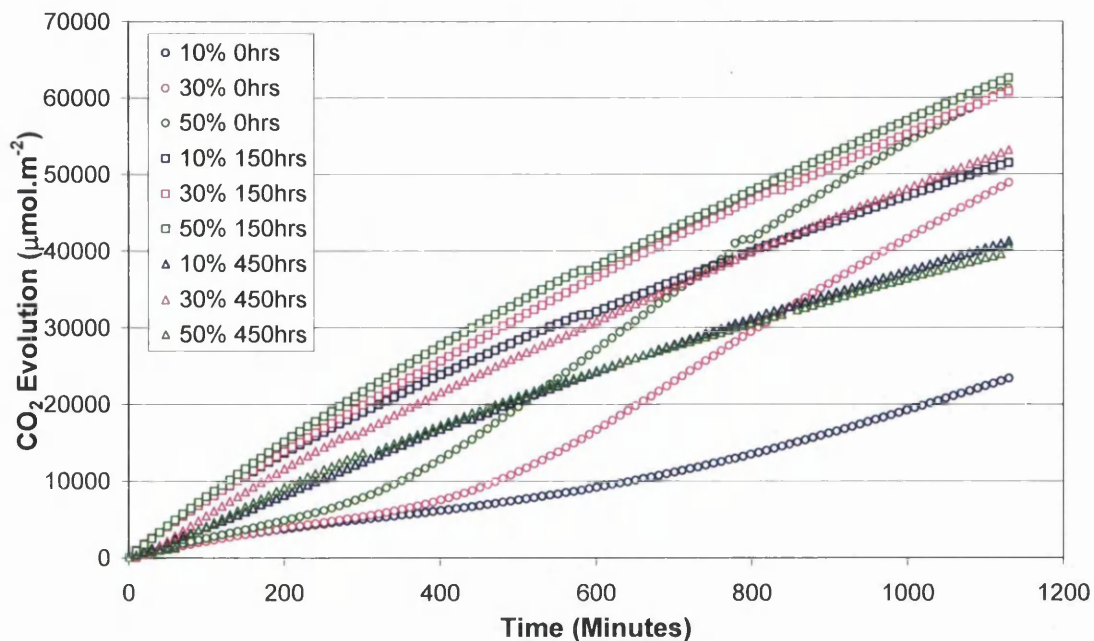


Figure 6-8 CO<sub>2</sub> Profiles for TiO<sub>2</sub> Pigmented PE after Varying QUV Exposure

On first inspection, the total CO<sub>2</sub> evolved for the virgin and stabilised samples follow the same trend as in 6.3.1, regardless of degree of weathering; Irganox most photoactive and Tinuvin the least. As previously shown, the rate of photo-oxidation in all samples is illustrated by comparing the rate on the profiles between 600 and 900 minutes. The CO<sub>2</sub> evolution rates are shown for the profiles measured at different degrees of weathering.

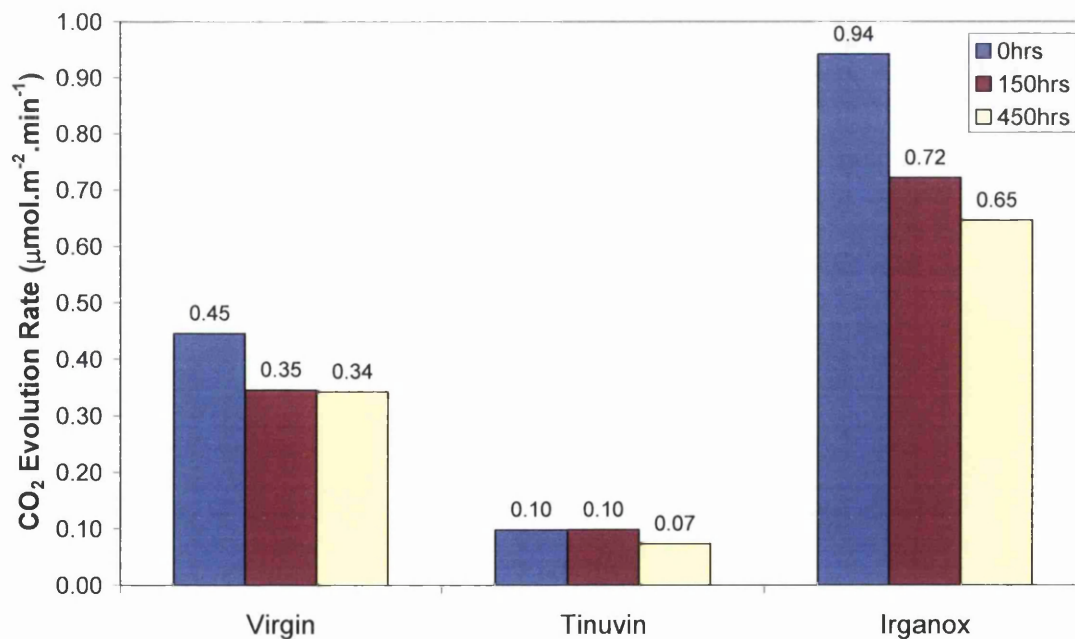


Figure 6-9 CO<sub>2</sub> Evolution Rates for Virgin and Stabilised PE after Varying QUV Exposure

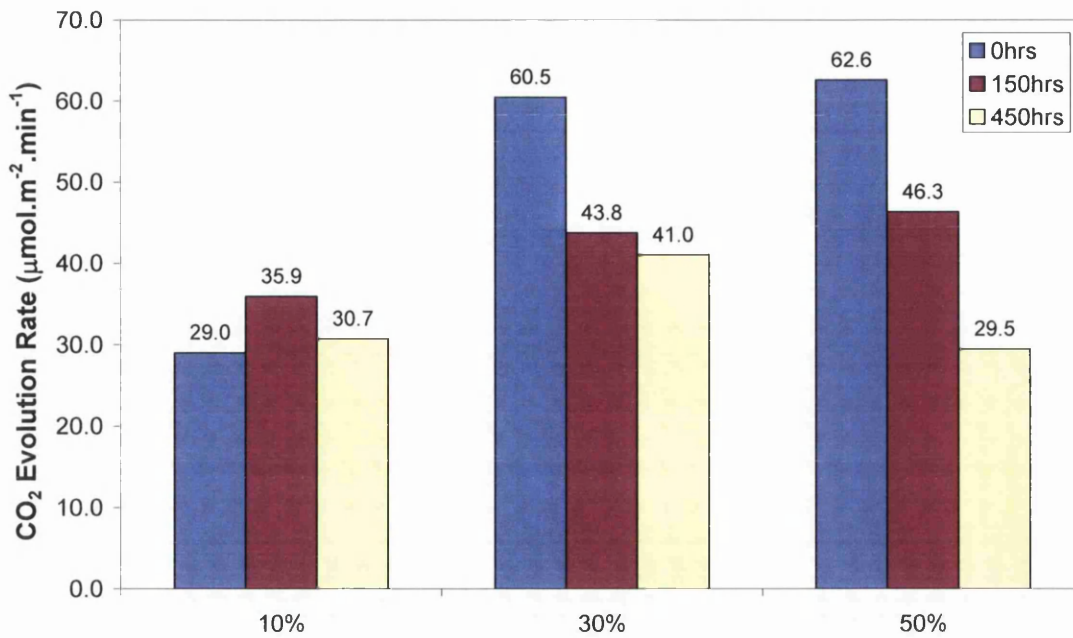


Figure 6-10 CO<sub>2</sub> Profiles TiO<sub>2</sub> Pigmented PE after Varying QUV Exposure

For all samples other than the 10% TiO<sub>2</sub> pigmented, it is evident that measuring the CO<sub>2</sub> evolution profile after weathering results in a decrease in the rate of photodegradation.

After only 150hrs weathering, the virgin PE shows a reduction in rate of almost 25%, which is quite significant given the stable nature of the polymer. Figure 6-11 illustrates more clearly the effect weathering has on the rate relative to the hours exposure, on the virgin and stabilised PE. After the initial drop in oxidation rate, the rate at which the CO<sub>2</sub> evolves plateaus at 450hrs. After the first initial exposure, the movement and loss of mobile polymer fragments and chain ends that are highly reactive means that subsequent degradation proves more difficult.

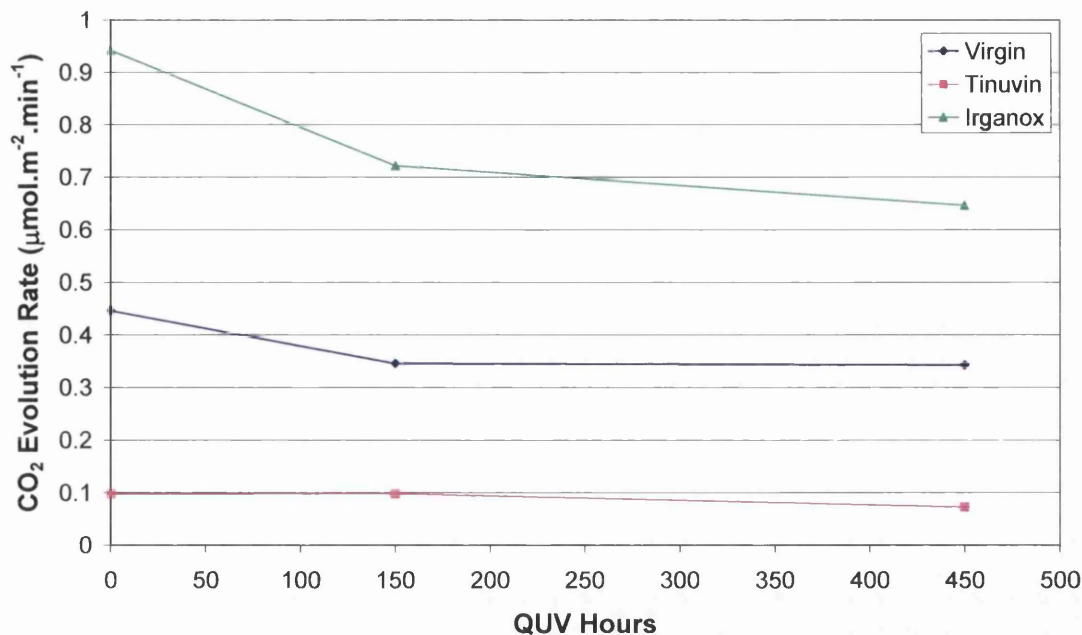


Figure 6-11 The Influence of QUV Exposure on Degradation Rate

Despite originally being a lot more active, the Irganox follows the same pattern. Already offering the greatest degree of stability of the two stabilisers, the drop in the evolution rate of the Tinuvin sample is a lot less severe, offering protection over time with minimal loss in its performance. As a UVA stabiliser, this was anticipated at this level of exposure, with maybe only a small loss in performance resulting from the leaching of the stabiliser during artificial weathering.

Clearly the addition of TiO<sub>2</sub> has a significant effect on the photoactivity of PE. The results for TiO<sub>2</sub> pigmented PE are however more complex. Evolution rates at 0 hours QUV exposure were symptomatic of that previously seen; a greater degree of TiO<sub>2</sub> pigmentation acts to increase the rate of degradation of the polymer in question. However, after 150hrs exposure, the rate increases for the 10% TiO<sub>2</sub> pigmented PE. Given the scale of this increase in relation to the quantities shown below, it is more likely this rate is in fact relatively linear. At such a small addition, in comparison to the other samples, this quantity is neither enough to significantly increase in rate, or alternatively provide a large screening protection to the polymer matrix.

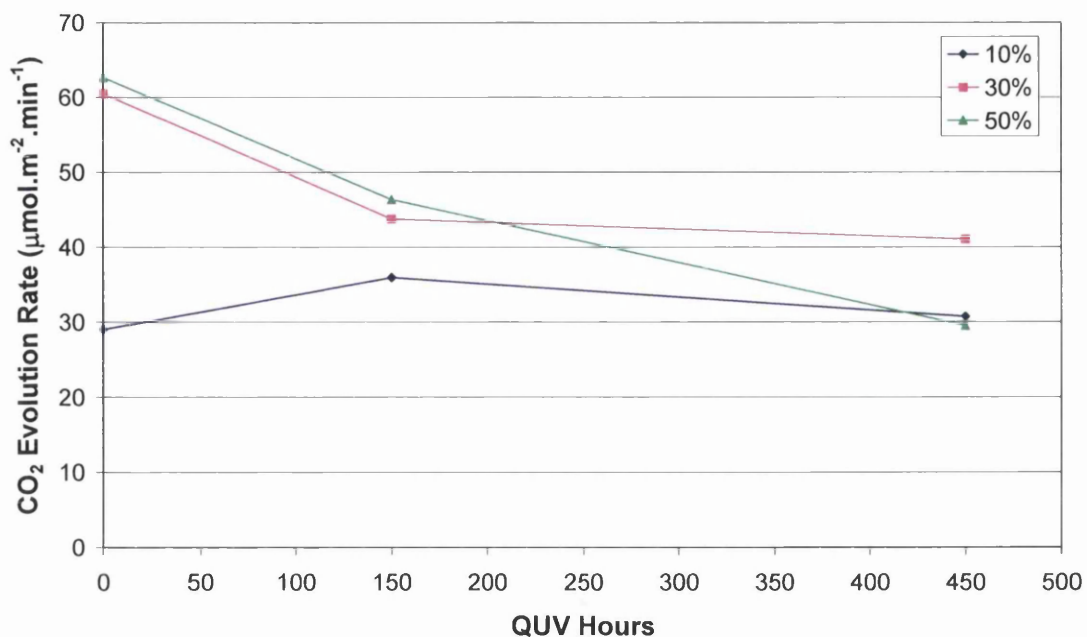


Figure 6-12 The Influence of QUV Exposure on Degradation Rate

At addition levels of 30% TiO<sub>2</sub>, the nature of the drop in degradation rate is similar to that of virgin PE; an initial decrease followed by a smaller drop, whereas 50% loading sees a dramatic continuous drop in evolution rate.

As previously mentioned, chalking was evident after 150 hours of weathering. During this time, there will have been significant oxidation of the polymer matrix surrounding the TiO<sub>2</sub> particles, leaving the TiO<sub>2</sub> more exposed at the surface layer. During UV exposure in the flat panel reactor, these exposed TiO<sub>2</sub> particles are now able to offer greater levels of screening protection to the underlying polymer, thus less CO<sub>2</sub> is evolved.

In the subsequent stage of QUV weathering, depending on the level of additive and how aggressive the degradation is, the same will occur. In the instance of 50% loading, the degradation of the surrounding PE matrix would have been more aggressive, leaving a more substantial 'protective' screening layer of exposed TiO<sub>2</sub>. Hence the dramatic decrease in the CO<sub>2</sub> evolved from the 50% pigmented PE sample, where little polymer surrounding the pigment was likely.

Similar studies [79] have shown a progressive increase in photodegradation with pre-exposure in QUV conditions for unpigmented and TiO<sub>2</sub> pigmented PE. These values were compared in terms of volumes evolved (as opposed to rates compared in this chapter), and the evolution was measured after a shorter time of 250 minutes. Results showed a definite increase in CO<sub>2</sub> evolved between 0 and 800 hours QUV exposure, however with lessening difference over 300 hours QUV. Comparing like results, Figure 6-13 shows the volume of CO<sub>2</sub> evolved 250 minutes into the experiment, at varying levels of exposure.

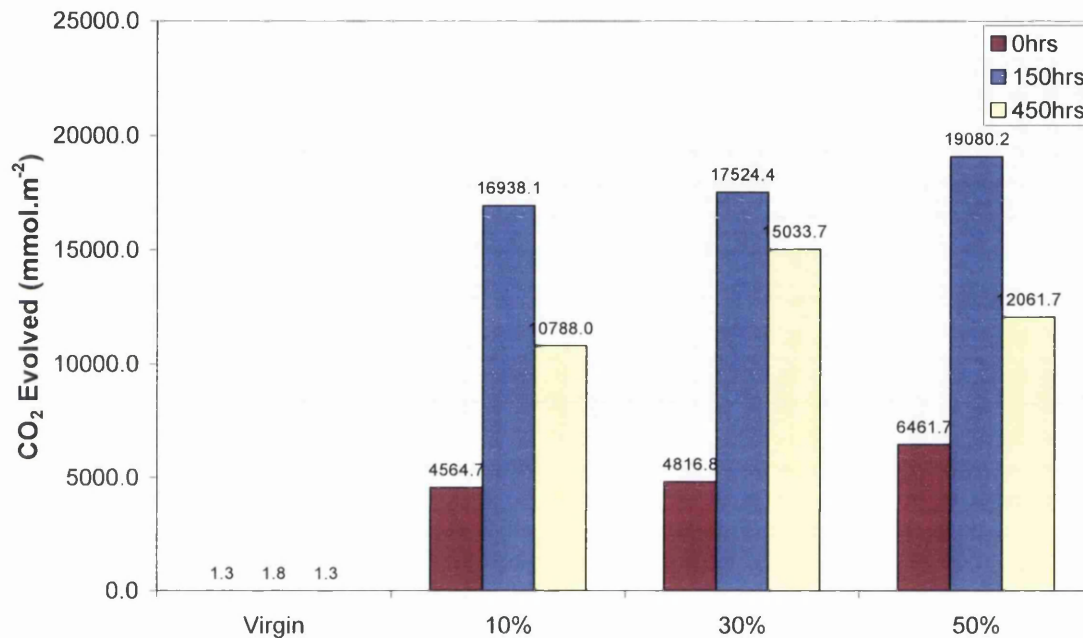


Figure 6-13 CO<sub>2</sub> Evolved at 250 Minutes of Testing In Flat Panel Reactor

The results shown here do not entirely follow the trend shown in the literature. Indeed an overall increase is evident; however at 450 hours exposure in all cases the volume evolved lowers. In the case of the TiO<sub>2</sub> pigmented samples, the level of addition in the literature was only 5%, so the level of photodegradation is likely to be less. However, this does not account for the case of the virgin PE. In this instance, the difference in results are likely to be attributed to different grades of PE with different molecular weights for example, and small levels of stabilisers (for production process) that are present in the commercially available grade that was used.

### 6.3.2.1 Removal Rate

The CO<sub>2</sub> evolution rates can be further used to calculate the loss of mass of polymer thus rate of removal of coating (Appendix A). Assuming the removal rate is directly proportional to UV intensity and taking into consideration volumes of additives, the cumulative reduction in coating thickness during the QUV cycle is shown below.

Table 6-3 Coating Removal Rate

| <b>Sample</b>        | <b>Reduction in Coating Thickness after 150hrs QUV Weathering (µm)</b> | <b>Cumulative Reduction in Coating Thickness after 450hrs QUV Weathering (µm)</b> |
|----------------------|--|---|
| Virgin PE            | 0.05   | 0.13  |
| Tinuvin              | 0.01   | 0.11  |
| Irganox              | 0.10   | 0.26  |
| 10% TiO <sub>2</sub> | 4.04   | 12.34   |
| 30% TiO <sub>2</sub> | 7.03   | 18.47   |
| 50% TiO <sub>2</sub> | 8.01   | 13.58   |

As expected, the loss of mass is much greater in the TiO<sub>2</sub> pigmented samples. The photo-oxidation of the polymer matrix is more aggressive in the presence of a pigment such as this, which accelerates the rate of oxidation of the PE. Interestingly, after 150hrs of weathering, the degree of reduction in coating thickness is relative to the level of TiO<sub>2</sub> addition, however after an additional 300hrs of weathering the 30% level addition sample undergoes a more significant degree of degradation and thus mass loss. This is attributed to a higher level of photodegradation than a 10% loading, but lesser degree of screening protection offered by the 50% loading.

The technique shown in this section is such that the manner in which the level of degradation is measured is based on a 'surface exposure' technique. The evolution of CO<sub>2</sub> has been seen to be a successful and reproducible test technique in measuring the photoactivity of polymer samples with a variety of additives, regardless of the stability of the sample in question. Whereas this technique has been more heavily verified with regard to its use in measuring the photo-activity of PVC coating systems (with supporting data such as colour and gloss loss), the following piece of

work in this chapter aims to add to and verify the portfolio of testing techniques used for alternative coatings such as a more stable polyethylene system.

One consideration that is of importance when using these methods to measure the degradation of a polymer such as PE, is the influencing factors such as crystallinity and whether the more 'surface orientated' techniques may be influenced by this. For example, in a semi-crystalline polymer such as this, the crystalline regions will be less susceptible to degradation. So in a sample where the surface layer is more crystalline, using testing techniques that measure surface effects only, may not be indicative to the degradation of the bulk polymer. The results in the following sections will later be coupled with the CO<sub>2</sub> evolution results and discussed.

### **6.3.3 Measurement of Oxidation Induction Temperatures (OIT)**

The DSC is a powerful tool in measuring the longevity of stabilisers in polymers, by means of measuring the oxidation characteristics, by determination of the oxidation induction parameters of materials. Often used to identify the longevity of anti-oxidant additives, it has been used here to identify the stability of the previously mentioned samples, before and during artificial weathering. As outlined in 6.2.5, due to the varying levels of stability of all samples, the oxidation induction temperature was chosen to be the comparable parameter.

Figure 6-14 illustrates a typical oxidation induction curve, whereby the oxidation induction temperature is shown as the point at which there is a significant change in the heat flow during heating in an oxygen atmosphere. It must be noted, that for this research and experiment, the positioning of the data on the y-axis is irrelevant to the oxidation induction characteristics.

The oxidation induction profiles of virgin PE following various degrees of weathering are shown in Figure 6-15. After investigating the nature of the profiles after weathering at 150 and 450hrs, it became apparent that there was broadening of the oxidation peak. To investigate this further, oxidation profiles were measured for the virgin PE after shorter QUV exposure times of 13, 32 and 45 hours.



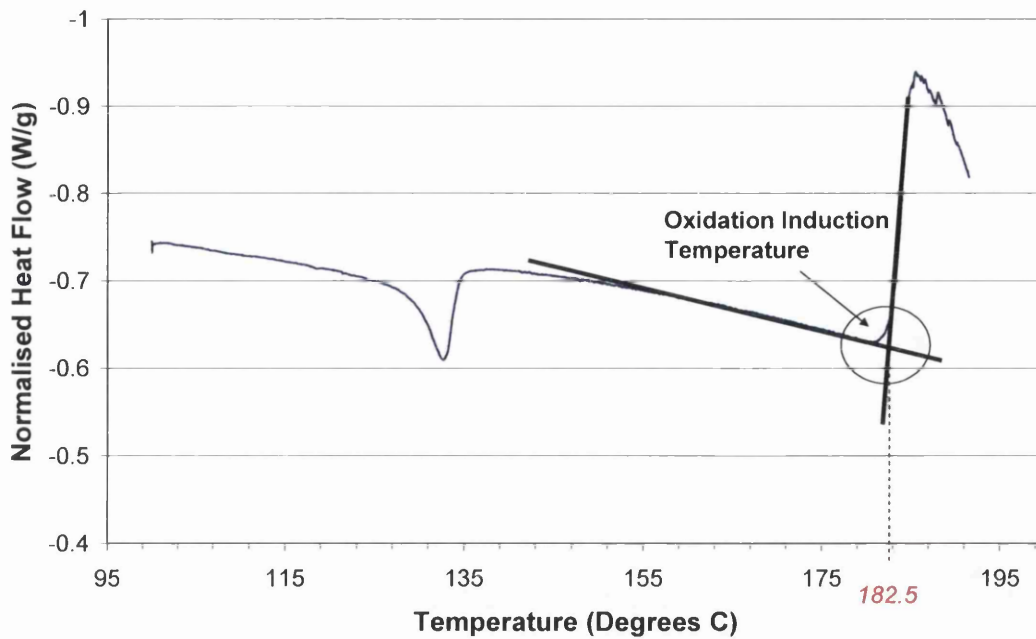


Figure 6-14 Typical PE DSC Oxidation Profile

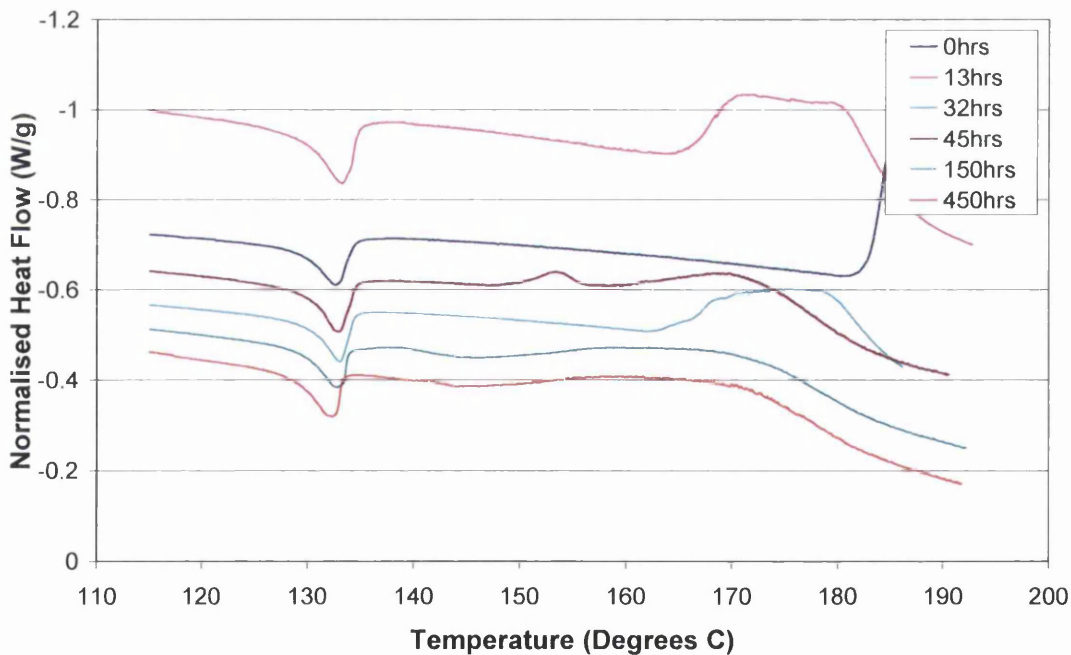


Figure 6-15 Oxidation Induction Profiles for Virgin PE after QUV Exposure

A reduction in the OIT of PE with increasing weathering was anticipated, with mobile reactive species in the polymer matrix present after photodegradation reducing the oxidative stability of the polymer during this experiment. However, on closer inspection and addition of 13, 32 and 45hr weathering profiles, it became



apparent that the broadening (and non-definitive OIT point) seen on the 150hr and 450hr profile was in fact an amalgamation of two OIT peaks that evolve after weathering and then appear to amalgamate again as the OIT reaches the melting point of the polymer.

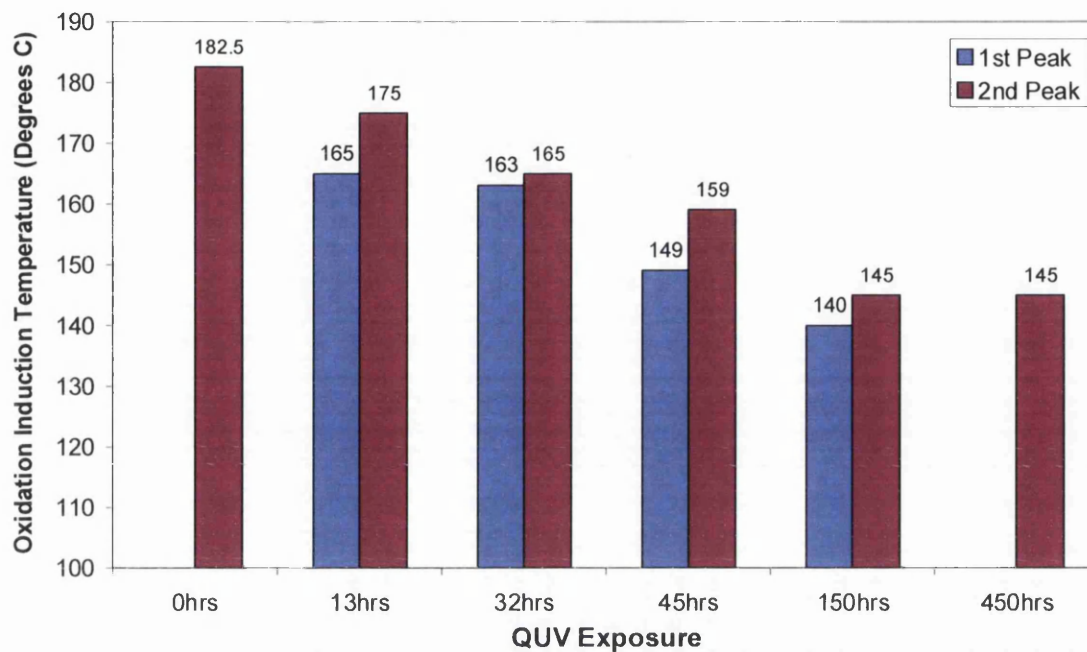


Figure 6-16 Peak Oxidation Induction Temperatures for Virgin PE

The early peak is likely to be a result of the polymer now comprising partially degraded polymer and lesser degraded material. The more severely degraded PE more readily oxidises at lower temperatures, followed by the second oxidation of the more stable PE.

The DSC curves for Irganox, Tinuvin and 50% TiO<sub>2</sub> pigmented systems can be seen in Figures 6-17 to 6-19. All curves have been compared to virgin PE, to highlight the influence of the additives.

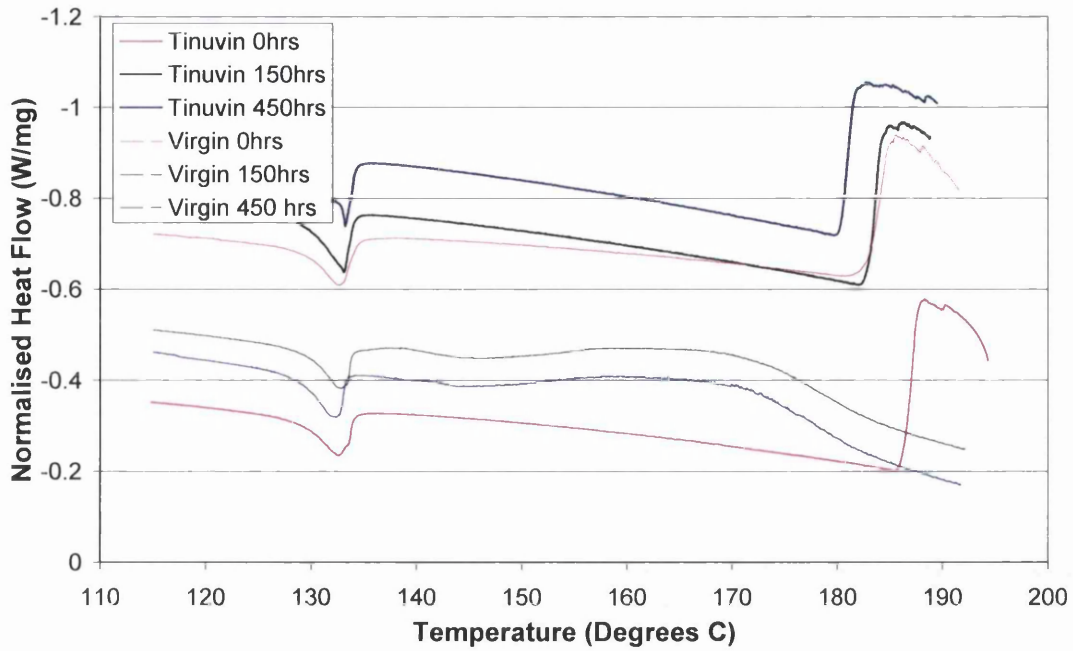


Figure 6-17 Oxidation Induction Profiles for Tinuvin and Virgin PE

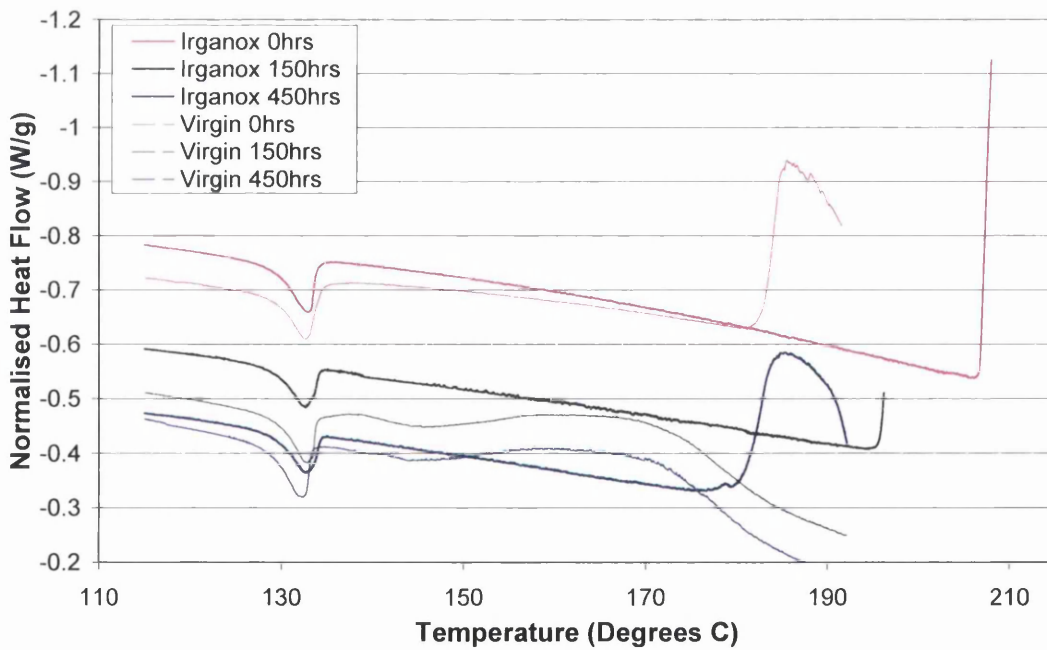


Figure 6-18 Oxidation Induction Profiles for Irganox and Virgin PE

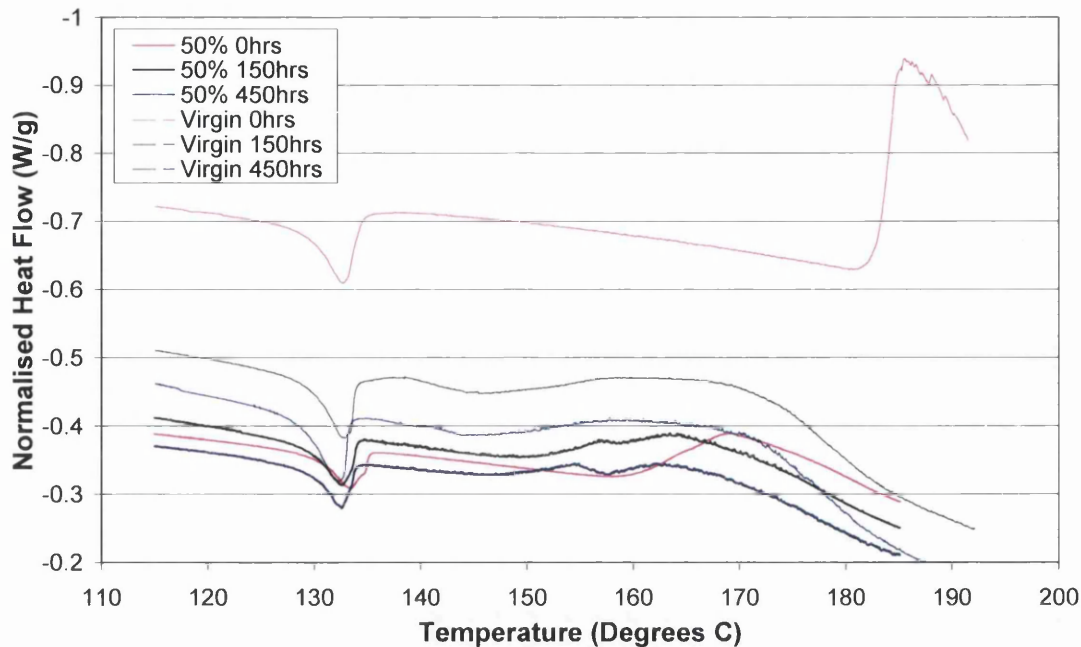


Figure 6-19 Oxidation Induction Profiles for 50% TiO<sub>2</sub> and Virgin PE

Looking briefly at the character of the DSC profiles, the influence of the additives is apparent in a shift of the oxidation induction temperatures. After weathering, the point at which oxidation occurs becomes less definite, whereas in non-irradiated samples it is clear. The ‘double peak’ that was evident with virgin PE is absent in all cases apart from the weathered 50% TiO<sub>2</sub> sample. Where this double oxidation has occurred in virgin PE, the OIT of the second peak is compared, as below.

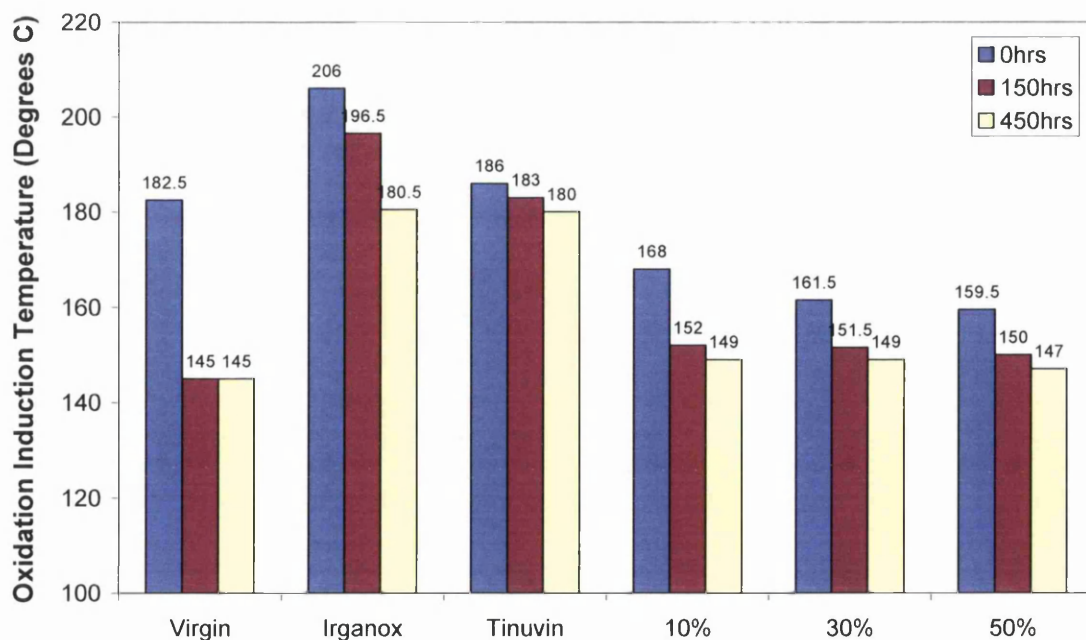


Figure 6-20 Oxidation Induction Times after QUV Exposure

As anticipated, examining the oxidation induction temperatures prior to weathering, Irganox, (AO) offers a degree of resistance to oxidation of the PE, increasing the OIT from 182.5°C to 206°C. Interestingly, the addition of TiO<sub>2</sub> appears to assist in the ease of oxidation, most likely actually aiding the onset of thermal degradation. This supports an earlier finding during the initial stages of this experimentation when a u-grade, photo-active TiO<sub>2</sub> pigment ‘P25’ (used in PVC experimentation) , was mixed with the PE at elevated temperatures. After the described mixing regime, the polymer was now pink in colour, typically characteristics of thermally degraded polymer. Increasing levels of TiO<sub>2</sub> appear to increase this degradation in the presence of heat.

It must therefore also be considered that due to the manner in which the thermoplastic samples were produced, a small degree of thermal degradation products may be present, and any reactive species may also contribute to the rate of degradation in the presence of UV. This is why, in industrially available polymeric coatings and products, the two stabilisers are found in synergy.

Comparing the OIT of the samples after weathering, Figure 6-21 illustrates the relative decrease in the OITs relative to exposure time.

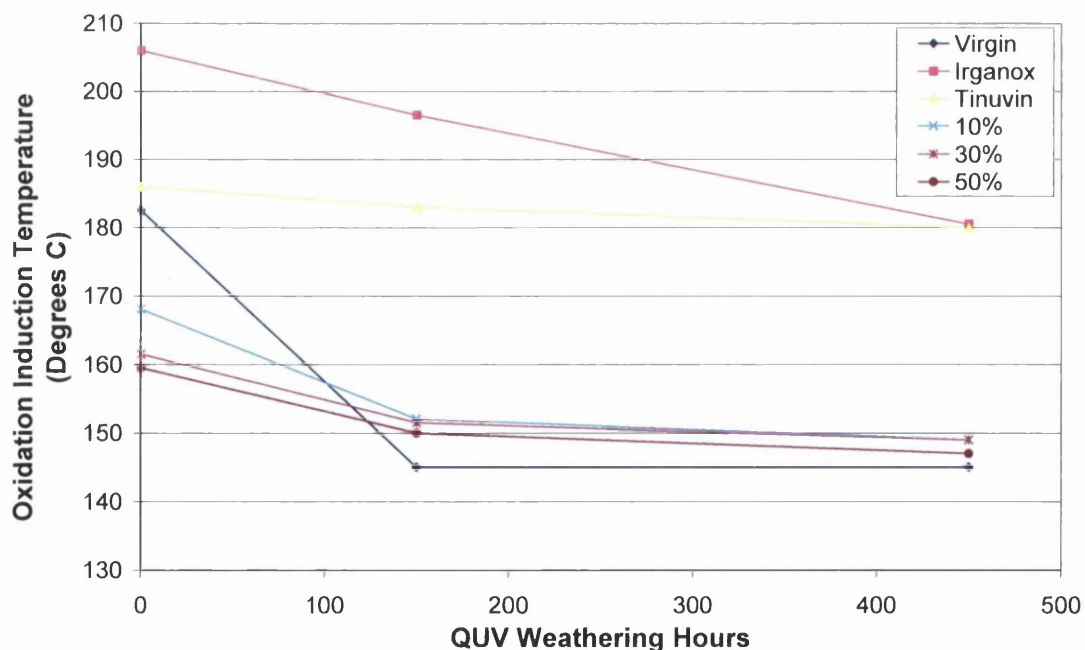


Figure 6-21 Influence of QUV Exposure on Oxidation Induction Temperature

Virgin PE undergoes the most significant decrease in OIT during the initial stages of weathering. This supports the CO<sub>2</sub> evolution data, in that after the first QUV exposure, the degradation level measured plateaus.

Although Irganox is a very effectively used AO for heat stability, the rate at which the OIT decreases is still relatively fast and linear in nature. In the absence of weathering, as expected it clearly outperforms all other additives in terms of delaying oxidation in the presence of elevated temperatures. However, as the CO<sub>2</sub> rates showed, in the presence of UV it is unstable, and compared to virgin PE has undergone vast oxidation leading to a reduction in the integrity of the polymer matrix. So therefore, a leaching of the stabiliser is a possibility, leading to a sustained reduction in the performance of the stabiliser.

The OIT of the Tinuvin containing PE sample also decreases, although to a much lesser extent, with it being the sample with the least change in OIT throughout the experiment. The CO<sub>2</sub> evolution experiments have shown it to be the least degrading of all the samples in the presence of UV, therefore leaving the integrity of the organic matrix high and the OIT data clearly indicates the system is also stable at high temperatures.

The performance of all the TiO<sub>2</sub> pigmented PE samples are very similar following a similar trend to virgin PE, with an initial drop in OIT, followed by a smaller drop after 450 hours QUV. However after 150 hours weathering, the TiO<sub>2</sub> samples have higher OITs than the virgin PE. Despite TiO<sub>2</sub> samples having CO<sub>2</sub> evolution rates significantly higher at all stages of weathering, this technique suggests that the PE with TiO<sub>2</sub> is more resistant to oxidative attack after weathering. However the accuracy of this is questionable, highlighting the limitation of such a technique, in that as the OITs approach temperatures in the region of the melting point, the accuracy of the OIT measured reduces.

### 6.3.3.1 Short Ramp

The parameters of this technique were designed in such a way to support a subsequent piece of work (6.3.4) whereby in-situ UV irradiation was investigated. In this instance it was preferential to have a longer test period with a slow heat-ramp, to encourage as much UV interaction as possible at low temperatures. It was necessary to use those conditions in this experiment also to allow for comparison.

To investigate if there is potential to overcome this problem of the melting point obscuring the OIT, a short heat ramp of 2°C per minute was used instead. As the sample spends less time at high temperatures, it resists oxidation up to a higher temperature, with no interference with the melting point.

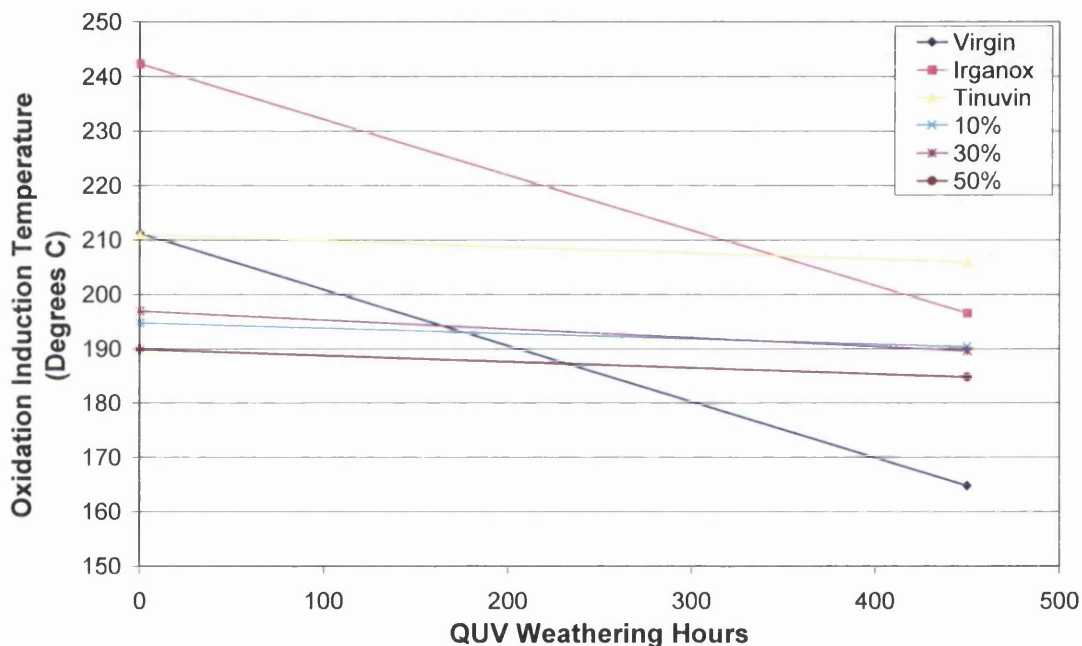


Figure 6-22 Influence of QUV Exposure on Oxidation Induction Temperature Using a Short DSC Ramp

Whilst there is no data available using the short ramp for 150hrs weathering, the same trend as when using a longer ramp is evident. It can therefore be concluded that results showing that after weathering the virgin PE is more unstable than all other samples is not in fact an artefact of the OIT infringing the melting point. This contradicts the results for the CO<sub>2</sub> evolution rates that indicated the virgin PE is one of the most stable samples. In the absence of any TiO<sub>2</sub>, assuming non-surface concentrated photodegradation occurs; it is likely that the degradation species are more mobile throughout the sample. During the CO<sub>2</sub> evolution experiment, rates



measured are less, as severe degradation does not occur within 1200 minutes as a result of surface UV irradiation. However, during the DSC experiment in its molten form, such species may contribute to reducing its oxidative stability.

### 6.3.3.2 Depth of Degradation

During such an experiment, the temperatures obviously exceed that of the melting point; therefore, this is a technique that measures the oxidation characteristics of the bulk sample and not just the surface. Literature [85] has illustrated that the phenomena of PE degradation is likely to not be limited to the immediate surface region and this has also been shown with the use of the DSC here. A virgin sample at 450hrs QUV exposure with sufficient UV degradation, manually had the top 30 $\mu$ m of the irradiated surface abraded and then the OIT measured. There was negligible difference in the results, indicating that the degradation is not concentrated at the surface. In comparison to this, the same test was carried out on a 30% TiO<sub>2</sub> pigmented sample, and a difference was noted as seen in Figure 6-23. Clearly despite being a known pro-degradant at levels of addition high enough, the screening effect does limit the degradation more to the surface layer.

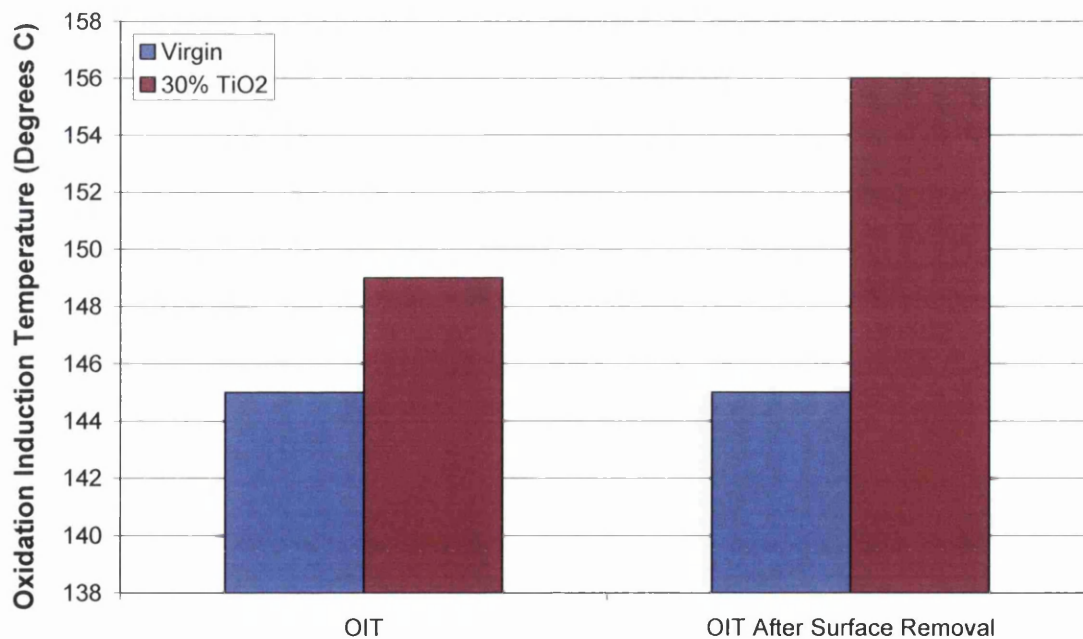


Figure 6-23 Influence of Surface Removal on OIT

It is therefore likely that in the case of a non-pigmented sample, indeed the degradation is not a surface phenomenon alone. However, where  $\text{TiO}_2$  is present and in sufficient quantities, there is the potential to screen and protect the bulk of the polymer, limiting the severe degradation to the surface region alone. During artificial weathering, the degraded organic matrix and degradation products were 'rinsed away', so one can assume that during an OIT test after some weathering, indeed the thin layer of degradation products will melt and be re-mixed. However, the amount of bulk PE that has undergone aggressive oxidative attack prior to this may actually be less than in the PE with  $\text{TiO}_2$ , accounting for the results discussed above.

#### **6.3.4 Development of In-situ UV Irradiated PE Oxidation Profiles**

With all accelerated test techniques, the ideal is to yield rapid results, but with information that is true to the long terms mechanisms that would naturally occur. The flat panel reactor and DSC coupled with the QUV were able to give an insight into degradation mechanisms of pigmented and stabilised PE after different degrees of degradation. This section now looks at the development of an alternative testing technique, integrating UV exposure with oxidative induction experiments.

The standard procedure for the OIT experiment is to heat the polymer sample in a closed furnace with either nitrogen or oxygen circulating. The test was adapted to allow for UV irradiation during the time the sample was subjected to an oxidative environment, combining two methods, that potentially offers a more rapid test technique that is able to replace the need for weathering then subsequent OIT testing.



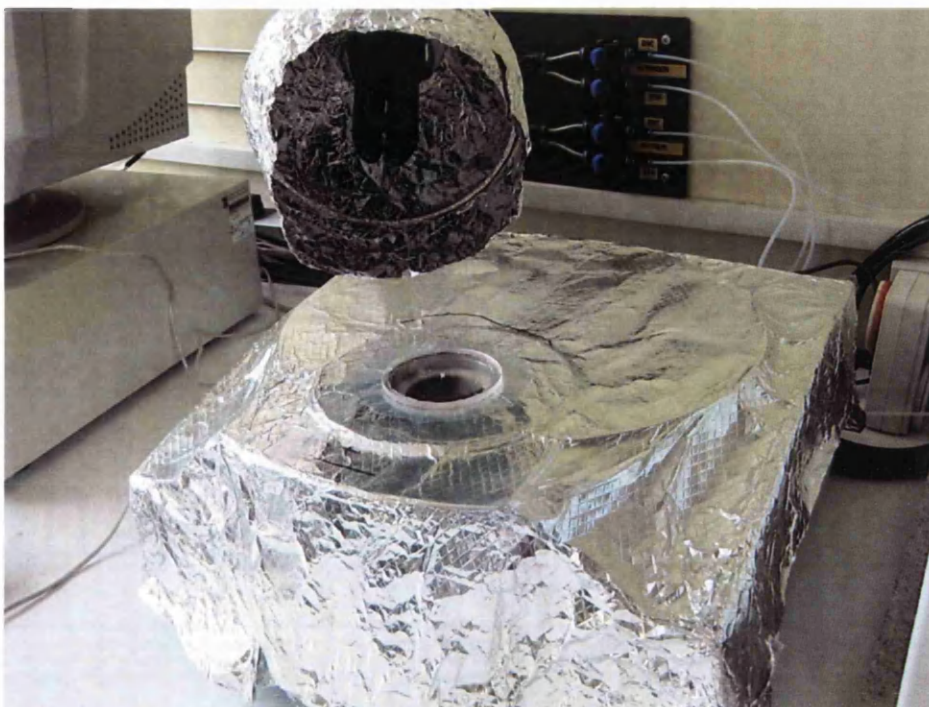


Figure 6-24 The In-situ UV-OIT Test Equipment

In the presence of UV irradiation, one would expect degradation to occur sooner and therefore at lower temperatures, lowering the OIT. The oxidation profiles of virgin PE samples after varying levels of UV exposure are shown both in the absence of UV, and during an in-situ UV irradiation in Figure 6-25. In addition to the QUV exposures discussed previously of 0, 150 and 450 hours, short irradiations are also shown. Whilst comparing the effect of the in-situ UV irradiation of all the weathered samples, the combination of samples tested has allowed for a comparison of the effect the ‘type’ or technique of exposure has had on the OIT but comparing total UV dosage i.e. some of the UV exposure occurring at elevated temperatures in the DSC.

Table 6-4 Levels of UV Exposure

| Sample    | QUV (hrs) | UV In-Situ | Total UV Exposure (MJ/m <sup>2</sup> ) |
|-----------|-----------|------------|--|
| 0hrs      | 0         | No         | 0                                      |
| 0hrs UV   | 0         | Yes        | 2                                      |
| 13hrs     | 13        | No         | 2                                      |
| 32hrs     | 32        | No         | 5                                      |
| 32hrs UV  | 32        | Yes        | 7                                      |
| 45hrs     | 45        | No         | 7                                      |
| 150hrs    | 150       | No         | 23                                     |
| 150hrs UV | 150       | Yes        | 25                                     |
| 450hrs    | 450       | No         | 69                                     |
| 450hrs UV | 450       | Yes        | 71                                     |

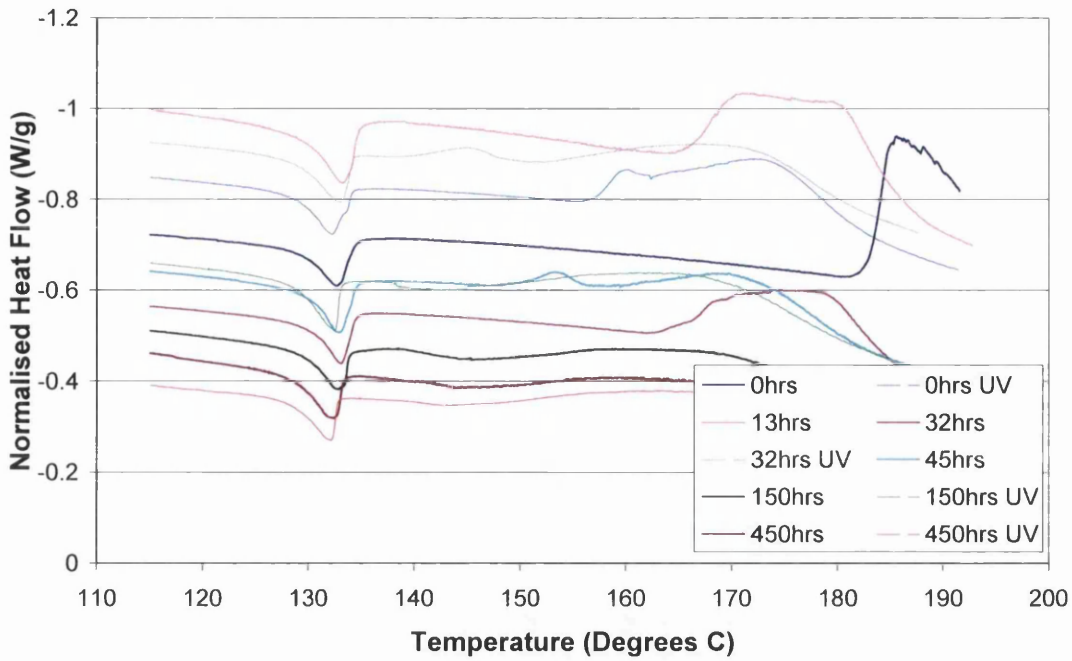


Figure 6-25 OIT Profiles for Exposed Virgin PE

As previously seen, the double oxidation peak phenomenon is evident during the in-situ experiment. The OITs for all samples are shown in Figure 6-26, identifying the total UV exposure throughout the test period. In all cases of like experimentation techniques, increasing the presence of UV reduces the OIT.

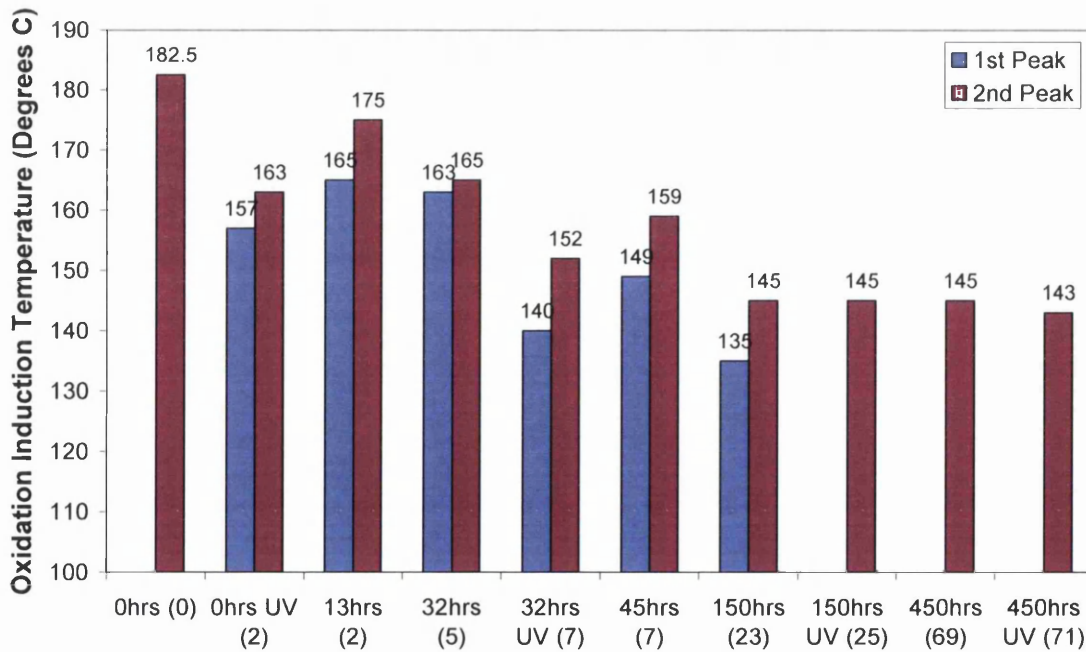


Figure 6-26 OIT for PE with Varying UV Exposure

It is evident for comparable UV exposures; the environment in which it occurs does influence the OIT. Figure 6-26 clearly illustrates that for the same level of UV dosage, if in part this occurs within the heated environment of the DSC, the OIT of this sample will be reduced. For example, 32 hours QUV and subsequent in-situ irradiation in the DSC is equivalent to 45 hours of QUV exposure (OIT measured in absence of any UV irradiation) and when measured, the DSC irradiation has a reduced OIT. This data highlights the influence that thermal degradation may be contributing to the results.

The DSC profiles can be seen for the Tinuvin, Irganox and 50% TiO<sub>2</sub> pigmented samples, all at the varying degrees of weathering, with and without UV exposure during the DSC experiment.

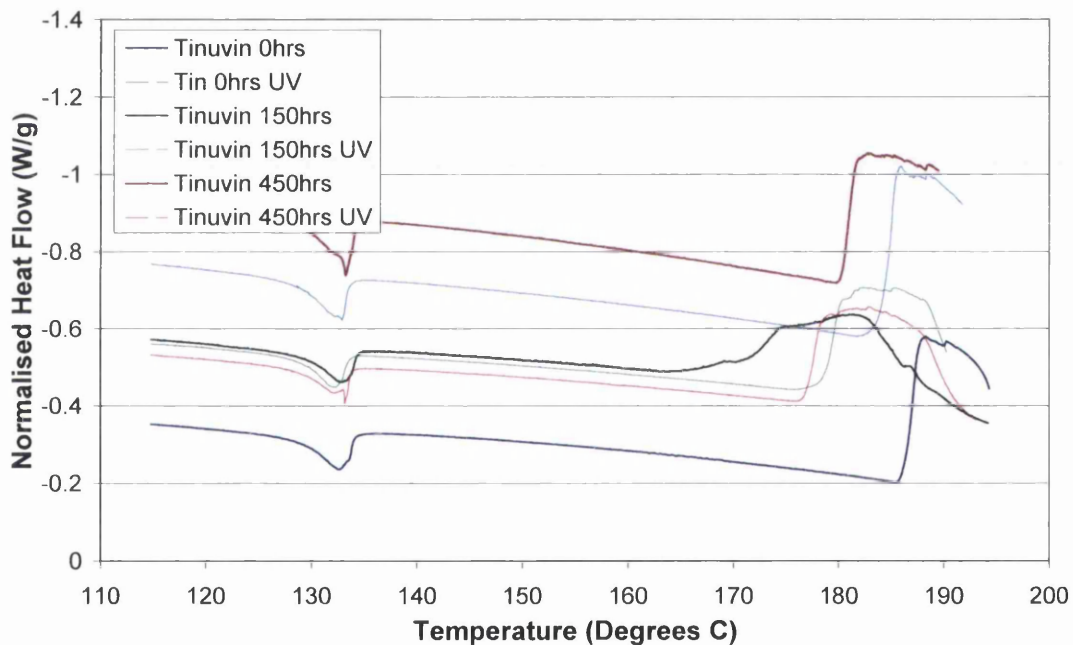


Figure 6-27 OIT Profiles for Tinuvin Stabilised PE

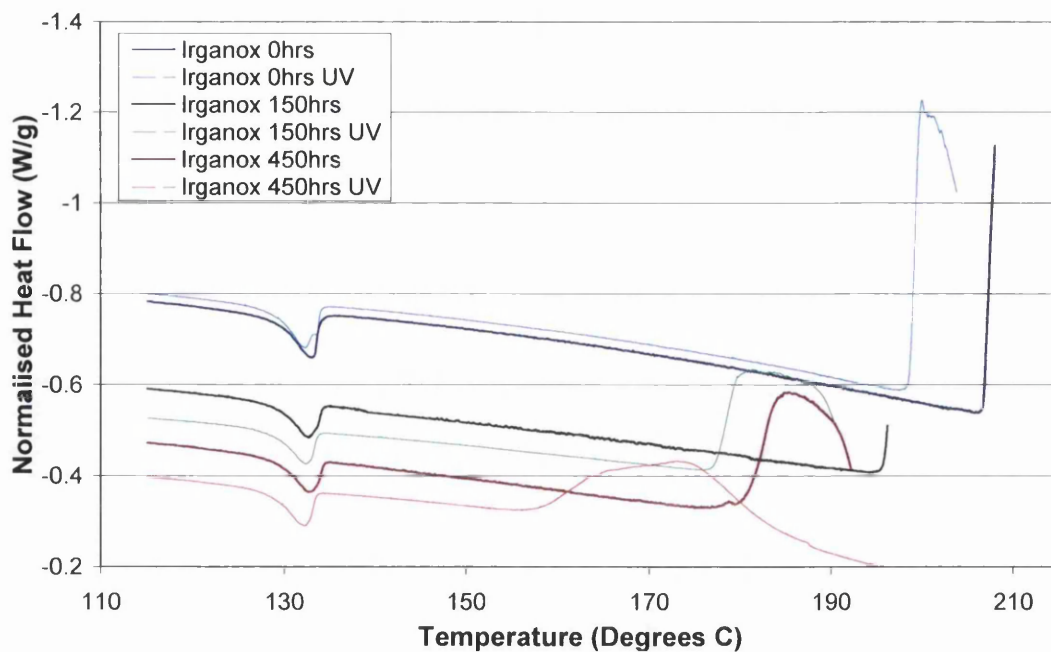


Figure 6-28 OIT Profiles for Irganox Stabilised Virgin PE

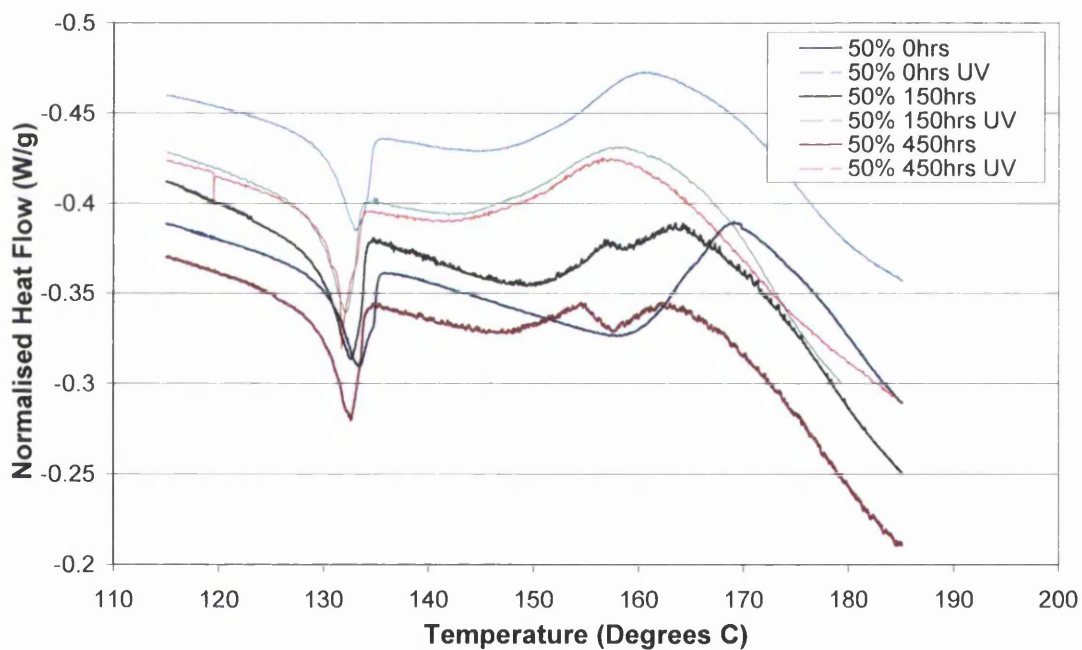


Figure 6-29 OIT Profiles for 50% TiO<sub>2</sub> Pigmented Virgin PE

In the presence of UV during the DSC test, a reduction in the OIT is apparent, although at times the exact point of oxidation becomes more unclear when significant levels of degradation have occurred. Figure 6-30 below illustrates for each sample the extent to which the UV irradiation actually decreases the OIT, looking first at the samples in the non-weathered state.



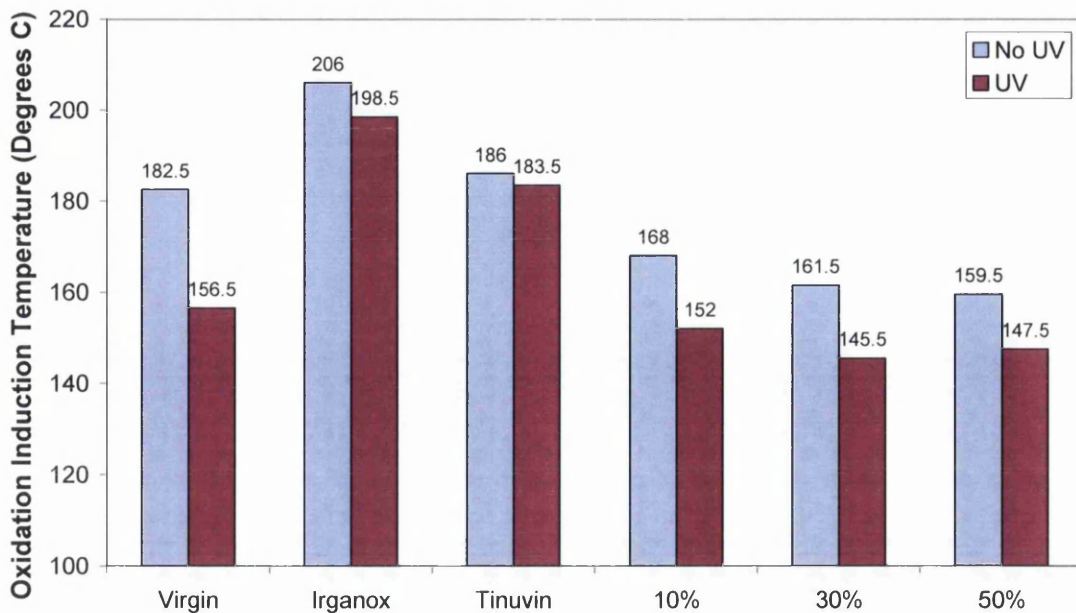


Figure 6-30 Influence of UV Irradiation on OIT during In-Situ Irradiation

The virgin PE is the most responsive to the presence of UV during the oxidative experiment, with a reduction in the OIT of 26°C. By virtue of the reactive nature of TiO<sub>2</sub>, a greater change in OIT was anticipated in the TiO<sub>2</sub> pigmented samples, with smaller reductions of 16 and 12°C respectively. As previously described, the presence of TiO<sub>2</sub> alone has the effect of reducing the OIT compared to virgin PE due to associated thermal degradation, so coupled with UV to accelerate degradation that is occurring, the effect is a lot less than would be expected. However, the time of experimentation is unlikely to have been sufficient enough to encourage severe degradation and a degree of screening is likely to have occurred.

As expected the UVA Tinuvin offered higher levels of stability over the virgin PE sample with a decrease in OIT of only 2.5°C in the presence of UV. It has proven to be stable and effective at offering UV protection, even at high temperatures as shown here. The Irganox is still the most stable of all the samples during this high temperature oxidative technique, with small change of 7.5°C likely to be caused by the non UV-stable nature of the additive shown previously.

Figure 6-31 shows the decrease in OIT caused by the in-situ UV irradiation following subsequent weathering.

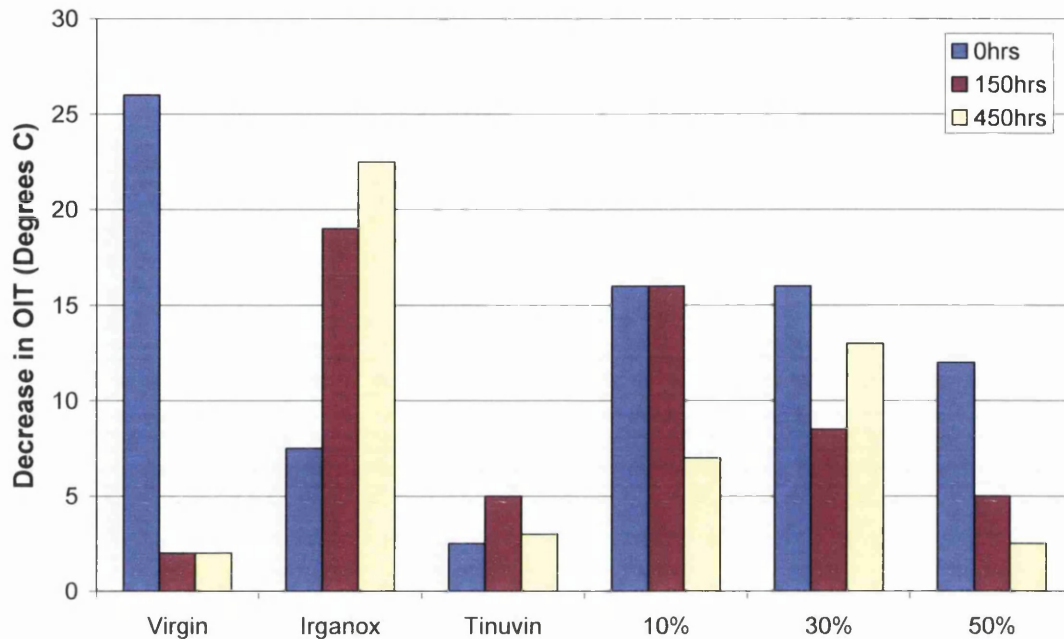


Figure 6-31 The Decrease in OIT as a Result of In-Situ UV Irradiation, after Exposure

Despite an initial significant influence on the OIT, the presence of UV irradiation after the virgin PE has been weathered has minimal impact, with a small decrease in OIT of only 5°C. This trend follows that seen in the CO<sub>2</sub> evolution profiles, where by the evolution rate dropped more significantly post weathering and then plateaus out. Evidently, as suggested before, after weathering, reactive species are less abundant, hence any interaction of the polymer with UV yields less of a degradation reaction.

In contrast to this, after weathering the Irganox sample in fact becomes more susceptible to a reducing OIT (oxidative degradation) induced by the in situ-UV irradiation. Despite providing a level of thermal stability, as shown in the CO<sub>2</sub> evolution profiles, it is itself is reactive to UV irradiation. During weathering, coupled with any loss of stabiliser by leaching, there is potential for the formation of mobile reactive species, which in turn will therefore more easily induce photo-oxidation in the sample during this experiment. It must be noted however, that even the presence of a small quantity of Irganox at this degree of weathering still provides

a sufficient level of thermal stability, when comparing the OITs of virgin PE and Irganox at 450hs with UV; 143 and 158°C respectively.

TiO<sub>2</sub> pigmented samples however, using this technique yield more complex results. In all cases, the trend shown is a reducing influence of UV irradiation on the oxidative degradation, but with a lesser degree of trend noted between the three levels of addition after weathering. Whereas in the CO<sub>2</sub> evolution experiment, the rate and extent of degradation measured is controlled by the surface of the sample, during the DSC experiment, the melting point of the sample is surpassed and thus all components of the system are melted and re-distributed. In this chapter and literature [54], part of the degradation mechanisms observed are attributed to the screening protection TiO<sub>2</sub> can offer. However, during such an experiment as this, at the point at which oxidation occurs, the surface layer of TiO<sub>2</sub> exposed (and reactive species) following weathering, is now re-distributed through-out the bulk polymer, itself further contributing to the thermal and UV degradation mechanism, rather than so heavily contributing to a 'screening' mechanism. This experimental technique is therefore not as indicative of the more surface concentrated reactions that may occur in natural weathering.

Despite having the highest loading of photo-reactive pigment, the OITs observed in the 50% pigmented sample have the overall smallest reductions in OITs of the TiO<sub>2</sub> pigmented samples, as a result of UV irradiation in-situ; indicating the UV has a low effect on the oxidation of this sample. A decrease in the CO<sub>2</sub> evolution rate of the 50% pigmented sample was attributed to the 'screening' phenomena mentioned, following the aggressive oxidation of bulk polymer exposing TiO<sub>2</sub> particles.

## **6.4 Conclusions**

Three techniques have been shown and discussed, that can be used in an effort to compare and understand degradation mechanisms and rates. The first of the three was the use of the flat panel reactor, to measure the rate at which CO<sub>2</sub> was evolved from a sample under UV irradiation, allowing for comparisons across samples. Subsequent weathering and further analysis gave an insight into the degradation mechanisms occurring.

This technique is fast and reproducible in nature and gives an indication of how reactive a sample is likely to be with an easy comparison of rates. Ranking the photo-reactivity of the samples using this in-situ technique, from most photo-active in the presence of UV irradiation to least the results concluded the following:

50% > 30% > 10% > Irganox > Virgin > Tinuvin

DSC oxidation induction profiles give no indication of the lifetime of a sample in a UV environment, although similarities may be present. Interestingly, it was evident that the TiO<sub>2</sub> present did have an influence on both the photo and thermal degradation characteristics of PE. Samples were exposed to artificial weathering for varying durations and the oxidation induction profiles collected intermittently. After 450 hours of weathering, chalking was evident on all TiO<sub>2</sub> pigmented samples, with no visible change in the other samples. Identifying where weathering had the greatest effect on the OIT, ranking of the photoactivity concluded the following using this technique:

Virgin > Irganox > 10% > 30% > 50% > Tinuvin

In this instance, even 150 hours had a considerable impact of the oxidative stability of virgin PE, indicating weathering had induced considerable polymer degradation. The Irganox sample was also considered to be less stable than the TiO<sub>2</sub> samples after weathering.

The final technique was developed in an effort to create a technique that would allow for UV irradiation in-situ whilst the OIT was being measured, eliminating the need for time consuming weathering and subsequent OIT profiles being collected. The degree of photo-activity of the sample thus being measured by effect the in-situ UV had on the OIT.

Virgin > 10% > 30% > 50% > Irganox > Tinuvin

All three techniques yield slightly different results, but in all cases Tinuvin was ranked the most photo-stable of all samples. In the DSC experiments virgin PE is considered the least stable despite there being little physical sign of photodegradation



after 450hrs in QUV, whereas the CO<sub>2</sub> technique measures it to be one of the slowest at degrading. It is a well-known phenomenon that a TiO<sub>2</sub> pigmented polymer will photodegrade significantly faster than the equivalent non-pigmented one, therefore it can be concluded that due to the inherent nature of the DSC technique (thermal based technique), oxygen diffusion characteristics through the molten samples with differing additives, is now influencing the oxidation characteristics measured that accompany degradation.

CO<sub>2</sub> evolution is a more surface based experiment measuring actual oxidation occurring, whereas OIT is an average through thickness indication of how susceptible a sample is to oxidation, also exploiting potential degradation, encouraging additional degradation at these test conditions. In order to allow for sufficient time for the UV to have an effect during the in-situ experiment, a very slow heating rate was used, therefore the test duration was lengthy and the polymer sample was held at elevated temperatures for too long. This is not ideal as the long time at high temperature means that the OIT decreases quickly for relatively short QUV exposures and you lose the ability to measure the OIT. It can be concluded that a short-ramp test of samples in the absence of UV, following QUV weathering, is more likely to be representative of the true extent of degradation.

Additional measures such as measuring sample surface hardness, mechanical properties, molecular weight and further weathering would build up a more thorough view on the effect UV irradiation has on the polymer samples tested.

## 6.5 References

1. Robinson, A.J., Searle, J.R., and Worsley, D.A., *Materials Science and Technology*, 2004. **20**(8): p. 1041-1048.
2. Worsley, D.A. and Searle, J.R., *Materials Science and Technology*, 2002. **18**(6): p. 681-684.
3. Diebold, M.P. Unconventional Effects of  $\text{TiO}_2$  on Paint Durability. in 5th Nürnberg Conference. 1999. Nuremberg, Germany
4. Jin, C.Q., *Ftir Studies of  $\text{TiO}_2$  Pigmented Polymer Photodegradation*. 2004.
5. Lundback, M., Hedenqvist, M.S., Mattozzi, A., and Gedde, U.W., *Polymer Degradation and Stability*, 2006. **91**(7): p. 1571-1580.
6. Fernando, S.S., *Spectroscopic Studies of Polyalkene and Polyester Photo-Oxidation*, in School of Chemical Engineering and Advanced Materials Newcastle University. 2007, PhD, Newcastle University.
7. White, J.R., Shyichuk, A.V., Turton, T.J., and Syrotynska, I.D., *Polymer Degradation and Stability*, 2005: p. 1-6.
8. Kumar, A.P., Depan, D., Singh Tomer, N., and Singh, R.P., *Progress in Polymer Science*, 2009. **34**(6): p. 479-515.

## **7 Conclusions and Future Work**

## 7.1 Conclusions

PVC plastisol coatings are widely used for pre-finished steel applications in external environments, such as construction. The onset of degradation can have detrimental effects on the appearance and substrate barrier properties.  $\text{TiO}_2$  is a widely used pigment in PVC coating systems and as explained in this thesis, also plays a significant role in the mechanisms of photo-degradation.

The rate of degradation of  $\text{TiO}_2$  pigmented PVC has been shown to be highly influenced by the atmosphere it is in. When exposed to UV irradiation in the presence of high relative humidities (~90%), the degradation rate observed was lower than that of a low relative humidity (~35%). Although, in dry conditions the rate measured was at a minimum. The production of acidic species, notably hydrochloric acid (HCl), catalyses the photodegradation of PVC. At high RH, the moisture content in the atmosphere is high enough to limit the evaporation of water produced during the degradation process, thus diluting the acidic effect of the HCl. A transition to the lowest degradation rate measured was apparent with moisture removal, when there was insufficient  $\text{H}_2\text{O}$  present to facilitate the production of HCl. The extent of this effect was reduced with the inclusion of a mineral clay pigment, Hydrotalcite, which reduces this effect by the removing chloride ions. Highlighting it as an effective potential stabiliser, its pigmentation in a PVC plastisol system for external application coatings could improve coating durability and limit the effect of atmospheric conditions on coating photodegradation.

$\text{TiO}_2$  pigmented polyethylene was also subjected to the same experimental investigation. As anticipated, the rate of degradation increases with increasing atmospheric relative humidity. As discussed, this phenomenon has previously been attributed to hydrolysis. However, noting that the nature of the  $\text{CO}_2$  evolution curve reflects that of PVC (transition in rate due to the production of acidic species) some further work would be required to eliminate the possibility of acidic species affecting the degradation mechanism. The addition of Hydrotalcite to the PE mix would help eliminate this possible theory, thus confirming the effect of hydrolysis.

Barrier coatings were shown to be an effective technique of reducing the extent of photodegradation that occurs in PVC coatings. Clear PVC plastisol coatings were applied to TiO<sub>2</sub> pigmented PVC plastisol basecoats, with the clear coats containing UVAs and HALS. Although the data reported in this thesis shows that an improvement to the weathering resistance of the PVC could be achieved by the addition of the lacquer alone (gloss retention of ~100% with clear lacquer alone), the requirement of the stabilisers was very evident in terms of the visual characteristics of the samples, as severe and localised degradation dark discolouration was evident.

In addition to the clear coats, the benefit of non-organic nano-scale coatings was shown. ITO, ZrOx, Ti, AlOx, Al and Cu were all deposited between 2nm and 200nm thicknesses onto a TiO<sub>2</sub> pigmented PVC coating. The extent of photodegradation was again measured by the CO<sub>2</sub> evolution during irradiation. The research highlighted that the choice and level of deposition material is very important to the integrity of the barrier layer and level of protection provided. For example, with ZrOx and AlOx barrier layers, increasing the deposition thickness from 2nm to 200nm caused an increase in CO<sub>2</sub> evolution and at thicknesses above 20nm, the AlOx barrier layer seemingly increased the CO<sub>2</sub> evolution rate by 15% above that of a reference sample with no additional barrier layer.

The use of the novel flat panel reactor in this thesis was concluded to be a useful and reproducible tool in the measurement of polyethylene photodegradation. Accompanying this research was the development of a new in-situ technique to measure the oxidative characteristics of different polyethylene samples. Whilst oxidation induction experiments were shown to be highly effective at indicating the stability of a system, coupled with in-situ irradiation, the thermal and photodynamics of the degradation were difficult to separate. It was therefore concluded, for accuracy and clear measure of the factors that influence the degradation, QUVA weathering followed by oxidation induction experimentation was still the most accurate of experiments of this type.

## 7.2 Future Work

As discussed in this thesis, the use of the novel flat panel reactor was a rapid and reproducible method of quantifying the photodegradation of a polymer sample. Throughout this research, the comparisons were drawn between the secondary rates of the evolution plots. The inflection point between the initial rate and this secondary rate is significant in that this is the point at which the rate of degradation rapidly increases, attributed to HCl production. A closer investigation into this inflection point, in terms of time to inflection and the initial rate of the evolution at differing humidities may prove an interesting insight into the HCl formation and use of HT to minimise the acid catalysis effect.

Whilst clear coats were seen to drastically improve the weathering resistance of a TiO<sub>2</sub> pigmented PVC coating, localised regions of dark discolouration were evident. Further investigations are required to confirm the cause of such discolouration, whether it be concentrated localised degradation and dehydrochlorination of the PVC, or leaching of corrosion products from the steel substrate through the coating. FTIR-ATR microscopy could be used to analyse the organic present in the region. Similarly, mechanically removing the coating may give an early insight.

It was evident that similar levels of weathering resistance improvement were achievable with the application of a PVD coating, however the exact mechanism by which this occurs is likely to be a combination of a few factors; UV screening provided by the nano-scale coating and a barrier layer to oxygen permeation. The deposition of the coatings onto glass panels then subjected to UV-Vis, could indicate the level of UV that is able to penetrate through to the PVC.

## **8 Appendices**

## 8.1 Appendix A

### Depth Removal of Polyethylene Samples

#### Assuming:

- i. 1 mol CO<sub>2</sub> = 44g
- ii. PE = CH<sub>2</sub>n
- iii. Density of PE = 0.95g/cm<sup>2</sup>
- iv. Density of TiO<sub>2</sub> = 4.3g/cm<sup>2</sup>
- v. For additions of 0.5% - volume fraction of PE is still considered 100%

#### Summary of Technique:

##### *Depth Removal Rate*

1 mol CO<sub>2</sub> is 1 mol C oxidised = 14g Oxidised PE

CO<sub>2</sub> evolution rate is measured as 'micro.mol/m<sup>2</sup>/min'

$$\begin{aligned} 1 \text{ micro.mol/m}^2/\text{min} &= 14 \times 10^{-6} \text{ g/m}^2/\text{min} \\ &= 8 \times 10^{-4} \text{ g/m}^2/\text{hr} \end{aligned}$$



Table 8-1 CO<sub>2</sub> Evolution Rates for Samples

| Sample  | Instantaneous Rate<br>(micro.mol/m <sup>2</sup> /min) |      |      |
|---------|---|------|------|
|         | Mins  |      |      |
|         | 0   | 150  | 450  |
| Virgin  | 0.45  | 0.35 | 0.34 |
| Tinuvin | 0.1   | 0.1  | 0.7  |
| Irganox | 0.94  | 0.72 | 0.65 |
| 10%     | 29  | 35.9 | 30.7 |
| 30%     | 60.5  | 43.8 | 41   |
| 50%     | 62.6  | 46.3 | 29.5 |

Table 8-2 Average CO<sub>2</sub> Evolution Rates

| Sample  | Average Rate<br>(micro.mol/m <sup>2</sup> /min) |           |
|---------|---|-----------|
|         | Mins  |           |
|         | 0 - 150   | 150 - 450 |
| Virgin  | 0.4   | 0.345     |
| Tinuvin | 0.1   | 0.4       |
| Irganox | 0.83  | 0.685     |
| 10%     | 32.45   | 33.3      |
| 30%     | 52.15   | 42.4      |
| 50%     | 54.45   | 37.9      |

*Volume Fraction*

Table 8-3 Volume Fraction of PE in Samples

| Sample  | Volume Fraction of<br>PE |
|---------|--------------------------|
| Virgin  | 1                        |
| Tinuvin | 1                        |
| Irganox | 1                        |
| 10%     | 0.9632                   |
| 30%     | 0.89                     |
| 50%     | 0.816                    |

Table 8-4 Depth Removal of Samples after Irradiation

| <b>Sample</b>  | <b>Cumulative Depth Removal (microns)</b> |               |
|----------------|---|---------------|
|                | <b>150hrs</b>                             | <b>450hrs</b> |
| <b>Virgin</b>  | <b>0.05</b>                               | <b>0.13</b>   |
| <b>Tinuvin</b> | <b>0.01</b>                               | <b>0.11</b>   |
| <b>Irganox</b> | <b>0.10</b>                               | <b>0.26</b>   |
| <b>10%</b>     | <b>4.04</b>                               | <b>12.34</b>  |
| <b>30%</b>     | <b>7.03</b>                               | <b>18.47</b>  |
| <b>50%</b>     | <b>8.01</b>                               | <b>13.58</b>  |